JANUARY 2016

Ph.D. in Civil Engineering

ZUHEIR ISMAEEL MOSA KARABASH

UNIVERSITY OF GAZİANTEP

GRADUATE SCHOOL OF

NATURAL & APPLIED SCIENCES

A STUDY OF THE TRIAXIAL SHEAR BEHAVIOUR OF SOME ARTIFICIALLY CEMENTED SAND SPECIMENS

Ph.D. THESIS

IN

CIVIL ENGINEERING

BY

ZUHEIR ISMAEEL MOSA KARABASH

JANUARY 2016

A Study of the Triaxial Shear Behaviour of Some Artificially Cemented Sand Specimens

Ph.D. Thesis

in

Civil Engineering

University of Gaziantep

Supervisor

Assoc. Prof. Dr. Ali Fırat ÇABALAR

by

Zuheir Ismaeel Mosa KARABASH

January 2016

REPUBLIC OF TURKEY
UNIVERSITY OF GAZİANTEP
GRADUATE SCHOOL OF NATURAL & APPLIED SCIENCES
CIVIL ENGINEERING DEPARTMENT

Name of the thesis: A Study of the Triaxial Shear Behaviour of Some Artificially Cemented Sand Specimens

Name of the student: Zuheir Ismaeel Mosa KARABASH
Exam date: 12.01.2016

Approval of the Graduate School of Natural and Applied Sciences

Prof. Dr. Metin BEDİR
Director

I certify that this thesis satisfies all the requirements as a thesis for the degree of Doctor of Philosophy.

Prof. Dr. Abdulkadir ÇEVİK
Head of Department

This is to certify that we have read this thesis and that in our opinion it is fully adequate, in scope and quality, as a thesis for the degree of Doctor of Philosophy.

Assoc. Prof. Dr. Ali Fırat ÇABALAR
Supervisor

Examining Committee Members	Signature
Prof. Dr. Abdulkadir ÇEVİK	.....
Assoc. Prof. Dr. Alper SEZER	.....
Assoc. Prof. Dr. Murat ÖRNEK	.....
Assist. Prof. Dr. Ahmet DEMİR	.....
Assoc. Prof. Dr. Ali Fırat ÇABALAR	.....

I hereby declare that all information in this document has been obtained and presented in accordance with academic rules and ethical conduct. I also declare that, as required by these rules and conduct, I have fully cited and referenced all material and results that are not original to this work.

Zuheir Ismaeel Mosa KARABASH

ABSTRACT

A STUDY OF THE TRIAXIAL SHEAR BEHAVIOUR OF SOME ARTIFICIALLY CEMENTED SAND SPECIMENS

KARABASH, Zuheir Ismaeel Mosa
Ph.D. in Civil Engineering
Supervisor: Assoc. Prof. Dr. Ali Fırat ÇABALAR
January 2016**,** 198 pages

The thesis describes an experimental study in the behaviour of cemented sand at small strain levels considering type of cementing material, sample preparation method, curing conditions, biocementation technique, and waste tire inclusion. In this study, the experiments were carried out using triaxial apparatus modified for local strain measurements for observation of the response of cemented sand at small strain levels. The influences of five different sample preparation methods, and four different cement types (gypsum, lime, calcite, and Portland cement) on the cemented sand behaviour were studied. It was observed that cement type has a significant effect on stress-strain and stiffness of cemented sand. Sample preparation techniques slightly affected the triaxial shear behaviour of cement stabilized sand; whereas specimens stabilized using other agents were significantly affected from sample preparation technique. A new method for the ground improvement, the biocementation of sand by induced formation of calcite from the bacterial activity was also investigated. The efficiency of the biocementation for improvement of the shear strength and the small strain stiffness in comparison with other cementation methods was investigated. The biocemented sand specimens were prepared under confining pressure at three levels of the cementation corresponding to the amount of the urea-calcium chloride flushes. Significant increases in the strength and stiffness of biocemented sand were observed due to the precipitated calcite. Response of the biocemented sand specimens was found to be similar to that of calcite and lime cemented specimens. Microscopic study was conducted to verify the formation of cementing material at three different concentrations. Furthermore, the effect of tire crumbs and cement addition on the response of clean and cemented sand was investigated.

Keywords: Triaxial test, cement type, biocementation, sample preparation, small strain stiffness.

ÖZET

BAZI YAPAY ÇIMENTOLANMIŞ KUM ÖRNEKLERININ ÜÇ EKSENLI KAYMA DAVRANIŞI ÜZERINE BIR ÇALIŞMA

KARABASH, Zuheir Ismaeel Mosa
Doktora Tezi, İnşaat Mühendisliği Bölümü
Tez Yöneticisi: Doç. Dr. Ali Fırat ÇABALAR
Ocak 2016, 198 sayfa

Bu tez, küçük deformasyon seviyelerinde, farklı bağlayıcı malzeme çeşitleri, numune hazırlama, kür koşulları, biyobağlama tekniği ve atık lastik içeriğine bağlı olarak çimentolanmış kum davranışını inceleyen deneysel bir çalışmayı anlatmaktadır. Bu çalışmada, deneyler, düşük deformasyon seviyelerindeki çimentolanmış kum davranışını gözlemlemek amacıyla, lokal deformasyon ölçümleri için değiştirilmiş üç eksenli cihazı ile gerçekleştirilmiştir. Beş farklı numune hazırlama yöntemi ve dört farklı çimento tipinin (alçı, kireç, kalsit ve Portland çimentosu) etkileri araştırılmıştır. Çimento tipinin, çimentolanmış kumun gerilme-deformasyon davranışı ve rijitlik üzerinde kayda değer bir etkisi olduğu gözlemlenmiştir. Numune hazırlama tekniğine bağlı olarak, kumların üç eksenli kesme davranışı, Portland çimentosuyla hazırlanan numunelerde önemsiz mikterlarda değişim göstermiş; ancak, diğer bağlayıcı malzemelerle oluşturulan numunelerde önemli ölçüde değişiklik gözlenmiştir. Yeni bir zemin iyileştirme yöntemi olarak, kalsit ile bakteriyel aktivite yoluyla kumda biyobağlanma özelliği incelenmiştir. Kayma mukavemetini ve düşük deformasyonlardaki rijitliği arttırmak amacıyla, biyobağlamanın verimliliği, diğer yöntemlerle kıyaslamalı olarak araştırılmıştır. Biyobağlanmış kum numuneleri, üç bağlanma seviyesindeki çevre basınçlarında hazırlanmıştır. Çökelmiş kalsit kullanıldığında, mukavemet ve sertlikte önemli artışlar olduğu görülmüştür. Biyobağlanmış kum numunelerinin davranışının kalsit ve kireçle çimentolanan numunelere benzer olduğu gözlenmiştir. Bağlayıcı malzeme oluşumunu doğrulamak amacıyla, üç farklı konsantrasyonda mikroskopik çalışma yapılmıştır. Ayrıca, lastik kırıntısı ve çimento eklenmesinin, temiz kum ve çimentolanmış kumun davranışları üzerindeki etkisi araştırılmıştır.

Anahtar Kelimeler: Üç eksenli deneyi, çimento tipi, biyobağlanma, numune hazırlama, küçük deformasyon sertliği.

To my family

Father,

Mother,

Brother and Sisters

ACKNOWLEDGEMENTS

I would like to express my deepest gratitude to my supervisor, Assoc. Prof. Dr. Ali Fırat Çabalar, for his unlimited guidance, patience and support during this research. Without his supervision and advice, this thesis would not have been possible.

I gratefully acknowledge Mosul University and the Ministry of Higher Education and Scientific Research in Iraq for the PhD scholarship provided by them.

I must acknowledge the financial assistance of the Scientific and Technical Council of Turkey (TÜBİTAK) provided under Project: 110M667.

I would like to extend my sincere gratitude to Professor Osman Erkmen for his assistance in the preparation of the biocementation bacteria solution.

I would also like to express my gratitude to all my colleagues at the department of civil engineering, Gaziantep University.

I would like to sincerely and gratefully thank my parents, father and mother, brother and sisters for their endless support and encouragement during my study period.

Finally, I would like to thank my wife for her endless support and sacrifice, and my wonderful kids for their endless energy, without their encouragement, I would not have finished this thesis.

CONTENTS

Page

LIST OF TABLES

Page

LIST OF FIGURES

Page

LIST OF SYMBOLS AND ABBREVIATIONS

SYMBOLS

B	Pore pressure coefficient
C	Portland cement
C_c	Coefficient of curvature
C_u	Coefficient of uniformity
D_r	Relative density (%)
E_u	Secant Young's modulus (MPa)
e	Void ratio
FY	First yield
BY	Bond yield
G_s	Specific gravity
p’	Mean effective stress (kPa)
q	Deviatoric stress (kPa)
TC	Tire crumb
u	Pore pressure (kPa)
ν	Specific volume
σ	Total axial stress (kPa)
ϕ	Angle of internal friction (°)
ϕ’	Effective angle of friction (°)

ABBREVIATIONS

ECS	Effective Confining Stress
EDX	Energy Dispersive X-Ray
EPS	Extracellular Polymeric Substances
CD	Consolidated Drained Triaxial Test
CIPS	Calcite in Situ Precipitation System
CIU	Isotropically Consolidated Undrained Triaxial Test
CPT	Cone Penetration Test
CU	Consolidated Undrained Triaxial Test
DNA	Deoxyribonucleic Acid
FRO	Full Range Output
LBS	Local Boundary Surface
LDS	Linear Displacement Sensor
LDT	Linear Differential Transformer
LVDT	Linear Variable Differential Transformer
MICP	Microbially Induced Calcite Precipitation
RNA	Ribonucleic Acid
SBS	State Boundary Surface
SEM	Scanning Electron Micrograph
USCS	Unified Soil Classification System
XRD	X-Ray Diffraction

CHAPTER 1

INTRODUCTION

1.1 General

The cemented sand and weak sandstone layers are widely distributed in the semi-arid regions of the earth. The cementation in the natural soils is generally formed due to the various geological processes such as chemical, biological, and mechanical processes that create bonding bridges between soil grains. All natural sand deposits possess some degree of cementation resulting from the deposition of the cementing materials. These materials are precipitated around the soil particles and at the grain contacts (Clayton et al., 2010). On the other hand, soil can artificially be cemented either by injection of cementing material or deep mixing. The cementation in sand is a type of the soil structuring as described by Burland (1990), and Leroueil and Vaughan (1990). They mentioned that the soil structure is represented by the combination of the soil fabric and the bonds between the particles.

The cementation in natural sand deposits may arise through a variety of processes, different cementing materials and percentages, different depths or loading conditions, different saturation and different environmental conditions. On the other hand, pervious knowledges on cemented sand behaviours were hampered by some difficulties in obtaining good quality specimens that cover all these variables and conditions. These difficulties also resulted from the disturbance of the soil structure that can occur during the sampling process (Clough et al., 1981; Abdulla and Kiousis, 1997; Ismail et al., 2002). Due to these difficulties, the researchers studied the behaviour of the artificially cemented sand to mimic the behaviour of the naturally cemented sands. However, the approaches of artificially cementation techniques may introduce many errors in describing the cementing structure and behaviours. The soil cementation that results through these techniques achieved under conditions does not accurately simulate the geological process and environmental conditions of the natural deposits.

The cementation in the sand layers produces significant increases in strength, small-strain stiffness of sand, dilative tendency, and resistance to liquefaction (Sangrey, 1972; Clayton, 1983; Yun and Santamarina, 2005). An important consideration for the cemented sand is that the small strain stiffness and the yielding responses depend on the characteristics of the cementation. From engineering point of view, small strain stiffness of the cemented soils has a great importance in several geotechnical applications, and especially in the context of tunnels and deep excavation (Jardine et al., 1986; Mair, 1993). The stiffness of the soils at small strains is relatively high, getting closer to the yield strain; stiffness becomes lower with increasing strain level (Atkinson, 2000). The accurate estimation of soil stiffness at the small strain in laboratory by triaxial equipments strongly depends on precisely measured strains. Therefore, for a better estimation of the axial strain, it is necessary to carry out tests on an apparatus with local transducers like linear variable differential transformers (LVDTs) (Jardine et al., 1984; Cuccovillo and Coop, 1997a; Heymann, 1998; Clayton, 2011).

Recently, the use of biocementation as a novel method of soil improvement techniques was proposed. This method consists of using the nonpathogenic bacteria, nutrients, and biological processes (DeJong et al., 2006). The biocementation processes utilizes urea hydrolysis as chemical reaction to increase the medium alkalinity and results of biominerals precipitation. The results of these processes produce cementing material (calcite) between the soil particles. The applicability of the biocementation in the field of the geotechnical engineering, the effect of the biocementation on the strength and stiffness was studied by many researchers (DeJong et al., 2006; Whiffin et al., 2007; Whiffin, 2007; Van Passen et al., 2009, 2010).

1.2 Aims and objectives

The main aim of the present research is to study the stiffness and the stress-strain behaviour of the cemented sand at small strains. To achieve this aim, a triaxial testing system was developed for a more accurate measurement of the soil stiffness using the local strain measurements. Also, the research encompasses to the effect of the sample preparation techniques, type of the cementing agents, waste material inclusion, and curing conditions on the stiffness and the behaviour of cemented sand. In addition, great attention was given to study the stiffness and stress-strain behaviour of the biocemented sand using bacterial activity.

In particular, the primary objectives of this research can be summarized as:

1- To modify and extend the capabilities of the triaxial testing system for accurate stiffness measurements at small strain zones.

2- To study the triaxial shear behaviour of the clean sand used in this study under different effective confining stress, relative density and consolidation period.

3- To investigate the effect of the sample preparation techniques, type of the cementing agents, curing conditions and confining stress on the behaviour of the cemented sand at small strain.

4- To explore the effect of the waste tire inclusion on the response of the clean and cemented sand.

5- To study the stress-strain behaviour and stiffness of the biocemented sand under three levels of treatments, and to compare the behaviour of the biocemented sand specimens with the cemented sand by conventional cementing agents.

6- To examine the distribution and percentage of the cementing material in the soil matrix by the microscopic study using Scanning Electron Microscope (SEM) and Energy Dispersive X-ray (EDX).

1.3 Layout of the thesis

The thesis consisted of five chapters and organized as follows:

Chapter 1 summarizes the general information, contribution, and the aim and objectives of the study.

Chapter 2 describes a brief review of the literature and investigations concerning the stiffness and stress-strain behaviour of the cemented geomaterials. Furthermore, the factors affecting the stiffness and strength of cemented soil was discussed in detail. The chapter also presents studies concerning soil biocementation technique. Also, the chapter summarizes studies related to use of the waste material and waste material with cementing agents in the soil improvements.

Chapter 3 illustrates the modification of the conventional triaxial system using local strain measurements and calibration of the instrumentations. In addition, the materials used and the methodology of the sample preparation techniques were explained in details. Finally, the chapter describes in particular the procedures for the preparation of biocementation solution and its application to the triaxial specimens.

Chapter 4 presents the results of the tests and analyses of the data obtained from the experimental studies. The stiffness and the stress-strain response of the cemented sand by the cementing agents and the biocemented sand are discussed, compared and interpreted.

Finally, Chapter 5 gives summary of the research, major conclusions, and recommendations for future studies.

CHAPTER 2

LITERATURE REVIEW

2.1 Introduction

This chapter presents a review of the investigations that reports the behaviour of cemented soils, and some of the latest experimental observations related to the response of the cemented sands. Emphasis was placed to present the studies of the naturally and artificially cemented sand and factors effecting on geotechnical behaviour of cemented soils. The chapter then describes briefly investigations concerning the stiffness of the cemented and uncemented soils and factors affecting soil stiffness. A sub-section of this chapter is focused on studies oriented to the low strain stiffness of the cemented sands, and local strain measurements using internal LVDTs. This is going followed by reviews of researches about the yielding of the cemented soils.

The literature survey presented in this chapter also includes current knowledge of the biocementation techniques through the bacterial activity. Types of the biocementation, geotechnical properties of biocemented soils, and the engineering applications of the biocementation technique are briefly presented. Finally, previous experimental investigations related to utilization of waste materials (waste tire crumbs in particuler) in soil improvements are discussed. The geotechnical properties of the soil improved using waste tire and cement are summarized.

2.2 Behaviour of the cemented geomaterials

2.2.1 Naturally cemented soils

The behaviour of soils cannot be completely understood unless the effects of the structure are considered. The importance of structure was first recognized by Terzaghi (1925) and confirmed by Casagrande (1932), and Skempton (1944). Soil structure was defined as the combination of geometric arrangement of soil particles with respect to each other (fabric) and interparticle attractions (bonding) (Mitchell,

1976 and Burland, 1990). Soils in-situ usually have a natural structure during both late or early stages of diagenesis, which enables them to behave differently from the same material in a reconstituted state (Burland, 1990, Cuccovillo and Coop, 1999). Therefore, investigation of the existence of different types of structures is of importance in understanding the behaviour of both naturally and synthetic artificially cemented geomaterials. As denoted by Sangrey (1972); Clough et al. (1981); and Mitchell (1993), the calcium carbonate, aluminum and iron hydroxide precipitates, organic compounds and amorphous manganese oxides are all possible cementing agents, any of them may be precipitated at the voids between the grains or at the grain contacts in the naturally cemented geomaterials.

The naturally cemented calcarenite behaviour was studied by Carter et al. (1988), and Airey and Fahey (1991). They showed that well defined yield point appears due to breakage of the cemented bonds when the cemented material loaded under isotropic compression. The individual stress-strain response of the naturally cemented geomaterials is the yield curve that identified by the fail of cementation, and independent to the pattern of effective stress or soil failure (Sangrey, 1972). The naturally cemented soils have high strength and rigidity if it compares to other uncemented material in the same geological history. The naturally cemented materials behave as linear up to the yield, and the volumetric strain up to the yield is linearly depending to the mean normal stress (Sangrey, 1972).

Leroueil and Vaughan (1990) showed that the stress-strain behaviour of soils depends on the critical state line of the non-structured remoulded soil, initial state and its position in relation to the yield curve. From the same concept, the typical stress-strain behaviour of naturally cemented sand tested at different confining pressures were emphasized by Leroueil and Vaughan (1990), and Coop and Atkinson (1993). The stress-strain response of the cemented soil depends basically on its initial state, its position related to the bonding yield curve, and the critical state line. This behaviour illustrated schematically in Figure 2.1. The first class of behaviour occurs when the soil reaches its yield stress during isotropic compression, in this case subsequent shearing of the cemented soil produces similar behaviour to the non-structured (uncemented) soil with no yield point and it is illustrated by the curve (1). The second class occurs at intermediate confining stress, in this category, it is proposed that bonds are broken during shearing and the frictional constituents of the

soil is control mainly the strength of the soil. The stress-strain curve might be expected to show a distinct yield point after linear behaviour. Finally, the third class occurs at low confining stress when compared to the bond strength of the cementing. A sharp peak in the stress-strain relations occurs at small strain levels and for stresses outside the limit state surface of the equivalent remoulded soil.

Two methods can be employed in such investigations; either the use of high quality specimens of natural soils or the use of artificially bonded synthetic geomaterials. Although, today, very high quality sampling techniques are available, implying very small disturbance, these high quality techniques (i.e., sherbrooke, laval) may still cause significant loss in structure, and further disturbance may be caused by specimen transportation and specimen preparation for an experimental investigation in a laboratory (Clayton et al., 1992, and Hight et al., 1992).

These investigations, however, presents some difficulties resulting from the disturbance of the structure that can occur during the sampling process (Clayton et al., 1992). In natural sands, Stokoe and Santamarina (2000), and Coop and Willson (2003) have noticed a loss of stiffness as a result of sampling disturbance of interparticle contacts and breakage of cement bonds. Fernandez and Santamarina (2001) concluded that a sand had been cemented under pressure could have its interparticle bonding damaged by unloading.

2.2.2 Artificially cemented soil and factors affecting the response of cemented soil

2.2.2.1 Effect of the cement type and content

Cementation in the soils is caused by either natural or artificial soil stabilization processes. In the natural, the strong and weak bonds formed between soil grains depends on the type and characteristics of cementing material. Silicates, carbonates, iron oxides and gypsum are usual cementing material. In addition, from the geological point of view, diagenesis describes the chemicals, physical and biological processes which occur in sediment after deposition or during lithification (Clayton, et al., 2010). The effects of cementing agent types, contents, and characteristics on the stress-strain behaviour of artificially and naturally cemented soils have been investigated by many researchers. The most commonly used cementing agents are

Portland cement (e.g., Clough et al., 1979, 1981; Acar and El-Tahir, 1986; Consoli et al., 2000, 2012; Haeri et al., 2006; Dalla Rosa et al., 2008; Suzuki, et al., 2014; Rios et al., 2014), gypsum (e.g., Huang and Airey, 1993; Coop and Atkinson, 1993; Ismail et al., 2002, Hamidi and Haeri, 2008), lime (e.g., Haeri et al., 2008; Consoli et al., 2014; Makki-Szymkiewicz et al., 2015) and calcite (e.g., Saxena and Lastrico, 1978; Ismail, 2000, 2002). Other materials usually used are kaolin (e.g., Maccarini, 1987; Bressani, 1990; Toll and Malandraki, 1993; Malandraki, 1994), sodium silicate (e.g., Christopher et al., 1989; Porcino, et al., 2012).

Abdulla and Kiousis (1997) examined in their study the effect of the Portland cement amount and the confining pressure on the stress-strain, softening, dilation characteristics and stiffness of the cemented sand. They concluded that the cohesion of the soil increases non-linearly, while the peak friction angle practically unaffected, as presented in Figures 2.4 and 2.5. They attributed this behaviour mainly to the coating method of cement material to the sand particles as the cement content increase in the soil matrix.

Ismail et al., (2002) performed a series of triaxial tests on cemented specimens to study the effect of cementation on the mechanical properties of the offshore calcareous sand. They investigated the influence of cement type on the shear behaviour of cemented calcareous soil at different level of density and cementation. They maintain the consistency of specimen density and unconfined compressive strength among different types of cementing agents, which were calcite, Portland cement, and gypsum. They concluded that specimens' effective stress paths and post-yield responses were different, despite having the same density and unconfined compressive strength. The reason of this behaviour as the authors mentioned is related to the intrinsic characteristics of each cementing agent and different volumetric response upon shearing. As can be seen from the Figures 2.2 and 2.3, specimens mixed with Portland cement give ductile yield followed by strong dilation, while cemented specimens with gypsum and calcite suffered from brittle yield, usually followed by contractive shear behaviour.

Haeri et al., (2006) conducted a series of triaxial compression tests to study the effect of the cementing agent type on the mechanical behaviour of the gravelly sand. Gypsum, Portland cement and lime were used. Several cement contents were

selected for the preparation of the test specimens (Figure 2.6). They concluded that the cemented specimens with gypsum induce strong brittleness among the cementing agents while the cemented specimens with Portland cement were found to be more ductile. Meanwhile, it showed the highest strength in higher cement content and lower confining pressure. In addition, the lime bonded specimens induced lower peak, ultimate shear strength and highest excess pore water pressure that generated during the undrained test. However, the cemented specimens with gypsum induced lower excess pore water pressure generation (Figure 2.7). They suggested that the effect of type of cementing agents in the drained test was greater than that in undrained test. Also, the cementing agents type effects increase as their contents increase within the soil matrix. The effect of the recent shearing path history on the weakly bonded soil was investigated by Malandraki and Toll (2001). They used 13% of fired kaolin as a cementing agent; the tests were performed on 38-mm-diameter, 76-mm-high triaxial specimens. They found that the previous shearing path history of the soil does not influence on yield strain level, and the yield occurred in zones that corresponded to a yield surface defined for the current shearing path direction. However, the specimen failure envelopes significantly depend on shearing path history of the soil.

Huang and Airey (1998) used gypsum as cementing agents to investigate the influence of cementation degree and density on the properties of the cemented sand. The results showed that the strength and stiffness increase with increasing cement content and density. Moreover, the effect of the cementation decreases as the density increases. Schnaid et al., (2001) studied the strain-stress behaviour of artificially cemented sand specimens that were improved by Portland cement. They showed that the shear strength parameters of cemented soil determined by conventional triaxial tests may be a function of the unconfined compressive strength and uncemented friction angle (Figure 2.8). The initial mean effective stress has not significantly influence to the deformation secant modulus of the cemented soil. An experimental study was conducted by Haeri et al., (2008) to model the Tehran cemented deposit. A series of triaxial compression tests (CD, CU) were conducted on hydrated lime cemented specimens. The effect of confining pressure, cement content and fines content were investigated in this research. The test results showed that there is an evident peak in shear stress for all cemented specimens. The peak was followed by

strain softening and a noticeable brittle response at failure, which increases with an increase in cement amount and decreases as the effective confining stress increase, and as the lime content increases the amount of the negative pore water pressure increase. Rotta et al., (2003) simulated the formation of sedimentary deposits in which cement bonding occurs after burial and under geostatic stresses. They pointed out the importance of the degree of cementation, and the void ratio during the formation of cement bonds.

Numerous of researchers used fired kaolin to investigate the influence of density and bond strength on yielding behaviour of the soil. They concluded that the strength of the bonds between the sand particles varied depending on the time of firing, temperature and density (Maccarini, 1987; Bressani, 1990; Malandraki, 1994).

2.2.2.2 Effect of the sample preparation techniques

The investigations of cemented geomaterials require sophisticated sample preparation and testing techniques. As mentioned by Clayton et al., (1992), and Fernandez and Santamarina (2001) natural and weakly cemented geomaterials can be disturbed partially and even completely during sampling. In addition, preparation of the cemented specimens in a laboratory needs special task. The cemented specimens prepared in the laboratory and tested must be simulate the field processes and environment that results cementation. There are two stress histories for the cementation can be identified; the soil bonded first and then loaded, or the soil loaded first and then bonded (Fernandez and Santamarina, 2001). In natural sands, Stokoe and Santamarina (2000), and Coop and Willson (2003) observed loss in stiffness as a result of sampling disturbance in the interparticle contacts and breakage of cement bonds. The stress-strain behaviour of soils tested in a laboratory is also affected by the sample preparation techniques. Differences between measured results in the laboratory and those obtained from field are usually explained by specimen disturbance, but this may also be due to the testing techniques employed (Bressani and Vaughan, 1989; Zhu et al., 1995; Consoli et al., 2000). For example, Fearon and Coop (2000) used three different sample preparation techniques in their investigation; (i) standard, (ii) reconstituted, and (iii) minced to investigate the dependency of the shear strength and compression behaviour of the soils to the sample preparation methods. They suggested that intrinsic properties of the

geomaterials may affected by the sample preparation methods. Mitchell (1976) concluded that the effort used in the reconstitution methods effects to the behaviour of reconstituted clay specimens. Rippa and Picarelli (1977) prepared reconstituted materials by different methods to evaluate the effects of preparation techniques based on the Atterberg limits. Burland (1990) suggested that reconstituted specimens can be made from a natural remoulded specimen by mixing the soil with water corresponds to water content between the liquid limit and 1.5 of liquid limit. Then the slurry subjected to one dimensional consolidation. Ideally, the water used for reconstitution must have the similar pore water chemistry. He referred to the parameters that determined in this manner as intrinsic, as these parameters were felt to be unique and inherent for a given soil type. Also, he proposed that the influence of soil structure could be measured by making a comparison between its natural behaviour and the intrinsic behaviour under all stress conditions.

Ismail et al., (2000) employed an innovative sample preparation technique defined as 'CIPS' (calcite in situ precipitation system). The process has been described by Kucharski et al., (1996) and the system was developed at the University of Western Australia. This method of sample preparation can provide preparation either by flushing cementation solutions through the soil, or by consolidation slurry of the cementing agents with the soil. Using this technique the calcite was deposited through the soil particles. CIPS seems to be a highly effective way that creates bonds between soil particles, leading to produce cementation between the soil particles that provide a better simulation of the naturally cemented stratums. Pathak and Dalv (2011) studied the effect of four sample preparation methods on stress-strain and liquefaction behaviour of the sand. During experimental work, different techniques of sample preparation methods were used, namely wet tamping, IS Code, dry deposition and moist placement techniques. They concluded that the specimens prepared by IS code technique have dilative behaviour and a greater resistance to liquefaction from the other techniques.

2.2.2.3 Effect of the curing condition

Cementation in natural sands arises through a variety of processes, different cementing materials and percentages, at different depths or loading conditions, and different environmental conditions. Some of the cemented soils in natural soil

deposits were formed under pressure, as can be observed in some marine deposits. Cemented sand in these deposits are formed due to precipitation of cementing agents under pressure (Murff, 1987, and Clough et al., 1981). As mentioned by Rotta et al. (2003) cementation may arise in the sand deposits naturally in a different process: (i) the cementing agents have been precipitated soon after the deposition and this occurred at the shallow depth (in this case cement bond formation is subsequent to burial). This process is typical in calcium carbonate from supersaturated pore water in carbonate sands (Clough et al., 1981; Airey and Fahey, 1991; Cuccovillo and Coop, 1993); (ii) the cementing agents have been precipitated at shallow depths too, but the cementing agent was iron oxide precipitated from water flowing through the soil. In this case the cementation occurs after it subjected to a strong overconsolidation through burial and erosion (Cuccovillo and Coop, 1999); (iii) cementation in many sand deposits occurs with burial at great depths, and this is more typical in the silica and chlorite cementing that generated in the quartzitic reservoir material (Coop and Willson, 2003).

Fewer researchers studied the cementation of sand under pressure. Consoli et al., (2000) studied the behaviour of an artificially cemented soil under drained triaxial compression at two distinct loading conditions. The first group of the specimens cured under confining pressure and the second group of the specimens cured without confining pressure. They confirmed that the stress state acting during the cementation process plays a fundamental role in the mechanical behaviour of cemented soils as presented in Figure 2.9. The peak angle of friction, stiffness and isotropic yield stress of the cemented specimens under pressure showed a more remarkable increase in comparison to the specimens cured under zero pressure. Also, they suggested that, in the case of naturally cemented materials, specimens should be taken from different depths to represent different geostatic stresses, and tested under their respective confining stresses to estimate their real mechanical behaviour. If these conditions not applicable, the triaxial tests should be conducted under confining stresses below stresses that cause bonding degradation or yield stress.

The effect of the confining pressure during the curing of cemented sand by Portland cement was investigated by Zhu et al., (1995). They concluded that the specimens subjected to zero confining pressure during curing period, the at-rest lateral earth pressure in cemented materials decreases significantly. The at-rest lateral pressure

becomes nonlinear and the value of K_o (at-rest lateral pressure coefficient) depends on the vertical stress. Furthermore, the lateral pressure decreases with curing period and density. For cemented sand specimens cured under vertical pressure, the value of the K_o during the removal of vertical stress depends on the cement content and the overconsolidation ratio. Rotta et al., (2003) studied the interparticle bonds in artificially cemented specimens. The cementation allowed to develop under atmospheric pressure before application of confining pressure. This method represents the cementing process for soils bonded close to the surface. Also, they mentioned that as in many calcarenites, this procedure does not represent the development of bonds if they occur after burial to depth. They concluded that at the same void ratio, the curing pressure of the cemented material effect on the primary yield pressure. Also, the increment of yield stress was not affected as presented in Figure 2.10. The cementation under pressure also significantly influence on the characteristics of the models required in the simulation stress-strain behavouir of soil strata (Dalla Rosa et al., 2008). Suzuki, et al. (2014) investigate the effects of one dimensional and isotropic consolidation pressures applied on cemented soils during curing period on undrained peak and residual shear strengths. They concluded that the peak shear strength of cemented soil cured under pressure increases with an increase in the consolidation pressure and curing period. The residual shear strength is affected by the consolidation pressure during curing and the specimens exhibit a higher residual strength as the curing pressure was increased.

The influence of the curing pressure alone, however, did not lead to noticeable changes in the small strain stiffness of the cemented soils, while the value of shear modulus was significantly affected when the cemented specimens were constituted under pressure, then subjected to cycles of loading before testing (Baig et al., 1996; Fernandez and Santamarina, 2001; and Alvarado et al., 2008). They concluded that cemented sand under pressure is prone to experience damage in interparticle bonds when it is subjected to unloading.

2.3 Stiffness of the cemented geomaterials

Soil stiffness is one of the important geotechnical parameters used in order to analyze the soil-structure interaction problems. Great efforts were given to develop new techniques for accurately measuring soil stiffness. Recently an advanced method for

soil stiffness measurement in the laboratory and the field were developed by Heymann, (1998); Clayton and Heymann, (2001). Soil stiffness depends on the stress history and soil deformations which are also time dependent. At very small strain levels, soil stiffness is approximately constant, but stiffness value may reduce as the strain level increase (Clayton, 2001). In this range of strain, soil behaviour is considered to be truly elastic. In addition the soil may exhibit a nonlinear stress-strain response. As mentioned by Atkinson (2000) the stiffness is relatively higher at small strain levels and the stiffness become lower at strain levels close to failure zone. The typical stiffness-strain curve for the soil was presented schematically in Figure 2.11. This figure was suggested by Atkinson and Sallfors (1991), and Mair (1993); and updated by Zimmermann et al., (2010). Actually, the strain levels in the geotechnical structures (e.g., foundations, retaining walls, and tunnels) are in the range where there is greatest variation in soil stiffness. Therefore, local strain measurement instruments are required to measure the variation in the stiffness relevant to failure strain levels in these structures (Atkinson and Sallfors, 1991; Mair, 1993). The stiffness of the geomaterials was affected by many geotechnical factors (e.g., void ratio, mean effective stress, stress history). Generally, the most important factors that effect on the stiffness of geomaterials are summarized below (Hardin and Drnevich, 1972; Clayton et al., 1984; Jardine, 1995; Heymann, 1998):

1- Void ratio: The stiffness of the soil increases as the void ratio decrease. Dense soil deforms by soil grain itself deformation, while loose soil deform by interparticle deformation.

2- Soil gradation, grain size and characteristics: The soil stiffness increases with the increasing average grain size, when large amounts of particles available per unit volume, high interparticle sliding occur. Soil stiffness increases with increasing coefficient of uniformity. In addition, soil stiffness decreases as the soil grain angularity increase (Park and Tatsuoka, 1994). Moreover, the grain surface roughness inhibits sliding therefore increase soil stiffness. Salgado et al. (2000) examine the effect of the silty size fine materials on the small-strain stiffness and shear strength of Ottawa sand. They concluded that the stiffness of loose sand decrease as the silt content is increased, although the shear strength of the mixture increases continuously with increasing fine content. Georgiannou (2006) made a series of triaxial tests to study the effect

of geomaterials in various shapes and sizes on the strength and stiffness of two types of sand. He concluded that the size and type of added fine materials have small effects on the sand stiffness in compression tests, while in extension tests; clean sand specimens are stiffer than the mixtures.

3- Soil plasticity and mineralogy: Soil stiffness increases as the soil mineral strength increase. In addition, the stiffness of the clean sand is greater than the stiffness of low plasticity clay-silt or clay-sand mixture, and the stiffness decreases as the plasticity of the mixture increase (Jardine, 1995).

4- Cementation and bonding: Soil stiffness increases with increasing the level of cementation. Soil grains sliding hampers by the bonds between the particles. The changes in the soil stiffness with the interparticle bonding have been investigated by Acar and El-Tahir (1986), and Cuccovillo and coop (1999). They concluded that soil stiffness increases as the cementation level between the soil particles increase. As mentioned by Leroueil and Vaughan (1990), the bonds results from the precipitation of the silica, carbonate, hydroxides and the organic matter in the grains contact. In addition, the bonding results from cold welding, re-crystallization of mineral, adsorbed water layer modification, and interparticle attractive force in the clay. The resulted bonds lead to increase the soil stiffness by reducing the effect of the mean effective stress. The initial stiffness of sand increase as a function of cement content (Abdulla and Kiousis, 1997).

5- Ageing and fabric: Soil ageing increases the stiffness of soil by increasing the creep and bonding. Soil creep reduces the void ratio, and bonding avoids grain sliding. Clayton et al., (1992) concluded that the material fabric effected on the stiffness of the clay, and the stiffness of the mottled clay greater than the bedded and laminated clay.

6- Degree of saturation: Degree of saturation has a great effect on the estimation of clay stiffness, while the soil saturation has a low effect on the estimation of sand stiffness. Generally, soil stiffness decrease as the degree of saturation increase.

7- Mean effective stress: Stiffness of geomaterials become higher as the mean effective stress increase. On the other hand, influence of the mean effective stress decreases as the bonding level increase. The influence of the mean effective stress on the soil stiffness decrease as the cementation level increase (Acar and El-Tahir, 1986). As mentioned by Porovir and Jardine (1994), and Viggiani and Atkinson (1995) stiffness of geomaterials is functional to the variation of the mean effective stress, and this variation becomes linear at the large strain. Cuccovilo and Coop (1997b) studied the effect of the mean effective stress on the intact and reconstituted soil. They concluded that the soil stiffness decrease as the mean effective stress becomes close to the yielding stress and when damage of the material occur. Heymann (1998), and Clayton and Heymann (2001) showed in their studies that the maximum stiffness of the undisturbed natural clay specimens depends and function of the mean effective stress. In addition, the mean effective stress effect on the maximum stiffness of the well bonded chalk specimens until destucturing take place.

8- Stress history: The effect of the recent stress history on the stiffness of geomaterials in the small and intermediate strain range was investigated by researchers (e.g., Atkinson et al., 1990; Jardine et al., 1991; Smith, 1992; Taheri and Tatsuoka, 2015). The influence of the recent stress history on the soil stiffness was studied by Atkinson et al., (1990). They confirmed four shear stage in the specimen of the reconstituted clay. The results showed that the stiffness was higher in the intermediate strain levels. Jardine et al., (1991) suggested that the soil creep might cause an incorrect stiffness measurement, and the soil must allow until completing soil creep. They showed that stiffness of the natural London clay becomes higher in the intermediate strain levels. Taheri and Tatsuoka (2015) conducted series of consolidated drained triaxial tests for cemented gravelly soil to study the influences of a loading history on small-strain and large-strain stiffness. They concluded that the loading histories have significant effects on the stiffness of cemented soil. Also, they mentioned that these effects depend on axial stress increases, creep strains, strain-hardening, and damage due to a loading history.

9- Shear stress and direction of the stress path: Soil stiffness was strongly affected by the stress path direction when the soils shear close to the yield surface. Moreover, soil stiffness becomes lower when the direction of the stress path is towards to yield surface (Jardine et al., 1991). Furthermore, Heymann (1998) concluded that the soil stiffness at the intermediate strain range is dependent on the current stress path direction. In addition, the stiffness at the intermediate strain level is more stiff if the direction of the stress path is away from the yield surface.

2.3.1 Small strain stiffness of the cemented geomaterials

The stiffness of geomaterials at small strain ranges has a great importance, especially in the context of tunnels and deep excavations as presented in Figure 2.11 (Atkinson and Sallfors, 1991, and Mair, 1993). Main limitations of the small strain stiffness measurement of the soil were the accuracy, resolution, and stability of the strain measurements (Nishimura, 2005). It was demonstrated by several researchers (e.g., Costa-Filho and Vaughan, 1980; Burland and Symes, 1982; Jardine et al., 1984; Cuccovillo and Coop, 1997a; Clayton, 2011) that small strain-measurement by global methods can be highly inaccurate. This inaccurecey is influenced from the imperfect platen-specimen bedding errors, specimen tilting and apparatus compliance. The small strain stiffness of the cemented and uncemented geomaterials were studied by numerous authors (e.g., Acar and El-Tahir, 1986; Cuccovillo and Coop, 1997b; Heymann, 1998; Clayton and Heymann, 2001; Clayton et al., 2010; Clayton, 2011; Cabalar, 2010; Taheri and Tatsuoka, 2015).

Clayton and Heymann (2001) studied the stiffness at very small levels of three different geomaterials (London clay representing the very stiff clay, Bothkennar clay representing the soft clay, and Chalk representing weak rock). They described the linear stress-strain response and stiffness degradation rate of naturally bonded materials. Also, they concluded in their study, that linear stress-strain behaviour appeared at very small strain levels for all three materials (see Figure 2.12). In addition, despite the maximum stiffness (E_{max}) in the two orders of magnitude, the linear behaviour of all three materials was extended in a similar way. The small strain stiffness for the three materials obtained from the triaxial test were found to be

similar to the stiffness measured from the geophysical methods although the effect of the sampling disturbance and the isotropy.

The study conducted by Cuccovillo and Coop (1997b) to investigate the yielding and low strain stiffness of two naturally cemented materials (calcarenite, which represent geomaterials with weak particles bonded by strong cement, and silica sandstone, which represent geomaterials with strong particles bonded by weak cement). Triaxial test device with the local strain measurement by LVDTs was used to determine the shear stiffness of the two materials in the intact and reconstituted state. The results showed that the shear stiffness of the structured sand was higher than that of equivalent reconstituted sand at the comparable state (Figure 2.13). Moreover, the stiffness at the low strain level decrease as structured sand yield, and with the development of the plastic strain when progressive bonding deterioration occurs as shown in Figure 2.14. Also, the stiffness of the structured sand depends on the stress state when the bond between the grains damage after the first yield. Acar and El-Tahir (1986) conducted a series of resonant column tests to study the stiffness of artificially cemented Monterey sand. The test results demonstrated that increasing the cement content up to 4% increased the cemented sand stiffness (Figure 2.15). They concluded that the cementing material at the soil grain contacts made confining to the sand particles and increase the shear stiffness. Also, the results showed that the effect of the mean effective stress decreases as the cementing level increase. The effect of the hydrated cementing material on the very small stiffness of two types of sand was investigated by Clayton et al., (2010). A series of resonant column tests were conducted. They concluded that the location of hydrated cementing material, its contents that fill the voids, size and shape of the particles have a significant influence on the small strain stiffness. Consoli et al., (2012) used bender element test to investigate the effect of the cement content on the stiffness. They showed that the porosity/cement ratio is a convenient parameter in the stiffness estimation of the cemented soil. They illustrated in their study that the small strain stiffness, increase as the cement content increase as presented in Figure 2.16. In contrast, the stiffness in the small strain decrease as the porosity increase. The results of the investigation made by Bhandari and Powrie (2013) for intact and reconstituted Reigate silver sand showed that the fabric structure in the intact sand modified the small strain stiffness.

2.3.2 Measurement of the small strain by LVDT

The measurement of the geomaterial stiffness using laboratory test required special attention in strain increment measurement. Also, the high-resolution displacement device required for recognition of non-linear stress-strain behaviours in soils. The external (global) strain measurement can be highly inaccurate for the stiffness determination in the small-strain levels due to the number of errors caused by (i) bedding errors, (ii) seating errors due to the gap between the device parts, (iii) the compliance of the apparatus (Costa-Filho and Vaughan, 1980; Burland and Symes, 1982; Jardine et al., 1984; Baldi et al., 1988; Heymann, 1998; Heymann et al., 2005). The importance of local measurements of axial strain in the triaxial test was first highlighted by Jardine et al., (1984). The response of triaxial specimens was measured with sufficient accuracy using internal transducers. In particular, the stiffness of the material was defined at small strain ranges relevant to the working load levels in the engineering structures (Cuccovillo and Coop, 1997a). A number of internal axial strain measuring instruments have been developed as shown in Figure 2.17. These include:

1- The electro-level inclinometer (Burland and Symes, 1982; Jardine et al., 1984; Kung, 2007).
2- The Hall Effect transducer (Clayton and Khatrush, 1987; Clayton et al., 1989; Kung, 2007).
3- The strain-gauged pendulum inclinometer (Ackerley et al., 1987; Kung, 2007).
4- The proximity transducers (Hird and Yung, 1989; Kung, 2007).
5- The strain-gauged local deformation transducers (LDTs) (Kokusho, 1980; Goto et al., 1991; Kung, 2007).
6- The linear variable differential transformers (LVDTs) (Brown and Snaith, 1974; Costa-Filho and Vaughan, 1985; Scholey et al., 1995; Cuccovillo and Coop, 1997a; Kung, 2007) (see Figure 2.18).
7- The Fabry-Perot laser interferometer (Heymann et al., 2005).

The typical characteristics, range, accuracy and resolution of the local axial displacement devices are shown in the Table 2.1 (Heymann, 1998).

The traditional local strain measuring instruments (LVDTs) are not suitable for measuring the local strain directly on the triaxial specimen due to its enoumous size, heavy weight, and low resolution. Recently, small LVDTs, low weight, with high resolution instruments have been developed and can be used for direct measurement of local strain on triaxial test specimens (Santagata, 1998; Kung, 2007).

The accuracy of the measurements which can be obtained from an LVDT instrument depends on its sensitivity, and it is required to choose the smallest range as it is possible to maximize the sensitivity and limit the physical size (Cuccovillo and Coop, 1997a). Two LVDTs were fixed to the triaxial specimen in diametrically opposite position on the specimen using mounts (brackets) as shown in Figure 2.18. Then, the average axial strain of the specimen during the shear can be estimated. In this way error resulting from the uneven deformation of the specimen can be limited (Cuccovillo and Coop, 1997a, and Kung, 2007).

Cuccovillo and Coop (1997a) investigated the stress-strain behaviour using two water-submersible internal transducers and an externally mounted LVDT. The results showed that the LVDTs allow strains to be accurately measured over six orders of magnitude, giving good agreement between the two transducers as shown in Figure 2.19. The data recorded from the transducers are continuous with no jumps or breaks even at very small strains. Also, the results showed that the electromagnetic field of the LVDTs is continuous and there is no tendency within the measuring system. The difference between the degradation of the granular soft rock stiffness measured by local and external strain measuring instrument is shown in Figure 2.20. The tangent stiffness in this study was obtained by oil-submersible LVDTs in a high-pressure triaxial apparatus. In such stiff materials, for definition the stiffness at small strain level, it is necessary to use very accurate device for small strain measurement (Cuccovillo and Coop, 1997a).

Cuccovillo (1995) suggested in her investigation that the study of the soft rock stiffness required re-examining the use of LVDTs. The definition of high stiffness at low strain required very accurate instruments. She stated that overall accuracy can be determined by summing up errors from non-linearity, hysteresis and drift. Moreover, she indicates that the output voltage small values result error was negligible if it is compared to the electrical noise.

2.4 Yielding of the cemented geomaterials

The term ‘yielding’ defined as the transition in the stress-strain from elastic to plastic behaviour. The yielding occurs when the sharp curvature appeared after the linear part in the stress-strain relationship (Kuwano and Jardine, 2007). The classical definition of yield in elastic-plastic theory describes the yielding as the end of the elastic region (linear or nonlinear) (Rolo, 2003). The laboratory investigation with clay led Jardine (1985, 1992) to identify three different yield surfaces, an outer bounding surface and three characteristic zones as can be seen in the Figure 2.21. The first zone was limited by Y1 surface, in this zone the soil response is perfectly linear elastic and the strains are fully recoverable. It is expected that the zone enclosed by Y1 might be in highly cemented soils. This zone is visible in strain ranges less than $6x10^{-5}$ and $2x10^{-5}$ in weakly cemented and reconstituted soils, respectively. Therefore, it is necessary to use very sensitive local small strain measurement instruments to assess for identifying this region (Jardine, 1995; Cuccovillo and Coop, 1997b).

The second zone, Y2 surface that defines the limit of non-linear recoverable parts. In this zone, plastic straining develops more rapidly, with markedly more energy being dissipated in unloading-reloading cycles, and the stress-strain behaviour becomes both rate dependent and subject to creep (Kuwano and Jardine, 2007). Smith et al., (1992) and Jardine et al., (1991, 2002) showed that in natural clay the Y2 surface depends on the limiting condition at hysteresis stress-strain loops developed in this zone, and to the sudden changes in the direction of the strain or stiffness drops. On the other hand, Kuwano (1999) suggested that in sandy soil the hysteresis loops developed in zone 2 fail to close. It has been considered that this surface corresponds to the range in which soil grain contacts fail and grain movements occur. Finally, the third zone Y3 surface, in this zone complete breaking of structure among soil particles occur and irrecoverable strains developed. In this zone that enclosed by Y3 surface, the soil particles start to slide over each other. The stress range at the Y3 surface is defined as a point where sudden drops in the stress-strain response occur when the yield points defined in the oedometer tests (Rolo, 2003).

The yield surface Y3 corresponds in normalized stress space to the local boundary surface (LBS), which cannot be crossed by undrained stress paths. The LBS provides

a boundary for an element of soil prone plastic deformation. It separates possible states from impossible states for all possible void ratios and effective stress states. The LBS develop within the more extensive state boundary surface (SBS), which introduce limitation between admissible and non-admissible normalized effective stress states (Jardine et al., 2004). As mentioned by Smith (1992) that the size of the boundary surface increases with increasing structure when defined in terms of normalized stress. Leroueil and Vaughan (1990) identified three zones of the yielding curve in which yield occur in different ways as shown in Figure 2.22. The zones of the yielding curve are; (i) 'compression yield' that developed away from the maximum shear strength, due to increasing in average shear stress, (ii) 'shearing yield' that appears before the shear failure, (iii) 'swelling yield' that occurs in swelling and positioned away from the failure envelope.

The yielding mechanism of cemented geomaterials was investigated by numerous of authors. Malandraki and Toll (1996) attempted to correct some of different definitions for the yield of bonded geomaterials. They compared the yield definitions and the terminology used to describe yielding behaviour within a framework proposed by Jardine (1992). Malandraki and Toll (2000, 2001) suggested the integrating of a 'bond yield' originally referred to as 'second yield', these points in addition to the yield surfaces defined by Jardine (1992) are: (i) Y1, first yield, for limit of linear elastic behaviour; (ii) Y2, for the limit of recoverable behaviour; (iii) Y3, final yield for complete destruction of any structure within the soil. They also suggested that the bond yield could be represented by the point where the major loss of the stiffness occurs in the stiffness versus axial strain graphs. Toll and Malandaki (1993, 2000) expected that the patterns of the behaviour of three different soils and rock as shown in Figure 2.23. Curve 1, no bond yield appears in the unbounded soils. Curve 2 for weakly bonded soils, they expected stiffness reduction at the Y1while a clear stiffness drops occurs at the bond yield. Curve 3 for the soft rock, a significant reduction in the stiffness was appeared while a very clear drop in the stiffness appears in the bond yield. As mentioned by Cuccovillo and Coop (1997b) yielding in the structured sands is marked by a rapid decrease of the stiffness and by a progressive deterioration of bonding. They denoted that after the first yield, the shear stiffness was dependent on the stress state.

Malandraki and Toll, (1996, 2000) identified four main zones of behaviour for bonded soils: the first zone, which is visible at low effective stresses, the behaviour of the soil up to the point of failure is controlled entirely by bonds. In the second zone, the soil behaviour at failure is controlled partially by bonds. In this zone, the soil demonstrates strength greater than those of the destructured material, and yielding of the bonds occur before failure. In addition, in the third zone, the soil has strength similar to that of the destructured soil. The yield of the bonds occurs during shear and do not contribute to the strength of the soil. In the fourth zone, the yield appears in isotropic compression. Also, the initial bonds do not contribute to the strength of the soil. Rotta et al. (2003) studied the characteristics of the isotropic yielding in the cemented sands using triaxial test results. They suggested that yielding stress of the cemented sands varied as a function of cement content and void ratio. Also, this variation is dependent on the curing stress and independent on the stress state. Coop and Atkinson (1993) showed that yield point could be identified by points corresponding to the starting deformation level of bond breakage. They denoted that for constant p' tests, yielding was defined by the plastic volumetric strain, while for drained tests, yielding was defined from the stress-strain graph discontinuity.

The first yield is defined using the stress-strain curves. It is at the end of linear part, and the second yield point is at section having greater curvature, possibly before point of failure (Maccarini, 1978; Airey, 1993). In contrast, in some of the past studies (e.g., Leroueil and Vaughan, 1990; Cuccovillo and Coop, 1997b; Ismail et al., 2002), the researchers discussed the difficulties in identification of yield points in cemented soils.

2.5 Biocementation

The use of the biocementation as an artificial soil improvement technique has been recently developed. Bacteria are the most dominant microorganisms in soil. There are approximately from 10^8 to 10^9 bacterial cells per gram of soil at the ground surface. However, the bacterial concentration generally decreases with soil depth (Ehrlich, 1996). Bacteria can be classified by the type of the wall, shape, nutrients, Deoxyribonucleic Acid (DNA) and Ribonucleic Acid (RNA) sequences, and biochemical transformation type (Mitchell and Santamarina, 2005). The shape of

bacteria is variable and may be rod-like, nearly round, or spiral. The bacterial cell size is usually in the range of 0.5 to 3 μm, and bacterial spores may be as small as 0.2 μm (Madikan and Martinko, 2003). The comparison between the soil grain size and the bacteria size is presented in Figure 2.24. As can be seen from this figure, soil bacteria are not expected to enter through pores of dimensions less than 0.4 μm (Mitchell and Santamarina, 2005; DeJong et al., 2010). Geochemical processes using bacterial activity regulated either through biostimulation (by stimulation the natural bacteria) or bioaugmentation (by adding the required bacterial cells into the soil) results several products. The primary product is typically the calcite precipitation to fill the voids and bind soil particles together (DeJong et al., 2013).

The biocementation has been used in several engineering applications. For example, use of microbes for remediation of cracks in concrete structure (Ramakrishnan et al., 1998, and Ramachandran et al., 2001), biocalcification in brick and bio-bricks (Sarda et al., 2009; Dosier, 2010; Bernardi, 2012), bioremediation (Ferris, 1996), metals stabilization as an environmental application (Etemadi et al., 2003), surface and ground water treatment (Hammes et al., 2003; Mitchell and Ferris, 2005), plugging of oil recovery in the lower yield oil reservoirs (Macleod et al., 1988), stabilization of the contaminated soils and dust suppression (Khachatoorian et al., 2003; Bang et al., 2011). Reduce the permeability of the coarse material and bioclogging (DeJong et al., 2006; Ivanov and Chu, 2008; Chu et al., 2014), improving the bearing capacity of soil (Bianco and Madonia, 2007; Martinez and DeJong, 2009; Sari, 2015), increasing the shear strength of the soil based on the filling of pores (DeJong et al., 2006; Whiffin et al., 2007; Van Passen et al., 2009, 2010; Al-Qabany and Soka, 2013), and use of bacterial activity to strengthen the liquefiable soil (Banagan et al., 2010; Burbank et al., 2011, 2013; Montoya et al., 2013). The most cited literatures related to the biocementation treatment using bacterial activity, type of the soils and tests, the microorganism and nutrient medium and their results are summarized in Table 2.2. Finally, the main applications and main advantages of the biotreatment through the bacterial activity are summarized by (DeJong et al., 2010) and presented in Tables 2.3 and 2.4. Also, DeJong et al. (2013) identified twenty four different biogeochemical applications according to the qualitative manner against the criteria of cost, implementation, probability of success, and social acceptance (Table 2.5). The disadvantage of soil biocementation in comparison with other treatment method

as mentioned by Ivanov and Chu (2008), the biocementation treatment process is usually slower, more complex, depends on several environmental factors (e.g., pH, temperature, electron concentrations, nutrients concentrations and diffusion rates, soil microbiological and applications of biocementation require data of the biological processes).

2.5.1 Types of the biocementation

The techniques of the soil biocementation using activated bacteria can be divided into three groups according to its products. The first one is microbial induced calcite precipitation (MICP). The product of this type is calcite. In this method the calcite achieved by many different processes, including urea hydrolysis, denitrification, sulfate reduction, and iron reduction (DeJong et al., 2013). *Bacillus pasteurii* (American Type Culture Collection 6453) is the most commonly prefered type in many studies due to its ability to produce calcite (Stocks-Fischer et al., 1999; Bang et al., 2001; DeJong et al., 2006, 2010, 2013; Whiffin et al., 2007; Ozdogan, 2010; Burbank et al., 2011, 2013; Al-Qabany and Soga, 2013; Montoya et al., 2013; Sari, 2015). The bacteria cells (*bacillus pasteurii*) use urea as a source of energy and make ammonium and carbonate, according to equation 2.1, in this case the pH of the medium increases. The process results precipitation of the Ca^{2+} and CO_3^{2-} as $CaCO_3$. The carbonate ions that produced from the reaction precipitate in the presence of calcium ions as calcite crystals according to the equation 2.2. The resulted calcite made bonding bridges between the sand grains. The chemical reaction, ureolysis process is shown schematically in Figure 2.25 (DeJong et al., 2006; Whiffin et al., 2007; Van Paassen, 2009; Al-Qabany and Soga, 2013).

$$CO(NH_2)_2 + 2H_2O \xrightarrow{\text{urease}} 2NH_4^+ + CO_3^{2-} \quad \text{..... (2.1)}$$

$$Ca^{2+} + CO_3^{2-} \rightarrow CaCO_3\,(s) \quad \text{..... (2.2)}$$

Biofilm is the second type of the bacteria products. Production of biofilms and other Extracellular Polymeric Substances (EPS) within the soil particles affected on physical properties of soils. These processes produce organic solids in the soil pore space. These materials have soft, ductile, elastic characteristic that reduces pore size, increase the ductility and reduces the rearrangement of soil grains during deformation. These changes in the physical properties lead to increase the erosion

resistance, reduce the hydraulic conductivity and increase the soil shear strength (Thullner and Baveye, 2008; Banagan et al., 2010; Stal, 2010; DeJong et al., 2013). *Flavobacterium johnsoniae* is one of the most important types of bacteria that produce biofilm (Banagan et al., 2010). Many researchers have found that biofilm formation reduces the hydraulic conductivity of the soil. For example, use of bioclogging to decrease the hydraulic conductivity of the soil under and through dams and levees, to decrease the infiltration in ponds, to reduce the permeability of the oil bearing layers, to reduce landfill leakage, and to reduce the groundwater migration through subsurface barriers (Seki et al., 1998; James et al., 2000; Lambert et al., 2010; DeJong et al., 2013).

The third type of the bacterial products is biogas generation. A variety of gases can be produced from denitrification or other microbial processes. For example, carbon dioxide, hydrogen, methane, and nitrogen. The generation of the biogas reduces soil degree of saturation and thereby increases pore space and its' compressibility, reduce excess pore pressure that generates from cyclic loading, and may mitigate liquefaction potential that resulted from earthquake (DeJong et al., 2013). The presence of the biogas bubbles within saturated soil results in a decrease in the P-wave velocities. In addition, small reduction in the soil saturation made a significant reduction in the liquefaction susceptibility (Rebata-Landa and Santamarina, 2012, and He et al., 2013).

2.5.2 Geotechnical properties of the biocemented geomaterials

The applications of the biocementation in the field of the geotechnical engineering have been investigated by several authors. Some of the studies focused on reducing the permeability of the soil. Gollapudi et al., (1995) used microbial calcite cementation to reduce the porosity of highly permeable structures. In this investigation, leaching of water through rock fractures was controlled by microbial plugging. Their results showed that microbial plugging was highly dependent on bacterial concentration, pH, flow rate of the water, and the presence of contaminants. Moreover, the permeability of the sand reduced by 15%-20% using the same technique as mentioned by Ferris et al., (1996). Whiffin et al., (2007) observed a reduction of 22%-75% in the hydraulic conductivity of the soil. They mentioned that the porosity of the sand decreased to 90% of the untreated material. The results of the

permeability test conducted by Al-Qabany and Soka (2013) showed that the permeability of the sand reduced to 20% of its original value.

The effects of the biocementation on the shear strength and stiffness of the sand have been studied by many researchers (DeJong et al., 2006; Whiffin et al., 2007; Whiffin, 2007; AL-Thawadi, 2008; Van Passen et al., 2009, 2010; Banagan et al., 2010; Cheng and Cord-Ruwisch, 2012; Al-Qabany and Soka, 2013; Chu et al., 2014). For example, DeJong et al., (2006) confirmed that microbially cemented specimens exhibit increases in strength when compared to uncemented specimens. They conducted a series of consolidated undrained triaxial tests for biocemented loose Ottowa sand specimens. They used the microorganism *Bacillus pasteurii* with a liquid growth medium, including urea and calcium chloride. Subsequent cementation treatments were applied to the specimen. Bacteria and nutrient solution were pumped into the specimens with a flow rate of 20 mL/min, for 20 minutes and then allowed to rest for 4 hours. The treatment processes were continued for 3-4 days. They used bender element test to monitor the shear wave velocity with treatment period until the wave velocity reached the maximum value. The results showed that biocemented specimens exhibit increase in the shear strength, initial stiffness, and elastic deformation capacity. In addition, the shear behaviour of the biocemented specimen is similar to that of gypsum-cemented soil (Figure 2.26). Ozdogan (2010) studied the effects of microbial calcite cementation on cohesionless soils using triaxial tests. She concluded that the biotreated specimens generally did not exhibit stress-strain behaviour that was significantly different from the control specimens. She observed that the shear strength and behaviour of the cemented soil depends on the amount of back pressure that applied during saturation. She concluded that any bonds formed during biotreatment process broken either during the saturation phase when back pressure applied or during consolidation phases of the test.

Whiffin et al., (2007) and Van Passen (2010) made a biotreatment model using five-meter-height sand column, which was treated with *Sporosarcina pasteurii* DSM 33 and reagents. The collected specimens were tested to estimate the influence of calcium carbonate precipitated along the column to the single-stage confined drained triaxial test results. The analyses of the results showed a significant improvement of strength and stiffness over several meters. Van Passen et al. (2009) and Van Passen (2010) investigated the mechanical characteristics of the biocemented sand. The

strength and deformation response of biocemented sand were determined. They studied the effect of the different levels of precipitated calcite, dry density and different confining pressures on specimens collected from a field scale experiment. The results were compared with other natural and artificially cemented sandstones. They concluded that there are significant increases in soil strength and stiffness of the treated sand if they compared with untreated sand.

Martinez and DeJong (2009) made a comparison footing model to explore the biocemented application performance as shown in the Figure 2.27. A zone of soil under footing model was treated with bio-mediated calcite precipitation. The deformation induced by load application from the footing was decreased by five times under footing pressure of about 30 kPa. The effect of the chemical concentration of the materials used in the MICP treatment on the amount of the calcite that precipitated and thus to the geotechnical properties of the treated soil was well investigated by Al-Qabany and Soga (2013). The results illustrate that there are decreases in the soil permeability and improvement in the strength of the treated specimens. Also, the results showed that materials (urea and calcium chloride) produce uniform and gradual reduction in permeability. On the other hand, the low chemical concentration results high strength specimens (Figure 2.28). DeJong et al., (2014) developed a scaled repeated five-spot treatment model for investigating the technique of biocementation by calcite precipitation in three-dimensional flow systems. The model provided with sensors, including bender elements and sampling wells, placed in accordance with the flow pattern defined by the stream and potential functions. Based on the results of microbial density monitoring and shear wave velocities via bender element, they suggested that the scaled repeated five-spot treatment model was successful at capturing a complex treatment scenario of biocemented soil improvement technology.

The biocementation improves the dynamic strength and stiffness of the treated soils; it provides a sufficient improvement to resist soil liquefaction as demonstrated by Burbank et al., (2011, 2013); Banagan et al., (2010); and Montoya et al., (2013). The variation of the shear wave velocity with the biocementation treatments was well investigated and mentioned in many researches (DeJong et al., 2006, 2010; Montoya et al., 2013). They concluded that the shear wave velocity increases with the increasing of biocementation treatment periods. Weil et al., (2011) examined the

applicability of P-wave, S-wave and resistivity measurements to control the treatment process, extension and spatial distribution of MICP in the sands. Burbank et al., (2011) and Burbank et al., (2013) studied the precipitation of calcite by indigenous microorganisms to strengthen liquefiable soils. They found using the result of XRD tests, that substantial cementation created in specimens treated with a biomineralization solution that contain urea and $CaCl_2$ (Figure 2.29). The high percentage of the Ca^{2+} indicates to higher calcite ($CaCO_3$) content. The CPT results showed a significant improvement in tip resistance for calcite precipitation levels as low as 1.8 to 2.4%. They anticipated that liquefaction resistance may be improved significantly for some geomaterial with calcite precipitation.

A trial test was performed by Dongliang et al., (2011) to determine the degree of cementation occurred by the biocementation treatments. They used microbes naturally inhabited in a pond. They found that some amount of cementation may be generated in the specimen of loose sand. Although the cementation was not uniform, the velocities of the shear wave that propagate through the specimen increased by approximately 10%. Montoya et al., (2013) used centrifuge test to study the response and integrity of the MICP cemented sand subjected to dynamic loading. The treatments were conducted at three levels of the cementation which was controlled by nondestructive measurements of shear wave velocities. The results from dynamic tests showed that there was a significant increase in resistance to liquefaction of biocemented sands compared to untreated loose sand.

2.5.3 Microscopic study of the biocemented geomaterials

The amount and distribution of the cementing material produced from the biocementation processes, the factors that effect on the calcite precipitation have been studied by many authors using SEM and XRD (Stocks-Fischer et al., 1999; Bang et al., 2001; DeJong et al., 2006, 2010; Wen Chou, 2007; AL-Thawadi, 2008; Ozdogan, 2010; Meyer et al., 2011; Sung-Jin et al., 2012; Burbank et al., 2012; Al-Qabany and Soka, 2013; Sel et al., 2015). As mentioned by DeJong et al., (2010) that the precipitated calcite covers the surfaces of soil grains relatively uniform and there is a high concentration of calcite at the interparticle contacts (Figure 2.30). Burbank et al., (2012) used SEM, XRD, and EDX to observe the distribution and amount of the calcite mineral in the treated soil matrix. They revealed that the cementing

material coats the sand grains, and forms clots and bridges. Also, they concluded that the amount of the calcite increase in the treated soil. Sel et al., (2015) observed using SEM that after biocementation treatments the group of the sand grains was attached to each other with a gummy likes bonds.

2.5.4 Field applications of the biocementation

There are few field trials of biocementation treatment using bacterial activity performed to date in the world. Generally, this method was actively used either to improve the strength and stiffness of soils by carbonate precipitation or to reduce the soil permeability by formation of biofilm (DeJong et al., 2013). Two trials of the MICP field application were mentioned in the papers. The first one performed by Visser and Smit Hanab in the Netherlands in 2010 for gravel stabilization in the gas pipeline. The stabilization was applied to a 1000 m^3 soil volume at 3-20 m depths. The second project was conducted at the Vadose Zone Research Park (VZRP) at the Idaho National Laboratory (INL) to immobilize the heavy metals (Fujita et al., 2010). The applications of the bioclogging have also been reported in the literature using biofilm formation. In Austria, nutrient solutions were used for injection in the screen of wells in the crest of an earth dam through the Danube River in Greifenstein. After completing the treatment process, a significant reduction in water flow rate was observed (Blauw et al., 2009; Lambert et al., 2010; DeJong et al., 2013). The other successful application using biofilm clogging was to reduce the hydraulic conductivity in a fractured dolostone in Southern Ontario, Canada (Lambert et al., 2010).

2.6 Behaviour of the soil and waste tire mixtures

The waste tires have been used in some engineering applications and thereby reduce the potential impact on the environment. Huge amounts of scrap tires are discarded annually and even larger numbers are currently stockpiled all around the world. Besides the economical and environmental benefits, tire wastes provide unique characteristics for many geotechnical applications. Tire wastes can be used in highway and earthwork constructions as lightweight fill material for example, retaining wall backfills, embankments, and bridge abutment, or in landfill applications as drainage material (Humphrey and Manion, 1992; Ahmad, 1993; Edil and Bosscher, 1994; Masad et al., 1996; Young et al., 2003; Tanchaisawat et al.,

2010). Properties of tire wastes such as strength, resiliency, durability, and high frictional resistance are important parameters in the design of highway embankments (Young et al., 2003; Edincliler et al., 2012). The typical piece shapes of different processed waste tires that use in the geotechnical application are tire chips, tire shreds, tire crumbs, and tire buffings as shown in Figure 2.31 (Edincliler et al., 2010).

Tire shreds have been used as lightweight fill material in many retaining structures and embankments (Humphrey and Manion, 1992; Bosscher et al., 1997; Tweedie et al., 1998; Lee et al., 1999; Dickson et al., 2001; Zornberg et al., 2004). The investigations illustrate that the use of waste tire-soil mixtures have higher shear strength and lower compressibility and thus show better engineering characteristics in comparison with waste tire shreds itself. Ahmad (1993) concluded that the density and resilient modulus of the tire-soil mixture decreases with increasing tire content and the relationship between tire content and density is almost linear. On the other hand, the compressibility of the tire-soil mixture increases as the tire content increase. Edil and Bosscher (1994) mentioned that including the tire shreds in sand layers vertically improves the shear strength along the plane that is perpendicular to the shred. Also, they showed that waste tire and tire-soil mixtures have high compressibility at low normal stresses. Masad et al., (1996) suggested that the Ottowa sand and shredded tires mixtures have a potential to be used in highway embankments over compressible soils as a lightweight fill material. The construction of embankments with waste tires-soil mixtures can potentially have steeper slopes because the backfill has lower unit weight and higher shear strength. Also, the settlement of underlying soil is reduced due to use of the lightweight material (Tatlisoz et al., 1997). Tsang (2008) suggested to use waste tires addition in underground tunnels, and around the foundation of a building.

2.6.1 Stress-strain response of sand-tire rubber mixtures

The stress-strain response of the tire rubber and sand mixture were investigated by numerous of authors. Particularly, the triaxial test was used to estimate the shear strength parameters of sand with different types of waste tires (Ahmad, 1993; Masad et al., 1996; Wu et al., 1997; Moo-Young et al., 2003; Zornberg et al., 2004; Gotteland et al., 2005; Edincliler et al., 2010). For example, Ahmad (1993) used

triaxial test to study the behaviour of sand with tire chips. He reported that adding tire chips increases shear strength of the mixture. The shear behaviour of the tire-sand mixture is mainly affected by the range of confining pressures and tire content, while compactive effort and tire grain size has inconsiderable effect on the shear behaviour of the mixture. The addition of tire chips to sand on the other hand provide an enhanced ability for energy dissipation due to the higher energy absorption capacity produced by tire chips (Edil and Bosscher, 1994). Large-scale triaxial tests were conducted by Zornberg et al., (2004) for clean waste tire and tire-sand mixtures to evaluate the optimum tire percent. They concluded that the shear strength increases with increasing tire percents, and the strength reached the maximum value for tire percentages up to 35% and then decreases. Edincliler et al., (2010) performed drained and undrained triaxial test to the sand-waste tire mixture and modeled the stress-strain behaviour with neural networks (NN).

Numerous researchers used the large scale direct shear test and conventional direct shear test to study the stress-strain behaviour of the waste tire and waste tire-soil mixtures (Humphrey et al., 1993; Foose et al., 1996; Tatlisoz et al., 1998; Edincliler et al., 2004; Ghazavi 2004; Attom, 2006; Ozkul and Baykal, 2006; Akbulut et al., 2007; Edincliler, 2007; Edincliler et al., 2010; Cabalar, 2010). For example Tatlisoz et al., (1998) conducted large-scale direct shear tests for waste tire and soil mixtures. They showed that the shear strength of the soil-tire mixtures improved with increasing waste tire percent up to 30%. Edincliler (2007) studied the shear strength response of tire buffings and tire buffings-sand mixtures. She observed an increase in shear strength of tire buffings-sand mixtures and she suggested to use the tire buffings as fiber reinforcement elements.

The influence of the waste tire to the dynamic properties of the geomaterials has been investigated by many researchers (Feng and Sutter, 2000; Pamukcu and Akbulut, 2006; Kim and Santamarina, 2008; Anastasiadis et al., 2009, 2011; Senatakis et al., 2012). For example Kim and Santamarina (2008) showed that up to an order of 20% content of tire chips mixed with sand, the shear wave velocity of the mixtures increases, and above that content the shear wave velocity of the mixture decreases. Similarly, an increase of small strain stiffness with a simultaneous increase of damping ratio as the content of waste tires increases in a mixture with sand, and up to a specific waste tires content was also realised by Feng and Sutter

(2000); Pamukcu and Akbulut (2006); and Anastasiadis et al., (2009). They conducted a series of resonant column tests on sand-waste tire mixtures, and showed that an increase of waste tire percentages leads to an increase of mixtures damping ratio and to a decrease of stiffness. They also realized that the behaviour of soil-waste tires mixtures become more linear as the content of waste tires increases in the range of medium to high strain level. Anastasiadis et al., (2009), and Senatakis et al., (2012) have recently studied the influence of confinement time on the behaviour of the soil-waste tires mixtures at various mix ratios, and the influence of size of specimens on the behaviour. They proposed analytical relationships for the calculation of the stiffness and damping ratio of granular soil-waste tires mixtures in a various strain levels.

2.6.2 Behaviours of the cemented sand and waste material mixtures

The mechanical properties improvement of the geomaterials was established, either by the addition of cementation materials or by the inclusion of randomly distributed discrete material such as fibers. The composite materials that include the cementing agents and fiber elements consist of soil stabilization and reinforcement (Consoli et al., 2009). The in-situ geotechnical application of fiber-reinforced cemented sand was proposed to increase the bearing capacity of spread foundations that construct over weak soils (Consoli et al., 2003).

The influence of the combined addition of the cementing agents and the fiber or waste material has been investigated by numerous of the researchers (Maher and Ho, 1993; Cai et al., 2006; Tang et al., 2007; Consoli et al., 2003, 2004, 2009, 2010; Park, 2011; Hamidi and Hooresfand, 2013). For example, Maher and Ho (1993) performed static triaxial, dynamic triaxial and splitting tension tests to study the behaviour of the cemented sands with randomly distributed glass fibers. They reported that the compressive strength, splitting tensile strength and brittleness index of cemented sand significantly increases. Also, they observed that the inclusion of fibers improved the cyclic strength of cemented sand. The fiber inclusion increases the number of cycles and the magnitude of strain required to damage the cemented sand. Consoli et al. (2004) conducted static drained triaxial tests to study the effect of three fiber types on the geotechnical behaviour of fiber-reinforced cemented soils. Their results illustrated that the addition of the fibers reduced the stiffness, increased

the peak friction angle of both cemented and uncemented sand, increased deviatoric stresses at failure and improved brittle behaviour of cemented soils.

The effect of the combined addition of the fiber and Portland cement on the behaviour of sand in a wide range of confining pressures has been investigated by Ud-din et al., (2011). Their results showed that the peak strength and the stiffness of sand increase with the inclusion of the fibers. However, confining pressure during the test effects on the behaviour of the fiber reinforced cemented soil. Few researches have been carried out studies on the influence of waste tire and cementing agents on the mechanical behaviour of geomaterials (Tsoi and Lee, 2011; Guleria and Dutta, 2012). Tsoi and Lee (2011) performed drained and undrained triaxial compression tests on mixtures of Portland cement, fly ash, sand and tire chips. They reported that the stress-strain properties of cemented tire chips-sand mixtures under triaxial tests are similar to the typical cemented soils, although high ductility produced by tire chips. The study made by Guleria and Dutta (2012) illustrated that the unconfined compressive strength of the fly ash-gypsum and lime mixtures improved by inclusion of tire chips. However, this behaviour was affected by the tire chip amount, curing method and curing period.

Table 2.1 Characteristics of the local displacement device (Heymann, 1998).

Instrument	Range (mm)	Accuracy (μm)	Resolution (μm)	Calibration instrument	Ref.
Electro level gauge	15	±2	< 1	LVDT with accuracy of 0.2μm	1, 8
Hall effect gauge	2.5 7	±6 ±30	< 1 -	Micrometer with 2.54μm resolution	4, 5
LDT	0.2	0.09	0.12	Micrometer with 2.54μm resolution	6
Proximity transducer	5	±2	1	Slip gauges with accuracy of ±2μm	7
LVDT	5 0.02	- 0.05	1 0.005	Micrometer	2, 3

1. Burland and Symes (1982)
2. Cuccovillo (1995)
3. Cuccovillo and Coop (1997a)
4. Clayton and Khatrush (1986)
5. Clayton et al. (1989)
6. Goto et al. (1991)
7. Hird and Yung (1989)
8. Jardine et al. (1984)

Table 2.2 Summary of literature review of studies concerning biocementation by bacteria.

No.	Authors	Soil Type	Microorganism	Nutrient medium	Nutrient period	Bacteria products	Test type	Test results
1-	Macleod et al., (1988)	Sintered glass bead cores	*Klebsiella pneumonia* (Starved and vegetative)	Sodium Citrate medium	-----	Biofilm (glacocalyx)	Permeability, SEM , DNA tests	Starved cell reduce the core permeability, deep penetrate and did not completely block while vegetative cell reduces to 1 % and can be used in the plugging of oil recovery
2-	Stocks-Fischer et al., (1999)	Sand	*Bacillus pasteurii* (ATCC 6453)	Urea and $CaCl_2$	10 Days	$CaCO_3$	X-ray and SEM	The rate of the precipitation with cell growth faster than that of chemical precipitation and suggest to use it in remediation of porous media
3-	Perkins et al., (2000)	Ottawa sand F-110	*Klebsiella oxytaca*	Biofilm nutrient solution	Min. 14 days	Biofilm	Triaxial, oedometer, and finite element model	Negligible effect on the strength and stiffness properties of sand. Yet increases creep deformation.
4-	Bang et al., (2001)	Polyurethane (PU), Cement mortar	*Bacillus Pasteur* (ATCC-11859) immobilizes by PU	Urea and $CaCl_2$	0 ,7 , 28, days	$CaCO_3$	SEM, Tensile strength, and compressive strength	Calcite precipitation didn't increase the tensile strength of the PU, and it increases the compressive strength of the cracked cement mortar cubes
5-	DeJong et al., (2006)	Ottawa sand 50-70	*Bacillus pasteurii* (ATCC-6453)	Urea and $CaCl_2$	3-4 days	$CaCO_3$	Triaxial test, SEM, XRD	An increase in the shear strength, increases in the initial stiffness, and the soil have no collapse behaviour
6-	Wen Chou (2007)	Silica sand, West Virginia	*Bacillus pasteurii* (11859)	Nutrient broth, urea, NH_4Cl, $NaHCO_3$, and CaCl2	74 and 29 hours	Calcite	Direct shear tests, CBR, SEM and EDX	Increase in the angle of internal friction, CBR, volume changes with live, resting, and dead cells, respectively
7-	Whiffin et al., (2007)	Itterbeck sand	*Sporosarcina pasteurii* (DSMZ 33)	Urea and $CaCl_2$	Pump 1 L/day	$CaCO_3$	Triaxial test, permeability	Porosity decrease by 90%, an improvement of the strength and the permeability slightly reduced.
8-	Waller III (2009)	Ottawa sand 50/70 (D_{50} = 0.21 mm)	*Sporoscarcina pasteurii*	Urea, $CaCl_2$, NH_4Cl, $NaHCO_3$	Until the target shear wave velocity	Calcite	Drained triaxial compression tests, X-ray, bender elements	Significant increase in peak deviator stress
9-	Bangan et al., (2010)	Ottawa sand 30	*Flovabacterum johusoniae* (UW101)	Casitone yeast extruct medium	5 days	Biofilm	Box model for liquefaction test	Increase the sand shear strength by the presence of biofilm.

Table 2.2 Summary of literature review of studies concerning biocementation by bacteria (continued).

No.	Authors	Soil Type	Microorganism	Nutrient medium	Nutrient period	Bacteria products	Test type	Test results
10-	Ozdogan (2010)	Ottawa sand	*Sporosarcina pasteurii* (ATCC-6453)	Urea and $CaCl_2$	14,19,25 days	$CaCO_3$	Triaxial test	A significant amount of microbial calcite was observed at grain contact, and the stress-strain behaviour was not significantly different from the control specimen.
11-	Burbank et al., (2011)	River sand	Indigenous microorganisms	Urea and $CaCl_2$	96 hrs	$CaCO_3$	CPT, XRD	1% of $CaCO_3$ have negligible effect, 1.8-2.4 % of $CaCO_3$ increase the CPT significantly
12-	Meyer et al., (2011)	Well graded sand	*Sporosarcina pasteurii* (ATCC 11859)	Urea nutrient broth and $CaCl_2$	1,2,4,7,14 days	$CaCO_3$	X-ray (EDS), wind erosion test (Wind tunnel)	Reduction in the soil mass loss and the method can be used an airborne fugitive dust control
13-	Weaver et al., (2011)	lane mountain silica sand 20/30	*Leptothrix discophoru* (SS-1)	$CaCl_2$, Iron, manganese solution	11 days	Iron and manganese oxides	Spectrophotometer	The results showed that 1 μM manganese and 0.2 μM iron in the treatment medium leads to a high percentage of manganese oxide precipitation
14-	Burbank et al., (2012)	Atlas sand and snake river sand	Natural indigenous bacteria	Urea, $CaCl_2$, Sodıum acetate, Molasses	3, 21 days	Calcite	CPT, Cyclic triaxial, EDX and SEM	A large increase in the CPT resistance and increases in the cyclic stress ratio, which required to induce liquefaction
15-	Sung-Jin et al., (2012)	Cement-sand mortar	*Exiguobacterium marinum* (KNUC513)	Urea and $CaCl_2$	3,7,28 days	Biofilm	Compressive strength and FE-SEM	Increase the compressive strength of the sand-cement mortar
16-	Al-Qabany and Soka, (2013)	Sand	*Sporosarcina pasteurii*	Urea, $CaCl_2$, ammonium chloride, sodium bicarbonate	------	Calcite	Permeability, UCS	Decrease in the soil permeability and improvement in the strength of the treated specimens
17-	Montoya et al., (2013)	Ottawa sand 50–70	*Sporosarcina pasteurii*	Urea, $CaCl_2$,	Until the target shear wave velocity	Calcite	Centrifuge model test, bender elements	A significant increase in resistance to liquefaction of bio-treated sands compared to untreated loose sand

Table 2.3 Main advantages of the biocementation treatment using bacterial activity (DeJong et al., 2010).

	Advantages of the biocementation
1-	Reduced costs: use of natural materials, reduced treatment injections.
2-	Reduced impact to the environment: use of natural materials that do not permanently alter subsurface conditions.
3-	Improved treatment uniformity: biological processes have potential to enhance spatial uniformity.
4-	Optimal treatment concentration: degree of treatment can be controlled and monitored.
5-	Adaptable duration: treatments can be removed if only temporary support needed (e.g. by reversal of chemical processes).
6-	Hydraulic and mechanical control: degree of treatment can be adjusted.
7-	Flexible implementation: methods can be used in new and retrofit construction.
8-	Penetration into soils w/fines: cells are typically 1–3μm in size and self-mobile.

Table 2.4 Main applications of the biocementation treatment using bacterial activity (DeJong et al., 2010).

	Applications of the biocementation
1-	Liquefaction prevention: cementation of subsurface to prevent liquefaction and its damage.
2-	Building settlement reduction: reduce settlement and increase bearing capacity for foundations.
3-	Dam and levee safety: upstream injection of technique would “plug” erosive piping.
4-	Tunneling: soil stabilization prior to tunneling would reduce disruption and increase efficiency.
5-	Scour/erosion prevention: treatment would increase resistance to erosive forces of water flow.
6-	Bluff and slope stabilization: treatment could provide additional stability needed to prevent failures.
7-	Impermeable barriers: barriers to stop/divert subsurface transport of contaminants.
8-	Reactive barriers: opportunity for creation of barriers that treat/clean ground water as it flows.
9-	Groundwater protection: treatment to immobilize materials before contamination of aquifers.
10-	Emergency immobilization: rapidly secure contaminants from hazards.
11-	Aquifer storage and recovery: treatment to enhance storage and reduce losses in aquifers.
12-	Energy (fuel) storage: used to create subsurface facilities for storage of liquefied natural gas.
13-	Carbon sequestration: used to create subsurface facilities for storage of CO_2.

Table 2.5 The evaluation of biocementation treatment application alternatives (DeJong et al., 2013).

Application	Implementation Easy: 5 Difficult: 1	Probability of success High: 5 Low: 1	Cost/viability Economic: 5 Expensive: 1	Societal acceptance High: 5 Low: 1	Total score out of 20
Structural repair	5	5	3	5	18
Erosion control	4	5	4	5	18
Co-precipitation/immobilisation of contaminants	5	4	4	5	18
Dust mitigation	4	5	4	5	18
Ground improvement for rural roads	5	5	3	4	17
Shallow carbon sequestration	5	3	4	5	17
Leak management	4	3	4	5	16
Rehabilitation of ancient monuments	3	3	5	5	16
Ground improvement for urban road subgrading	5	3	3	4	15
Soil liquefaction mitigation (MICP)	3	5	3	3	14
Ground improvement for ash ponds	1	4	4	5	14
Recycling/reuse of dredging materials	3	2	3	5	13
Soil liquefaction mitigation (biogas)	3	3	3	3	12
Enhanced water/oil/gas recovery	1	3	3	5	12
De-desertification	1	5	1	5	12
Sediment weakening by fluidisation	3	2	3	3	11
Underground creation (pipeline)	3	4	1	3	11
Stabilisation of sinkholes	1	3	2	5	11
Landfills as new energy resource	3	4	1	2	10
Construction products (bricks)using soil-biocementation	2	4	1	3	10
Water storage	3	2	2	2	9
De-swelling of clays	1	1	1	4	7
Deep carbon sequestration	1	1	1	3	6
Underground creation (tunnel)	1	1	2	1	5

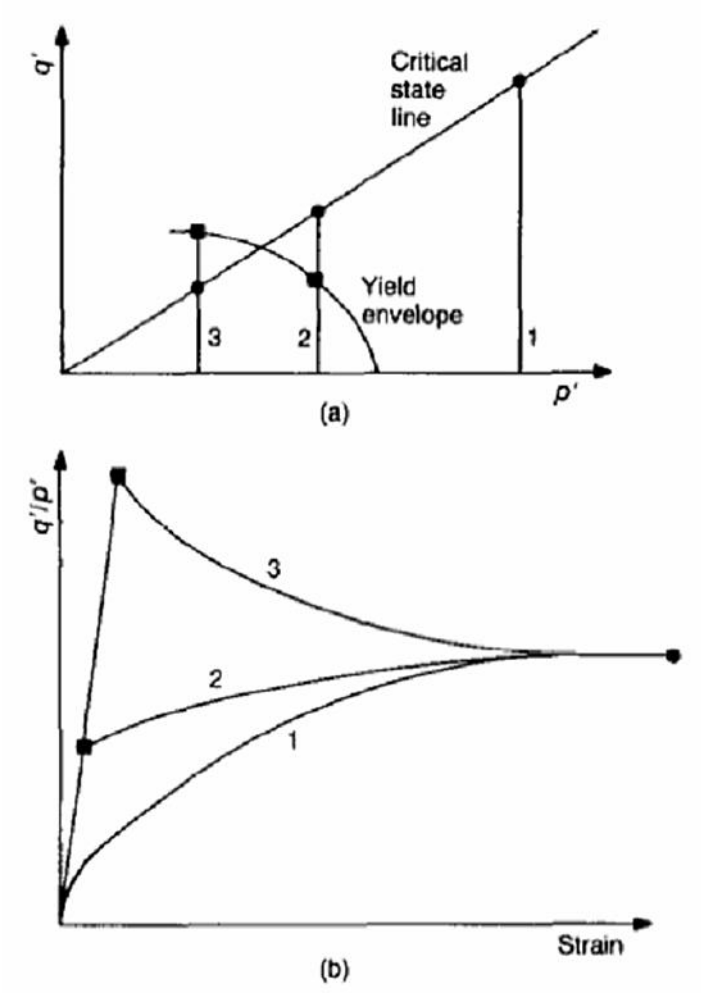

Figure 2.1 The cemented soils idealized behaviour: (a) stress path (b) stress-strain behaviour (Coop and Atkinson, 1993).

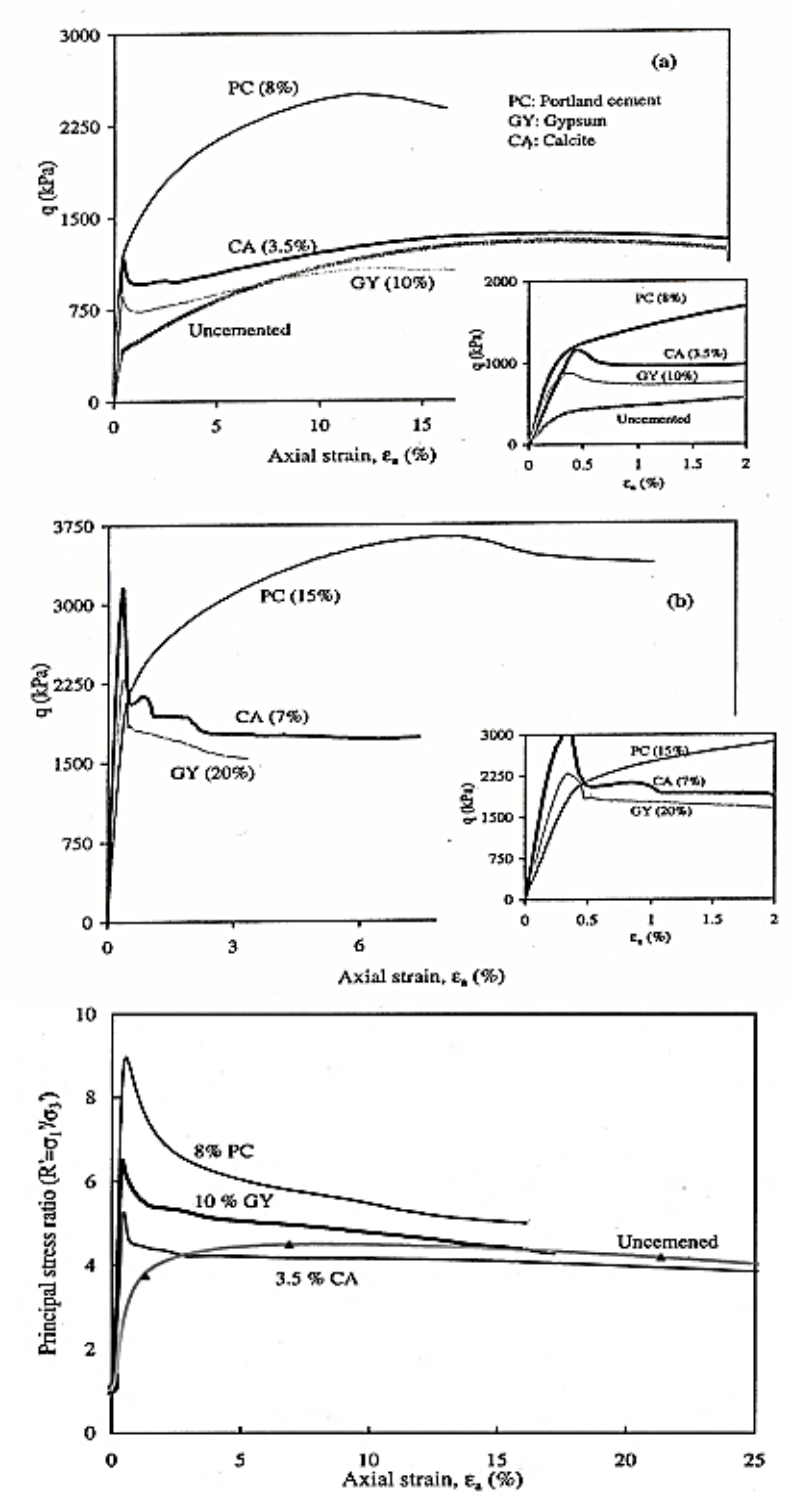

Figure 2.2 Stress-strain response of specimens treated with different cementing materials in CIU triaxial test (Ismail et al., 2002).

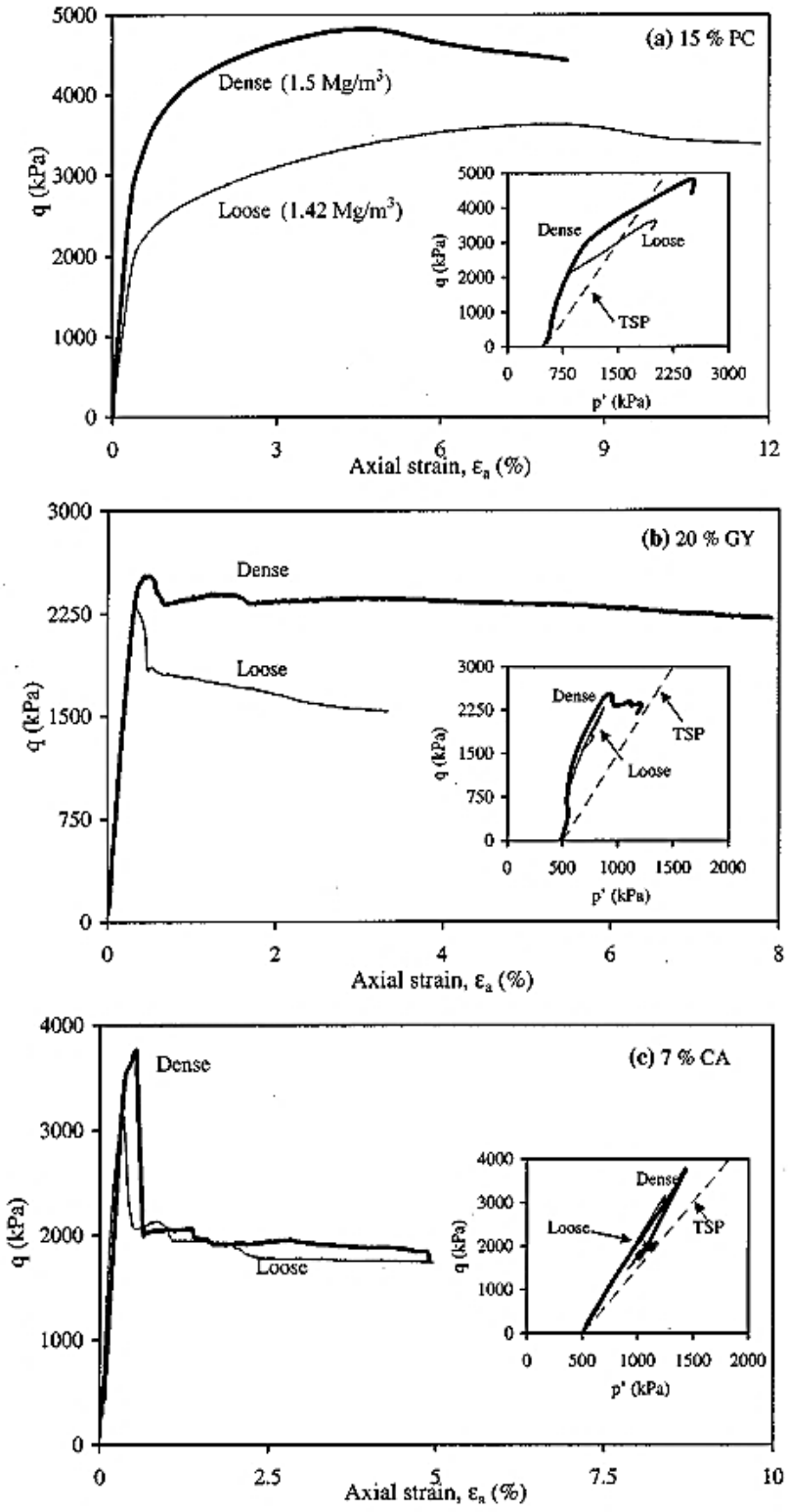

Figure 2.3 Influence of the density on the behaviour of the treated sand with different cementing agents (Ismail et al., 2002).

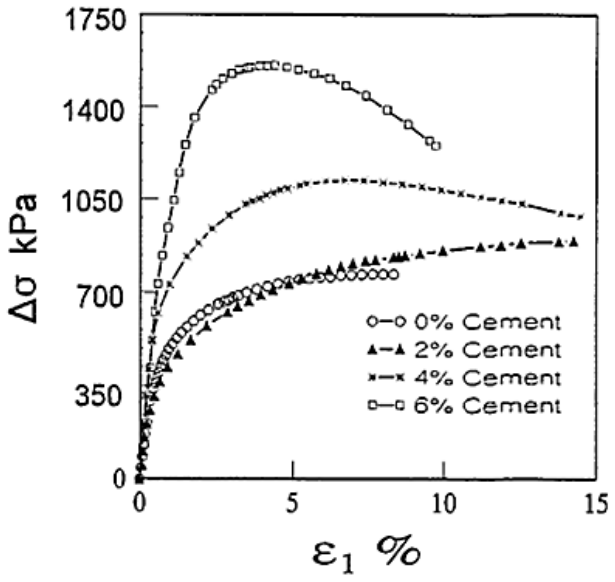

Figure 2.4 Effects of the cement contents on the stress-strain relations for σ_3 = 200 kPa (Abdulla and Kiousis, 1997).

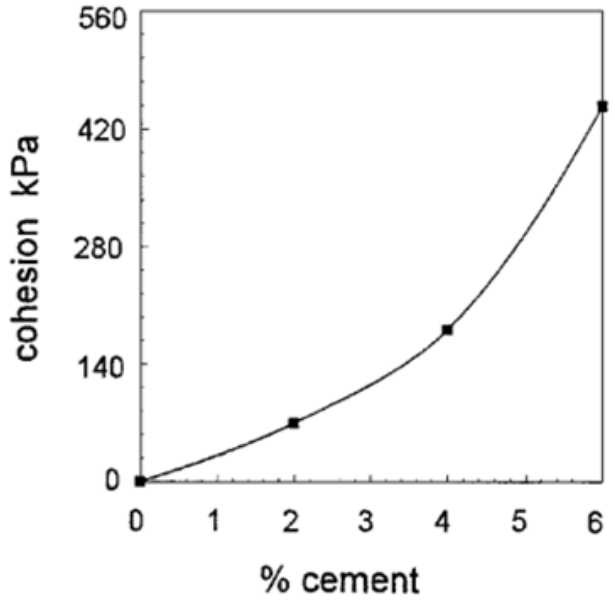

Figure 2.5 Effects of the cement contents on cohesion (Abdulla and Kiousis, 1997).

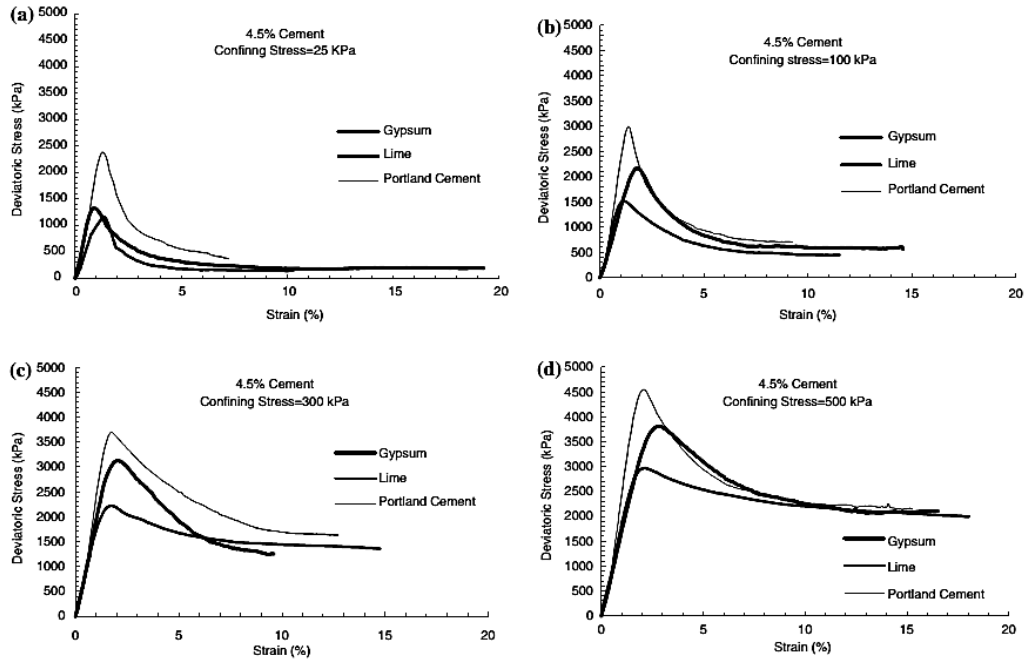

Figure 2.6 Stress-strain curves for cemented soils in drained condition (Haeri et al., 2006).

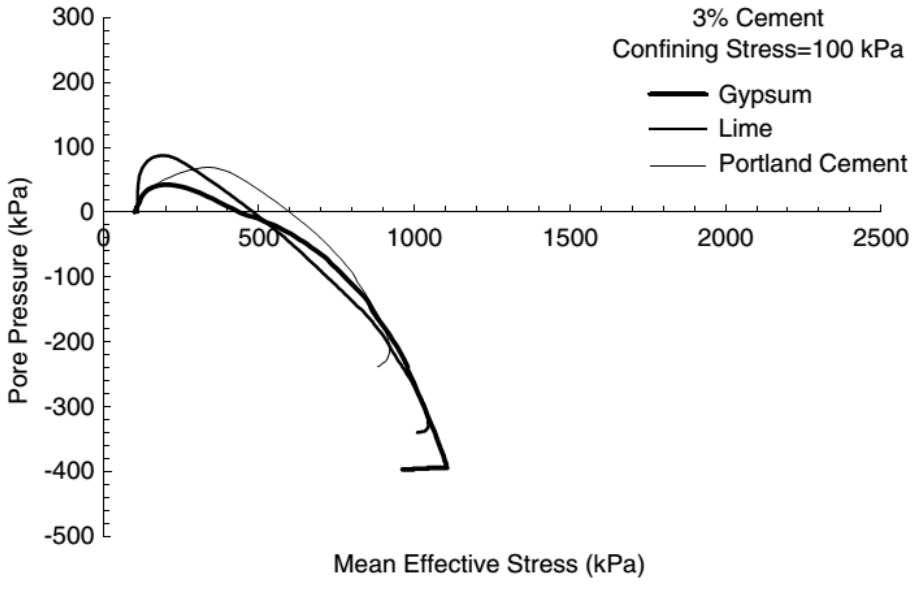

Figure 2.7 Relationship between pore pressure and mean effective stress for three types of cementing agents (Haeri et al., 2006).

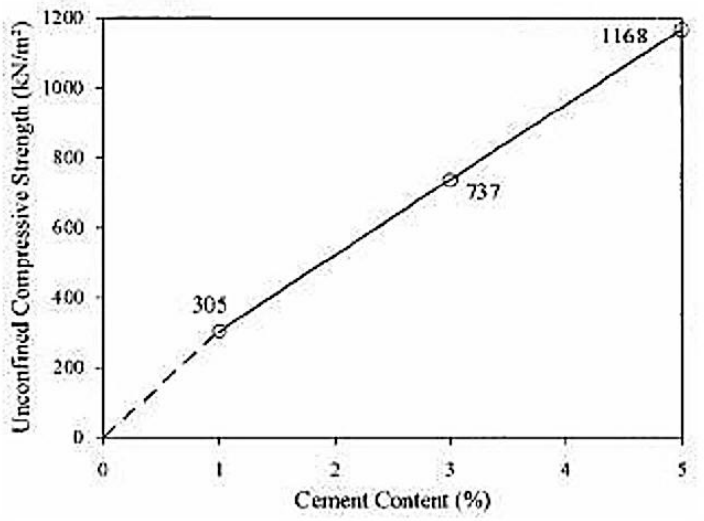

Figure 2.8 Variation of the unconfined compressive strength with the cement content (Schnaid et al., 2001).

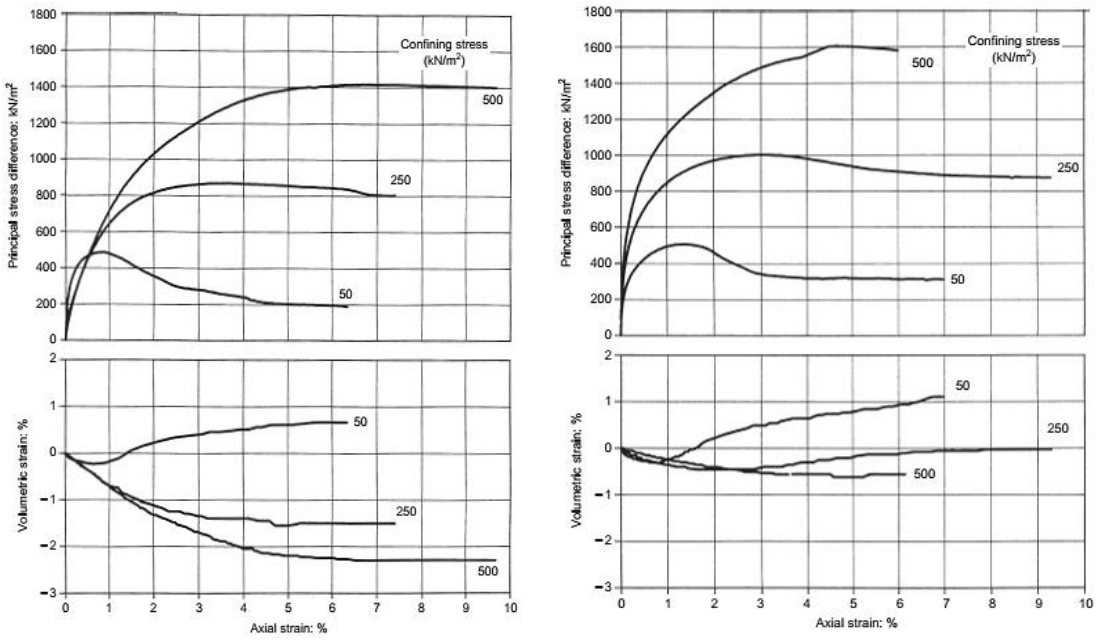

(a) (b)

Figure 2.9 Stress-strain behaviour of cemented soil (a) cured under zero pressure (b) cured under pressure (Consoli et al., 2000).

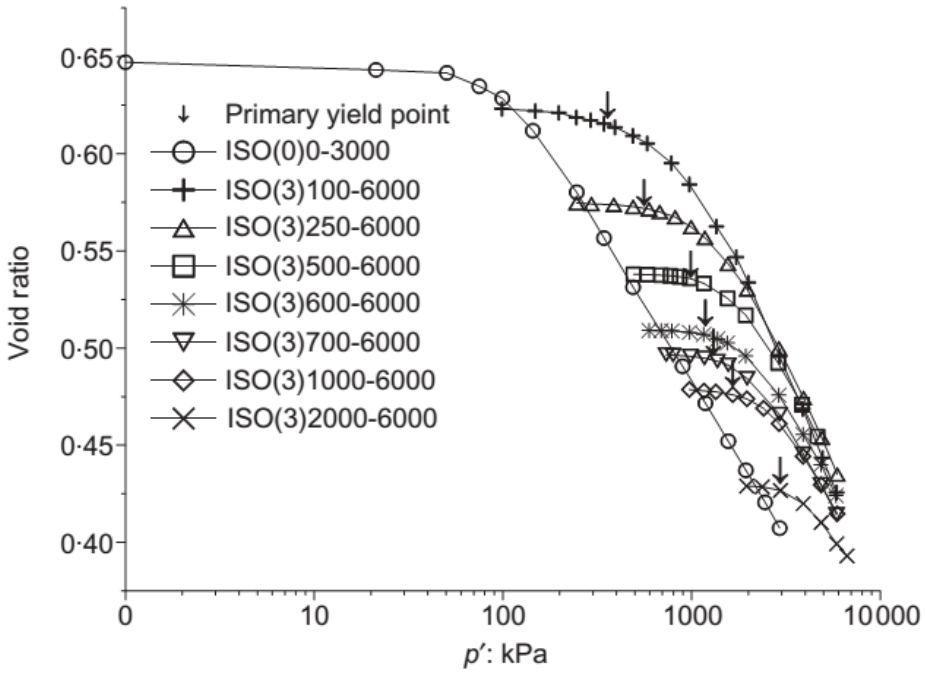

Figure 2.10 Isotropic compression response of the cemented specimens (Rotta et al., 2003).

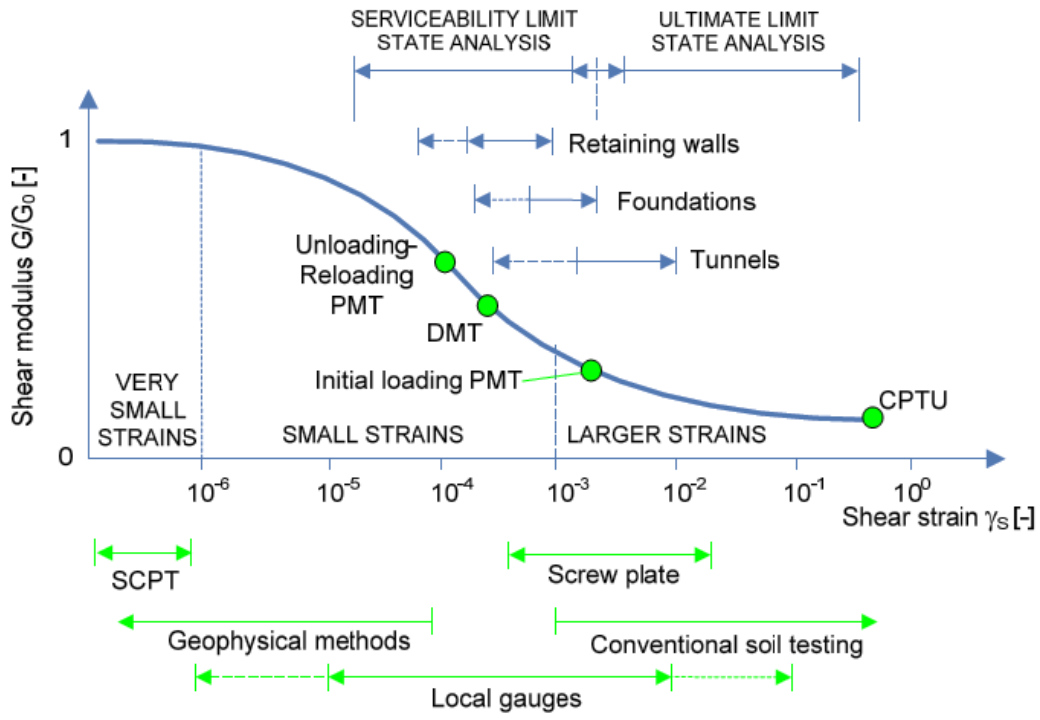

Figure 2.11 Typical representations of stiffness degradation with the shear strain amplitudes; related to the ranges of typical geotechnical applications and different tests (suggested by Atkinson and Sallfors, 1991, and Mair, 1993; and updated by Zimmermann et al., 2010).

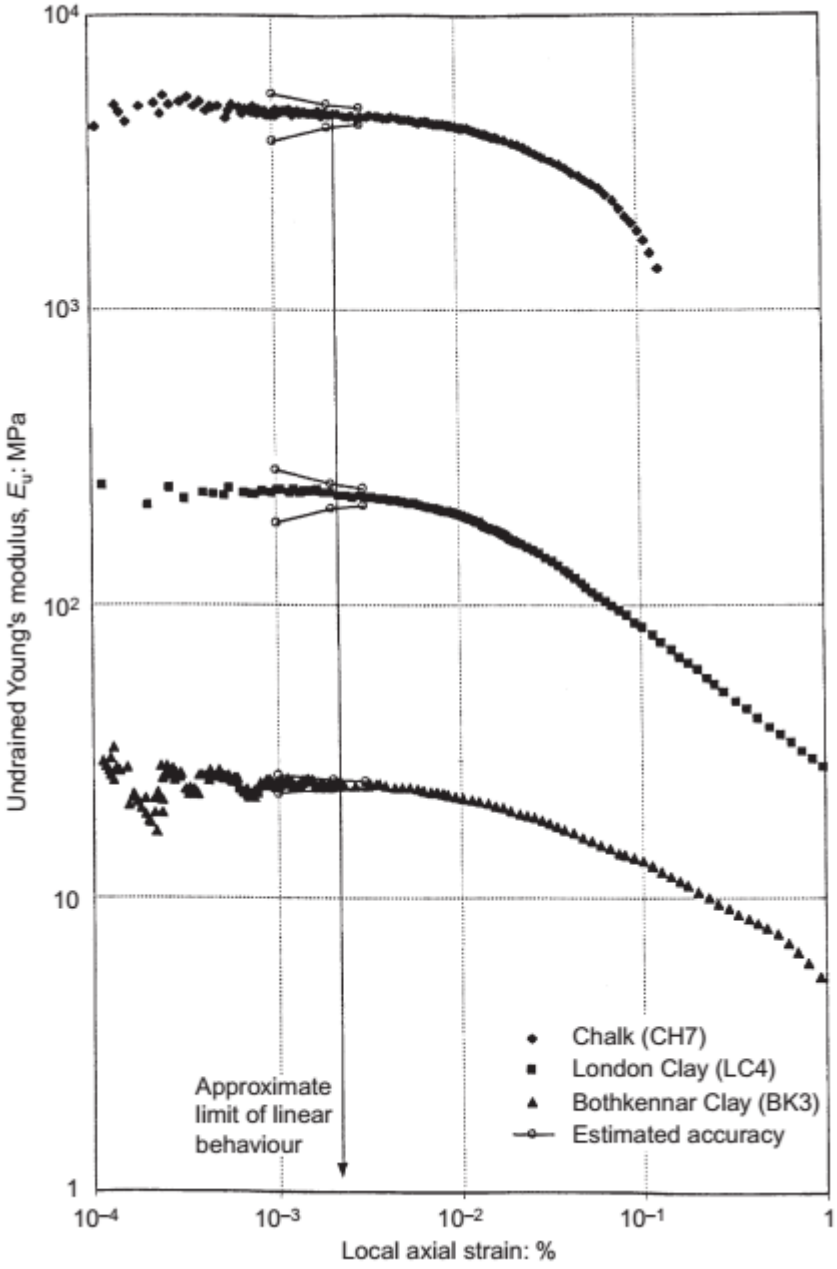

Figure 2.12 Comparison of the stiffness of three materials (Clayton and Heymann, 2001).

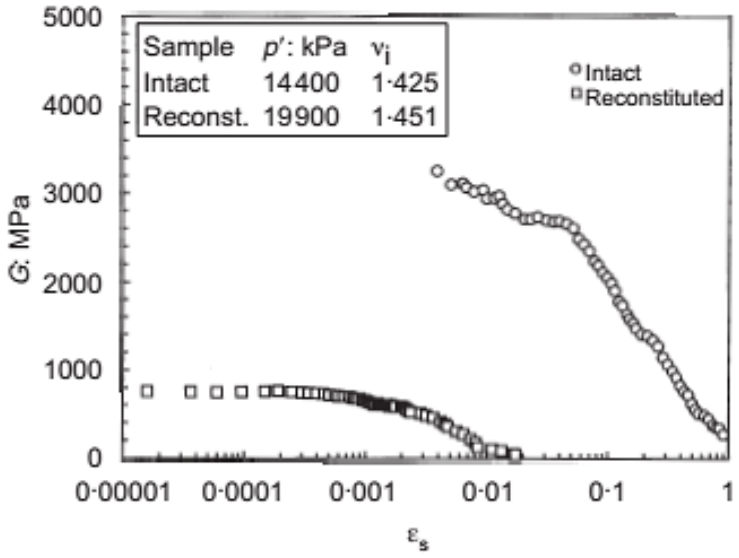

Figure 2.13 Comparison between the stiffness of the intact and reconstituted silca sandstone (Cuccovillo and Coop, 1997b).

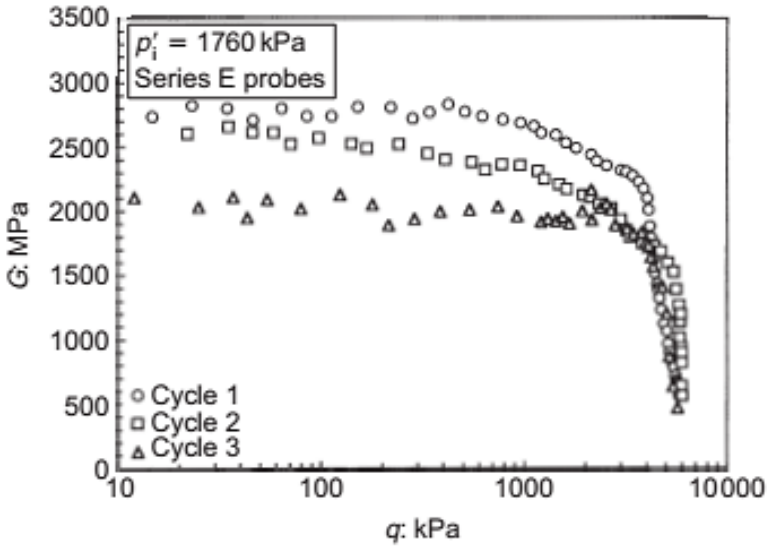

Figure 2.14 Variation of the stiffness with the undrained cycles of loading for the Silca sandstone (Cuccovillo and Coop, 1997b).

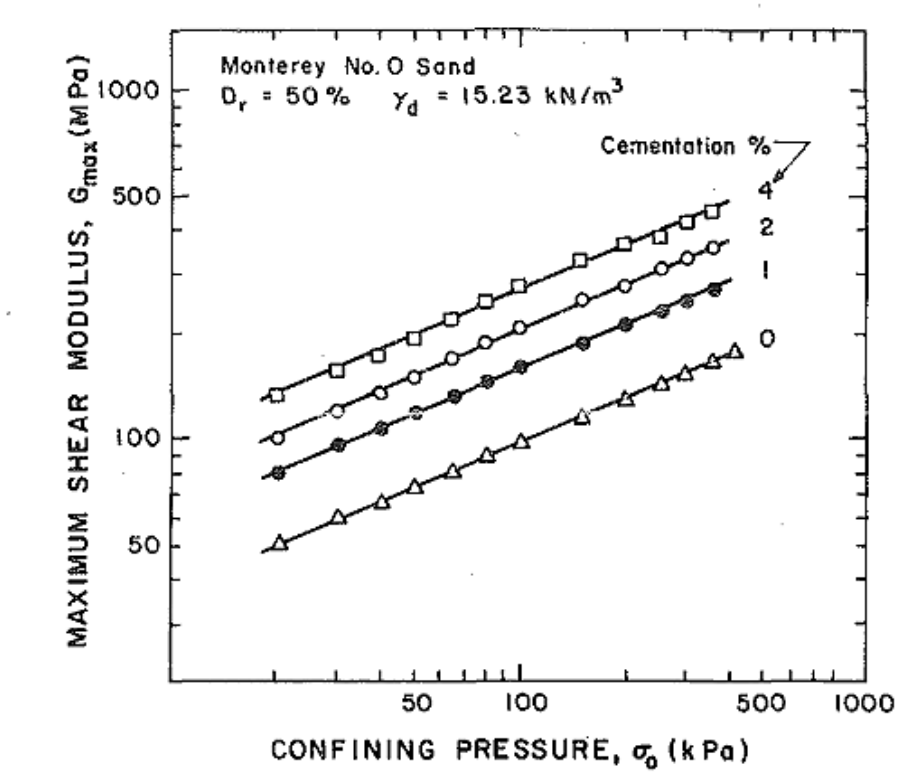

Figure 2.15 Effect of the cement amount on the stiffness of the cemented sand (Acar and El-Tahir, 1986).

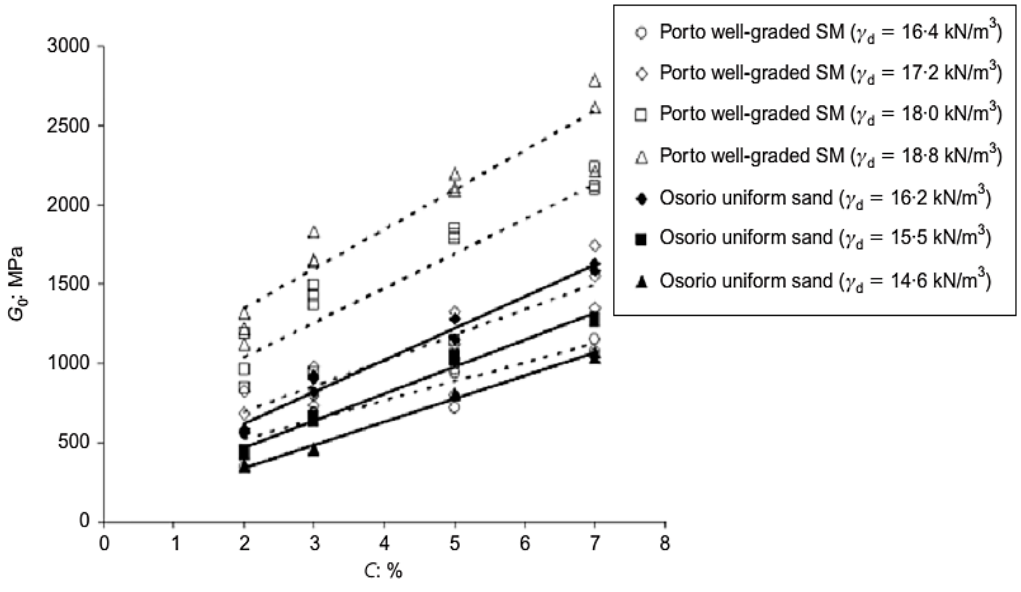

Figure 2.16 Variation of the stiffness with cement amount for well-graded Porto silty sand (Consoli et al., 2012).

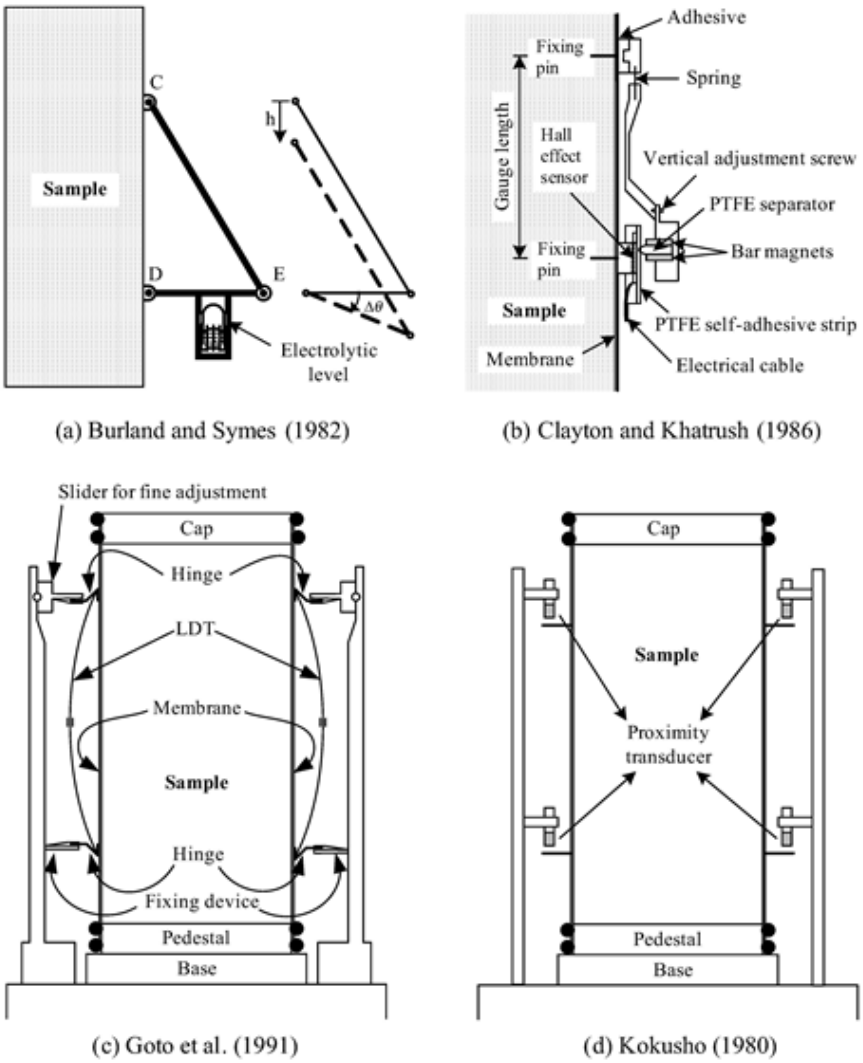

Figure 2.17 Types of internal axial strain measuring instruments (Kung, 2007).

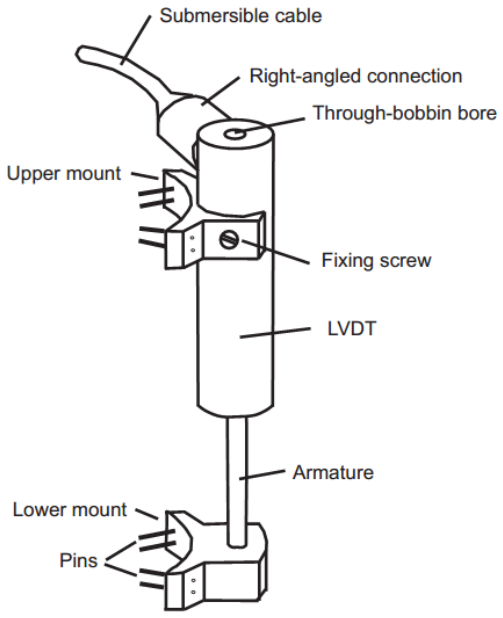

Figure 2.18 The LVDT mounts (Cuccovillo and Coop, 1997a).

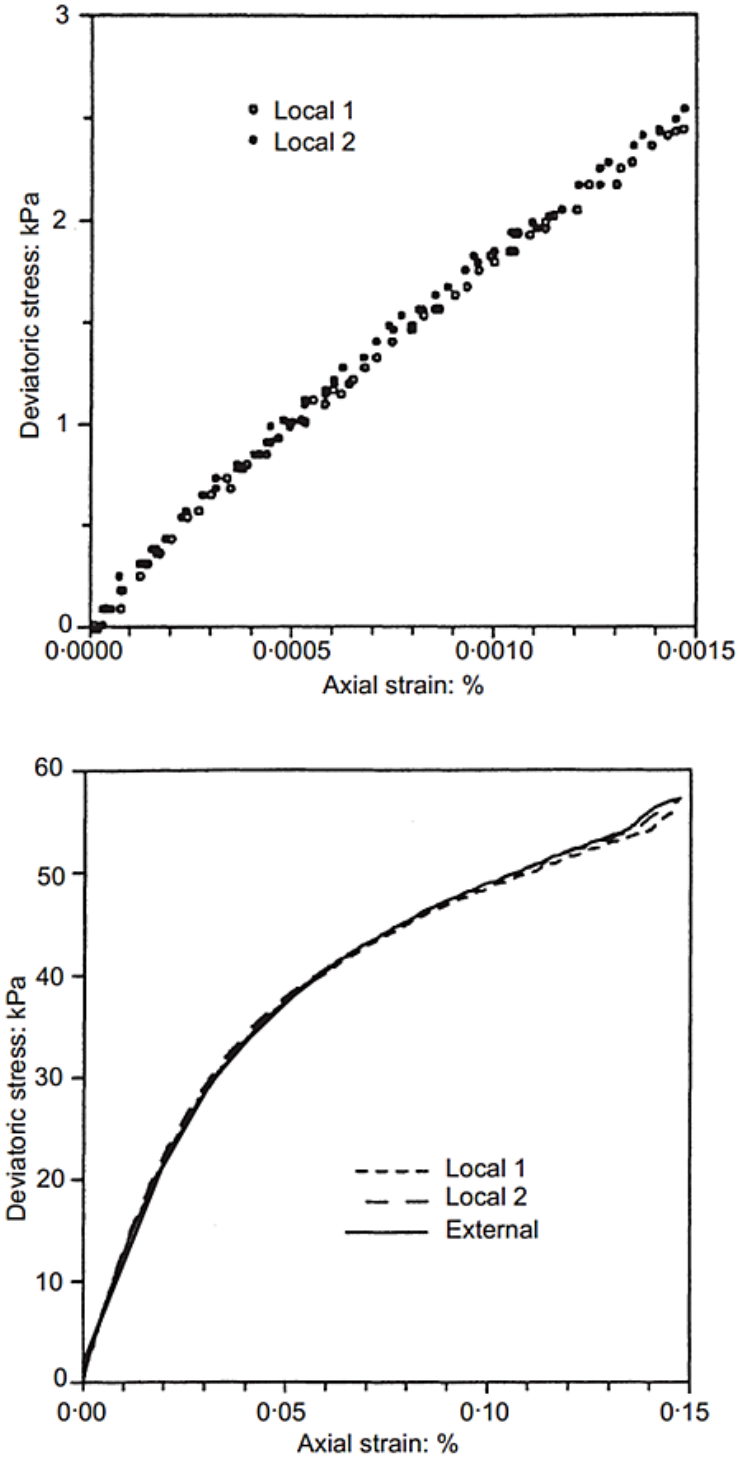

Figure 2.19 The performance of the LVDT in stress-strain analysis for undrained test (Cuccovillo and Coop, 1997a).

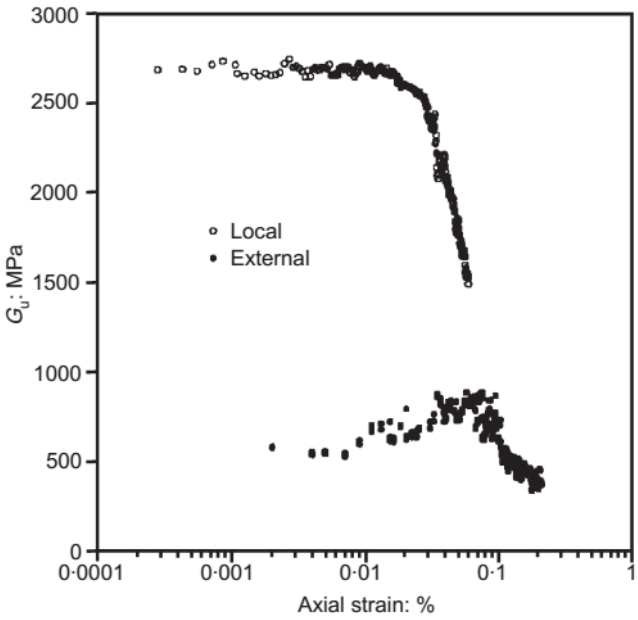

Figure 2.20 Variation of the stiffness between the local and external strain measurement (Cuccovillo and Coop, 1997a).

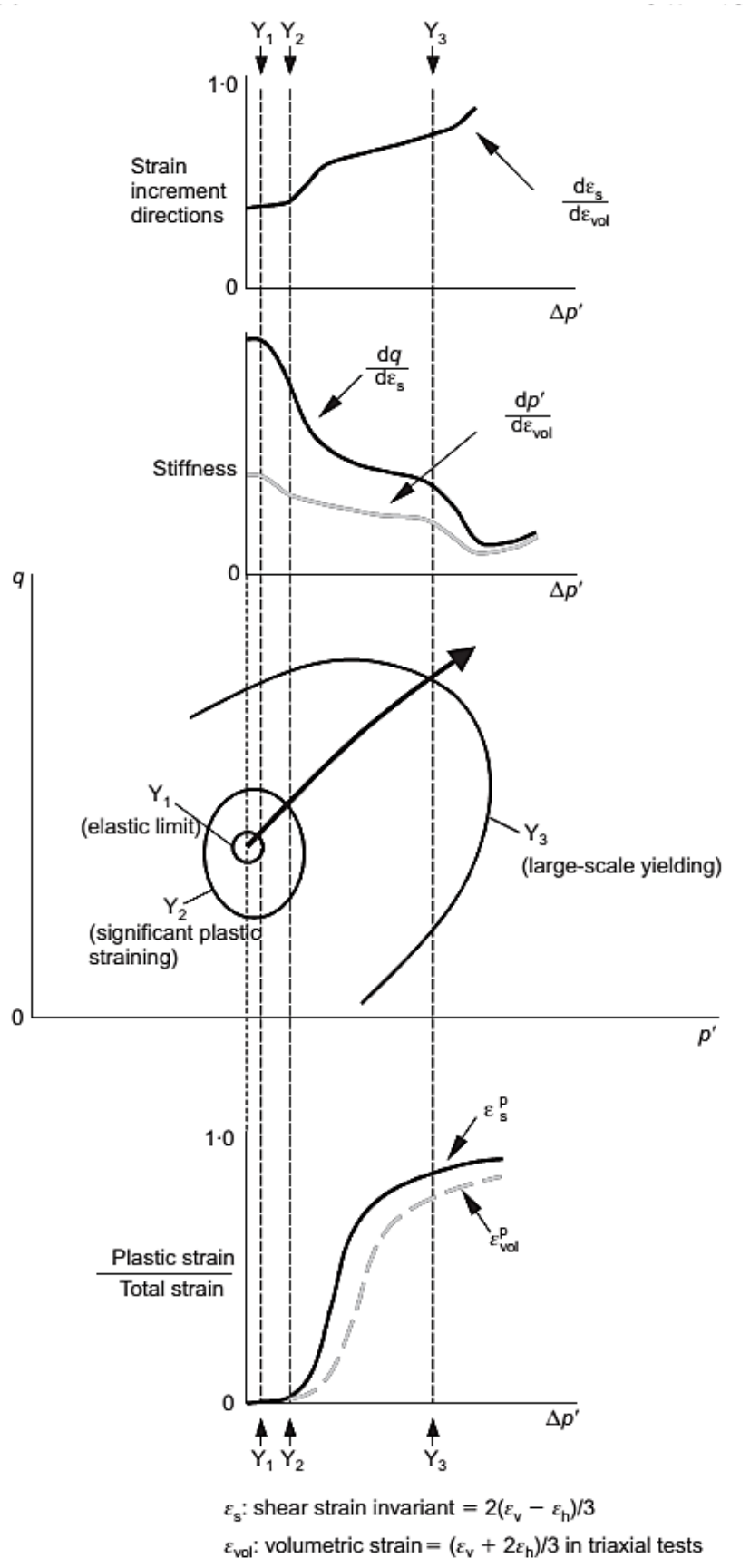

Figure 2.21 Scheme of multiple yield surfaces (Jardine, 1995)

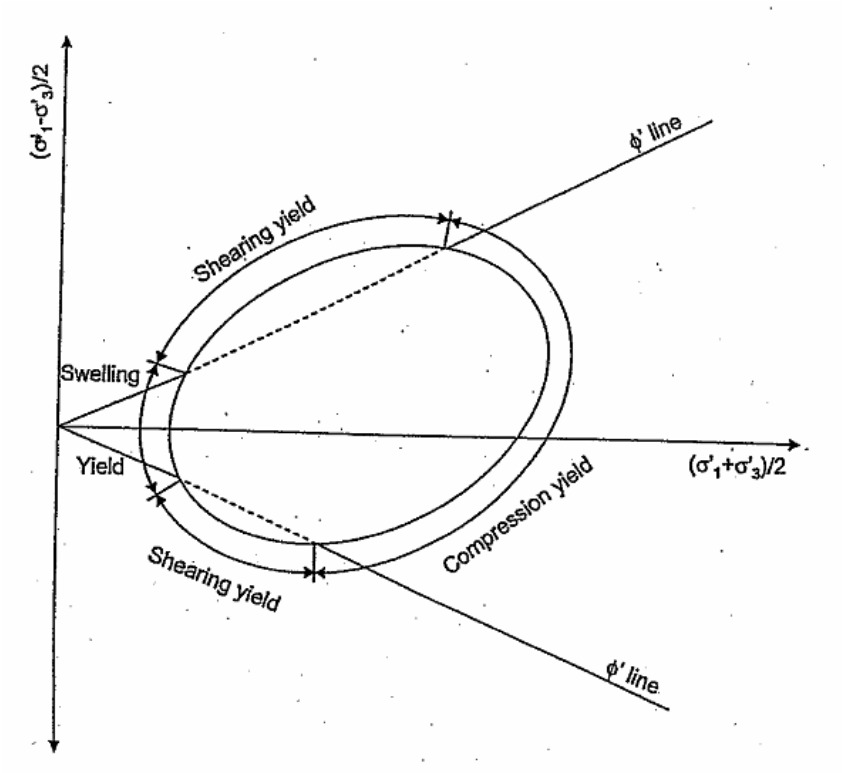

Figure 2.22 Types of the yielding as suggested by Leroueil and Vaughan (1990).

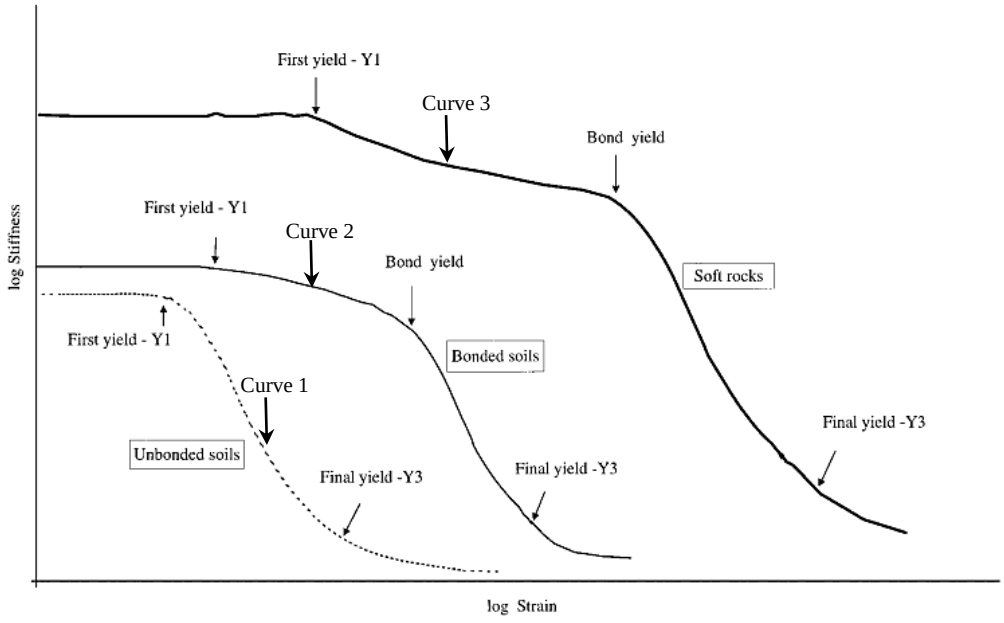

Figure 2.23 Yielding points for the bonded material (Toll and Malandraki, 2000).

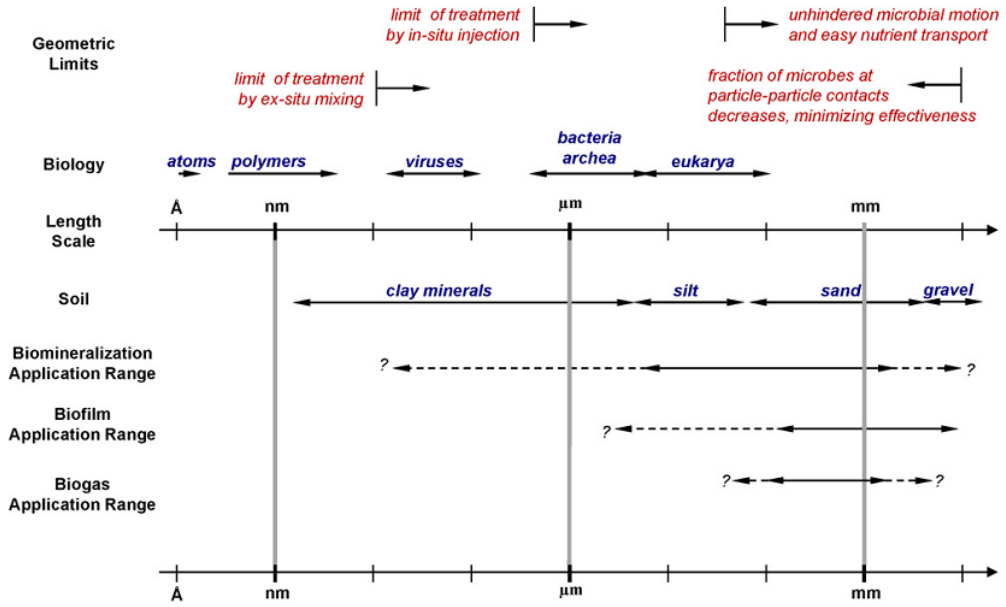

Figure 2.24 Comparison of soil grains and bacteria typical sizes, and approximate ranges of different treatment techniques (extended from Mitchell and Santamarina, 2005) (DeJong et al., 2010).

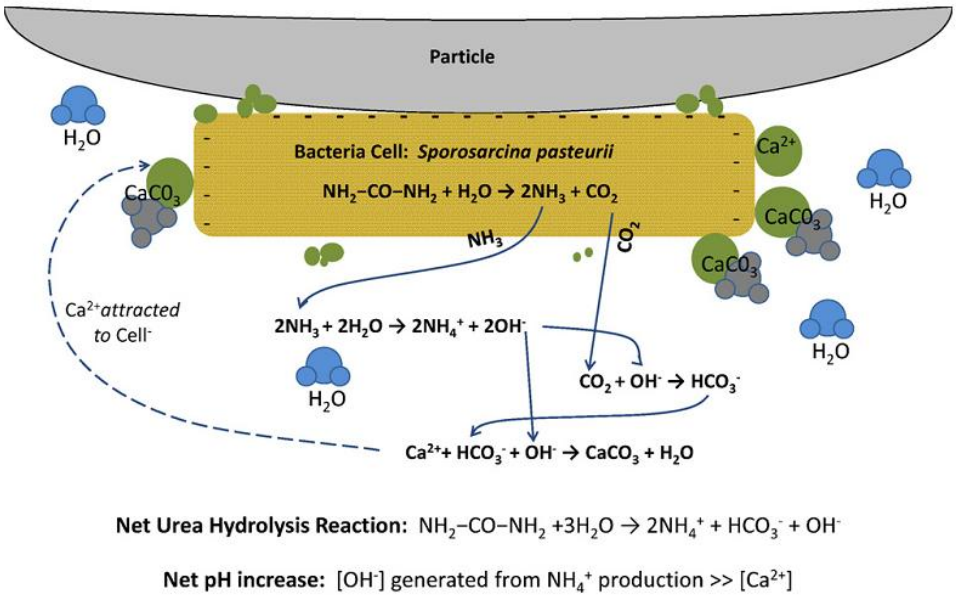

Figure 2.25 Schematic view for the biochemical reactions of calcite precipitation between sand grains (DeJong et al., 2010).

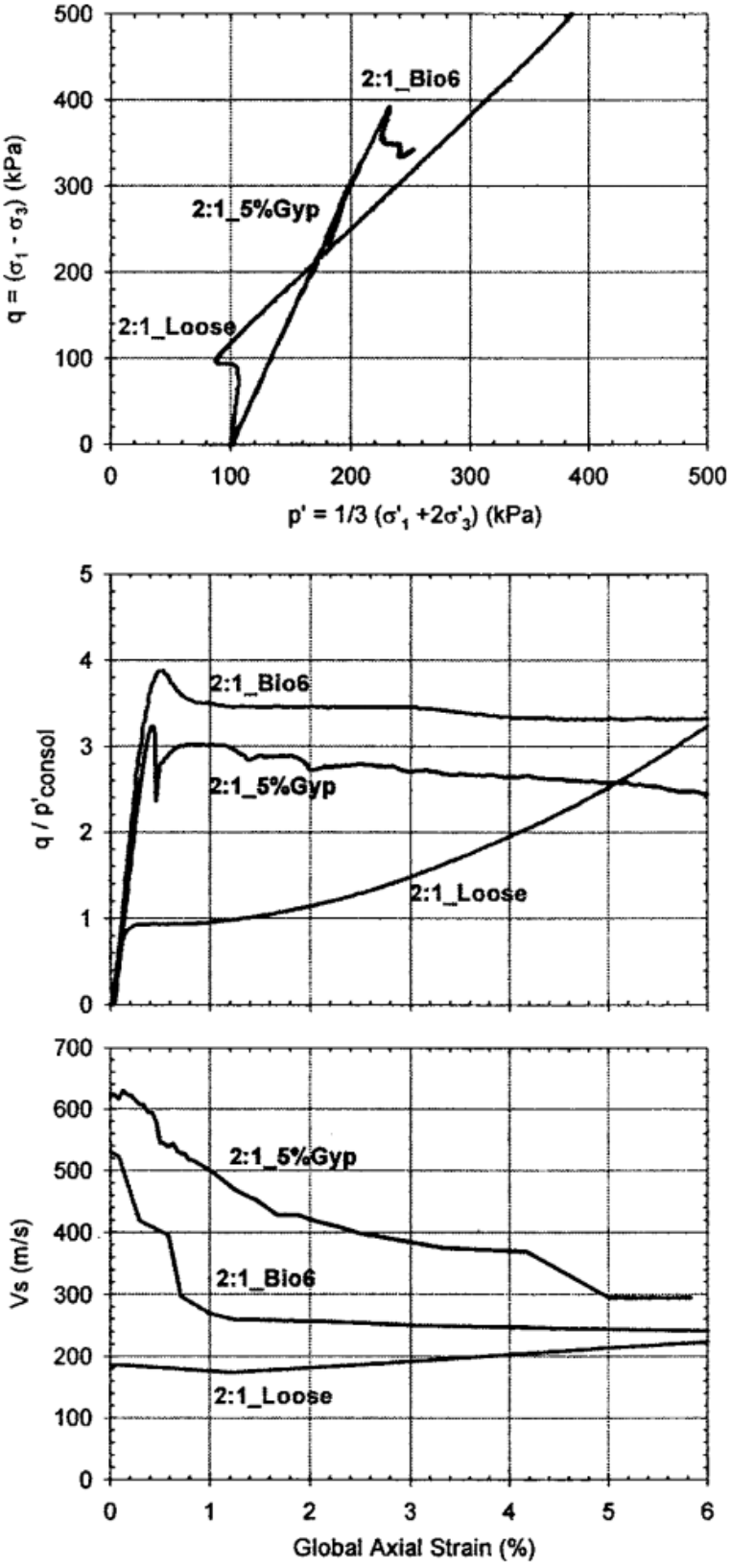

Figure 2.26 Undrained triaxial test results for biocemented specimens (DeJong et al., 2006).

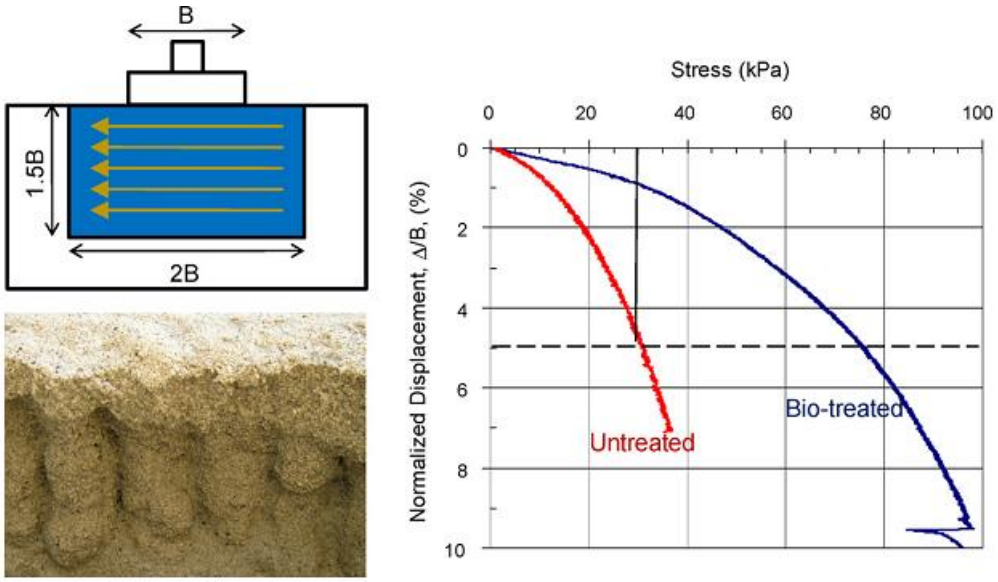

Figure 2.27 Field test results from biocemented soil improvement under a shallow foundation (Martinez and DeJong, 2009).

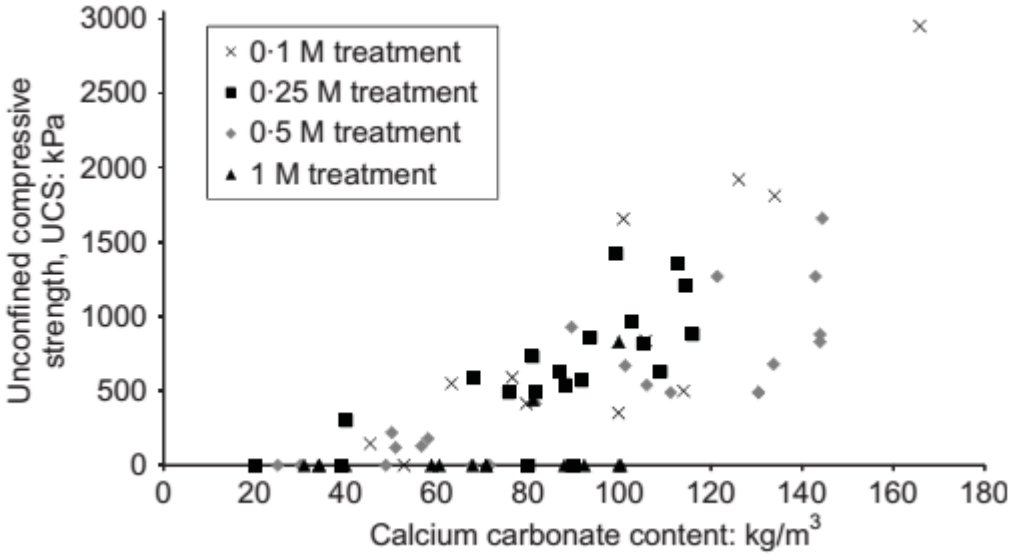

Figure 2.28 The results of unconfined compressive strength test for different chemical concentration of the treatment (Al-Qabany and Soga, 2013).

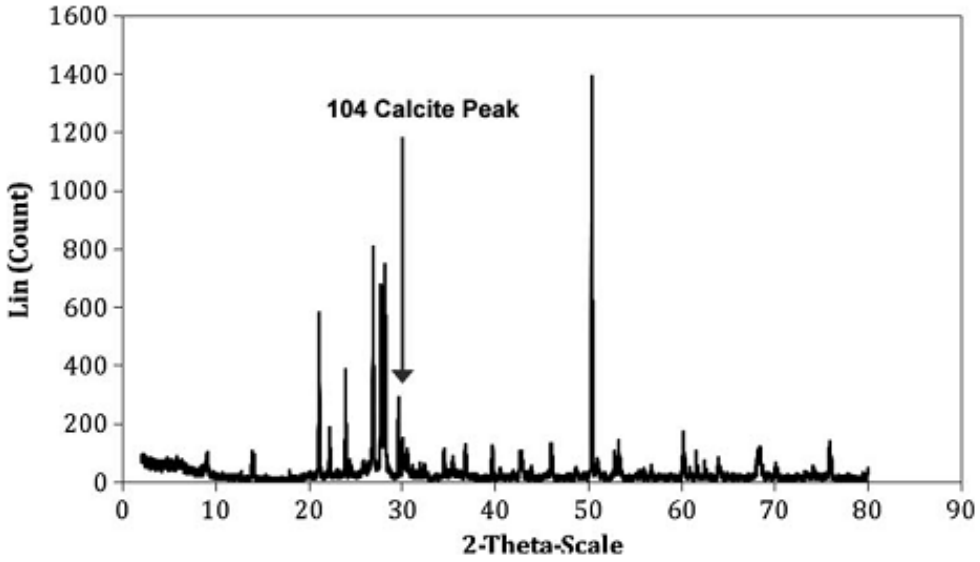

Figure 2.29 XRD scan of treated soil specimen (Burbank et al., 2011).

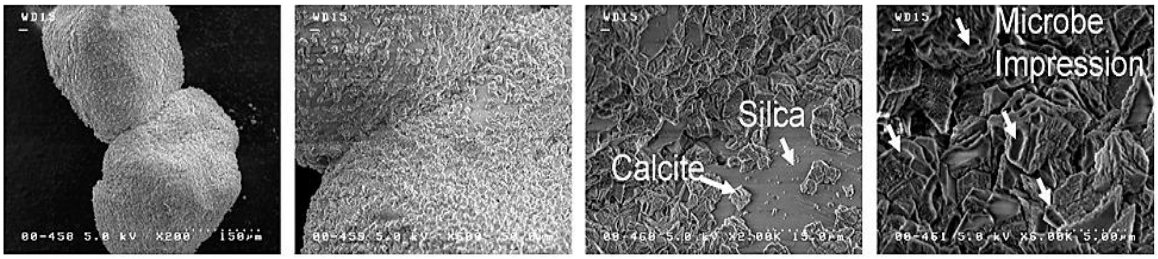

Figure 2.30 SEM images of calcite precipitated on the sand grains (DeJong et al., 2010).

Figure 2.31 Typical piece shapes of different processed waste tires (Edincliler et al., 2010).

CHAPTER 3

MATERIALS AND EXPERIMENTAL TECHNIQUES

This chapter presents the characteristics of the soil and cementing agents used in this study. This is followed by a description of the basic design and modification of the conventional triaxial apparatus that was provided with local strain measurements by internal LVDTs. Also, the instrumentations setup and their calibrations were illustrated. The chapter describes the procedures and details of sample preparation techniques of tests that were carried out to investigate the effects of various cementing agents and sample preparation techniques on stress-strain and stiffness of cemented sand. In addition, the sample preparation procedures for sand with waste tire and cement were also presented. In the following sections, the preparation of the biocementation bacteria medium solution, sample preparation, and method of introducing the bacteria solution to the soil specimen were reported. Scanning Electron Microscopy (SEM) analyses that performed to study the distribution of calcite over sand grains were described.

3.1 Material properties

Sand

The type of the soil used in all tests of this study was river sand taken from Narli, near Gaziantep city, Turkey. Two sizes from this sand were used. First size of the sand was fixed between the 0.3-1.0 mm, and prepared by sieving it through standard sieves. The sand was washed several times until it becomes clean, and then dried using 100 °C oven to use it in all tests. The grain size distribution of this sand was determined according to ASTM D422. The resulted grain size distribution curve is presented in Figure 3.1. From this figure, it can be clearly seen that D_{10}, D_{30} and D_{60} sizes are about 0.33, 0.40 and 0.54 mm, respectively. Thus, the coefficient of uniformity (C_u) and the coefficient of curvature (C_c) have been calculated as 1.63 and 0.9, respectively. The soil specimen based on these properties classified as poorly graded sand (SP) according to the Unified Soil Classification System (USCS). The

specific gravity of the sand grains, maximum and minimum dry densities were found to be 2.67, 1.71 g/cm^3, and 1.44 g/cm^3, respectively. The minimum and maximum dry densities were determined according to ASTM D4253 and ASTM D4254, respectively. Size and shape of the sand grains were evaluated using SEM as shown in Figure 3.2.a.

The second size of the sand falling between 0.6 mm and 1.18 mm were artificially selected and used in the preparation of the cemented sand/waste tire specimens. The gradation curve was presented in Figure 3.1. The D_{10}, D_{30} and D_{60} sizes are around 0.67, 0.78, and 0.92 mm, respectively. Thus, the coefficient of uniformity (C_u) and the coefficient of curvature (C_c) have been calculated as 1.37 and 0.99, respectively. The specific gravity of the grains equal to 2.67, the sand was classified as poorly graded sand (SP) according to the Unified Soil Classification System (USCS). The sand has maximum and minimum dry densities of 1.65 g/cm^3 and 1.41 g/cm^3, respectively.

Tire crumb

Commercially available tire crumb was used in the experimental study. It is a granular material obtained by processing of waste tires. The grain size distribution of the tire is presented in the Figure 3.1. As can be seen from the figure, the values of D_{10}, D_{30} and D_{60} were found to be around 1.2, 1.3, and 1.7 mm, respectively. Thus, the coefficient of uniformity (C_u) and the coefficient of curvature (C_c) have been calculated as 1.42 and 0.83, respectively. The waste tire grains have a specific gravity equal to 1.12. The size and shape of the tire crumb and sand grains were evaluated using SEM and presented in Figure 3.2.b.

Cementing agents

Gypsum

The type of gypsum used in the experimental study was a sulfate mineral composed of calcium sulfate dehydrate obtained from a company in Batman, Turkey. Size of the gypsum particles was less than 0.045 mm. Size and shape of the gypsum particles were evaluated using SEM and presented in Figure 3.2.c. The chemical compositions of the gypsum are illustrated in Table 3.1.

Lime

The type of lime used in this study was quick lime obtained from a company in Gaziantep, Turkey. Size of the lime particles was less than 0.063 mm. The lime was stored in the laboratory within a plastic bag, which is inside a sealed container to prevent the carbonation effect by the CO_2. Size and shape of the lime particles were evaluated using SEM and presented in the Figure 3.2.d. The chemical compositions of the lime are illustrated in Table 3.1.

Calcite

The type of calcite used in the experiments was a carbonate material obtained from a company in Ankara, Turkey. Size of the calcite particles was less than 0.045 mm. Size and shape of the calcite particles were evaluated using SEM and presented in the Figure 3.2.e. The chemical compositions of the calcite are illustrated in Table 3.1.

Cement

The type of cement used in the experimental study was calcium aluminate cement (ISIDAÇ 40: Turkish acronym) which is high-early-strength cement obtained from a Turkish cement and building materials company (ÇIMSA: Turkish acronym) in Mersin, Turkey. The cement has a compressive strength of a range of 22-40 MPa in 6 hours, specific gravity of 3.25, and a specific surface area of 3000 cm^2/gm. Size of the cement particles was less than 0.063 mm. Size and shape of the cement particles were evaluated using SEM and presented in Figure 3.2.f. The chemical compositions of the Portland cement are illustrated in Table 3.1.

3.2 Triaxial testing system

3.2.1 Triaxial testing machine

Triaxial tests for clean sand specimens and cemented sand specimens were performed using a conventional 70 mm diameter ELE triaxial machine with a 50-kN load capacity. The load can be applied with selected rate under strain control. The main machine of the system was placed on pneumatic mounts in order to reduce the effect of external vibration. The triaxial system is shown in the Figure 3.3, and schematic view is shown in Figure 3.4. As can be seen from the Figures, the triaxial

system set-up consists of load ring, an external displacement transducer (LDS), linear variable differential transformers (LVDTs), pore pressure transducers, pressure volume controllers, and data acquisition system.

A new triaxial cell was manufactured by local company. The cell that made by perspex material had an inside diameter and height of 280 mm and 470 mm, respectively. In addition, it had a base pedestal diameter of 70 mm. The cell had a working pressure capacity of 1700 kPa. The cell was designed and manufactured in a bigger size to give better clearness between the local instrumentation such as internal LVDTs and inside of the cell. The cell base was provided with three holes to insert three ports for connecting the local measurement instrumentation cables. The load ram passed into the cell through brass fitting which provided by o-ring. The cell was held by six external tie rods. The cell was provided by two vent holes in the cell top for allowing the air to be expelled from the cell during water filling (Figures 3.3, 3.4).

3.2.2 Instrumentation

The deviatoric stress was measured by 4.5 kN capacity load ring produced by ELE. The load ring was calibrated and connected to the data logger (Figure 3.3). The calibration result was uploaded to the data acquisition software; the calibration graph for the load cell was presented in Figure 3.5. The figure shows approximately 6.6 N maximum errors.

A linear displacement sensor (LDS) produced by ELE was used for external axial strain measurement. The LDS has a maximum capacity of 11 mm and sensitivity 0.5 μm. The LDS was calibrated and the calibration result data was uploaded to the data acquisition software. The calibration graph for the LDS was presented in Figure 3.6. This figure shows approximately 0.062 mm maximum error over the 11 mm calibration range. The external LDS was fixed on the frame of the machine by magnetic rod as shown in Figure 3.3.

Two volume-pressure controllers produced by GDS (Geotechnical Digital System Limited) have been used as part of triaxial system. Each pressure controller had a maximum pressure capacity of 2000 kPa and maximum water storage capacity of 200 cm^3. The volume-pressure controller had an accuracy of 1.0 kPa in the pressure

application and $1mm^3$ in the water volume measurements. The volume-pressure controller was used to apply and control the cell and back pressures, and to estimate the volume change during the drained tests. The two volume-pressure controllers were connected directly to the PC and measured data was trensfered to data acquisition software (Figure 3.3).

In order to measure back and cell pressures, and for determination of effective stress in the undrained tests, the pore water measurements were required. Two separate pressure transducers were used and connected to the back pressure and cell pressure lines (Figures 3.3, 3.4). The type of the pressure transducers was PDCR 810 produced by Druck Limited, each transducer had a 10 bar pressure capacity, ±1.5% total error band, and operating temperature range between -20°C and +80°C. The two transducers were calibrated using the volume-pressure controller. The calibration results were uploaded to the data acquisition software. The calibration results graphs of the two pressure transducers are presented in Figures 3.7, 3.8. These figures show a 0.8 kPa maximum error for pore water pressure transducer (PDCR S/N 2850055), and similarly around 0.9 kPa maximum errors for cell pressure transducer (PDCR S/N 2850056) over a calibration range of 600 kPa pressures.

The stability and resolution of the strain measurements were the main limitations of stiffness measurement at small strains. Therefore, for more accurate estimation of the soil stiffness at small strain, two submersible linear variable differential transformers (LVDTs) produced by GDS Instruments Limited have been used for local axial deformation measurements. The submersible linear variable differential transformers LVDTs were employed to measure the axial displacement in the middle third of the specimen. The LVDT had an accuracy of 0.1 % FRO, working range of ± 5 mm (Maximum transducer measuring range 10 mm), resolution of 0.2 μm, -20 to 60°C temperature range, and maximum operating pressure of 3500 kPa in water or oil. The two LVDTs were calibrated and the calibration results were uploaded to the data acquisition software, the calibration graphs are presented in Figures 3.9, 3.10. The maximum error as shown from the figures are equal to 0.021 mm for LVDT2 (SN 134078) and 0.018mm for the LVDT1 (SN 134079) over the 9 mm calibration range. The two transducers were set up diametrically opposite to each other on the specimen using the brackets (mounts) and special type of glue (super glue 502). The LVDTs

were used over a 66 mm gauge height (center to center distance) between the two brackets. The LVDT body was held in position by the top bracket and fixed with screw on the bracket, the armature of the LVDT was rested on the pad slammed to the bottom bracket. The set-up of the LVDT and the brackets were designed to ensure correct alignment and positioning the brackets. Therefore, the two brackets were clamped to an alignment tool at a desired position and this was only removed once the bracket had been glued to the specimen as shown in Figure 3.11.

3.2.3 Data logger and data acquisition system

The 8 channels and 16 bit data logger was used in the triaxial system for logging the data output from the instrumentations. In addition, output of the two LVDTs was logged by another two channel data logger which is connected to the main data logger, the two channel data logger work in parallel with the main data logger (Figure 3.3). The windows based software GDSLAB v2.0.8 package produced by GDS Instruments Limited was used to control and data acquisition during the tests.

3.3 Sample preparation technique

The procedure adopted in preparation of the triaxial test specimens for the clean sand and cemented sand was air-pluviation. This approach simulates natural deposition methods more accurate than other commonly used sample preparation methods such as compaction, moist tamping, or vibration (Polito, 1999). The research mainly focuses on the mechanical effects of various sample preparation, curing techniques and cementing agents on the behaviour of sand. To study the mechanical properties of specimens tested, it is crucial to maintain consistency between the specimens prepared for the tests. Therefore, great care was given to provide reasonable repeatability during the preparing of the specimens to be tested. Details of the preparation techniques for the samples are as follows:

I) <u>Descriptions of triaxial sample preparation of clean sand without local strain measurement:</u>

   In the initial phase of this research, a series of preliminary tests at consolidated undrained and consolidated drained conditions were conducted without local strain measurements. These series of tests aimed to study the behaviour of clean

sand. Also, to study the effect of the effective confining pressure, consolidation period, and the relative density on the stress-strain response of clean sand.

A. The specimens consolidated for 18 hours (loose state):

1- A filter paper was placed on the pedestal, the membrane was attached to the pedestal, and then two O-rings were pushed into place over the membrane using an O-ring stretcher.
2- A two-part split mold was placed around the pedestal to retain the shape of the specimen during construction and to support the specimen until a vacuum is applied. The split mold was used as a forming jacket for the specimens. Top of the membrane was folded back over the mold to fit the membrane and mold. A vacuum was applied between inside wall of the split mold and the membrane to attach the membrane tightly to the split mold inner surface.
3- Desired amount of the sand was weighed which gives the required relative density of the loose sand (relative density of about 35%). The sand was poured via a funnel inside the mold; the sand was placed in a loose state without any segregation by pouring it from a shallow drop-height that can be raised steadily at a constant rate.
4- When the mold was completely filled, top of the specimen was flattened using a spatula to provide a uniform top and without any loss of sand particles. Applying additional vibration to the mold may be required to place the desired amount of sand.
5- The specimen top was then covered by placing a filter paper on top of the sand. Top-cap was placed on the filter paper without disturbing the specimen. Top part of the membrane was pulled off the split mold, stretched around the top-cap and was secured by two O-rings without disturbing the specimen.
6- Saturation of soil specimen was made by flushing the water to the specimen through back pressure channel, the water was flushed from the bottom to the top in a slow rate.
7- Approximately 10 kPa of vacuum was applied to the specimen. The vacuum was maintained by specifying a target pressure of -10 kPa to the GDS volume-pressure controller that connected to the pedestal.

8- After the pore pressure was fixed at the -10 kPa pressure value, the two part split-mold was carefully removed to prevent disturbance of the specimen.
9- The diameter and height of specimens were then measured at three different locations using a digital caliper and ruler. Average of the measurements was taken, and was used with the weight of the specimen to calculate the volume, dry density, void ratio, and relative density of the test specimen.
10- The triaxial cell was assembled and filled with water.
11- Back pressure inside the specimen was increased with gradually increasing the confining water pressure by small values until the desired pressures value were achieved (400 kPa back pressure and 500 kPa cell pressure). The specimen was kept under the specified pressures overnight (about 18 hours) for consolidation.
12- Check the B-value by closing the drainage valve, increasing the cell pressure of 10 kPa, measuring the associated change in specimen pore water pressure caused by the change in confining pressure. After checking the B-value, the cell pressure was decreased by 10 kPa, then the drainage valve was re-opened.

B. The specimens consolidated for 3 hours (loose state):

The same steps from 1 to 12 of the sample preparation as illustrated in section I-A have been followed. Except, the specimen was kept under consolidation pressure for about 3 hours to study the effect of the consolidation period on the stress-strain and stiffness behaviour of the clean sand.

C. The specimens prepared in medium and dense state:

1- The steps from 1 to 3 as in the procedures that illustrated in sections I-A, I-B for preparation of triaxial specimen in loose state have been followed.

2- Desired amount of sand corresponds to the medium or dense state of the specimen was weighed, which gives relative density of 63% and 85%, respectively.

3- Desired amount of the sand poured via funnel inside the mold in three layers. Each layer was subjected to densification by vibration or compaction with a

150 g steel rod dropping at a height of 30.0 cm. The vibration or compaction energy increases as the required relative density increase to occupy the desired amount of sand.

4- Steps from 4 to 12 of the procedure for preparation of triaxial specimen in loose state as illustrated in section I-A have been repeated.

II) Descriptions of triaxial sample preparation of the sand, tire crumb and cement mixture without local strain measurement:

A series of consolidated undrained (CU) tests were performed to investigate the effect of the tire crumb contents on triaxial behaviour of the sand, and to study the triaxial behaviour of sand with tire crumb and cement. Amounts of the tire crumbs used in the experimental study were 0%, 3%, 7%, and 15% by dry weight of the mixture. 0%, 1%, 3%, and 5% of cement by dry weight of the mixtures were added to specimens of the sand with tire crumbs at 15% mix ratio. 3% of cement by dry weight of the mixtures was also added to the sand with tire crumbs specimens at all percentages. The specimens of the sand, tire crumbs and cement were prepared as the following steps:

1- The steps from 1 to 3 as in the procedure that illustrated in sections I-A for preparation of triaxial specimen in loose state have been followed.
2- The required amount of sand (0.6-1.18 mm), tire crumbs, and cement was weighed, mixed in the dry state according to the mixture percentages, and was poured via a funnel into the mold. The relative density values here in this investigation were aimed to be kept at a constant range (loose to medium). Dry densities of the specimens tested were calculated as 14.45 kN/m^3 for clean sand, 14.10 kN/m^3 for sand with 3% tire crumb, 13.21 kN/m^3 for sand with 7% tire crumb, and 11.99 kN/m^3 for 15% tire crumb.
3- Steps from 4 to 12 of the procedure for preparation of triaxial specimen in loose state as illustrated in section I-A were then repeated.
4- The specimen formation in the way described here could result in the cement hydration during the saturation phase, and cementation under a consolidation pressure.

III) Description of sample preparation of the clean sand with local strain measurement using LVDTs:

A. The specimens prepared in saturated state:

1- The same steps from 1 to 6 of the procedure as in the section I-A for preparation of triaxial specimen in loose state have been followed (Figure 3.12.a, b).
2- Approximately 20 kPa of vacuum was applied to the specimen. The vacuum was maintained by specifying a target pressure of -20 kPa to the GDS volume-pressure controller that connected to the pedestal.
3- The two part split-mold was carefully removed after the pore pressure fixed at the -20 kPa pressure value (Figure 3.12.c).
4- Each specimen dimensions (diameter and height) were then measured at three different locations using a digital caliper and a ruler.
5- The LVDT brackets (mounts) were attached to the membrane surface with super glue, two LVDTs were fixed to the specimens sides in the same diametrically position in the middle third of the specimen. To ensure correct alignment and position of the brackets, both brackets were clamped to the alignment tool (aluminum fixing struts) to the desired position and this was only removed once the brackets had been glued to the specimen membrane (Figures 3.11, 3.12.d). The LVDTs were then inserted in the place with screw on the side of the brackets, then the armature was rested on the pad clamped to the bottom bracket. The gauge length of the LVDTs was adjusted to ensure the maximum linear range, and this was done by adjusting the screw (Figure 3.12.e). The aluminum fixing struts used for the two brackets alignment were removed (Figure 3.12.f). (If necessary) Elastic bands were placed around the brackets and cables for additional support. Note, this step needs to be carried out as quickly as possible, and as carefully as possible.
6- The triaxial cell was placed around the specimen; the load ram was carefully placed on the top-cap. The triaxial tie rods were attached to hold the cell together under pressure, then the cell was filled with water.
7- Back pressure inside the specimen was increased with increasing confining water pressure at small increments until the desired pressure values were

achieved (400 kPa back pressure and 500 kPa cell pressure). The specimen was kept under the specified pressures overnight (18 hours) for consolidation, and to ensure any air trapped in the specimen would dissolve into the pore fluid.

13- B-value was checked by closing the drainage valve, increasing the cell pressure by 10 kPa, and measuring the associated change in specimen pore water pressure caused by the change in confining pressure. After checking the B-value, the cell pressure was decreased by 10 kPa, then the drainage valve was re-opened.

8- Next day, after completing consolidation of the specimen, the test was commenced. Figure 3.12 illustrates the steps of the sample preparation techniques.

B. The specimens prepared in dry state:

1- The steps from 1 to 6 of the procedures as in the section I-A for preparation of triaxial specimen in loose state have been followed. The specimen is not flushed or filled with water for saturated and it prepared in dry state.

2- Approximately 20 kPa vacuum was applied to the specimen. The vacuum was maintained by specifying a target pressure of -20 kPa to the GDS volume-pressure controller that connected to the pedestal.

3- After the vacuum pressure fixed at the -20 kPa pressure value, the two-part split mold was carefully removed to prevent disturbance of the specimen.

4- The specimen diameter and height were then measured at three different locations using a digital caliper and ruler. Average of the measurements was taken, and was used with the weight of the specimen to calculate the volume, dry density, void ratio, and relative density of the test specimen.

5- The procedures illustrated in steps 5 and 6, section III-A have been followed.

6- Back pressure inside the specimen was increased with increasing the confining water pressure at small increments until the desired pressure values were achieved (100 kPa back pressure and 0 kPa cell pressure). The specimen was kept under the specified pressures for 1hour and then tested.

C. The specimens prepared in partially saturated state

1- The steps from 1 to 6 of the procedures as illustrated in section I-A for preparation of triaxial specimen in loose state have been followed.
2- Saturation of the soil specimen was made by flushing the water to the specimen through the back pressure channel. Water was flushed from bottom to top of the specimen in a slow rate, then the water was emptied from the specimen after a period of 1hour from water flushing.
3- The procedures followed in steps 2 to 6 for the preparation of the triaxial specimen as illustrated in section III-A have been repeated.
4- Back pressure inside the specimen was increased with gradually increasing the confining water pressure by small values until the desired value was achieved (100 kPa confining pressure and 0 kPa back pressure). The specimen was kept for 4 days under 100 kPa effective confining pressure and then tested. The specimen prepared according to this method was taken as a benchmark for biocemented sand specimens.

IV) <u>Descriptions of sample preparation steps of the cemented sand with local strain measurement using LVDTs</u>:

The triaxial test specimens of the cemented sand for all cementing agents were prepared in five different methods to represent the cases of the cementation that occur in the nature. The cemented sand specimens were prepared in various cementing agents type and content, saturation status and curing under confining pressure. The cemented sample preparation technique steps were illustrated below:

A. First method of the sample preparation for cemented sand (M1):

1- The filter paper was placed on the pedestal, the membrane was then attached to the pedestal, two O-rings were pushed into place using an O-ring stretcher.
2- A two-part split mold was placed around the pedestal to retain the shape of the specimen during construction and to support the specimen until a required vacuum applied. Top of the membrane was folded back over the mold to fit the membrane and mold. A vacuum was applied between the inside wall of

the split mold and the membrane to attach the membrane tightly to the split mold sides.

3- The required amount of sand and 4% of cementing agent mixture was weighed. The weight of the mixture was determined to give relative density correspond to loose state of sand (relative density of 35%). The materials were mixed in the dry state and poured via a funnel into the mold. The mixture was placed without any segregation by pouring it from a shallow drop-height that can be raised steadily at a constant rate.
4- When the mold was completely filled, top of the specimen was flattened using a spatula to provide a uniform top. Applying additional vibration to the mold may be required to place the desired amount of the mixture.
5- The second filter paper was placed on top of the specimen; the top-cap was placed on the filter paper without disturbing the specimen. Top portion of the membrane was pulled off the split mold, stretched around the top-cap and was secured by two O-rings without disturbing the specimen.
6- Saturation of soil specimen was made by flushing the water to the specimen through back pressure channel, the water was flushed from the bottom to top of the specimen at a slow rate.
7- The same steps 2 to 9 of the procedures as illustrated in section III-A for triaxial sample preparation of loose sand have been followed. The specimens were kept under pressure for consolidation and curing for overnight for about 15 hours. The specimen formation in the way described here could result in the cement hydration during the saturation phase, and cementation under confining pressure.

B. Second method of the sample preparation for cemented sand (M2):

A very similar procedure to the method described in IV-A was followed. The differences between the two methods were the amount of cementing agent, and the curing time. In this method (M2), amount of cementing agent was 12% (by weight) instead of 4%, and the curing time was four days instead of 15 hours. Therefore, the difference between this method and the previous method is that cementing agent content and curing period was increased.

C. Third method of the sample preparation for cemented sand (M3):

1- The same steps 1 to 5 of the procedures as illustrated in section IV-A for preparation of the triaxial specimen have been repeated.
2- Saturation of soil specimen was made by flushing the water to the specimen through the back pressure channel, the water was flushed from the bottom to top of the specimen at a slow rate.
3- Water was flushed from bottom to top of the specimen, then the specimen was kept for one hour after it was completely filled with water for purpose of saturation of the specimen and hydration of the cementing agent. After completing the saturation and hydration steps both valves at bottom and top of the specimen were kept open to drain out the water from the specimen.
4- The specimen was kept under this condition for curing for four days, in this case the curing of the hydrated cementing agents occur in the unsaturated conditions.
5- At the end of four days, the specimen was refilled with water, the top cap valve was then closed.
6- The procedures followed in steps 2 to 9 for the preparation of the triaxial specimen as illustrated in the section III-A have been repeated.

D. Fourth method of the sample preparation for cemented sand (M4):

1- The triaxial specimens in this method were prepared using plastic split mold, the plastic split mold has 70 mm diameter and 147 mm height.
2- Initially, the required amount of the sand and 12% of cementing agent mixture was weighed, and mixed in a dry state. Then, a 15% of water by the dry weight of the mixture was added to the mixture of sand and cementing agent, and mixed until obtaining a homogenous paste. The weight of the mixture was determined to give the same dry density of the specimens prepared by the other methods.
3- The sand-cementing agent-water mixture was placed in the plastic split mold in three layers. The mixture was placed inside the mold in homogenous low dry density by compacting it with a 150 g steel rod dropping at a height of 30 cm. The rod has a 1.0 cm diameter and 30 cm

height. Each layer of the specimen was compacted by 25 drops. When the mold was completely filled, a great care was taken to flatten the top of the specimen using a spatula to provide a uniform surface.

4- The compacted specimen was kept in a closed plastic bag for a period of 2-day for curing purpose. After stripping the plastic bag and disassemble the split mold, the specimen was kept open to the air in a constant temperature room (25^{o}C) during the next two days for more curing.

5- Once the curing period completed the specimen was placed on the pedestal of the triaxial testing machine. After that, the membrane was attached to the specimen, and the filter paper and top cap were placed on the specimen, the specimen was saturated with water. Then, 20 kPa vacuum was applied.

7- The procedures followed in steps 2 to 9 for the preparation of the triaxial specimen as illustrated in section III-A have been repeated.

E. Fifth method of the sample preparation for cemented sand (M5):

The specimen preparation technique followed here in this method was very similar to the last method IV-D. The only difference between the two methods was the saturation case.

1- The procedures followed in steps 1 to 4 for the preparation of the triaxial specimen as illustrated in section IV-D have been repeated.

2- Once the curing period was completed, the specimen was placed above the pedestal of triaxial cell. After that, the membrane was attached to the specimen, the filter paper and top cap were placed on the specimen, and then the specimen was subjected to 20 kPa vacuum pressures without saturation with water.

3- The specimen dimensions (diameter and height) were then measured at three different locations using digital caliper and ruler.

4- The LVDTs were fixed to the specimen according to the procedure described in step 5 in section III-A.

5- The triaxial cell was placed around the specimen; the load ram was carefully placed on the top cap. The triaxial tie rods were attached to hold the cell together under pressure and the cell filled with water.

6- The back pressure inside the specimen was increased with gradually increasing the confining water pressure by small increments until the desired value was reached at 100 kPa confining pressure with a back pressure of 0 kPa. The specimens were kept under these pressures for a 1 hour before shearing.

3.4 Test procedure of shearing steps:

3.4.1 Test procedure for specimens without local strain measurement

Isotropically consolidated undrained and drained triaxial compression tests were conducted on clean sand specimens prepared according to the procedures outlined in the preceding section to determine the shear behaviour of the sand. Tests in this study were applied to fully saturated specimens sheared in consolidated-undrained and consolidated-drained triaxial compression. Following the consolidation step, the drainage valve to the specimen were closed for undrained tests, and kept open during the drained tests. The load ram has been brought into just above the specimen, then zero of the external LDS and proving ring were set. Compressive load was applied using strain controlled load frame. The rate of loading of 0.1 mm/min for undrained tests and 0.05 mm/min for drained tests were used. During the test, the data was governed by 10 second-logging rates. For each logging the measurements of deviatoric load, external axial deformation, base pore pressure and volume change were recorded.

The test procedure for the cemented tire sand mixtures performed as follows; after completing the consolidation and curing period for the cemented specimens for overnight (18 hours) the test started. The drainage valve to the specimen was closed. The load ram has been brought into just above the specimen and zero of the external LDS and proving ring were set. A standard machine rate of displacement, equivalent to 0.15 mm/min was used throughout the testing. During shear, measurements of deviatoric load, external axial deformation, and base pore pressure were made at approximately 10 sec intervals. Triaxial specimens were sheared until an axial strain of 15% had been reached.

3.4.2 Test procedure for specimens with local strain measurement

The test procedure for clean sand and cemented sand with the conventional cementing agents conducted with local strain measurements were performed as follows; after completing the sample preparation, consolidation and curing period for the cemented specimens the test started. The drainage valve to the specimen (back pressure channel) was closed. The load ram has been brought into just above the specimen. The zero reading was set for the reading of the external LDS, internal LVDTs and proving ring. A standard machine rate of displacement, equivalent to 0.025 mm/min was used throughout the testing. During shear, deviatoric load, local strain measurement by internal LVDTs, external axial deformation, and base pore pressure were recorded at 2 seconds intervals. The specimen was sheared until an axial strain of 5% had been reached. The examples of typical test results obtained in the experimental study are shown in Figures 3.13-3.17. Figure 3.13 presents the local axial displacement estimated from the LVDT1 and LVDT2 and the average values of the estimated axial displacement. Variation of the deviatoric stress versus the average local axial strain at very small strain levels is presented in Figure 3.14. Variations of the deviatoric stress and pore water pressure versus the average local axial strain of the clean sand specimens overall strain range are shown in Figure 3.15. The stress path space of the clean sand in the term of q and p' is presented in Figure 3.16. The typical degradation curve of the clean sand stiffness with the axial strain is shown in Figure 3.17. It is clearly observed from these figures that the data obtained from the LVDTs are very steady and without any oscillation.

3.5 Biocemented samples preparation

3.5.1 Preparation of the biocementation bacteria medium solution

1- Bacteria and growth conditions

Freeze-dried *Bacillus pasteurii* ATCC was obtained from the American Type Culture Collection, Manassas, VA. This culture was activated using Tris-yeast extract broth (Tris-YEB) by incubation at 30^{o}C for 24 hours under aerobic condition. The activated broth culture was inoculated onto a Tris-yeast extract agar (Tris-YEA) slant and Tris-YEA slant was incubated at 30^{o}C for 48 hours under aerobic condition. Tris-YEA slant culture was stored in the refrigerator to use in experimental research.

Tris-YEB contained the following ingredients per one liter of distilled water: Tris-HCl, 130 mM (pH 9.0); $(NH_4)_2SO_4$, 10 g and yeast extract, 20 g. Tris-YEA was prepared by adding 15 g of agar into Tris-YEB to prepare solid medium. The medium was autoclaved.

Bacillus pasteurii from Tris-YEA slant culture was inoculated into 10 ml of Tris-YEB and incubated at 30 ^{o}C for 24 hours. After incubation, *Bacillus pasteurii* Tris-YEB culture was inoculated to two 250 mL flask containing 125 mL of thoroughly mixed Tris-YEB. The flasks were placed into a bench type water bath shaker (ST-402 NÜVE, Sanayi Malzemeleri İmalat ve Ticaret A. S., İstanbul, Turkey) and wrist shaken at 30°C for 24 hours. After completing the incubation process, 250 mL bacterium culture from two flasks was transferred to a series of 50 mL sterile centrifuge tubes. Tubes were centrifuged at 1000 rpm for 15 minutes to separate the bacterial cells from the supernatant. The supernatant was removed by pouring it into a separate flask, and the remaining bacterial pellet was re-suspended in the urea medium, then re-suspended cell was used for the biocementation process that was applied to each soil specimen.

2- Bacterial treatment solution preparation process

The bacterial treatment solution was prepared according to following procedure: the urea medium was used as a main component. The following ingredients were mixed to prepare the urea medium: nutrient broth (3 g), urea (20 g), NH_4Cl (10 g), $NaHCO_3$ (2.12 g) and 1 L distilled water. The solid ingredients were mixed thoroughly with distilled water until they dissolved and the pH of the resulting urea medium solution was adjusted to 6.0 with 5 N HCl before autoclaving. After autoclaving, the pH of the urea medium was measured to be 7.0. The resulting urea medium was divided into two separate 400 mL batches. The pH of one of the 400 mL urea medium solution batches was then adjusted by stirring the solution to aerate it, the process continued until the pH was increased from an initial value of approximately 7.0 to approximately 8.0, as measured by a pH meter. The remaining 400 mL solution batches were stored for other specimens. This 400 mL of aerated solution was divided into two portions, one 80 mL and one 320 mL. The 80 mL portion of the aerated urea medium was added to the tube containing the spun *Bacillus pasteurii* cells and the tube were gently agitated to re-suspend the cells. A 12 mL volume of

calcium chloride solution (18.5 g $CaCl_2$/100 mL distilled water) was then added to the aerated urea 320 mL, which lowered slightly the pH of the treatment solution. The re-suspended bacterial solution (now a little more than 80 mL) was then added to the urea-calcium chloride solution (now 332 mL). The combined solution consisting of urea, calcium chloride and *Bacillus pasteurii* cells (about $1x10^7$ cells/mL, as initial content) were then quickly pumped from the base of the triaxial specimen over a period of approximately 20 minutes. The procedure for the preparation of biocementation treatment solution by the bacterial activity was similar to the methods illustrated by DeJong et al., (2006) and Ozdogan (2010).

3.5.2 Triaxial test sample preparation of the biocemented specimens

The specimens of the biocemented sand were prepared in a similar way to the sample preparation method of clean sand in the dry state as illustrated in section III-B:

1- The procedures followed in steps 1 to 6 for the preparation of the triaxial specimen as illustrated in section I-A have been repeated. The specimen is not flushed or filled with water for saturated and it prepared in dry state. The sand used in the biocementation tests was first subjected to heat sterilization by 180 °C for 24 hours. Two plastic wire mesh No. 100 was used at bottom and top of the specimen instead of filter papers to provide a better drainage of bacterial treatment solution.
2- Approximately 20 kPa of vacuum was applied to the specimen. The vacuum was maintained by specifying a target pressure of -20 kPa to the GDS pressure controller that connected to the pedestal. After the vacuum pressure fixed at the -20 kPa pressure value. The two-part split mold was carefully removed to prevent disturbance of the specimen.
3- The specimen diameter and height were then measured at three different locations using a digital caliper and ruler.
4- The LVDTs were fixed according to the methods illustrated in step 5 as illustrated in section III-A.
5- The triaxial cell was placed around the specimen; the load ram was carefully placed on the top-cap. The triaxial tie rods were attached to hold the cell together under pressure and the cell filled with water.

6- The back pressure inside the specimen was increased with gradually increasing the confining water pressure by small values until the desired value was achieved (145kPa cell pressure and 10 kPa back pressure). The cell pressure was increased to 145 kPa because the biocementation solution pumping pressure may rises to 45 kPa during the circulation of the treatment solution, and to keep the difference between the cell and back pressure not less than 100 kPa, then the biocementation process was initiated.

7- At the beginning, the bacteria solution which was prepared as the procedures that described in the bacteria solution preparation section was pumped inside the specimen. The bacteria solution was pumped using the GDS pressure-volume controller, the cell with membrane, and the 500 mL flask with magnetic stirrer. Mixing of treatment solution was continued during pumping step to avoid precipitation of solution contents. The biocementation treatment system set-up sketch was illustrated in Figure 3.18. The treatment solution consisting of *Bacillus pasteurii* cells, urea, and calcium chloride was then quickly pumped inside the specimen over a period of approximately 20 minutes, and pumping rate was approximately 20 mL/min.

8- This initial "biological treatment" was then allowed to set overnight for about 15 hours, during this period the *Bacillus pasteurii* cells were attached to the surface of sand grains.

9- After 15 hours and when the microbes bonded to the soil grains subsequent treatment cycles were passed through the specimen. A 400 ml nutrient treatment solution consisting of aerated urea and $CaCl_2$ (25.2 mM) were pumped through the specimen at a flow rate of 5 ml/min, for a period of 80 minutes. Every subsequent treatment solution was identical and consisted of a urea growth medium solution and $CaCl_2$.

10- This nutrient treatment process was then periodically repeated twice per day over the period of 3, 6, and 9 days, which correspond the BT1, BT2, and BT3, respectively. The biocementation specimens BT1, BT2, and BT3 represent the lightly, moderately and heavily cemented sands, respectively. The preparation of the biocemented specimens, treatment process and the curing of the biocemented specimens conducted in a constant temperature room 28°C.

11- At the end of the biocementation processes the specimen was emptied from the treatment solution. The biocemented specimen was kept under 100 kPa confining pressure for a period of 4 days for more curing and setting the cementing material.

12- The specimens were tested in undrained condition under pressures equal to "100 kPa cell pressure and 0 kPa back pressure". Figures 3.18 and 3.19 illustrate the schematic view of the biocementation treatment setup. The overview of the triaxial testing system of the biocemented specimens was presented in Figure 3.20.

3.5.3 Test procedure for the biocemented triaxial specimens

Triaxial testing procedures for biocemented sand specimens with local strain measurements were performed as follows; after completing the sample preparation, biocementation process and curing period for the cemented specimens, the test was started. The drainage valve to the specimen (back pressure channel) was closed. The load ram has been brought into just above the specimen. The reading of the external LDS, internal LVDTs and proving ring were set to zero. The specimens were loaded under strain control with the rate of displacement equal to 0.025 mm/min. During shear, measurements of deviator load, local strain measurement by internal LVDTs, external axial deformation, and base pore pressure were made at 2 seconds intervals. The specimen was sheared until an axial strain of 5% had been reached.

3.6 Scanning Electron Microscopy and EDX analyses

The microscopic study and microstructure examination of the untreated and cemented sand grains were carried out using a scanning electron microscope that produced by JEOL limited (joel 6390 LV, operating at 15 kV accelerating voltage). For further study the mineral composition of the untreated and cemented sand, energy dispersive X-ray (EDX) analyses were conducted. The specimens for SEM and EDX analyses were obtained from the middle part of the tested specimen. The SEM specimens were placed onto the stub and coated with a thin layer of gold prior to testing with SEM.

Table 3.1 The chemical compositions of the cementing agents.

Compositions (%)	Gypsum ($CaSO_4.2H_2O$)	Lime (CaO)	Calcite ($CaCO_3$)	Portland cement
SiO_2	1.063	0.242	0.126	20.600
Al_2O_3	2.538	0.192	0.099	4.344
Fe_2O_3	0.162	0.068	0.028	0.2524
TiO_2	0.014	0.0015	0.0015	0.1282
CaO	31.20	88.02	55.56	64.270
MgO	5.961	1.145	1.058	2.388
Na_2O	0.369	0.241	0.238	0.3131
K_2O	0.03	0.043	0.028	0.333
Cr_2O_3	0.002	0.0007	0.0007	0.0007
SO_3	39.13	0.298	0.040	3.230
P_2O_5	0.0012	0.0012	0.0012	0.039
MnO	0.011	0.011	0.0001	0.014

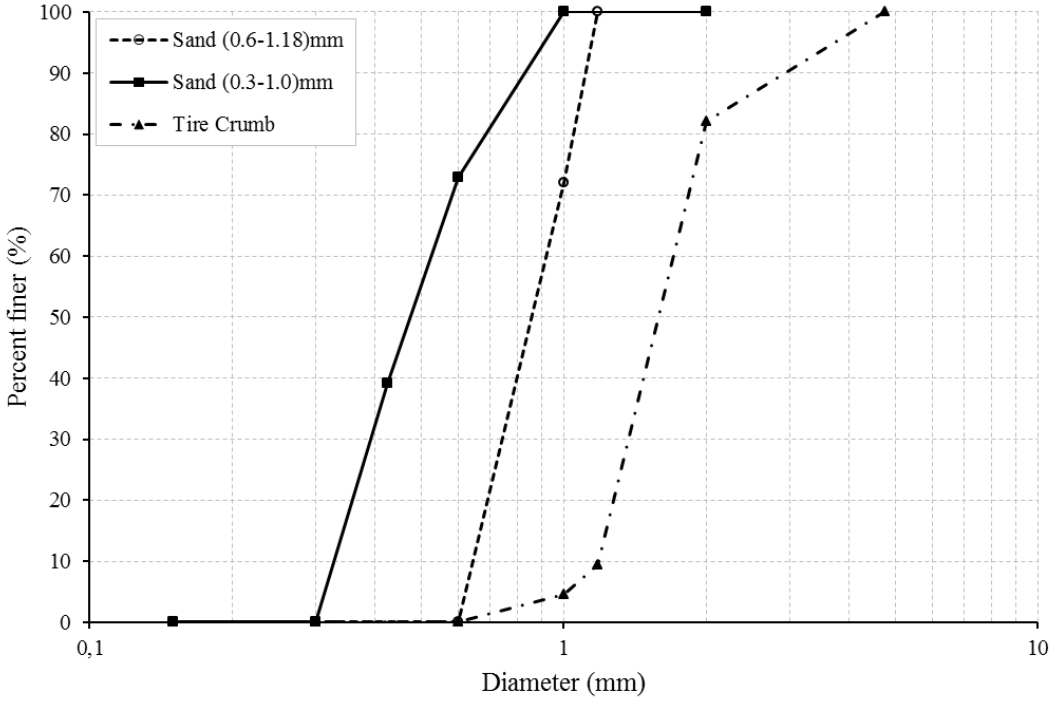

Figure 3.1 Grain size distribution curves of the materials used in this study.

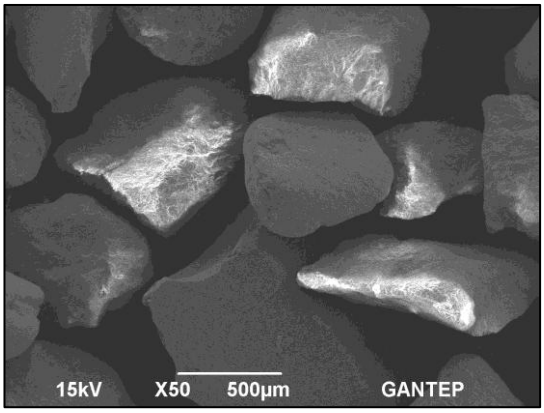

(a) Sand

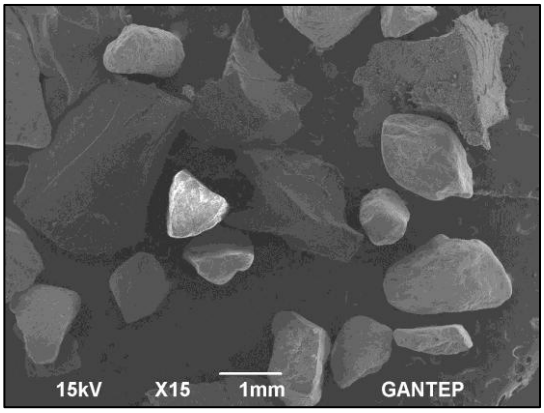

(b) Sand with tire crumb

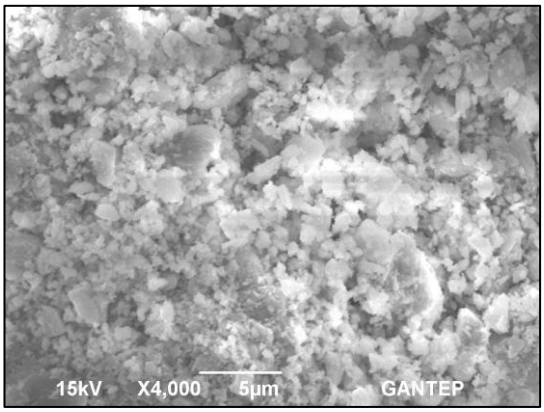

(c) Gypsum

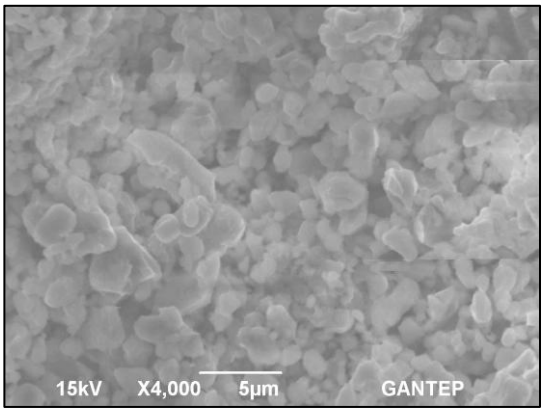

(d) Lime

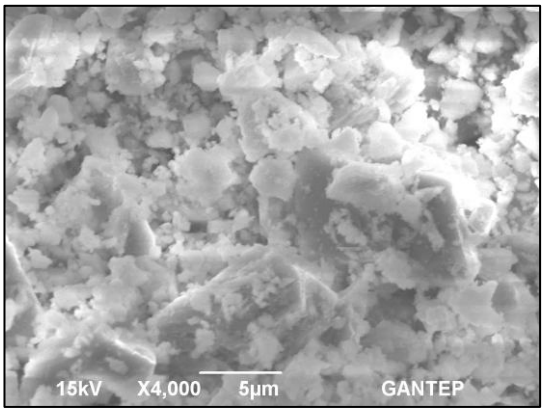

(e) Calcite

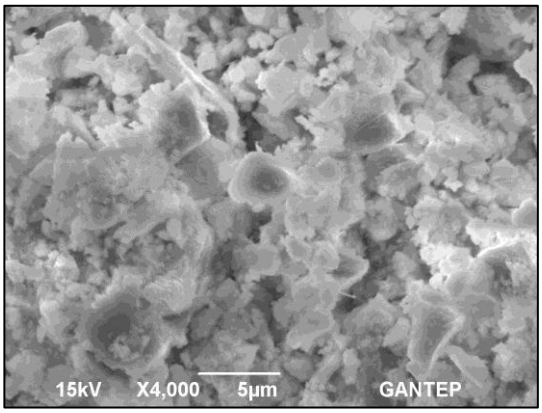

(f) Cement

Figure 3.2 Scanning Electron Micrograph (SEM) of the materials used during the experimental study.

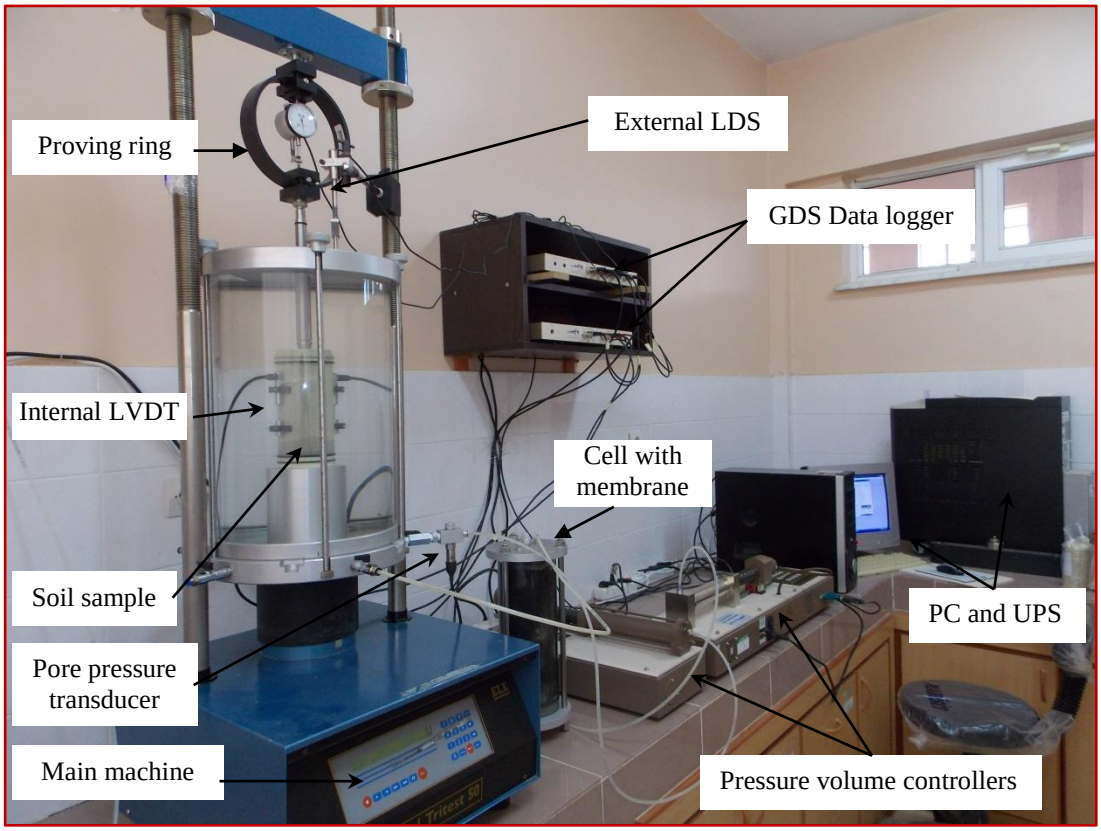

Figure 3.3 An overview of the triaxial testing system.

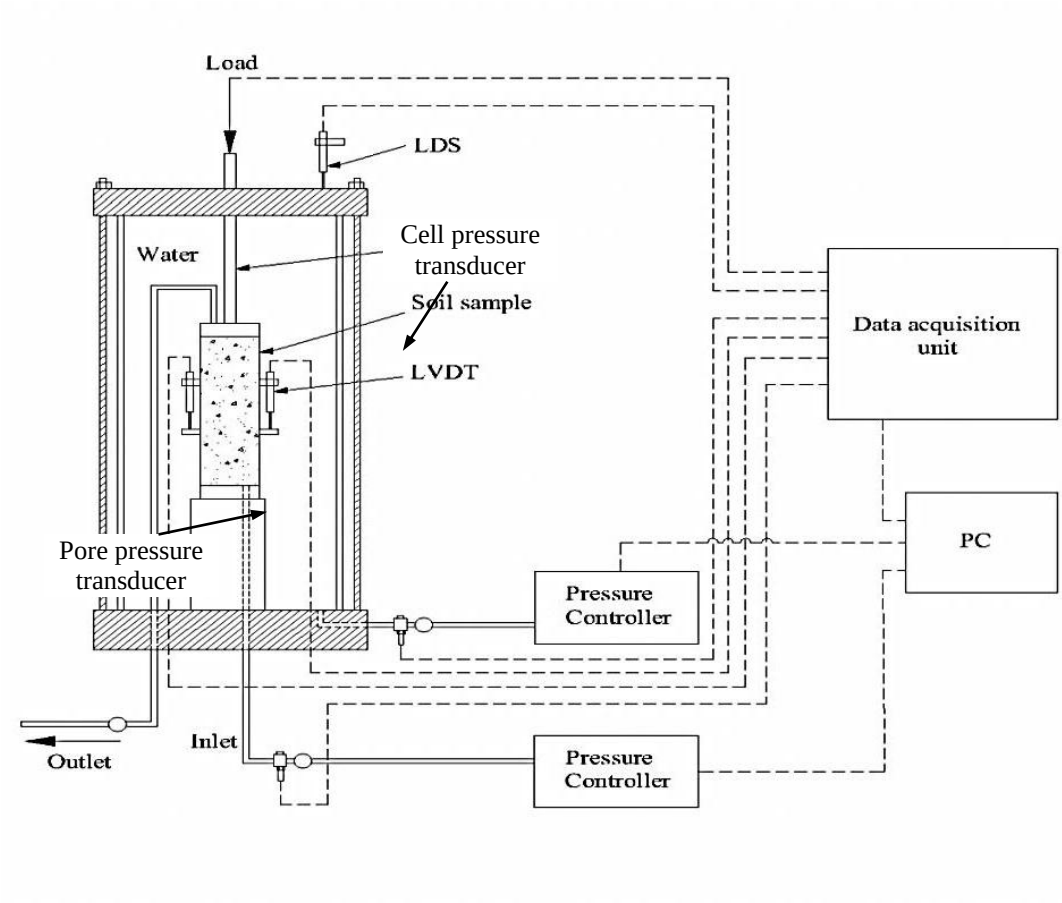

Figure 3.4 Triaxial testing system setup sketch.

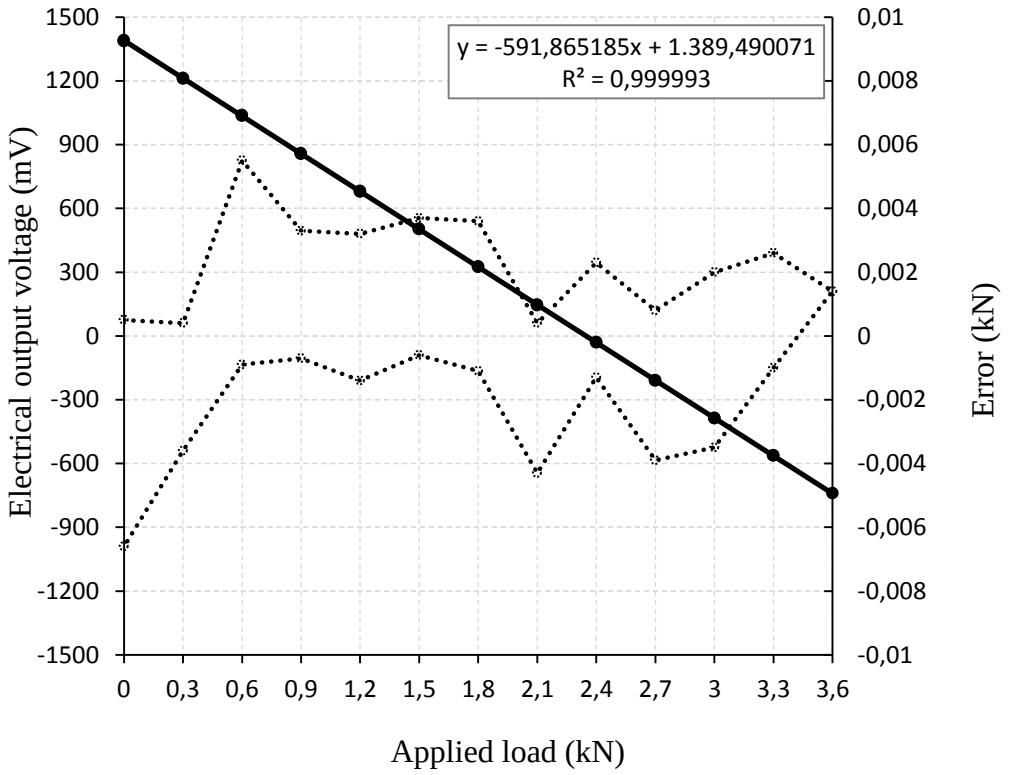

Figure 3.5 Calibration graph for the 4.5-kN load ring, ELE S/N 1155-12-13341.

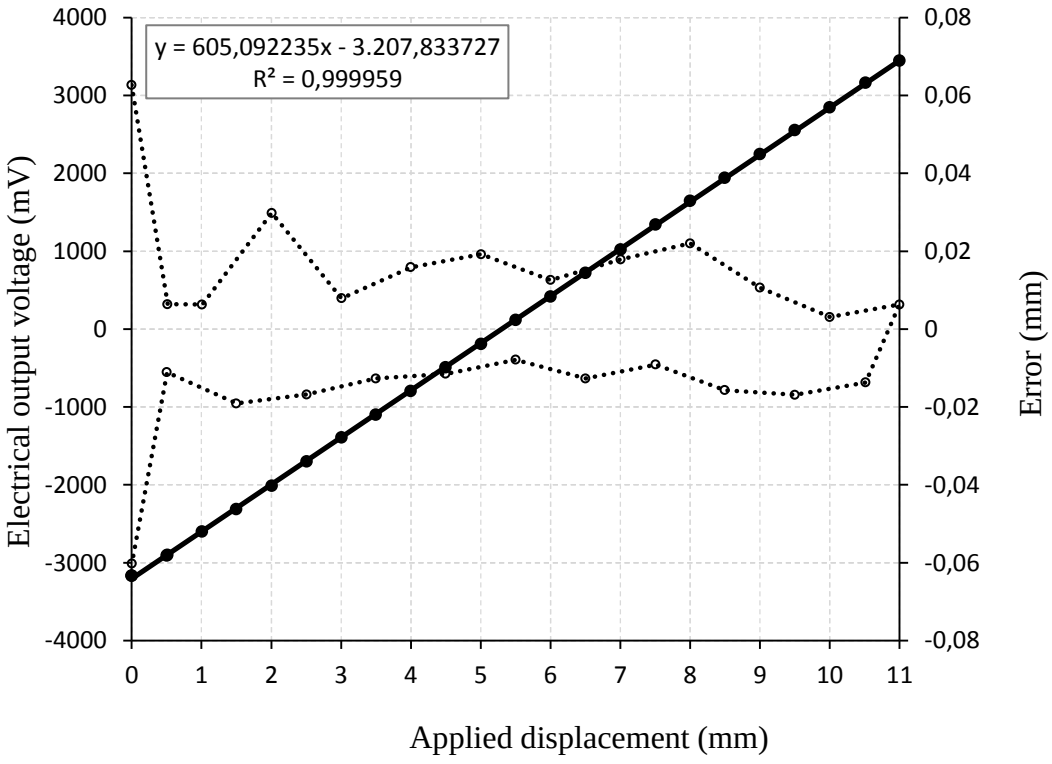

Figure 3.6 Calibration graph for the external LDS, ELE S/N M858440-03.

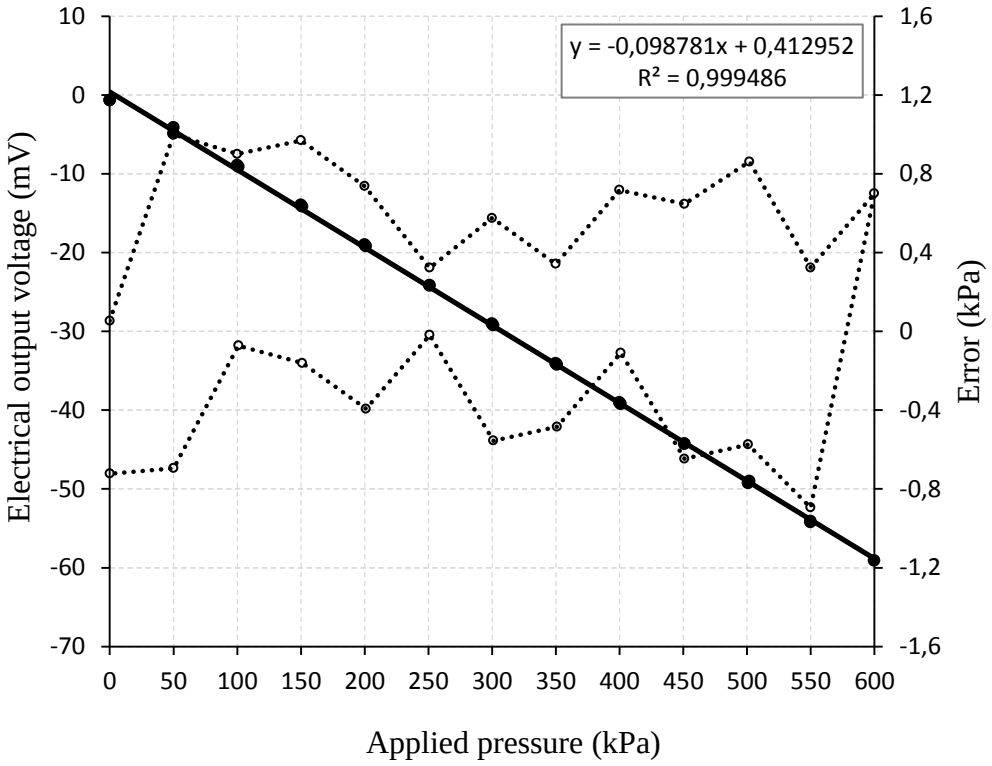

Figure 3.7 Calibration graph for the cell pressure transducer, PDCR 810 S/N 2850056.

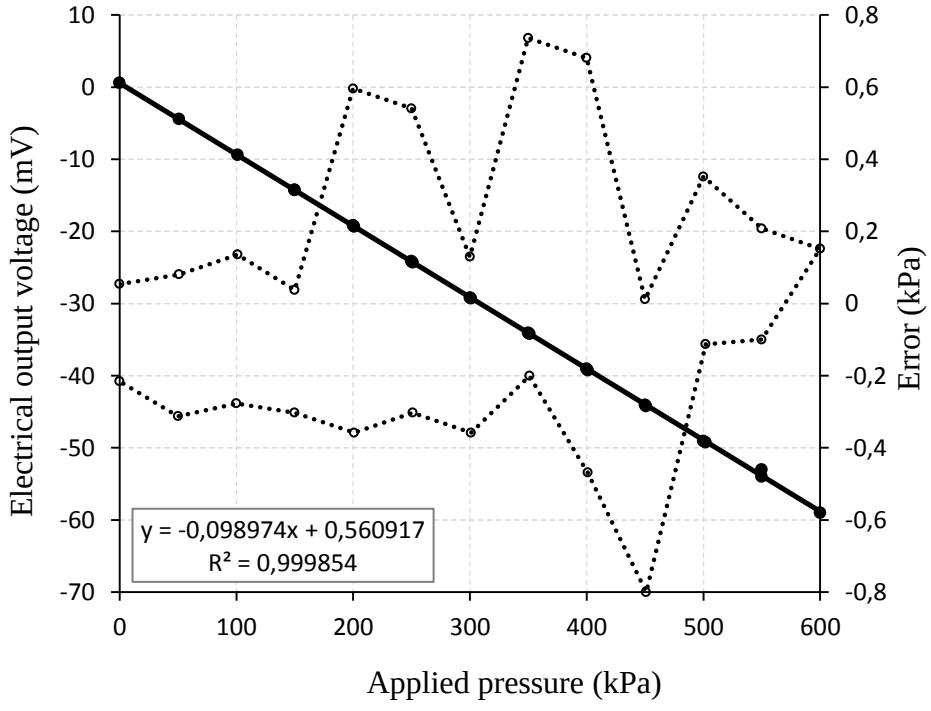

Figure 3.8 Calibration graph for the pore pressure transducer, PDCR 810 S/N 2850055.

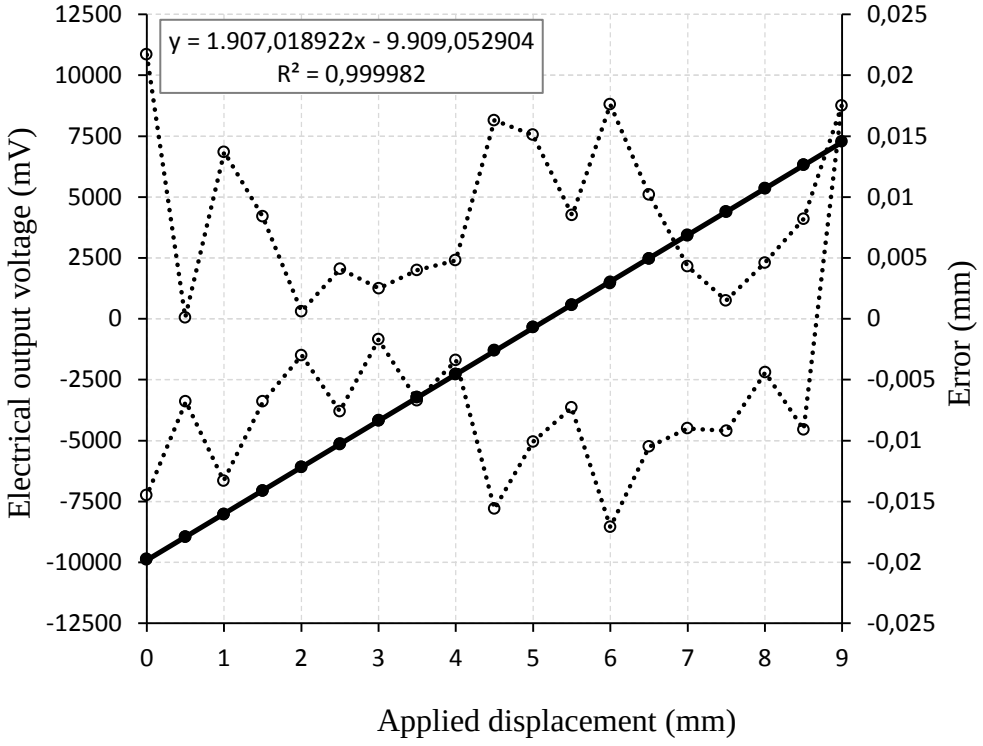

Figure 3.9 Calibration graph for the internal LVDT, GDS S/N 134078.

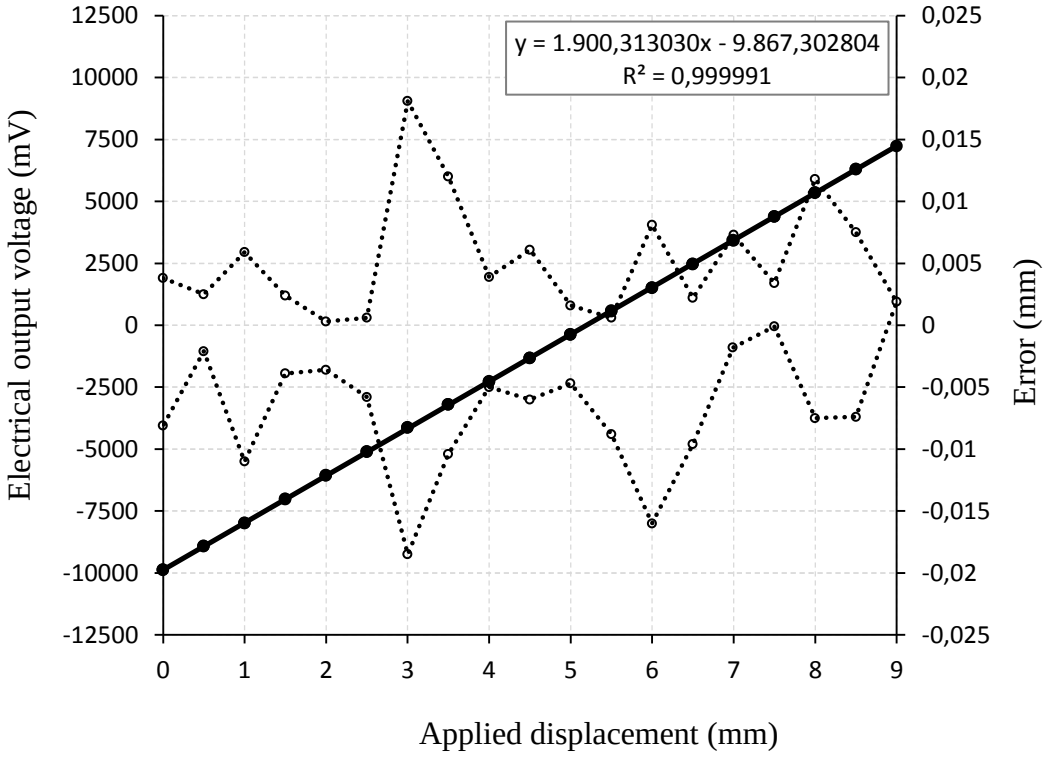

Figure 3.10 Calibration graph for the internal LVDT, GDS S/N 134079.

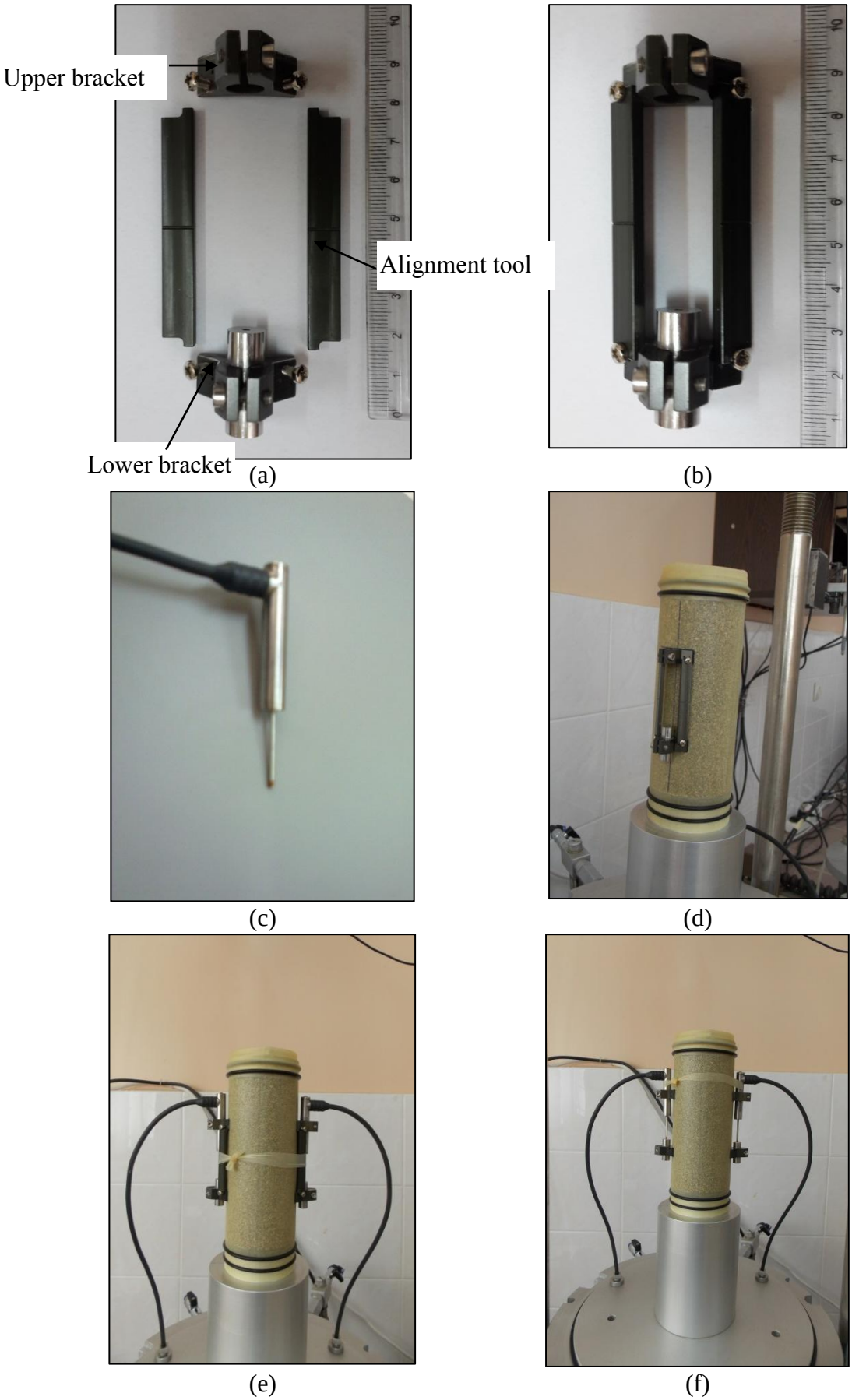

Figure 3.11 Setting up the submersible local strain measurement (LVDT).

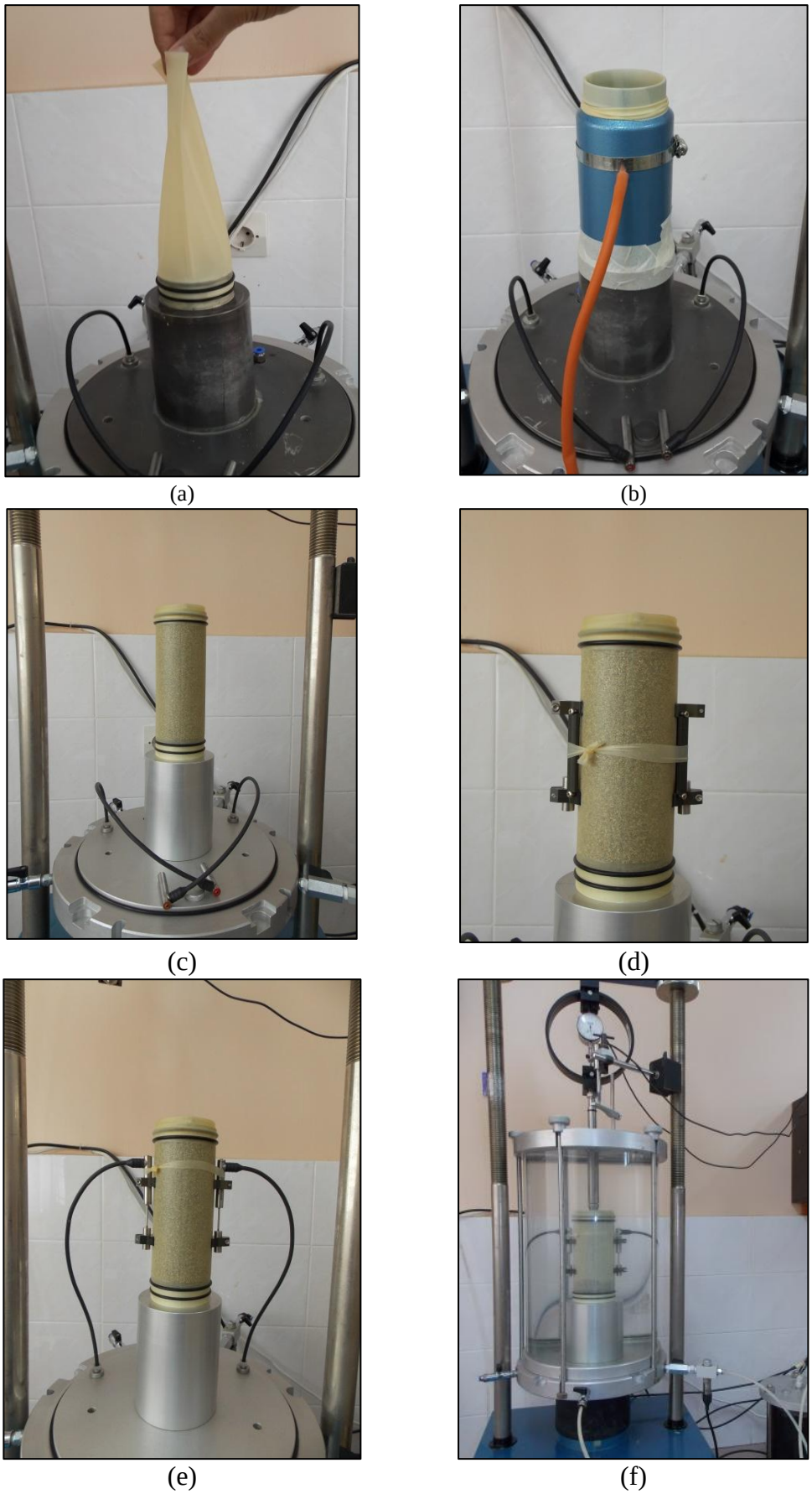

(a) (b) (c) (d) (e) (f)

Figure 3.12 Illustration of the sample preparation techniques with the local strain measurements.

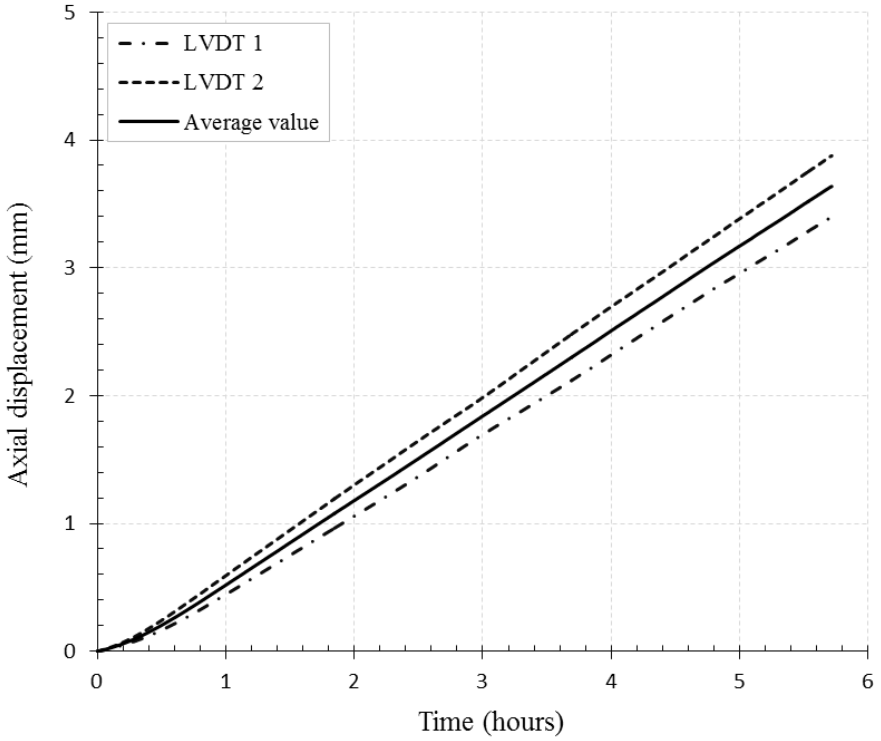

Figure 3.13 Axial displacement measured from the two LVDTs during the test.

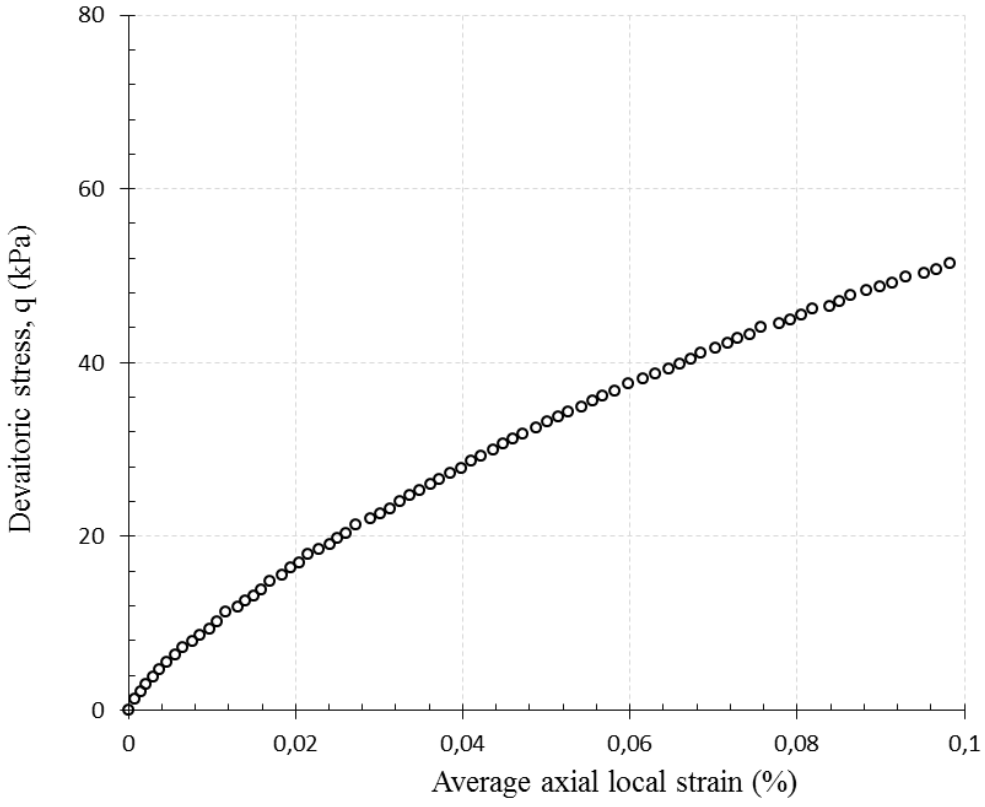

Figure 3.14 Accuracy of the stress-strain curves using local strain measurements at small strain levels.

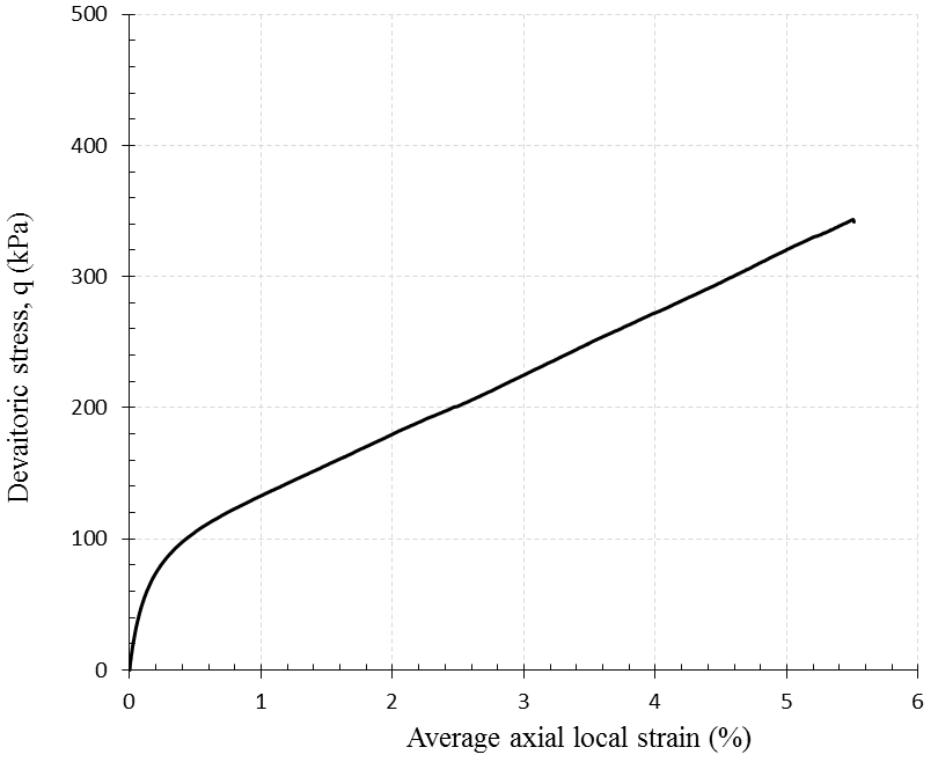

(a)

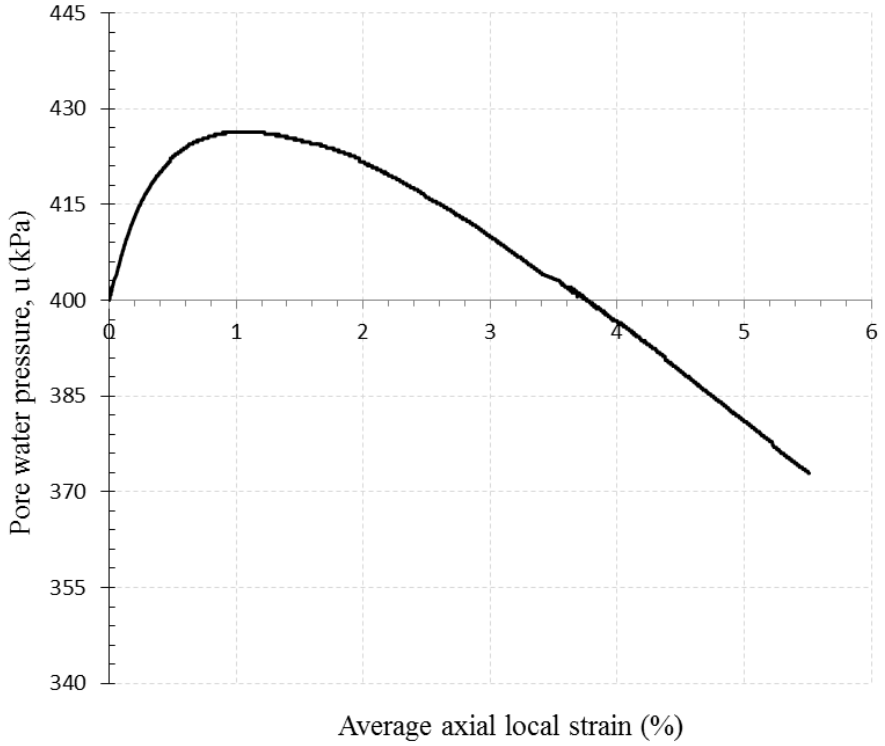

(b)

Figure 3.15 Examples of variation of the (a) deviatoric stress (b) pore water generation with average axial local strain.

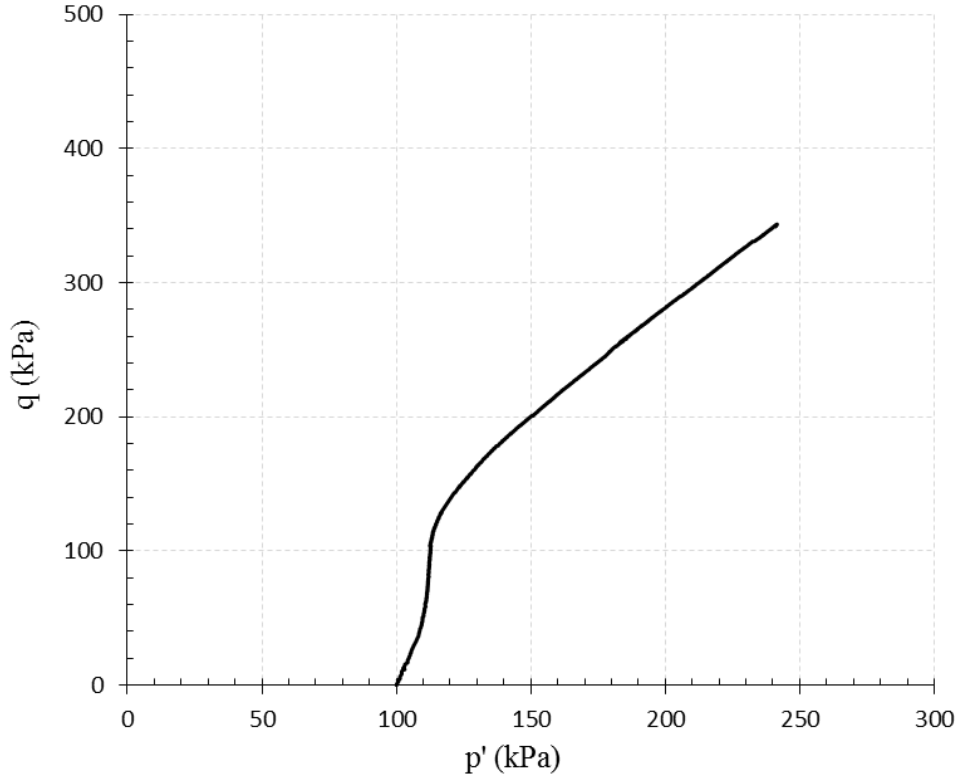

Figure 3.16 Example of stress space paths of clean sand using q-p' values.

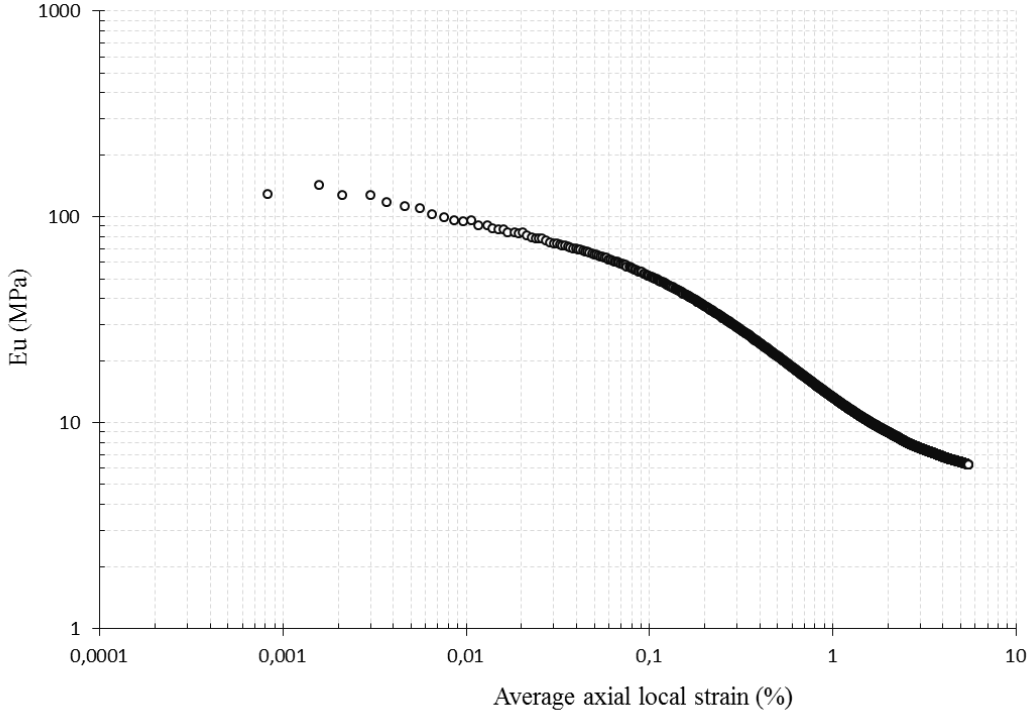

Figure 3.17 Example of the stiffness (secant Young's modulus) degradation curve with the average axial local strain.

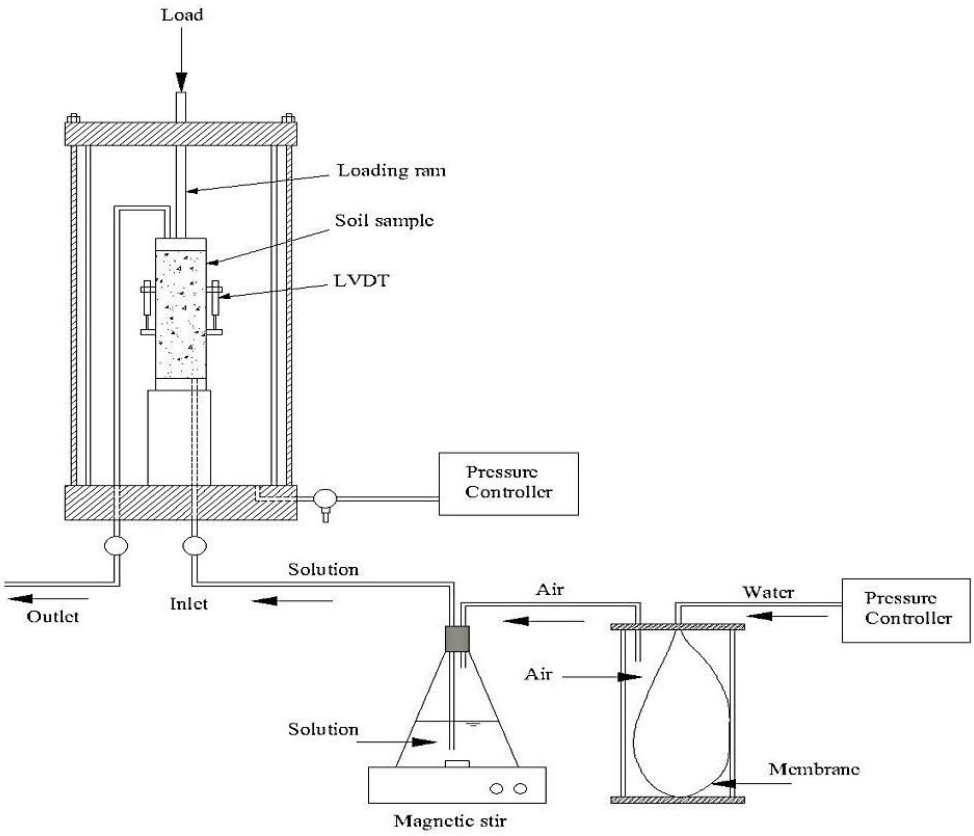

Figure 3.18 The biocementation treatment system set-up sketch.

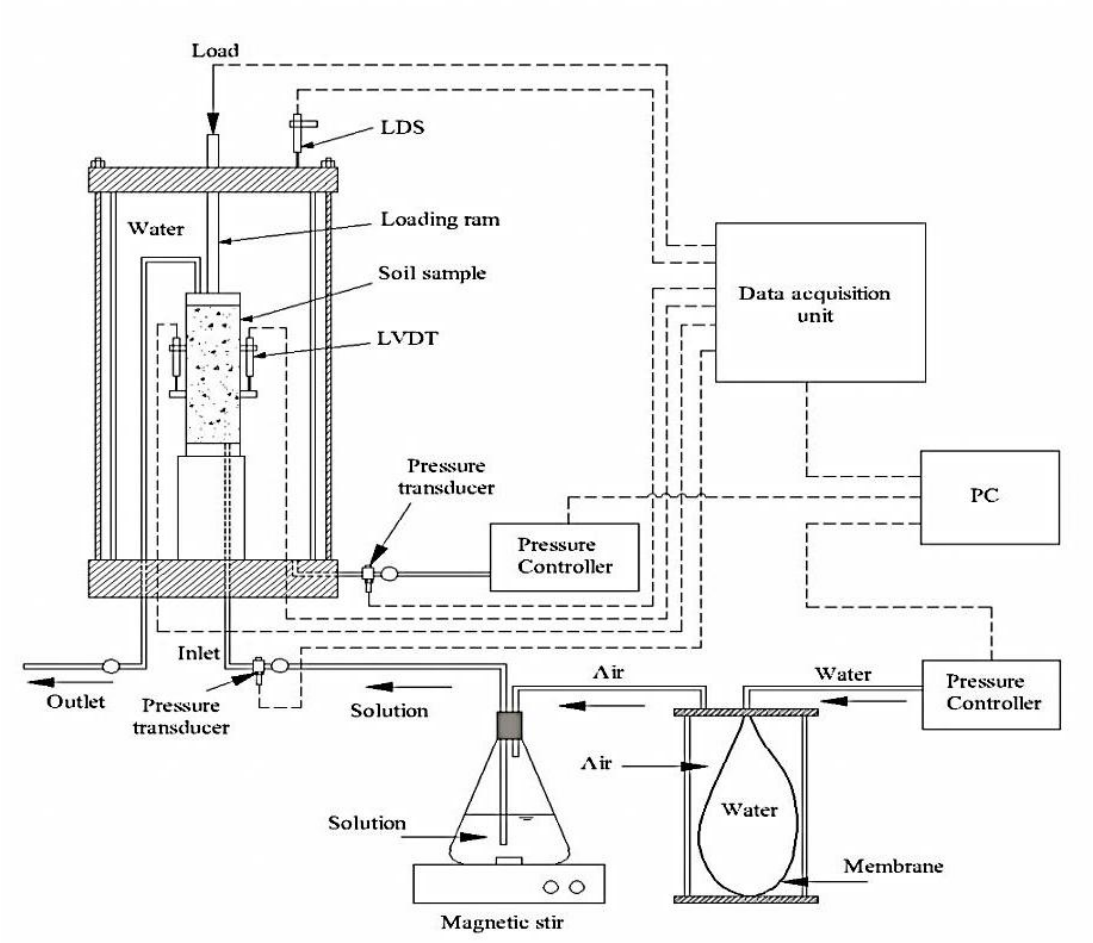

Figure 3.19 Triaxial testing system set-up sketch for the biocementation treatments.

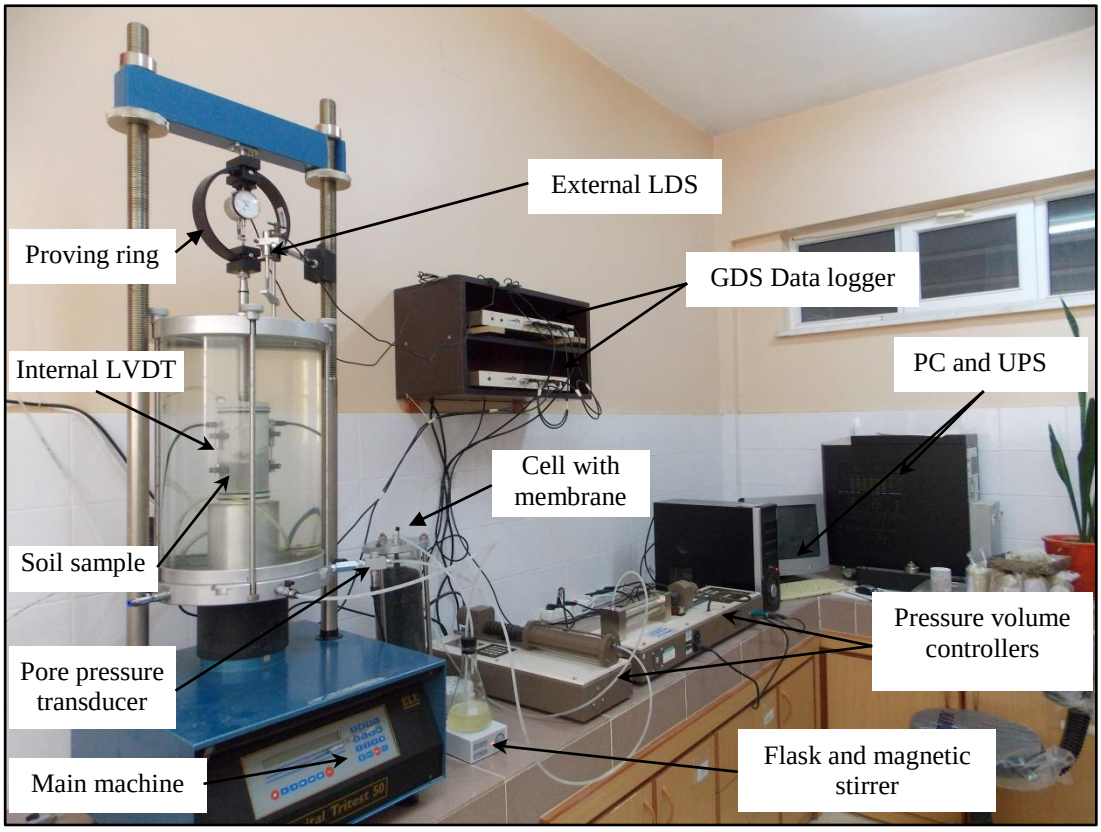

Figure 3.20 An overview of the triaxial system for the biocemented specimens.

CHAPTER 4

RESULTS AND DISCUSSION

In this chapter, results of the triaxial tests were presented and discussed. The experimental study was consisted of two main phases; an initial preliminary study and subsequent detailed studies. The results of the preliminary studies were presented considering the results of the triaxial tests of clean sand at various confining pressures, consolidation period, relative density and type of the triaxial test. These tests provide basic information about the shear strength and stiffness of clean sand. Results and the discussion of the tests that focused on the effect of the tire crumb inclusion on the response of the cemented sand were illustrated. Later, detailed tests were mainly conducted on cemented sand with local strain measurements using LVDT. Result of the tests that were conducted to study the effect of the type of the cementing agents and sample preparation techniques on the stress-strain response and low strain stiffness of the cemented sand were presented. Also, the chapter consists of results of the tests on the biocemented specimens, which performed at three levels of cementation. Emphasis was given to present the variation of the stiffness degradation with the treatment period. The discussions of the results were confirmed by the results of the microscopic study.

4.1 Preliminary triaxial tests on clean sand

In the initial phase of this study, a series of triaxial tests were conducted to investigate the preliminary behaviour of clean sand without local strain measurements. Influence of the effective confining pressure, isotropic consolidation period, type of the triaxial test, and relative density were studied during these tests. The specimens were prepared and consolidated according to the sample preparation techniques that explained in Chapter 3.

4.1.1 Response of clean sand in various confining pressure and consolidation period

The triaxial shear response of clean sand was investigated in various effective confining pressure and consolidation period. Two series of triaxial tests were conducted. The first series of the triaxial tests was conducted under consolidated undrained conditions (CU) and the second series of the tests was conducted under consolidated drained conditions (CD). For each series of the triaxial tests, three effective confining pressure and two consolidation period were selected, namely; 50 kPa, 100 kPa and 150 kPa for effective confining pressure, 3 hours and 18 hours for the consolidation period.

In the first series of tests, the triaxial specimens were tested in undrained condition (CU). The specimens were prepared in a loose state by following the sample preparation techniques as described in Chapter 3 sections I-A and I-B. Figure 4.1 shows the variation of the deviatoric stress versus axial strain, and pore pressure generation versus axial strain for clean sand at three different effective confining pressures and two consolidation periods. As can be seen from the Figure 4.1, for both triaxial tests that consolidated for 3hrs and 18 hrs, the deviatoric stress increases as axial strain increase, and no peak shear stress values were observed in all clean sand specimens within this range of axial strain. Also, the deviatoric stress and excess pore water pressure generation increase as the effective confining pressure increases within the measured strain level. In addition, for all tests, regardless the effect of the confining pressure and consolidation period the specimens exhibited strain hardening behaviour as the axial strain increased. On the other hand, for all effective confining pressures the deviatoric stress increased and excess pore water pressure generation decreased as the consolidation period increases. However, effect of the consolidation period is significantly lower in low effective confining pressure. The results present a good agreement with the results reported by Park and Jeong (2015) and Della et al. (2011). As the confining pressure is increased the maximum deviatoric stress and peak strength increased.

The stress path space graphs of the clean sand in CU condition for three confining pressures and two different consolidation periods are illustrated in Figure 4.2. In this Figure, q represents the deviatoric stress, and p’ represents mean effective stress. It is

clearly observed that the change in the effective confining pressure does not significantly influence the contractive and the dilative behaviour of the clean sand. However, effect of the consolidation period on the stress path space results increase as the effective confining pressure increases. The specimens exhibit more contraction at low consolidation periods. This behaviour may be attributed to high excess pore water pressure that was generated during shear.

Figure 4.3 shows the variation of clean sand stiffness with the axial strain for specimens consolidated and sheared under different effective confining pressure and different consolidation period. In general, the clean sand stiffness was degraded as the axial strain increases. The specimens that were consolidated and sheared at high effective confining pressure have higher stiffness value than the specimens at low effective confining pressure. On the other hand, the specimens that were consolidated for a longer period (18 hrs) have higher stiffness than the specimens that were consolidated for a shorter period (3 hrs). Also, effect of the consolidation period decreases as the effective confining pressure becomes low as in pressure equal to 50 kPa.

In the second series of the preliminary triaxial tests of clean sand, the specimens were tested in drained condition (CD). As for the CU tests the specimens were prepared by following the sample preparation techniques as illustrated in Chapter 3 sections I-A and I-B. The CD triaxial tests were conducted in three different effective confining pressures and two consolidation periods. The results are presented in the Figures 4.4-4.9. The deviatoric stress increases with the axial strain and peak shear stress values were not visible in all the specimens within this range of axial strain. Also, the deviatoric stress and volume change during shear increase as the confining pressure increases within the measured strain level, while changes in the consolidation period have lower influences on the deviatoric stress and volume change variation versus axial strain. A comparison of the stress space results for clean sand that tested in CD condition in various effective confining pressure and consolidation period are given in Figure 4.5. It is observed from this Figure that shape of the stress path space of the clean sand in all effective confining pressures was not clearly affected by the consolidation period change.

Figure 4.6 presents the degradation of the soil stiffness with the axial strain for CD test series. Soil stiffness in the drained condition and especially at the low strain level has a higher value and this value is significantly affected by the value of effective confining pressure and consolidation period. In addition, the influence of the effective confining pressure and consolidation period decrease as the axial strain increases during shear and as the effective confining pressure decreases. Variation of the volumetric strain and the void ratio with axial strain are presented in Figure 4.7 and Figure 4.8, respectively. Changes of the volumetric strain and void ratio with the axial strains become higher at the high values of the effective confining pressure, while it was not clearly affected by the change in the consolidation period. Also, variation of the specific volume during shear with the mean effective stress was influenced by the change in effective confining pressure, while the consolidation periods were not significantly effective on the specific volume of the specimens as presented in Figure 4.9.

The stress-strain behaviour variation of the clean sand with the type of the triaxial test for the 18 hrs consolidation period is presented in Figure 4.10. As can be seen from this figure, the deviatoric stress of clean sand and especially at the low strain (less than 4% axial strain) in drained condition higher than the deviatoric stress value in undrained condition. This behaviour is similar for all confining pressures. As mentioned by Chen (2006), and Park and Jeong (2015) the deviatoric stress obtained from the drained tests was higher than their values in the case of the undrained tests. They attributed this response of the clean sand in the drained condition to strain hardening behaviour during the test. The comparison between the stress path results of the CU and CD tests of the clean sand is presented in Figure 4.11. The specimens were tested in the CU condition and for all effective confining pressures, exhibit contraction behaviour more evident, in comparison with specimens that were tested in CD conditions. The author attributed this behaviour to the generation of the positive excess pore water pressure at the beginning of the test. Figure 4.12 presents the difference in the stiffness degradation with the axial strain between the specimens were tested in the CU and CD conditions. It can be clearly observed that for all effective confining pressures, Stiffness of the clean sand at the small strain in the CD condition higher than its value in the CU condition. However, as the axial strain increases the stiffness values become closer each to other. The author believes that

this behaviour is also due to the generation of the excess pore water pressure that may reduce the friction between the soil grains.

The Mohr circles and failure envelopes of the two series of tests in loose state of clean sand are presented in the Figures 4.13-4.17. The failure envelope and angle of the internal friction were determined for the CU condition based on total stress and effective stress (Figures 4.13 and 4.14). In the case of the total stress, there is considerable difference in the angle of internal friction between the specimens consolidated for 3 hrs and specimens consolidated for 18 hrs. However, in the case of the Mohr circles drawn based on effective stresses for the same series of the triaxial tests, little influence of the consolidation period on the friction angle values was noticed. Also, as it is observed from the two Figures, in the case of the results based on total stress a small value of the cohesion appeared in the both consolidation periods. However, in the results based on effective stress, no value for the cohesion was appeared. Figure 4.15 presents the Mohr circles and failure envelopes of the specimens in the CD condition based on effective stresses. The results showed that there is a little difference (about 1.6°) in the angle of internal friction between the specimens consolidated for 3 hrs and others consolidated for 18 hrs. The comparisons between the Mohr circles, failure envelopes and the angle of internal friction between the CD and CU triaxial tests of clean sand are illustrated in Figures 4.16 and 4.17. For both consolidation periods (3 hrs and 18 hrs), the angle of internal friction determined from the CD tests is small greater than its value in the case of CU tests. This behaviour may be due to the generation of the pore water pressure during the undrained tests.

4.1.2 Effect of the relative density on the triaxial response of clean sand

A series of consolidated undrained triaxial tests were conducted to investigate the effect of relative density on the response of clean sand. The triaxial tests were conducted for three different relative densities, namely; 35%, 63% and 85%, corresponding to loose, medium and dense states of the sand, respectively. Clean sand specimens of the triaxial tests were prepared by following the sample preparation techniques as illustrated in Chapter 3 sections I-A, I-B, and I-C. The tests were conducted under 100 kPa effective confining pressure and 3 hrs consolidation period. The series of the tests were repeated under the same condition for the 18 hrs

consolidation period. Figure 4.18 presents the variation of the deviatoric stress and pore water pressure versus the axial strain. As the relative density of the clean sand increases the deviatoric stress increases and the pore water pressure generation decreases. These behaviours might be due to increase in the area of contact between the soil grains that lead to increase in frictional resistance among them. On the other hand, high densities may lead to a better interlocking between the grains. As mentioned by Ismail et al., (2002) number of the contact points between the soil particles depends on the degree of the compactness of the soil skeleton.

The stress path space graphs of clean sand specimens that were prepared under different relative densities are illustrated in Figure 4.19. It is clearly observed that for the two consolidation period, the material behaviour becomes more contractive as the relative density decreases. Reason of this behaviour as the author believes, is that decreases of soil density lead to generation of high pore water pressure. Figure 4.20 presents the curves of stiffness degradation versus axial strain of the sand specimens prepared under different relative densities. The stiffness of the sand increase as the relative density become higher and this behaviour is similar in the two consolidation periods. Also, as for the deviatoric stress, this behaviour is related to the friction and interlocking between soil grains. Effect of the relative densities on the Mohr circle parameters based on total stresses and effective stresses is shown in Figure 4.21 and 4.22. As can be seen from the Figures, the consolidation period and the relative densities have a considerable effect on the Mohr circles and its parameters.

4.2 Response of the sand mixed with the tire crumbs and cement

The effect of tire crumbs with small amount of cement on the stiffness, strength, and pore water pressure characteristics of sand were investigated to assess the contributions to the overall behaviour of the mixture. These series of the triaxial tests were aimed from one hand to study the effect of the change in the fabric structure of the sand by including tire crumb pieces on the behaviour of the sand. On the other hand, the tests were directed to investigate the applicability of a waste material in the soil improvements. Also, the tests were focused to explore the effect of the small percentages of cement on the behaviour of the sand-waste material mixtures.

4.2.1 Triaxial response of the sand and tire crumbs mixture

A series of consolidated triaxial tests were conducted to clean sand and sand tire crumbs mixtures. The specimens of the triaxial test for this series were prepared by following the sample preparation technique as illustrated in section II of Chapter 3. Triaxial testing specimen contract or dilate substantially during tests in accordance with the relative density values (Vesic and Clough, 1968). Some of the engineering properties, including shear strength, compressibility, and permeability of a given soil depend on the relative density. Therefore, the relative density values here in this investigation were aimed to be kept at a constant range (loose to medium). Dry densities of the specimens tested were calculated as 14.45 kN/m^3 for clean sand, 14.10 kN/m^3 for sand with 3% tire crumb, 13.21 kN/m^3 for sand with 7% tire crumb, and 11.99 kN/m^3 for 15% tire crumb. Comparing the relative density of the specimen prepared in this study with those proposed by Terzaghi and Peck (1962), it can be seen that the materials tested could almost exclusively be classified as loose to medium dense.

Figure 4.23 shows deviatoric stress versus axial strain, and pore water pressure versus axial strain of the clean sand, and sand with different amount of tire crumbs at 100 kPa effective confining pressure. The untreated specimen (clean sand) responses to triaxial loading was served as a benchmark from which the treatment in shear response by adding tire crumbs and cement could be assessed. Figure 4.23 presents results of four different experiments, which are the (i) clean sand specimens, and sand with (ii) 3% tire crumb, (iii) 7% tire crumb, (iv) 15% tire crumb. As can be seen from Figure 4.23.a, deviatoric stress decreases as the tire crumbs content increases within the measured strain level. No peak shear stress values are observed in all the specimens, and the deviatoric stress continues to increase with increasing axial strain. Figure 4.23.b presents the pore water pressure generation corresponding to the tests described in Figure 4.23.a. It is seen that the pore water pressure in the clean sand generates higher values than their values in sand with tire crumbs specimens in particular at the low strain level, and as the axial strain increases the pore water pressure of clean sand becomes lower than its value in the sand with tire crumbs specimens. In addition, generation of the pore water pressure decreases as the tire crumb content increases. Although a clear dilation can be observed in the specimen

tested using clean sand, the tests on the sand with tire crumbs do not show dilation within the measured strain range. The results are in the contrast with the results were obtained by Ahmad (1993), Zornberg et al., (2004), and Edincliler, 2007. They concluded that the shear strength of the material increases as the content of waste tire pieces increase in the mixture. But, increasing or decreasing in the soil strength with the inclusion of waste tire pieces depends on many factors, for example, type of the soil used, type of the test, and shape and type of the tire pieces.

The clean sand grains are assumed to be in clean contact with each other in the specimen tested without tire crumbs, and hence the mechanical behaviour of this specimen was governed by the sand particles only. As the amount of tire crumbs increase, the contacts between the sand particles reduce, and the behaviour of the specimens are controlled by the tire crumbs. Actually, sand and tire crumb grains can rearrange themselves into various modes depending on the initial conditions and applied stress. The rearrangements of sand and tire crumbs grains and the surface characteristics of each material's grain may influence on the friction and interlocking of the grains. Also, the compressibility behaviour of the tire crumbs particles play an important role and may effect on the response of sand-tire crumbs mixture during loading.

The stress path results of the sand and tire crumbs mixture specimens were given in Figure 4.24. The most striking point in these plots is that the contraction increases as the tire crumbs content increases. This response can be attributed to the compressible behaviour of the tire crumbs under pressure. As reported by Edil and Bosscher (1994) waste tire are much more compressible during the initial stages of loading than soils, and the compressibility of tire-soil mixtures can be relatively high, depending on density and the tire-soil mixing ratio. Figure 4.25 presents the variation of the sand and tire crumbs specimen's stiffness with the axial strain. The stiffness of all mixture percentages degraded with the axial strain, and the stiffness of the specimens decreased by adding tire crumbs. The stiffness values for the specimens tested using various tire crumbs contents are fairly close to each other at the strain level after the 2% strain level. However, the stiffness result of the sand-tire crumb specimens differed from each other at relatively small strain levels. In particular; before the 1% axial strain, the characteristics of the plots for the specimens with tire

crumbs considerably change. The individual tire pieces have stiffness, lower than that of sand grains, this may be one of the reasons that lead to stiffness decrease. Also, rearrangement in the soil structure after tire crumbs inclusion and the higher compressibility of its grains may be another reason that reduces the stiffness of the mixture.

4.2.2 Behaviour of the cemented sand and tire crumb mixture

As it was concluded from the analysis of triaxial testing results in the previous section, the strength and stiffness of the sand decrease as tire crumb was included in the mixture. Therefore, in this study an attempt was made to improve the strength, stiffness, ductile and contractive behaviour of sand and tire crumbs mixture by adding small amounts of cement. A series of the consolidated undrained tests were conducted on the sand, tire crumbs and cement mixture. The specimens were prepared by following the sample preparation methods that illustrated in section II of Chapter 3. In the first group of the tests, the tire crumb percentage was fixed at 15% by the dry weight of the mixture, which was selected as a worst case (the lowest stress value). Hence, the cement contents were selected as 0%, 1%, 3%, and 5% by the dry weight of the mixture. In the second group of the tests, the cement content was fixed at 3% by the dry weight of the mixture, which was the optimum percentage with the all percentages of tire crumbs which were 0%, 3%, 7%, and 15%.

The effect of cement content at various ratios on the deviatoric stress-axial strain, and pore water pressure-axial strain responses of the sand are shown in Figure 4.26. As the specimens with tire crumbs only, the specimens with both tire crumbs and cement have no observed peak deviatoric stress values within the measured axial strain range (Figure 4.26.a). Type of the failure in the cemented sand-tire crumb mixture was barrelling type without a distinct failure plane. It is seen that 3% and 5% cement contents have a significant effect on the deviatoric stress. As the cement content increases, the deviatoric stress values, and the energy absorption increase. Energy absorption can be found by calculating the area under the stress-axial strain curve (Hamidi and Hooresfand, 2013). As shown in Figure 4.26.a, energy absorption has higher values within relatively small strain levels. The author interpreted that this behaviour might be attributed to an artificial bonding between the sand grains and

tire crumb particles because of the hydrated cement that was cured for 17 hrs. It is considered that the hydrated cement covers the tire crumbs particles as well as sand grains, and reduces their size and compressibility characteristics, while it is being kept under a 100 kPa effective stress. The SEM pictures indicate that cementation occurs between the sand and tire crumb grains (Figure 4.27). Also, the SEM pictures illustrate that the hydrated cement covers the sand and tire crumb particles. Therefore, the compressibility of the tire crumb pieces reduces after curing the hydrated cement. The results of this series of the tests in a good agreement with the results of the test conducted to the cemented soil and fiber mixtures made by Tsoi and Lee (2011), Guleria and Dutta (2012), Consoli et al., (2004), and Maher and Ho (1993). Figure 4.26.b presents the effect of the cement content on the generation of the pore water pressure for the sand-tire crumb mixtures. This Figure shows the pore water pressure generation corresponding to the tests described in Figure 4.26.a. The tests on the specimens with less amount of cement exhibit a higher pore water generation, in particular at larger strain levels.

Figure 4.28 describes the stress path of the clean sand, 15% tire crumb mixtures and cement at various ratios. It is observed that the dilatancy increases as the cement content increases. The author considers that the bonding (cementation) could result in a lower ductility. Also, increases in dilation behaviour may be attributed by the inclusion of hydrated cement that covers the mixture grains from one hand and on the other hand, it causes bonding between the mixture grains at the contact points. The modification in the stiffness of the sand and 15 % tire crumbs mixtures due to the addition of the various percentages of cement is presented in Figure 4.29. Stiffness of the mixture increase significantly with increasing cement content. It is observed from the Figure that the stiffness values for all the specimens tested using various cement ratios are fairly close to each other at the strain level after the 2% strain level. On the other hand, the stiffness result of the sand-tire crumb specimens with cement differed from each other at relatively smaller strains, in particular before the 1% strain level. Stiffness of the sand that reduced due to the inclusion of the tire crumbs and achieved its lower value in the 15% tire crumbs was improved by cement addition. In addition, stiffness of the mixture was retained to its initial value corresponds to the stiffness of the clean sand. Also, the stiffness of the specimens of sand with 15 % tire crumbs and cement increases as the cement content increase.

Figure 4.30 indicates the behaviour of sand and various contents (0%, 3%, 7%, and 15%) of tire crumbs mixtures with and without 3% cement additions. Considering the overall testing result, the author has preferred to use 3% cement content in sand with various contents of tire crumbs. Because, the authors interpreted that such cement content could be an optimum value to modify effectively the behaviour of various sand-tire crumb mixtures. It can be seen from the Figure 3.30.a, the deviatoric stress values for the specimens with 3% cement increase as the tire crumb content decrease. Figure 3.30.b shows the pore water pressure generation corresponding to the tests described in Figure 4.30.a. It is observed that the tests on the specimens with less tire crumb content exhibit a lower pore water generation with a peak at a smaller strain level (at about 1%).

The stress path results of the specimens with various content of tire crumbs with and without 3% of cement are illustrated in Figure 4.31. As can be seen from this figure, the specimens behaviour becomes more contractive as the tire content in the mixture is increased. The specimens with and without cement exhibit similar trends in the case of specimens with tire crumbs. Figure 4.32 presents the stiffness degradation curves with the axial strain for specimens corresponding to the results in Figure 4.30. The specimens of sand and tire crumbs mixture with and without cement addition get close in the stiffness values at the strain level after the 2% strain level. Also, the cemented specimens by 3% cement have higher stiffness values. As the tire content increases in the mixture the stiffness values decrease regardless of cement existence. The author believes that this behaviour may be attributed to the compressible behaviour of the tire pieces.

4.3 Behaviour of the sand at the small strain using local strain measurement

Importance of the local strain measurements using internal LVDTs was first highlighted by Jardine et al., (1984). They mentioned that conventional triaxial results with external displacement measurement contain errors which are frequently so large, and their use in the determination of soil stress-strain behaviour and the stiffness at the working level of stress is invalid. These errors resulted from bedding at the end platens, tilting of the specimen and due to the effect of the apparatus compliance. Therefore, most triaxial tests tend to give inaccurate stress-strain behaviour and the apparent soil stiffnesses far lower than those inferred from field

behaviour. Due to these reasons, the local strain measurement by internal LVDTs were used in this study for an accurate evaluation the stress-strain and stiffness behaviours of the clean and cemented sand at small strain level.

In this context, difference between the external axial displacement measurements and local axial displacement measurements and its effect on the stress-strain and stiffness of the sand was observed. A consolidated undrained triaxial test was conducted for clean sand using local strain measurements by two LVDTs. The specimens were prepared by following the sample preparation technique, which was explained in details in section III-A of Chapter 3. Figure 4.33 presents the deviatoric stress versus axial strain using local strain and global strain measurements. It can be clearly observed that the stress-strain response at small strain levels using local strain measurements by LVDTs can be assessed with more accuracy. Furthermore, the deviatoric stress appeared in higher value when it plotted versus local axial strain. This experimental result presents a good agreement with Clayton and Khatrush (1987), Clayton and Heymann (2001), and Cuccovillo and Coop (1997a).

Figure 4.34 presents the variation of the pore water pressure versus the axial strain using local and global strain measurements corresponding to the results presented in the Figure 4.33. It can be seen that the pore water pressure is higher at low strain levels when it is plotted against the local strain. Variation of the stiffness of clean sand considering the secant Young's modulus versus the axial strain is presented in Figure 4.35. The figure indicates that the secant Young's modulus degradation curve can be derived to as small as 0.002% axial strain. As mentioned by Jardine et al., (1986) and Mair (1993), the strains around foundations, excavations and tunnels are except in the small areas that undergo yield, generally very small and typically of the order of 10^{-2}-10^{-1}% axial strain. In general, stiffness of the clean sand that was estimated depending on local strain measurements is higher than its value when it was estimated depending on the global strain and especially at the strain lower that 0.4%. Also, it can be seen that degradation in the stiffness value that was derived from the local strain measurement is higher than its degradation in the case of external strain measurement (Figure 4.35).

4.4 Behaviour of the cemented sand

One of the main objectives of this study was to investigate the stress-strain behaviour and stiffness of the cemented sand at small strain zones. During the experimental study, emphasis was given to study the effect of cementing agent type and sample preparation techniques on the behaviour of cemented sand. In the context of sample preparation technique, the effect of cementing agent content, curing period, curing under pressure and saturation were considered. A series of the consolidated undrained triaxial tests using local strain measurement by two internal LVDTs were conducted. The specimens were prepared according to five different sample preparation techniques considering the above variables. Four types of the cementing agents were selected, namely; gypsum, lime, calcite and cement. The triaxial specimens for each cementing agent prepared by five methods (i.e., M1, M2, M3, M4, and M5). The details of the sample preparation techniques for each method were explained in the section IV of Chapter 3.

4.4.1 Stress-strain response of the cemented sand prepared by various methods

The variations of deviatoric stress and pore water pressure as a function of average local axial strain for the specimens are presented through the Figures 4.36-4.41. The figures reveal a clear difference in the behaviour of artificially cemented sands prepared by different techniques and cementing agents (i.e., Gypsum, lime, calcite, cement). Figure 4.36.a shows the influence of preparation techniques on the behaviour of sand cemented with gypsum. The effect of gypsum on the behaviour of the specimens differs depending on the preparation and curing conditions. For the specimen tested by employing method M4 and M5, However, the specimen cured and tested in the dry state which represent by method M5 has strength greater than the cemented sand tested in the saturated state which represent by method M4. On the other hand, the specimens tested in the dry state have more brittle behaviour and have an immediate yielding at lower stain near to the 0.05% axial strain. As an overall view, as the strain level increases the specimen shows a sharp increase in strength. Conversely, for the cemented specimens tested by employing other techniques (i.e., M1, M2, and M3), produce deviatoric stress lower than the uncemented sand. Also, the confining pressure during the curing period has a little effect on the strength of the cemented soil due to breakage of the cementing bonds

during the saturation phase. In addition, cementation of the cementing agent is very small in the saturated state. Generally in the tests employing methods M1, M2 and M3, the increasing of the cementing agent content reduces the specimen strength because these specimens cured in the saturated state. Therefore, no cementation occurs in the submersed condition at low curing period, and this leads the cementing agents to behave as a fine material. Figure 4.36.b illustrates the pore water pressure variation as a function of axial strain for the specimens. It is seen that the clean sand generates the lowest values of pore water pressure within the measured strain level and the pore water pressure generation increases as the cementing agent content increase in the mixture. This behaviour may be attributed to the reduction in the void ratio and increasing in the density as the cementing agents amount increase in the specimens.

It is clearly observed from the Figure 4.36 and 4.37 that the behaviour of cemented sand specimens with the gypsum and calcite is qualitatively similar. However, the behaviour of the specimens cemented by calcite and tested by employing method M5 would probably be different from other methods because of the bonding degradation during sample preparation in the other methods. The results are in an agreement with most of the testing results reported in literature (Ismail, et al., 2000; Consoli et al., 2000; and Rotta et al., 2003). Comparing the results obtained by the techniques M2 and M3 reveals that the stress applied during the curing period has a little effect on stress-strain behaviour of the specimens. It is likely to be possible to conclude, that phenomenon is due to the deterioration of cementation bonds during saturation of the specimens. The results suggest that specimen formation in the way used in M2 and M3 methods could suppress dilatancy. Therefore, it is postulated that the mechanism observed in the specimens prepared by employing the techniques M1, M2, and M3 could be due to fact that the cementing agents behave as 'fine materials' rather than a 'binder'. In the light of the studies by Thevanagayam (1998), Monkul and Ozden (2007), Cabalar (2010), Cabalar and Clayton (2010), Cabalar and Hasan (2013), the interpretation of the authors provide a consistent explanation of the reduction in deviatoric stress with increase in the amount of cementing agents. The specimens with calcite result in similar patterns in deviatoric stress and pore water pressure generation (Figure 4.37).

Variations of the deviatoric stress versus the average local axial strain and the pore water pressure versus the average local axial strain for the specimens cemented with lime are presented in Figure 4.38. The specimens cemented with lime have similar behaviour to the cemented specimens with gypsum and calcite. However, the specimen cemented with lime and prepared by following the technique M4 was failed in the early phase of the shearing (Figure 4.38.a). This behviour may be due to the cementing bonds lose from its strength during the saturation and consolidation steps of the test. In addition, due to the combined effect of the saturation and the confining pressure, the effect of the curing under pressure was not clearly observed. Also, the pore water pressure generates in higher values as the cementation increase in the specimen as can be seen in Figure 4.38.b.

Figure 4.39 illustrates the variation of the stress-strain behaviour and the variation of pore water pressure with the average local strain of the specimens cemented with Portland cement. The specimens cemented with Portland cement showed quite different responses from the specimens cemented with other cementing agents. It is observed that the amount of the Portland cement in the specimen plays a key role in the overall behaviour, the deviatoric stress increase as the amount of the Portland cement increases in the specimens. However, sample preparation techniques and curing conditions were not significantly effective on the triaxial response of the specimens with Portland cement. For the specimens prepared using the technique M1, as the stress level increases, the specimen shows a noticeable increase in stiffness. The specimens prepared by employing other methods showed a sharp increase in deviatoric stress within very small strain levels. The author attributed this behaviour to higher cement amount in the other methods. Ismail et al., (2002) consider that it is possible to use the results of specimens with gypsum, calcite, and lime for modeling natural deposits. While, for the specimens with Portland cement, there is no agreement between the results obtained here in this study and the results given by Ismail et al., (2002), as they reported no brittle response. The author considers that the reason of such difference could be because of the type of Portland cement used, sample preparation, curing conditions, and curing time.

Figures 4.40 and 4.41 present the variation of triaxial response for the specimens cemented with different cementing agents and prepared by following the techniques

M4 and M5, respectively. It is observed that the specimens with cement and lime exhibit a much higher deviatoric stress, and fail at very small strain levels (Figure 4.40.a). The difference in the behaviour (yield strength and yield strain) among the cemented specimens with different agents depends on the mineral compositions of each cementing agent and the percentages of these minerals within the cementing agent will be discussed in detail in forthcoming sections in this chapter. Figure 4.40.b shows the change in pore water pressure generation versus the average local strain. It is clearly observed that there are similarity in the pore water pressure trends versus the axial strain between the specimens cemented by cement and specimens cemented by lime from one hand, and between the specimens cemented by calcite and specimens cemented by gypsum on the other hand. Also, the pore water pressure values for the first two cementing agents (cement and lime) are greater than their values in the other two cementing agents (gypsum and calcite). The specimens cemented with cement produce low negative pore water generation at the beginning of the test. The results are in a good agreement with the results obtained by Haeri et al., (2006). It is postulated that differences in the response depend on the mineral composition and the amount of each cementing agent.

Application of the technique M5 has resulted in higher deviatoric stress values in the specimens cemented by Portland cement or gypsum than the other cemented specimens tested (Figure 4.41). Also, it was observed that the specimens with calcite or lime prepared by employing the technique M5 have similar behaviours. These responses of the cemented samples may be related to the mineral composition of each cementing agent and with the curing conditions that needs for each of them individually. The response of the clean sand has exhibited always much smaller deviatoric stress than the other specimens within the measured strain level.

4.4.2 Variation of the stress path space of cemented sand prepared by various methods

Figures 4.42-4.45 present the stress path space for the specimens with various cementing agents and various sample preparation techniques. The most striking point in these plots is that the specimens with gypsum, calcite, and lime exhibit similar behaviour. The clean sand specimen exhibits a dilation process. However, the specimens with the three cementing agents show a contractive behaviour, which

increases as the amount of cementing agent increase. The causes of such behaviour are thought to be a weak or no cementation between the sand grains, where the cementing agents behave like fine materials. Therefore, the specimens with increasing amount of cementing agent results in a more contractive behaviour, especially in the method M1, M2 and M3. The cemented specimens were prepared by employing the technique M4 exhibit dilative behaviour at the beginning of the shear and then the behaviour changed to contractive behaviour as the test continued. This behaviour may be due to breakage of the cementing bonds as the axial strain increase or could be because of the pore water generation. As reported by Ismail et al., (2002), the yield occurs due to broken of the bonds that created by hydration of cementing agent. He mentioned that the shearing mechanism before yield is primarily cohesive with stress mainly carried through the cement bond and little frictional strength. Therefore, the yielding pattern will be functional to the strength and the nature of the cementing agents as well as to the bonding mechanism created by cementing agents. It is observed from the Figure 4.45 that the specimens cemented by Portland cement exhibit dilative behaviour, and the sample preparation techniques employed in the specimens with this cementing agent were not very much effective on the stress path results.

Figures 4.46 and 4.47 make a comparison between the stress path results of the specimens cemented with various cementing agents and tested by employing the techniques M4 and M5, respectively. Figure 4.46 indicates a clear difference between the results obtained using gypsum, calcite, lime and Portland cement. Also, the specimen cemented with Portland cement exhibits strong dilation from the beginning of the test. The author considers that the results observed in the Figure 4.46 were because of the cementing agents which actively take part as “bonds” or as “fine materials” in the specimens. The results were in agreement with the conclusion reported by Ismail et al., (2002). However, the specimens cemented with any cementing agent prepared by the procedures described in M5 produce the same responses (Figure 4.47). The effects of the cementing agents could not be observed in the Figure 4.47. It is interpreted that the cementing agents were not activated because of the lack of water. It is also thought that the amount of non-activated cementing agents taken place in the pores were not enough to change the overall behaviour of the specimens. In addition, similarity in the stress path response may be due to the

specimens tested in the unsaturated state and there is no excess pore water pressure generated during shearing of the specimens. Moreover, the generation of the excess pore water pressure itself depends on the type, properties of the cementing agents and level of the cementation.

4.4.3 Small strain stiffness of the cemented sand prepared by various methods

Variations of the undrained stiffness considering the variation of the Young's modulus of the cemented specimens versus the average local axial strain, on a log-log scale are presented in the Figures 4.48-4.53. For accurate measurements of the small strain stiffness, the axial strain was measured locally using LVDTs. Degradation of the undrained secant Young's modulus of the specimens tested was measured at effective confining pressures of 100 kPa. Variation of the secant Young's modulus results for the specimens with various cementing agents prepared using different methods was studied. In order to have an understanding if the Young's modulus and yielding of the cemented specimens is a function of cementing agent type and sample preparation method, the results were compared within the range of 0.001% to 5% strain levels. In general, for all types of the cementing agents and for all sample preparation methods, there are degradations in the specimen stiffness with the axial strain.

It is observed from the Figures 4.48-4.50 that the specimens cemented with gypsum, calcite, and lime that were prepared by employing the techniques M1, M2, and M3 exhibit stiffness values close to the stiffness of clean sand or stiffness values less than its value in clean sand specimen. However, the same specimens tested by employing the techniques M4 or M5 exhibit higher stiffness values within the measured strain level. The author considered that a cementation did not take place, or it was broken after loading in the techniques M1, M2, and M3. Also, the cemented specimens prepared employing the method M5 have higher stiffness values than their values in the method M4. This behaviour is similar in all types of cementing agents. This response might be due to cementing bonds may lose from their strength during the saturation and consolidation steps of the test.

The locations of the first yield (FY) and bond yield (BY) estimations were made based on the Malandraki and Toll (2000). First drops and second drops in the secant

Young's modulus-strain curves were described as 'first yield' and 'bond yield (second yield)', respectively. Location of the first yield (FY) and bond yield (BY) in the specimens tested by employing the different techniques were indicated on the curves. The yielding points (first yield and bond yield) clearly appeared in the cemented specimens that prepared employing methods M4 and M5. Strikingly, for the cemented specimens with the calcite and lime, the first and bond yield of the cemented specimens employing method M4 locate at strain levels less than their strain in the specimens prepared employing the method M5 (Figure 4.49 and 4.50). This behaviour might be attributed to broken of the some bonds between the soil grains during the saturation and consolidation steps of the triaxial test. Since yielding occurs at small strain levels, the significance of the development of local displacement transducers can be seen. The fact is that local strain instrumentation with high accuracy and precision in laboratory testing techniques has shed new light on soil behaviour at small strains (Burland and Symes, 1982; Jardine et. al, 1984; Clayton and Khatrush, 1987; Clayton and Heymann, 2001).

Unlike cemented specimens with the gypsum, lime, and calcite, the cemented specimens with Portland cement exhibited stiffness values greater than the uncemented specimens regardless of the effect of the sample preparation methods as shown in Figure 4.51. The first yield and bond yield for the cemented specimen with Portland cement for all sample preparation methods locate in positions near each to other. Table 4.1 presents the rate of stiffness degradation with local axial strain. The stiffnesses measured at 0.01%, 0.1% and 1% axial strain are given as ratios of the maximum stiffness (E_{max}). E_{max} generally appears at very small strain levels and in this study the stiffness value correspond to 0.001% axial strain was taken as E_{max}. As can be seen from the Table 4.2 a great degradation in the stiffnesses of the cemented sand specimens was occurred after 0.01% axial strain, which was the zone of the bond yield that will be discussed in later sections. In general, this behaviour was appeared in particular in specimens that were tested by following method M4 and M5 and cemented with gypsum, calcite and lime, and all sample preparation technique for specimens with Portland cement.

Figures 4.52-4.53 present comparison of stiffness degradation versus the local axial strain for the specimens prepared and tested using the techniques M4 and M5 for all

cementing agents. As can be seen from the plots, the stiffness of the cemented specimens with cement and lime were greater than those of specimens including gypsum and calcite for the specimens prepared using M4 method. Stiffness of the cement stabilized specimens prepared using the M5 method were greater than the rest of specimens. Also, the stiffness of the specimens with other three cementing agents are close each to other. In particular, stiffness values for the specimens with Portland cement were higher than the others for all testing techniques. From the study by Hamidi and Haeri (2008), the response of cemented sand was thought to be dependent on the physical properties (i.e., grain size, grain shape), and mineral composition of the cementing agents and used sand. The location of the first yield and bond yield differed depending on the type of cementing agents and sample preparation techniques. The location of the first yield varied between 0.0003%-0.003% and 0.0004%-0.0025% axial strain for the method M4 and M5, respectively, while the location of the bond yield varied between 0.003%-0.006% and 0.002% - 0.02% axial strain for the method M4 and M5, respectively. Coop and Willson (2003) highlighted that yield during isotropic compression can be induced by either soil grains crushing or bond breakage and which one of these mechanisms acts first would depend on the grain strength, bond strength and density.

Variations of the cemented sand stiffness versus the deviatoric stress for different types of cementing agents and sample preparation method are presented in Figures 4.54-4.59. In general, for all the cementing agents and sample preparation techniques, it can be observed that there is a well-defined plateau in the stiffness values which extend to relatively high values of the deviatoric stress. This plateau was followed by a sharp decrease in the stiffness values as yielding is approached. Similar results were reported by Cuccovillo and Coop (1997b). As in the stiffness degradation versus average axial strain curves, the stiffness of the cemented sand degrades by increasing deviatoric stress (Figures 4.54-4.56). It is observed from these Figures that stiffness of the cemented specimens with gypsum; calcite and lime employing the M4 and M5 sample preparation technique exhibit higher stiffness values than their values in other methods. This response may be due to cementation may not be occurred in the specimens prepared by following methods M1, M2 and M3, and the cementing materials in this case behave as fine materials as discussed in previous sections. The first yield and the bond yield for the cemented specimens with

gypsum and calcite prepared by following the method M5 occur at a deviatoric stress greater than their values in the method M4. Conversely, the yielding points for the cemented specimens with lime and prepared by following the method M5 occur in deviatoric stress value lower than its value in the method M4. Figure 4.57 shows the variation of the stiffness of the cemented sand with Portland cement versus the deviatoric stress. It can be seen that the sample preparation method did not remarkably affect on the stiffness variation with the deviatoric stress, and yielding points located close to each other.

Figures 4.58and 4.59 present the variation of the stiffness versus the deviatoric stress for the cemented sand with all cementing agents and prepared by following methods M4 and M5. The stiffness of the cemented specimens with cement and lime prepared by following method M4 were higher than those stabilized with gypsum and calcite. Also, in specimens including lime and cement, the yielding points (first and bond yield) were appeared at deviatoric stresses greater than those including gypsum and calcite. Cemented specimens with gypsum, calcite and lime prepared via method M5 produced very close stiffness values and lower than those including Portland cement. In addition, the yield points in the specimens of three cementing agents were appeared at deviatoric stresses close each to other, and lower than its value in the case of specimens with Portland cement. These behaviours may be related to the stiffness and yielding behaviour of the cementing agents themselves that depend on the mineral composition of each of the cementing agents. Therefore, each cementing agent according to its composition needs particular curing condition to produce better strength and behaviour. The photos of cemented sand specimens with all cementing agents after shear are presented in Figure 4.60. The zone of the bond yield clearly appears in the cemented specimens with the gypsum, calcite and lime.

4.4.4 Microscopic study of the cemented sand

The changes of sand microstructure due to gypsum, lime, calcite, and Portland cement play significant role in the mechanical behaviour of these stabilized soils. Cubical specimens of the cemented sands were prepared and dried at 25 ^{o}C and subsequently subjected to a vacuum. The specimens were glued on aluminum holders for scanning. Surfaces of the specimens were coated with gold to obtain images at a good quality. Observations of scanning electron micrograph pictures and

energy dispersive x-ray spectroscopy results are shown through the Figures 4.61-4.62. These Figures give information about textural properties, grain shape, surface roughness, and mineralogy. The SEM pictures of the clean sand, gypsum, lime, calcite, and Portland cement were already presented in the Figures 3.2. It was seen that the sand used consists of relatively sub-rounded coarse grains, however the cementing agents consist of sheetlike or flaky grains. This confirms that the reduction in deviatoric stress observed in the specimens tested by employing the techniques M1, M2, and M3 was due to the cementing agents behaving like as 'fine materials' instead of a 'bonds'. Figure 4.61 shows the SEM pictures of the sand with hydrated gypsum, lime, calcite, and Portland cement, respectively. It is clearly observed that the sand grains were covered by hydrated cement products, and the voids were filled with the cementing agents and the contacts between the soil grains welded with the hydrated cementing agents. A similar observation was made by Ismail et al. (2002). EDX results carried out to investigate the mineralogical aspects of the bonding between sand grains and the cementing agents. The results were presented in Figure 4.62. It was observed that the amount of silicon (Si^{4+}) and calcium (Ca^{2+}) elements varies with cementing agent types. As an overall view, the amount of Ca^{2+} increases while the amount of Si^{4+} reduces with various ratios of bonding that takes place due to various cementing agents.

4.5 Behaviour of biocemented sands

A series of the undrained triaxial tests were conducted to investigate the behaviour of the biocemented sand specimens. This series of tests was mainly directed towards the stress-strain behaviour and small strain stiffness of biocemented sand specimens. The specimens cemented with three different levels of microbial products, which represents the light (BT1), moderate (BT2) and heavy cementation (BT3), were prepared and tested under 100 kPa effective confining stress. The specimens of biocemented sand were prepared by following the sample preparation method that explained in details in the section 3.5.2 and tested according to procedure illustrated in section 3.5.3 in chapter 3. A second group of the tests was conducted for natural sand in the three saturation states, namely dry, fully saturated and partially saturated state to study the behaviour of the natural sand in these conditions and the last one

was taken as a benchmark for biocemented sand tests. The efficiency of the biocementation method was compared with the rest of methods.

4.5.1 Stress-strain response of biocemented sand

The biocemented triaxial specimens were sheared after completing the biocementation process and curing of the cementing material that precipitated within the soil matrix. To neglect the effect of the back pressure on the cemented calcite that may break calcite bonds between sand grains, the biocemented triaxial specimen tests were performed under 100 kPa cell pressure and 0 kPa back pressure.

Variation of the deviatoric stress with the local axial strain for the three levels of biocementation was presented in Figure 4.63. The deviatoric stress versus axial strain behaviour of the specimens significantly changes with the employed techniques that provide different amounts of microbial products for cementation. The sand grains are assumed to be in clean contact with each other in the clean sand specimen, and hence the mechanical behaviour of this specimen was governed by the sand grains only. However, cementing material (calcite) formed by biocementation process covers the sand grains and creates cementing bonds between them, and the mechanical behaviour of the cemented specimens was initially governed by the bonds. Also, a significant increase in the deviatoric stress values was observed as the duration of application of biological treatment increases. The author considers that the biological treatment of the specimens under a certain confining pressure plays an important role in the strength increase. The fact is that an increase in duration of the biological treatment process, which corresponds to the number of urea-calcium chloride cycles, resulted in an increase in the amount of calcite precipitating on and between the sand grains. These results were improved by the microscopic analyses SEM and EDX which are presented in the last two figures. It is clearly observed from EDX results that the amount of the Ca^{4+} increases in the treated specimens as the treatment period increases. The increases of the Ca^{4+} in the treated specimens tend to increase the amount of the cementing calcite ($CaCO_3$). Similar results were obtained by DeJong et al., (2006), Whiffin et al., (2007), and Al-Qabany and Soga (2013). They observed an increase in the shear strength of the biocemented specimens, and verified the calcite precipitation on the sand grains by microscopic investigations. Contrery to these, Ozdogan (2010) concluded that bio-treated specimens generally did not exhibit

stress-strain behaviour that was significantly different than the control specimens. She thought that the cemented specimens were disturbed during the saturation by application of back pressure. Therefore, in this study to neglect the specimen disturbance and brokage of cementation bonds, the flushing of the bacteria solution at the beginning and the urea-calcium chloride during the treatment process and curing of the cemented specimens were conducted under confining pressure. The treatment of the specimens under confining pressure and the curing of the cementing material after finishing the treatment process play an important role in the increasing strength. From the microscopic studies made and mentioned by Bang et al., (2001), Dejong et al., (2006), Ozdogan (2010), and Al-Qabany and Soka (2013), the calcite ($CaCO_3$) that precipitated within the soil matrix covers the sand particles from one hand and makes a bonding bridge between the sand grains at the grains contact on the other hand. Therefore, an improvement occurs in the stress-strain and stiffness of the sand.

Efficiency of the biocementation method was compared with cemented specimens with conventional cementing agents. Under this objective the specimens were cemented with gypsum, lime and calcite and prepared by following method M5 were selected. Figure 4.64 shows deviatoric stress versus local axial strain variation for the clean sand (fully saturated, partially saturated and dry), biocemented sands (BT1, BT2 and BT3) and sands cemented with conventional agents (gypsum, calcite and lime). The clean sand tested at fully saturated state has the lowest deviatoric stress values, as expected, in all strain levels. As an overall view, it was seen that there is a similarity between the response of biocemented sand with BT3 and that of sand cemented with calcite and lime. This behaviour is due to chemical compositions of the biominerals may be similar to chemical compositions of calcite and lime rather than gypsum's compositions which composed of calcium and sulphate minerals. The cemented sands with BT1 and BT2 have a relatively lower deviatoric stresses over the measured range of strain if its compared with BT3 specimens. This behaviour is due to formation of low amount of calcite in BT1 and BT2 relative to its amount in BT3.

4.5.2 Small strain stiffness of biocemented sand

The small strain stiffness of the natural and cemented sand as mentioned in the previous sections play an important role in the geotechnical applications as indicated by Jardine et al. (1987), Cucovillo and Coop (1997b), and Clayton and Heymann (2001). Therefore, it is a good opportunity to improve the small strain stiffness of the sand by the biocementation. For accurate measurement of the stiffness at small strain levels, the LVDTs were used in the present study to allow the accurate measurements of displacement over a certain range of strains which are interesting to geotechnical engineers. Variation of the stiffness of biocemented sands with the local axial strain was presented in Figure 4.65. As can be seen from the Figure 4.65.a, stiffness of the biocemented sand specimen at strain levels less than 1% increases as the treatment duration increase. Also, stiffness values for the three specimens were very close to each other at a strain range higher than 1% axial strain level. This behaviour may be the cementation between the sand grains was broken during shear; the stiffness of the biocemented specimens degrades to stiffness values close to the stiffness of clean sand. The stiffnesses for clean sand and biocemented sand specimens (BT1, BT2, and BT3) appear to exhibit a plateau at strain levels less than 0.001% (Figure 4.65.b). In particular, the limit of the plateau appeared different in the BT3 treated sand, and was found to be in a wider range of axial strain. Actually, such a plateau is an indicative of linear stress-strain behaviour of a geomaterials (Clayton and Heymann, 2001). Stiffnesses of the four specimens were found to be markedly different. Figure 4.65 shows that the maximum stiffness measured at small strains (less than 0.001%) were approximately 818.17 MPa, 496.62 MPa, 220.77 MPa and 141.9 MPa for the BT3 treated sand, BT2 treated sand, BT1 treated sand and clean sand, respectively. Degradation of stiffnesses for all four specimens was presented using four different strain levels (0.001%, 0.01%, 0.1% and 1%) in Table 4.2. The stiffness degradation for the biocemented specimens was found to be higher than that for the clean sand; this may be due to bonding breakage. Figure 4.66 indicates the stiffness variation with deviatoric stress for the biocemented specimens and clean sand. A slight decrease followed by a sharp decrease in the stiffness of biocemented specimen was observed, while a gradual decrease in the stiffness of clean sand was observed. The sharp decrease, due to the bonding breakage, is a distinctive behaviour of typical

artificially cemented sand. Figure 4.67 presents the pictures of specimens immediately after the test. The specimens were found to be cemented.

Figure 4.68 presents the degradation of stiffnesses with local axial strain for the clean sand (fully saturated, partially saturated and dry), biocemented sands (BT1, BT2 and BT3) and sands cemented with conventional cementing agents (gypsum, calcite and lime). The cemented sand specimens with conventional cementing agents were prepared by following the method M5, because this method was similar to the sample preparation and testing condition of the biocemented specimens. In general, the stiffness values at the small strain level of the biocemented sand specimens (BT2 and BT3) were found to be closer to the stiffness values of the cemented specimens with 12% of cementing agents (gypsum, calcite and lime). Also, as the strain increase the biocemented specimens exhibit sharp degradation in the stiffness values as other cemented specimens with the cementing agents, and their values become closer to the stiffness of uncemented specimens. The similarity in this behaviour may be depends on the properties of the cementing material itself, including the mineral composition and the stiffness of this material. As stated out by Malandraki and Toll (2000), and Cuccovillo and Coop (1997b) a sharp drop in the stiffness-axial strain curve point out bond yield. Degradation of stiffness with the strain for all geomaterials tested was pointed out using four different strain levels (0.001%, 0.01%, 0.1% and 1%) and given in Table 4.2. The significant degradations in the stiffness of the cemented sands were appeared between 0.1%-0.001 % axial strains. Therefore, this zone of the axial strain (0.1%-0.001 %) as the author interpreted may be the bond yield zone.

The stiffness variation versus deviatoric stress for clean sand in all saturation conditions, biocemented sands in all treatment levels, and cemented sands with conventional cementing agents were presented in Figure 6.69. There are plateaus in the stiffness values with the deviatoric stress and the difference in behaviour between the cemented and uncemented sand specimen is confirmed by the relatively high deviatoric stress values at the failure. In addition, a sharp drop appears in the stiffness of the cemented specimens as the deviatoric stress increases (before 300 kPa for untreated sand and before 400 kPa for cemented sand). The sharp drops may indicate to broken of the cemented bonds. In addition, it is clearly observed that the

response of the biocemented sand and especially the BT2 and BT3 were close to the lime and calcite cemented specimens.

4.5.3 Microscopic study of the biocemented specimens

Microscopic study of the biocemented specimens was performed to direct observation the distribution and characteristics of the cementing materials produced from the bacterial activity. Microscopic investigation of the clean sand and biocemented sand specimens was performed using SEM and EDX analyses, which were shown in Figures 4.70 and 4.71. It is seen that the calcite crystals were precipitated on to grains' surface as well as on contacts between grains (Figure 4.71). Amount of the precipitated calcite was seen to be higher as the duration of biocementation treatment increases. Increasing in the amount of the calcite with the treatment period was predicted from the amount of the Ca^{4+} that becomes higher as the treatment level increase (Figure 4.70). Observations made using the SEM pictures and EDX analyses revealed that increase in strength and stiffness of the biocemented sand specimens is likely due to precipitated calcite in soil matrix. The biominerals that precipitate in the soil matrix cover the soil grain surfaces which change the surface roughness, precipitate on the grain contacts which make bonding bridge between sand grains, and fill the voids between the grains which increase soil density. Similar observations were made by Stocks-Fischer et al., (1999); Bang et al., (2001); DeJong et al., (2006, 2010); Ozdogan, (2010); Meyer et al., (2011); Burbank et al., (2012); Al-Qabany and Soka (2013); and Sel et al., (2015).

Table 4.1 Stiffness degradation with local axial strain.

Specimens	Cementing agents	$E_{0.001}$ (MPa)	$E_{0.01}$ (MPa)	$E_{0.1}$ (MPa)	$E_{1.0}$ (MPa)	$E_{0.01}/E_{0.001}$	$E_{0.1}/E_{0.001}$	$E_{1.0}/E_{0.001}$
Sand	----	130.1	96.2	51.71	13.28	0.74	0.40	0.10
Sand + 4% cement M1	Cement	370.5	273.7	122.24	26.47	0.74	0.33	0.07
Sand + 12% cement M2	Cement	4693.49	3314.18	Failed	Failed	0.71	Failed	Failed
Sand + 12% cement M3	Cement	5522.98	4630.03	Failed	Failed	0.84	Failed	Failed
Sand + 12% cement M4	Cement	3344.77	3296.63	Failed	Failed	0.98	Failed	Failed
Sand + 12% cement M5	Cement	3571.37	2106.8	Failed	Failed	0.59	Failed	Failed
Sand + 4% lime M1	Lime	63.63	71.19	33.18	9.39	1.12	0.52	0.15
Sand + 12% lime M2	Lime	90.21	87.95	31.34	4.29	0.97	0.35	0.05
Sand + 12% lime M3	Lime	139.61	52.98	31.48	5.65	0.38	0.23	0.04
Sand + 12% lime M4	Lime	2115.61	1165.82	138.15	Failed	0.55	0.06	Failed
Sand + 12% lime M5	Lime	512.13	403	180.29	32.83	0.79	0.35	0.06
Sand + 4% gypsum M1	Gypsum	83.42	82.51	40.99	9.35	0.99	0.49	0.11
Sand + 12% gypsum M2	Gypsum	149.55	107.44	58.95	7.87	0.72	0.39	0.05
Sand + 12% gypsum M3	Gypsum	92.26	89.69	38.5	6.39	0.97	0.42	0.07
Sand + 12% gypsum M4	Gypsum	155.93	167.3	73.62	12.5	1.07	0.47	0.08
Sand + 12% gypsum M5	Gypsum	805.16	468.48	148	Failed	0.58	0.18	Failed
Sand + 4% calcite M1	Calcite	100.22	91.26	35.44	8.08	0.91	0.35	0.08
Sand + 12% calcite M2	Calcite	119.47	100.11	46.51	6.62	0.84	0.39	0.05
Sand + 12% calcite M3	Calcite	91.36	73.44	34.43	5.88	0.80	0.38	0.06
Sand + 12% calcite M4	Calcite	128.2	89.22	46.17	13	0.69	0.36	0.10
Sand + 12% calcite M5	Calcite	288.18	269.83	114.03	35.86	0.94	0.39	0.12

Table 4.2 Stiffness degradation of biocemented specimens with local axial strain.

Specimens	Cementation method	$E_{0.001}$ (MPa)	$E_{0.01}$ (MPa)	$E_{0.1}$ (MPa)	$E_{1.0}$ (MPa)	$E_{0.01}/E_{0.001}$	$E_{0.1}/E_{0.001}$	$E_{1.0}/E_{0.001}$
Sand	----	141.908	92.585	47.383	17.229	0.652	0.333	0.121
Sand (dry state)	----	155.041	115.003	61.273	21.869	0.741	0.395	0.141
Sand (saturated state)	----	130.15	95.072	51.715	13.276	0.730	0.397	0.102
Sand + BT1	Biocemented	220.175	132.626	66.263	18.057	0.602	0.300	0.082
Sand + BT2	Biocemented	496.62	215,835	95.874	23.787	0.434	0.193	0.047
Sand + BT3	Biocemented	818.471	675.763	217.166	32.187	0.825	0,265	0.039
Sand + gypsum	Gypsum	805,169	468.479	148.002	Failed	0.541	0.171	Failed
Sand + lime	Lime	512.139	393.707	180.296	32.839	0.768	0.352	0.064
Sand + calcite	Calcite	288.181	269.829	114,027	35.862	0.936	0.395	0.124

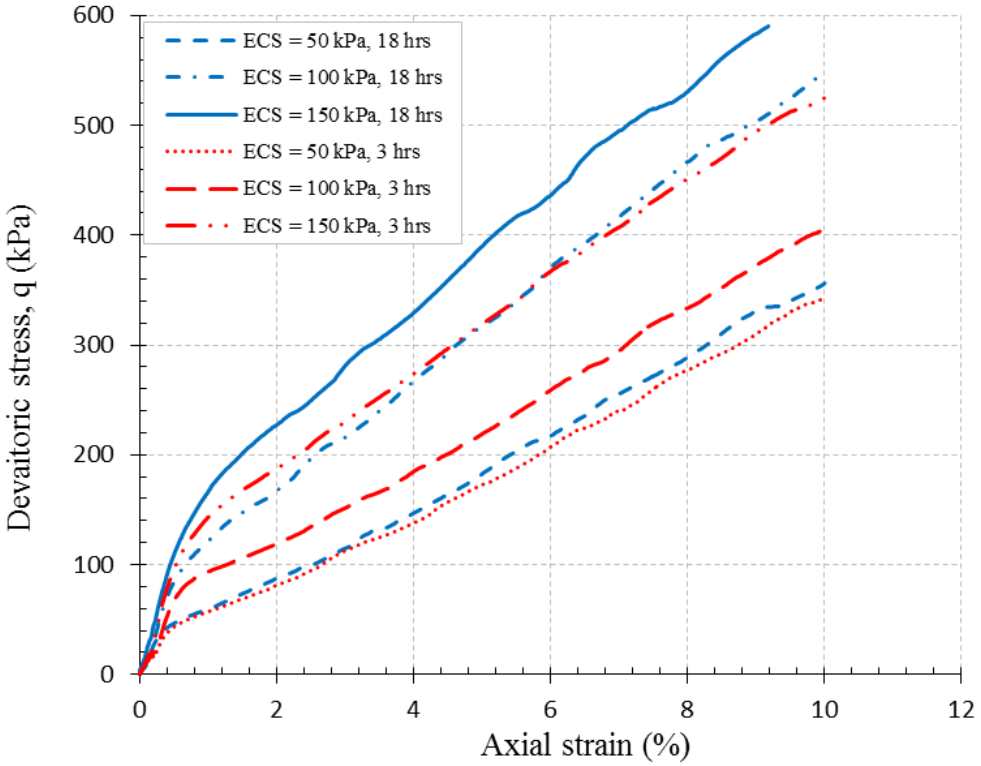

(a)

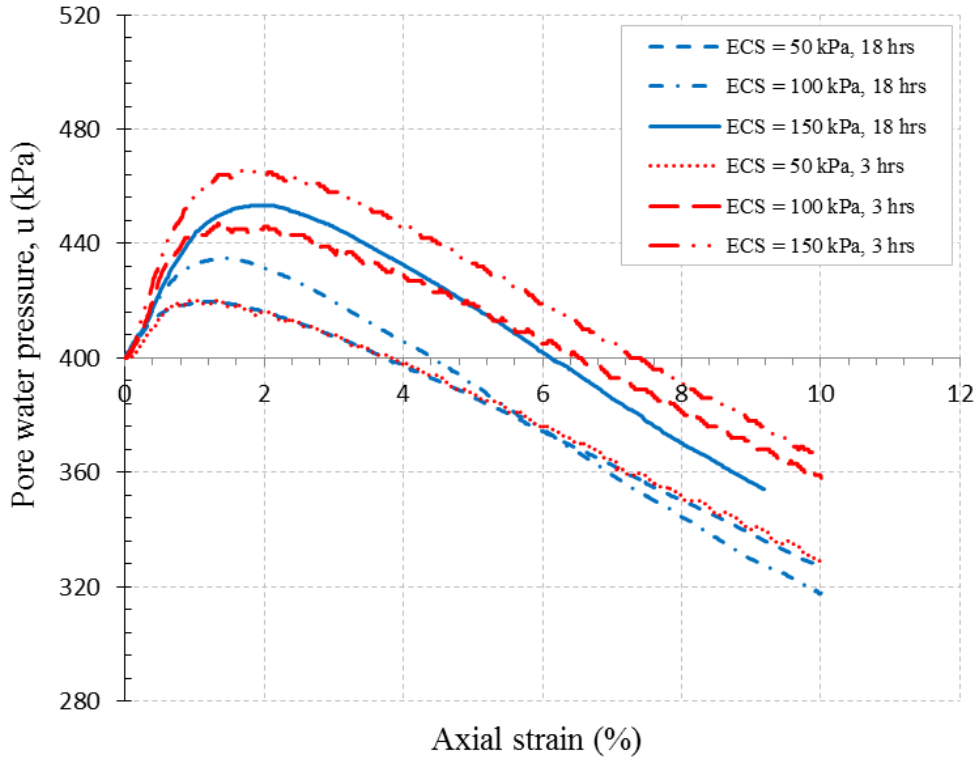

(b)

Figure 4.1 (a) Stress-strain and, (b) pore water pressure versus axial strain curves for clean sand tested in CU condition with 18 and 3-hours isotropic consolidation period.

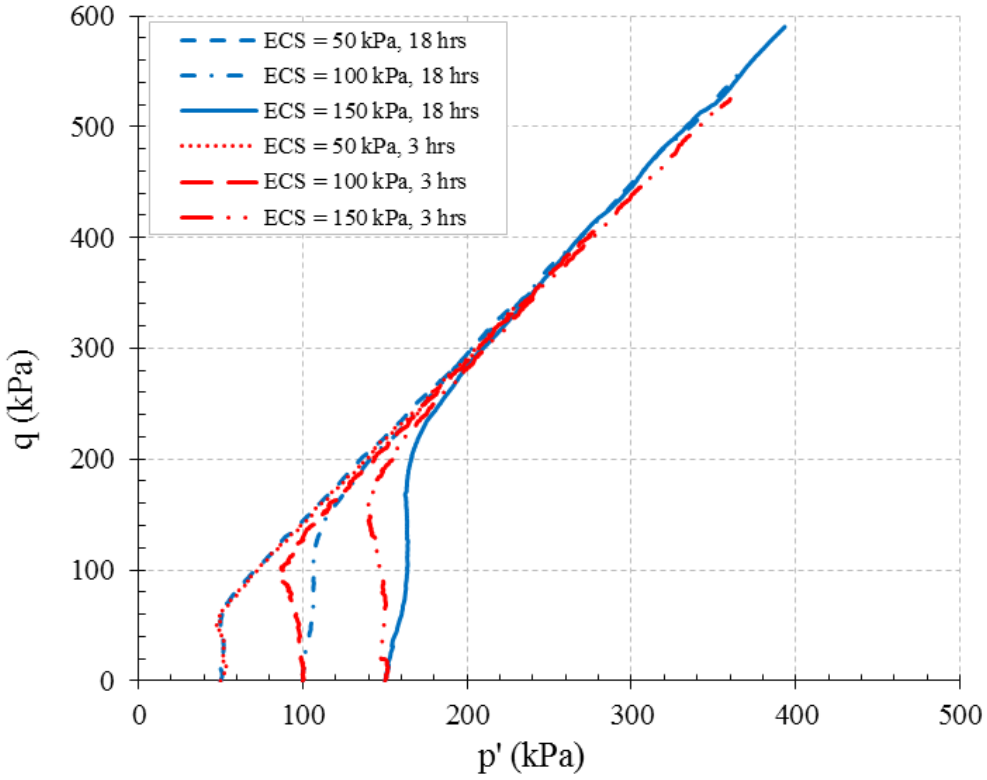

Figure 4.2 Stress path space of clean sand tested in CU condition with 18 and 3-hours isotropic consolidation period.

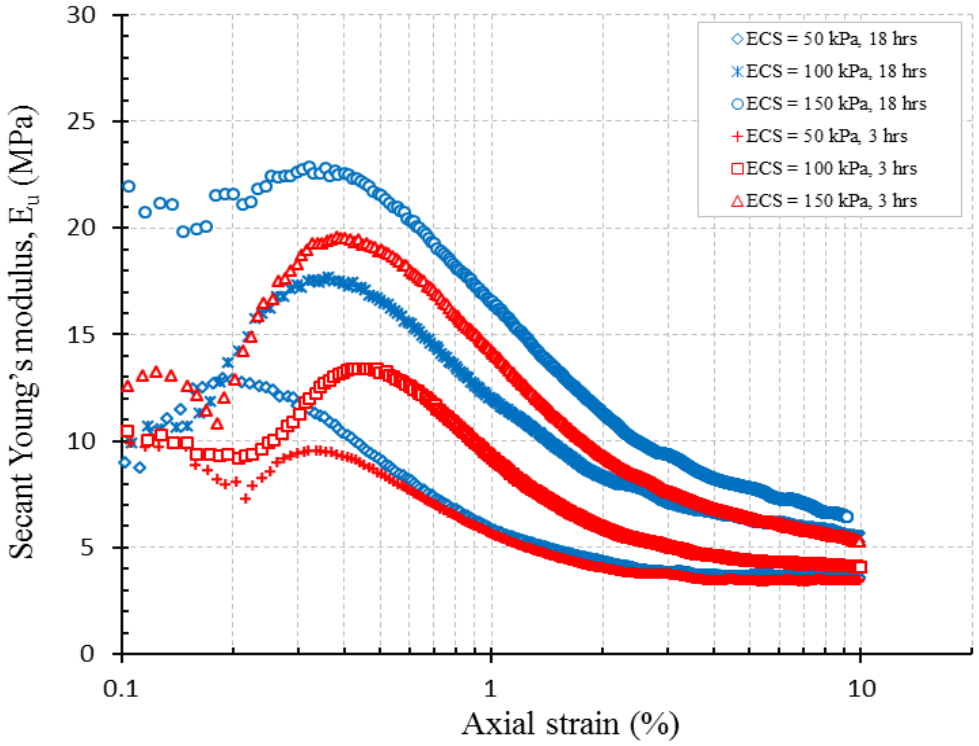

Figure 4.3 Comparison of secant Young's modulus for clean sand tested in CU condition with 18 and 3-hours isotropic consolidation period.

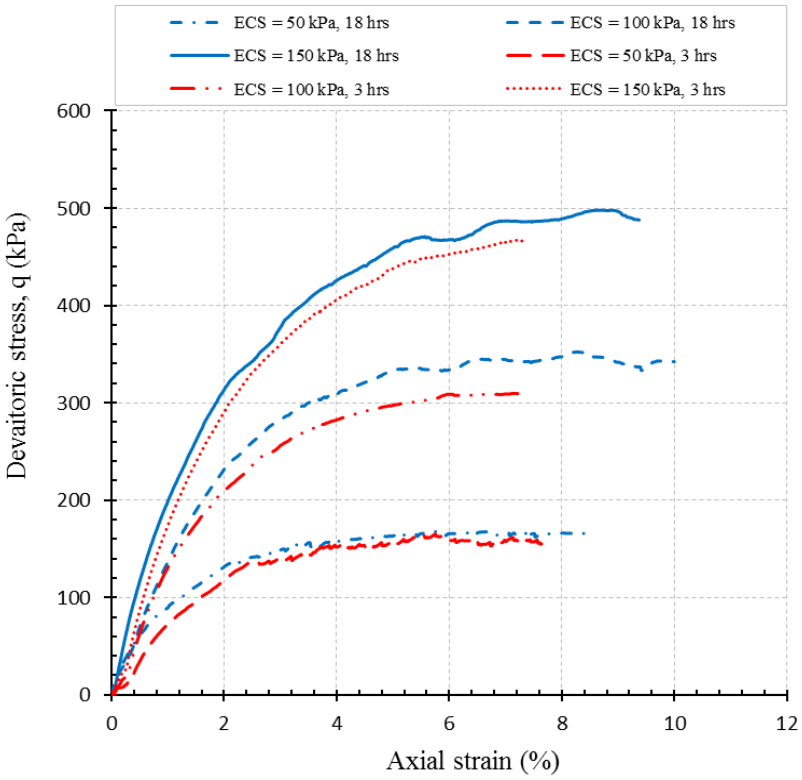

(a)

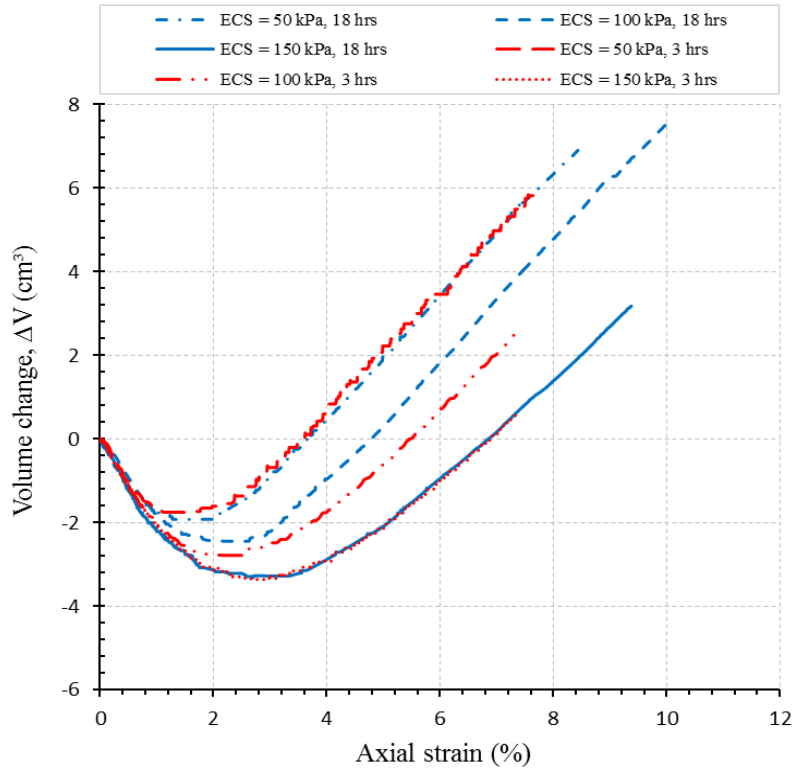

(b)

Figure 4.4 (a) Stress-strain and, (b) volume change versus axial strain curves for clean sand tested in CD condition with 18 and 3-hours isotropic consolidation period.

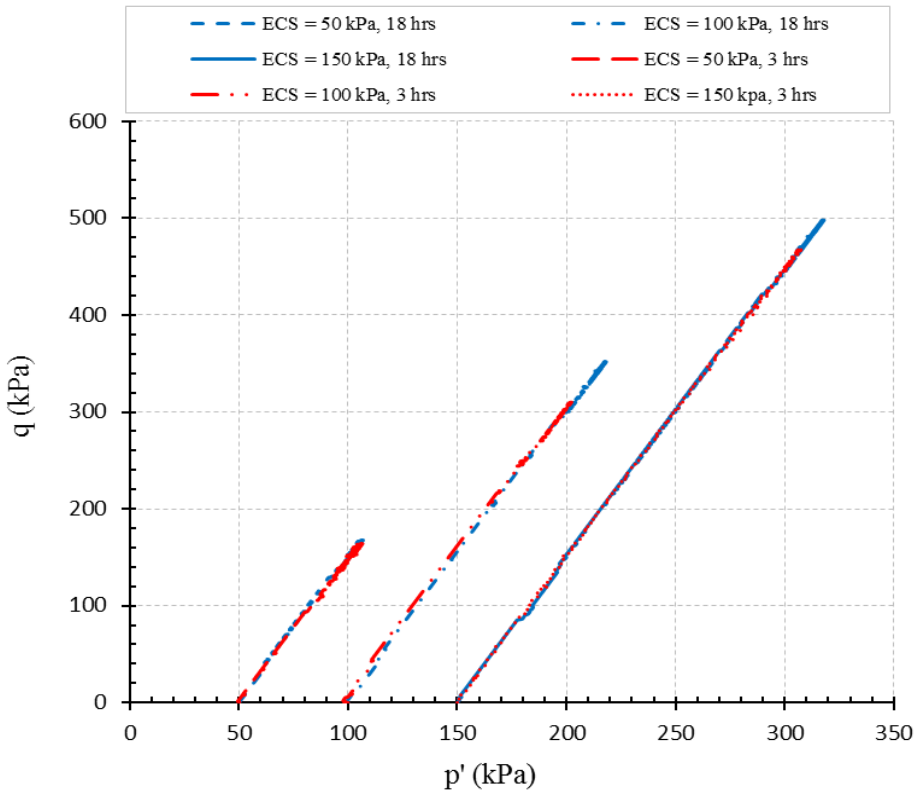

Figure 4.5 Stress path space of clean sand tested in CD condition with 18 and 3-hours isotropic consolidation period.

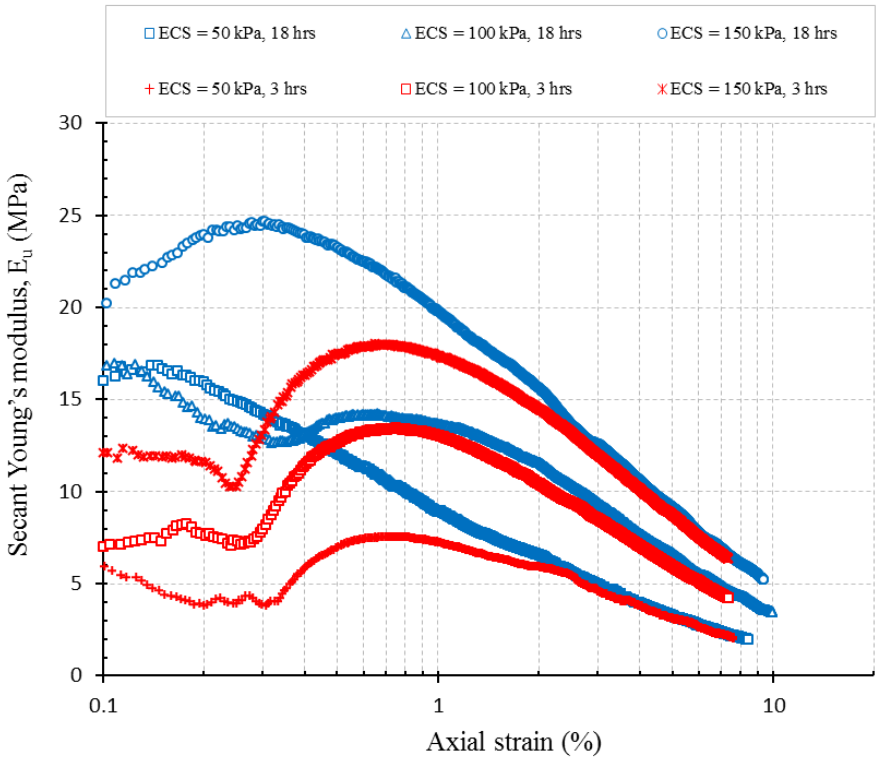

Figure 4.6 Comparison of secant Young's modulus for clean sand tested in CD condition with 18 and 3-hours isotropic consolidation period.

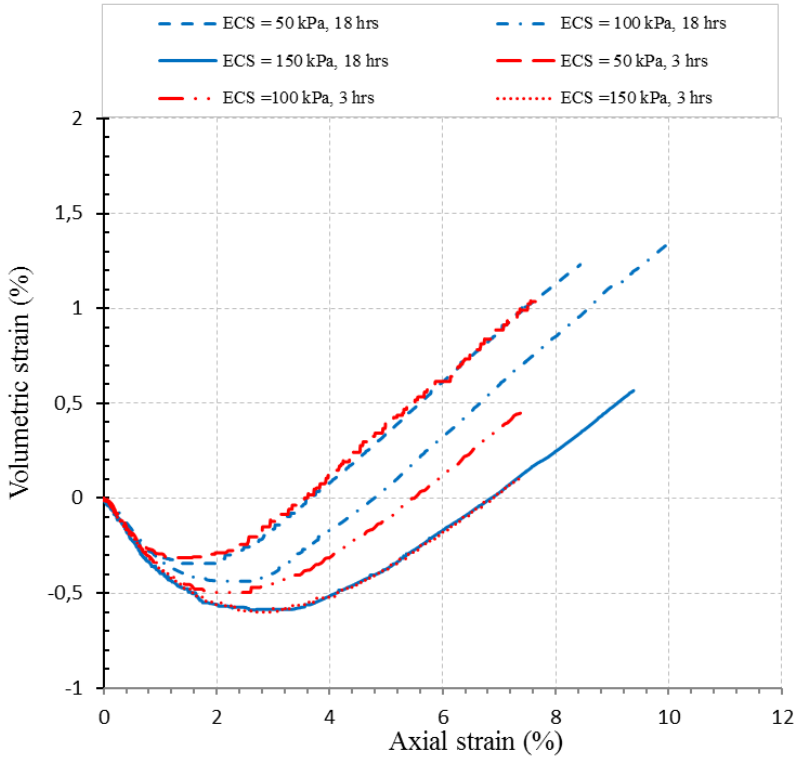

Figure 4.7 Volumetric strain changes with axial strain for clean sand tested in CD condition with 18 and 3-hours isotropic consolidation period.

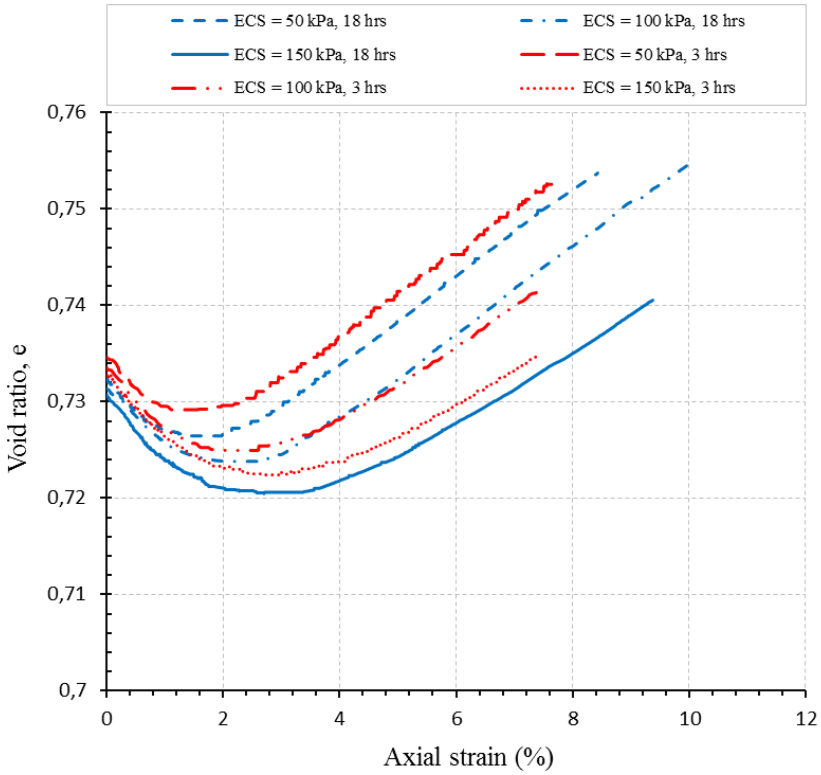

Figure 4.8 Variation of the void ratio with axial strain for clean sand tested in CD condition with 18 and 3-hours isotropic consolidation period.

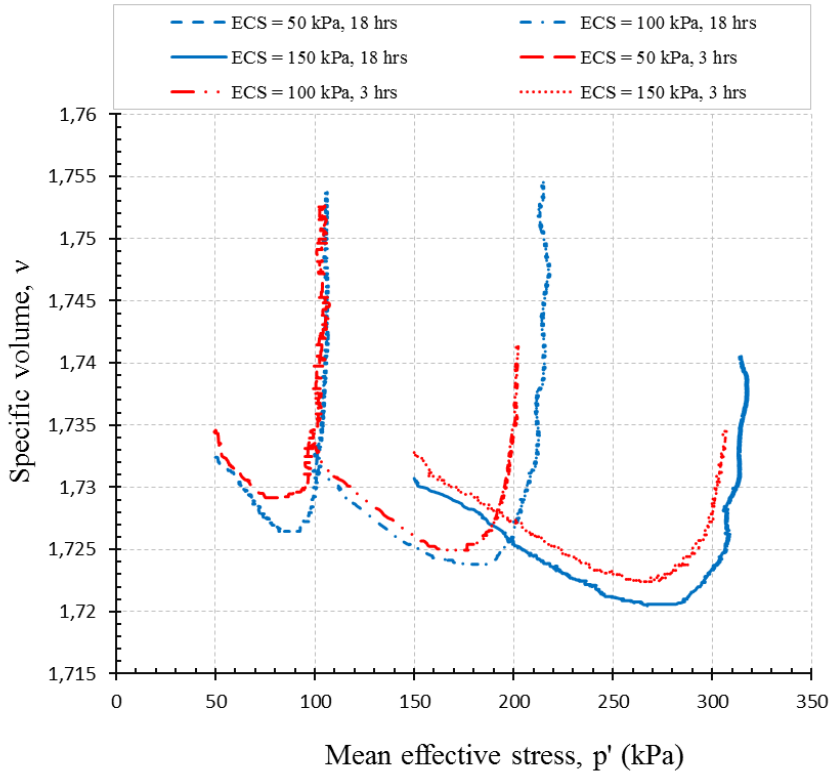

Figure 4.9 Variation of the specific volume with the mean effective stress for clean sand tested in CD condition with 18 and 3-hours isotropic consolidation period.

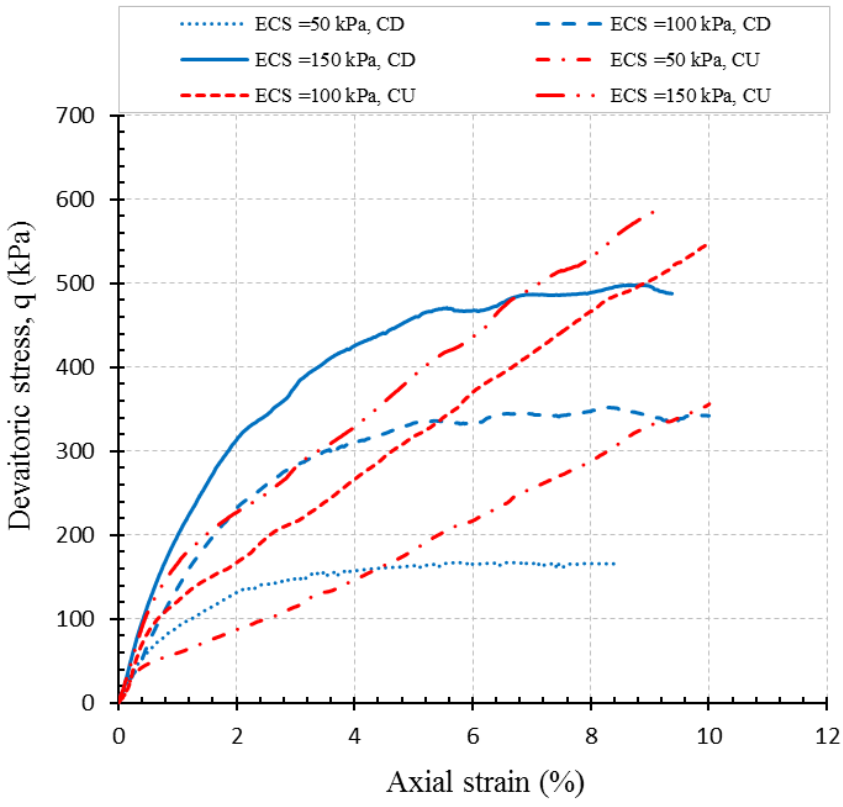

Figure 4.10 Stress-strain behaviour variation between CU and CD tests of clean sand with 18 hour isotropic consolidation period.

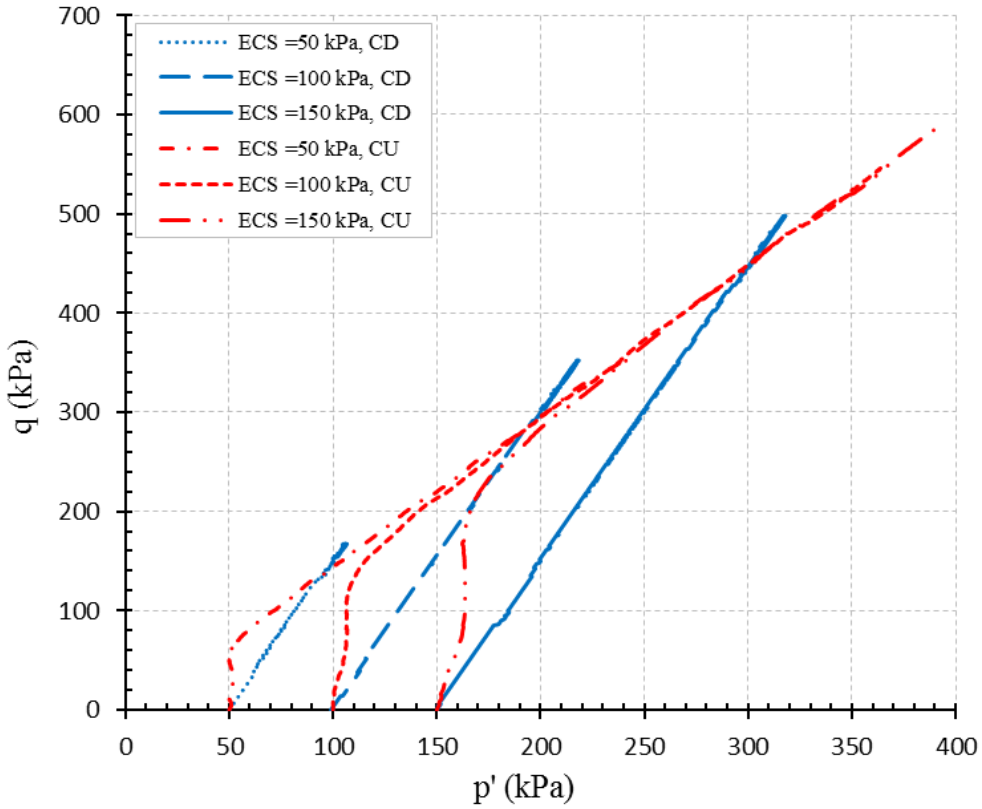

Figure 4.11 Stress path space graphs variation between CU and CD tests for clean sand with 18 hour isotropic consolidation period.

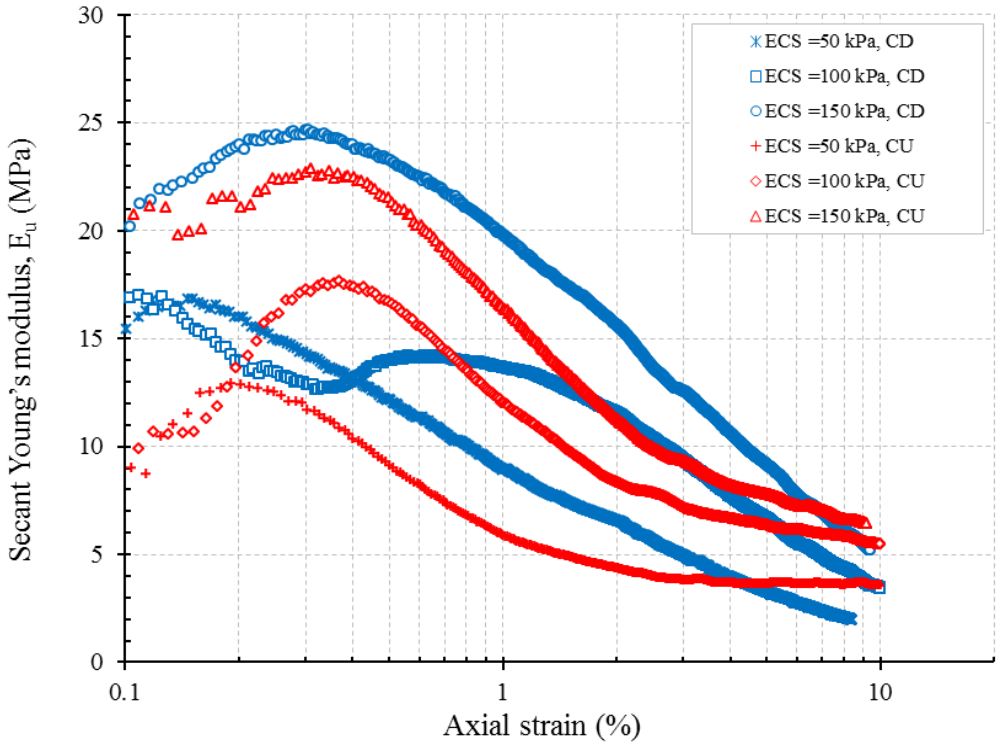

Figure 4.12 The secant Young's modulus degradation with strain of CU and CD tests of clean sand with 18 hours isotropic consolidation period.

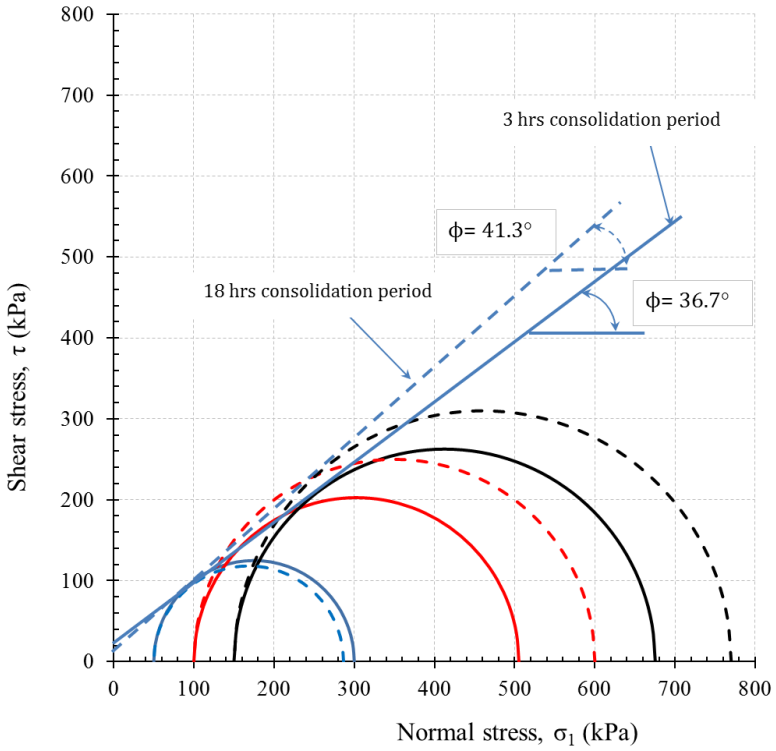

Figure 4.13 Effects of consolidation period on the failure envelopes of clean sand, CU tests (total stresses).

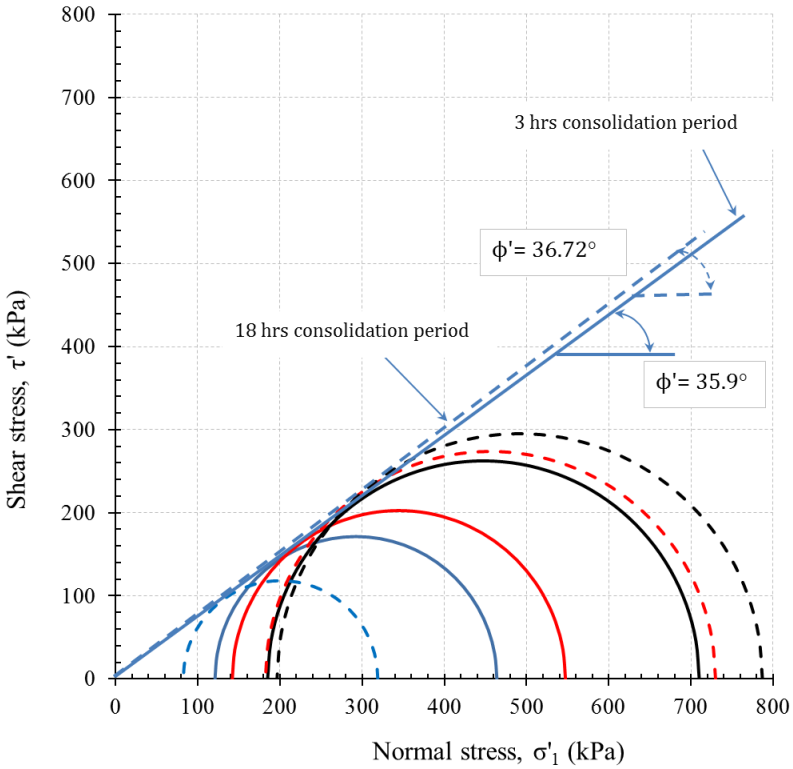

Figure 4.14 Effects of consolidation period on the failure envelopes of clean sand, CU tests (effective stresses).

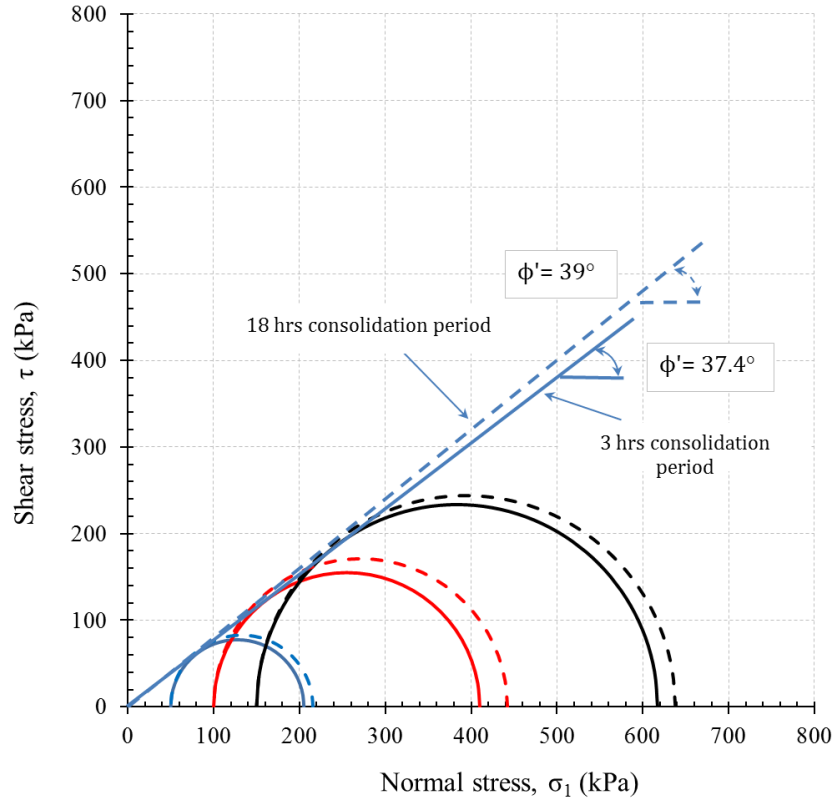

Figure 4.15 Effects of consolidation period on the failure envelopes of clean sand, CD tests.

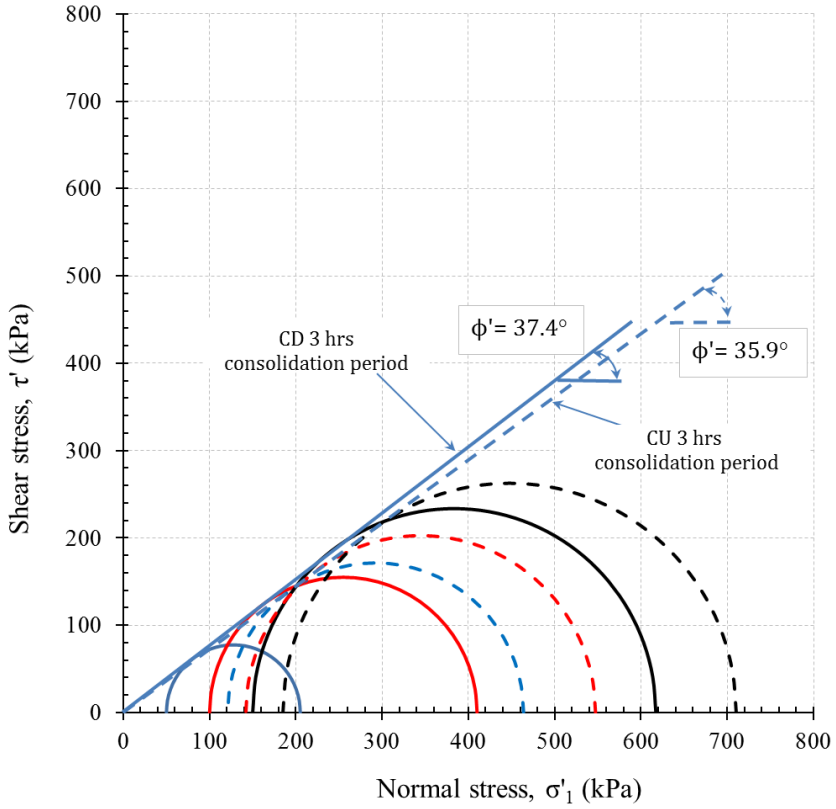

Figure 4.16 Failure envelopes of clean sand tested in CU and CD conditions with 3 hours consolidation period (effective stresses).

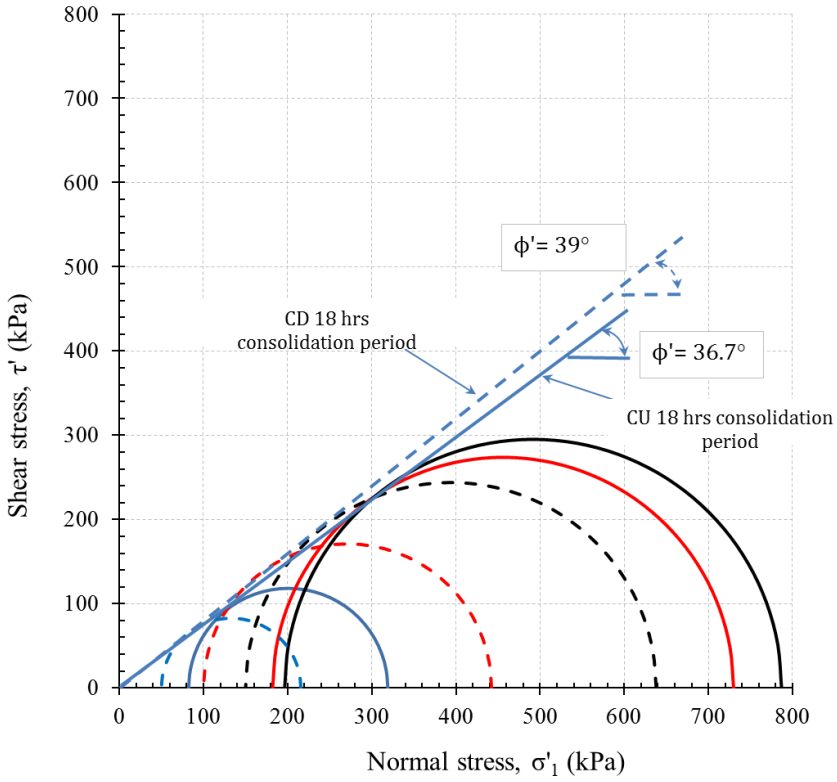

Figure 4.17 Failure envelopes of clean sand tested in CU and CD conditions with 18 hours consolidation period, (effective stresses).

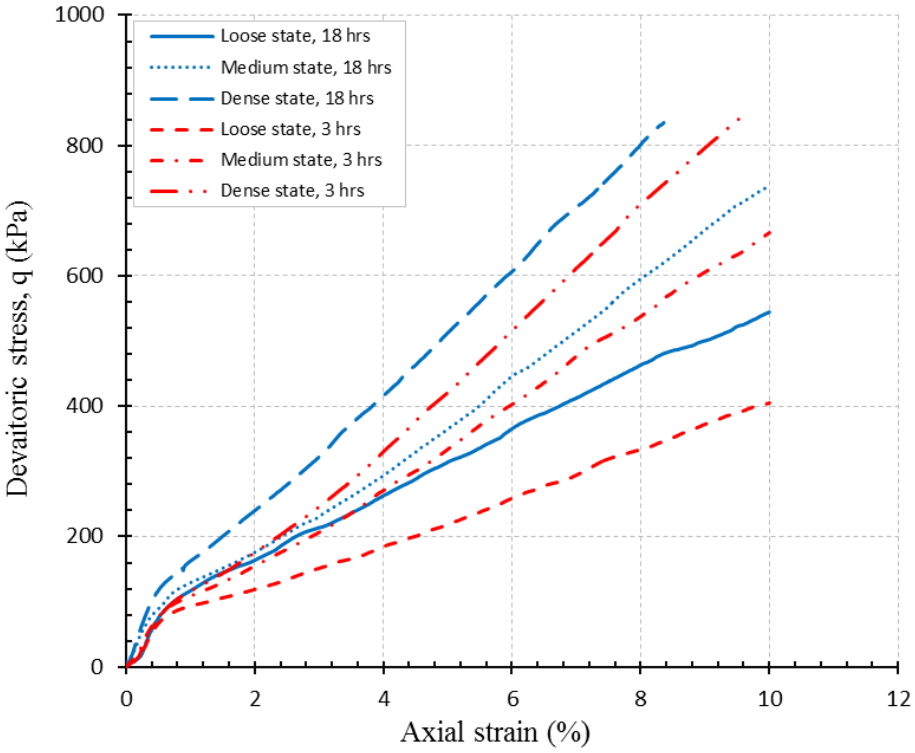

(a)

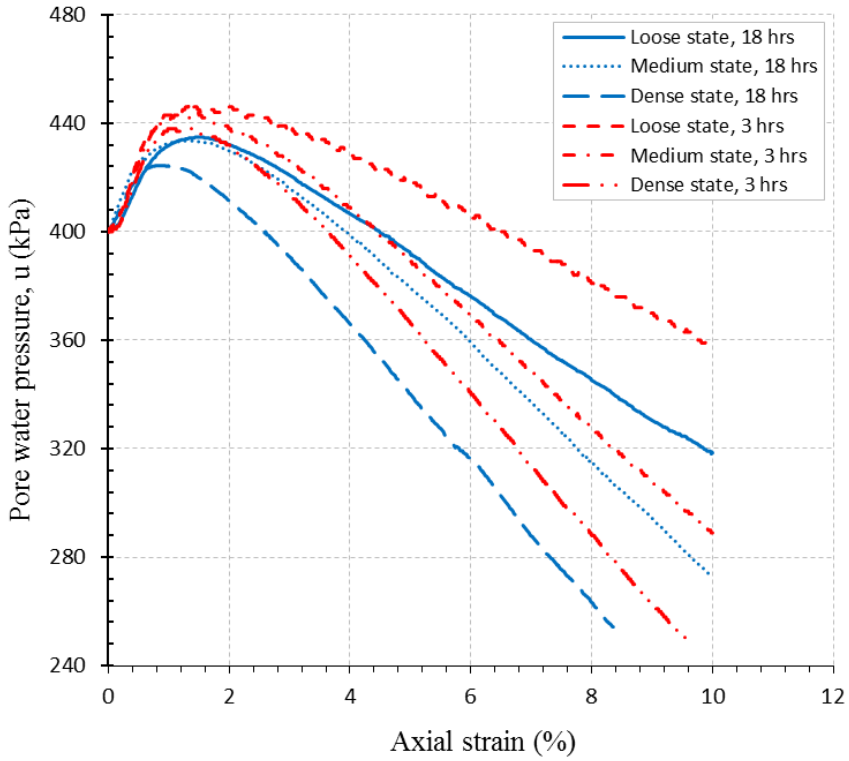

(b)

Figure 4.18 Effects of the relative density on the (a) stress-strain behaviour (b) pore water pressure generation of the specimens tested in CU conditions and consolidated at 18 and 3-hours.

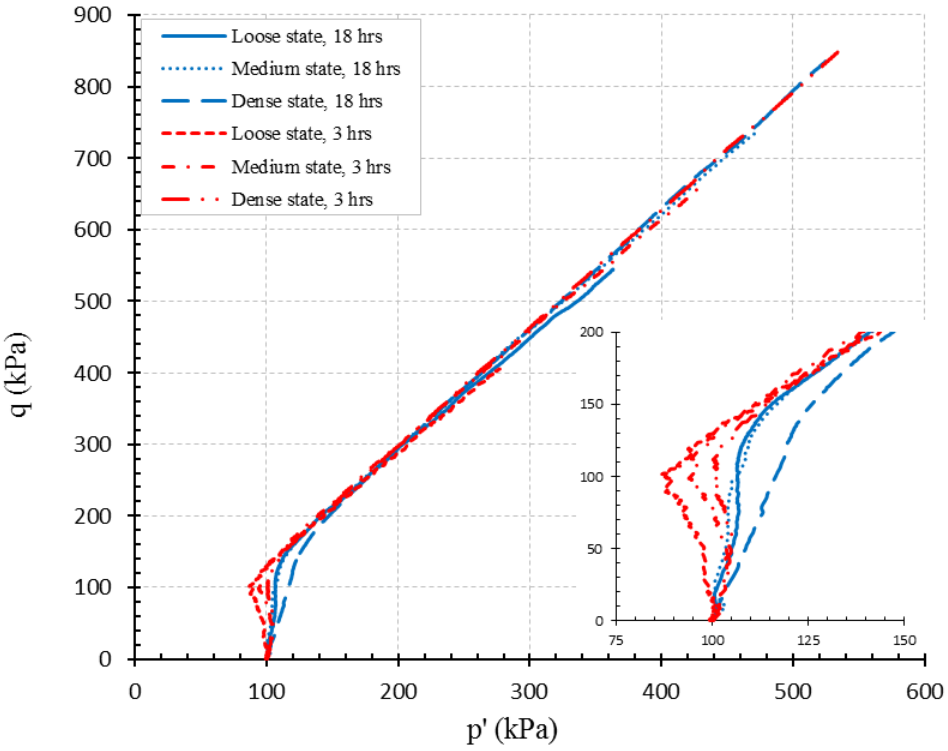

Figure 4.19 Effects of the relative density on the stress path space graph of the specimens tested in CU conditions and consolidated at 18 and 3-hours.

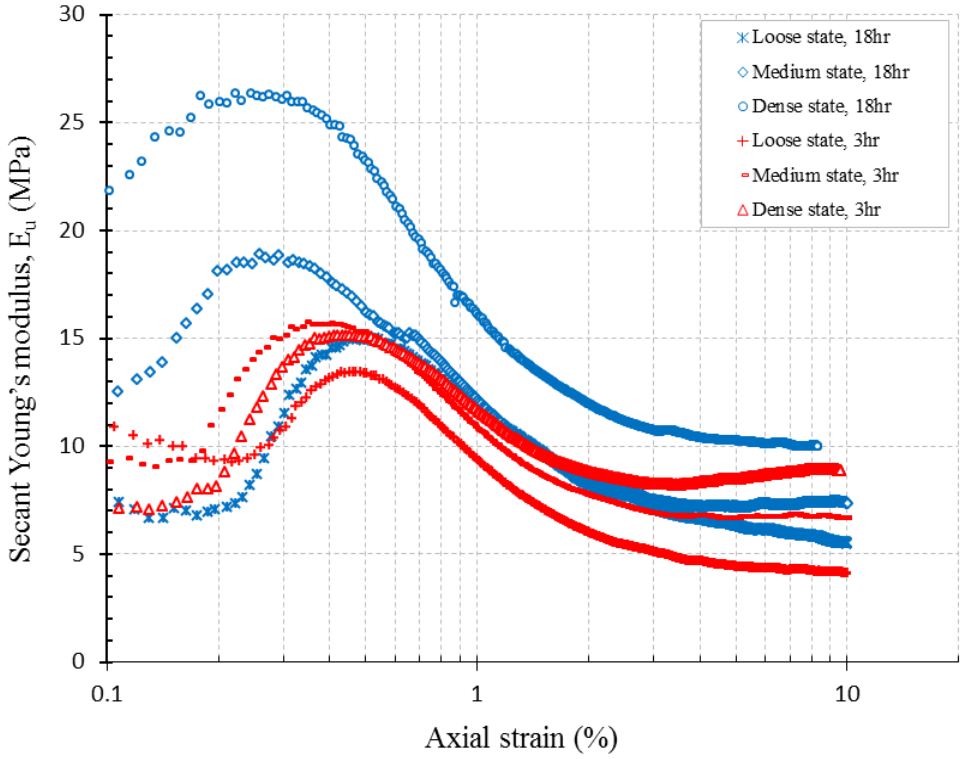

Figure 4.20 Effects of the relative density on secant Young's modulus degradation with axial strain of the specimens tested in CU conditions and consolidated at 18 and 3-hours.

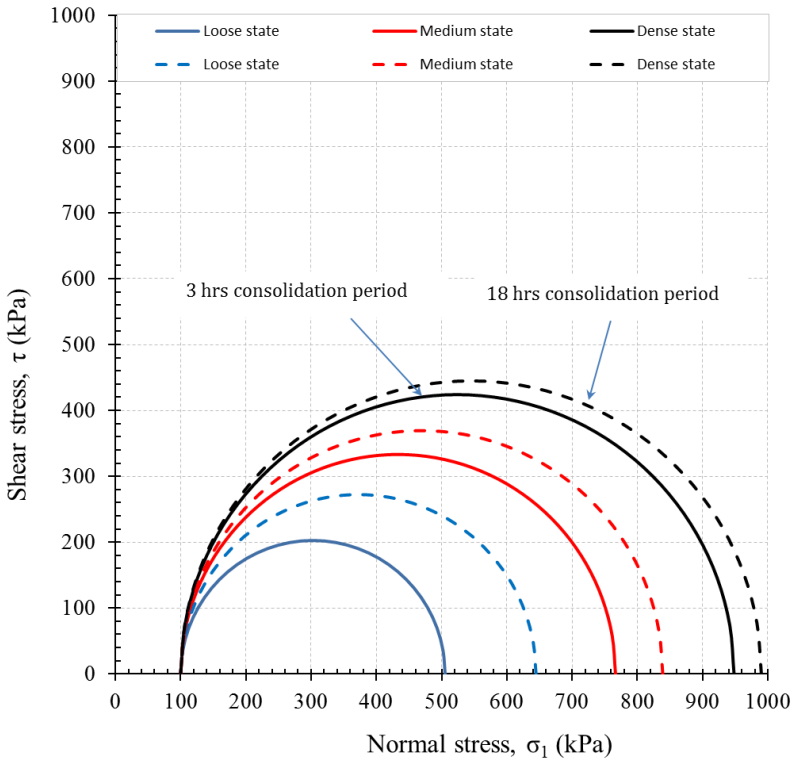

Figure 4.21 Effects of the relative density on the Mohr circles of the specimens tested in CU conditions and consolidated at 18 and 3-hours (total stresses).

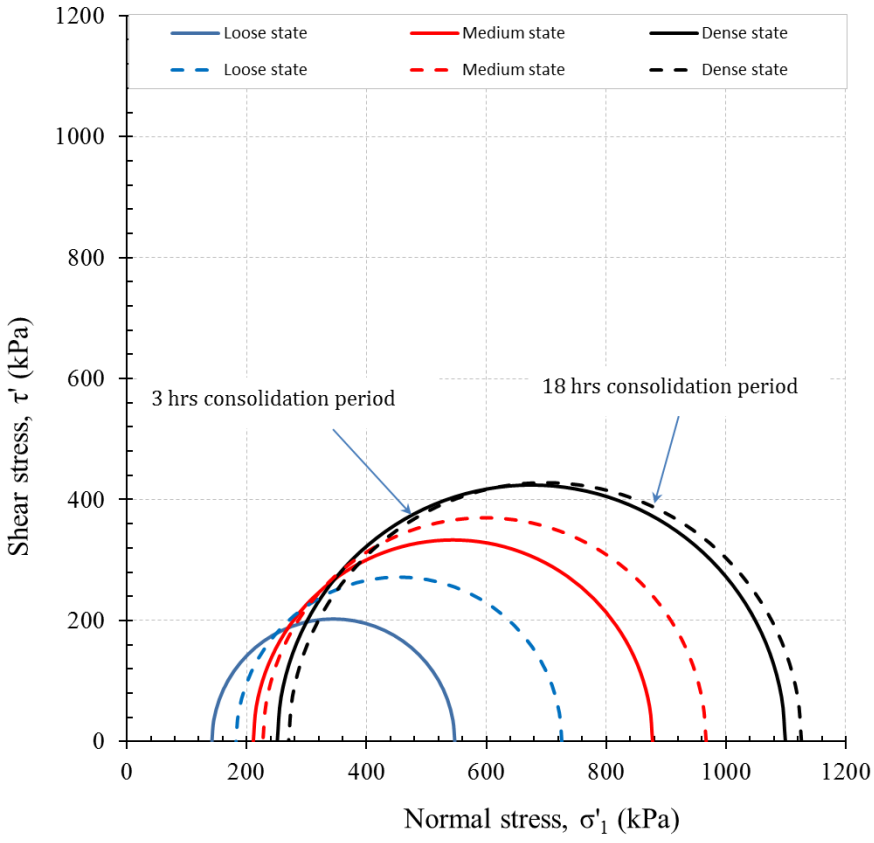

Figure 4.22 Effects of the relative density on the Mohr circles of the specimens tested in CU conditions and consolidated at 18 and 3-hours (effective stresses).

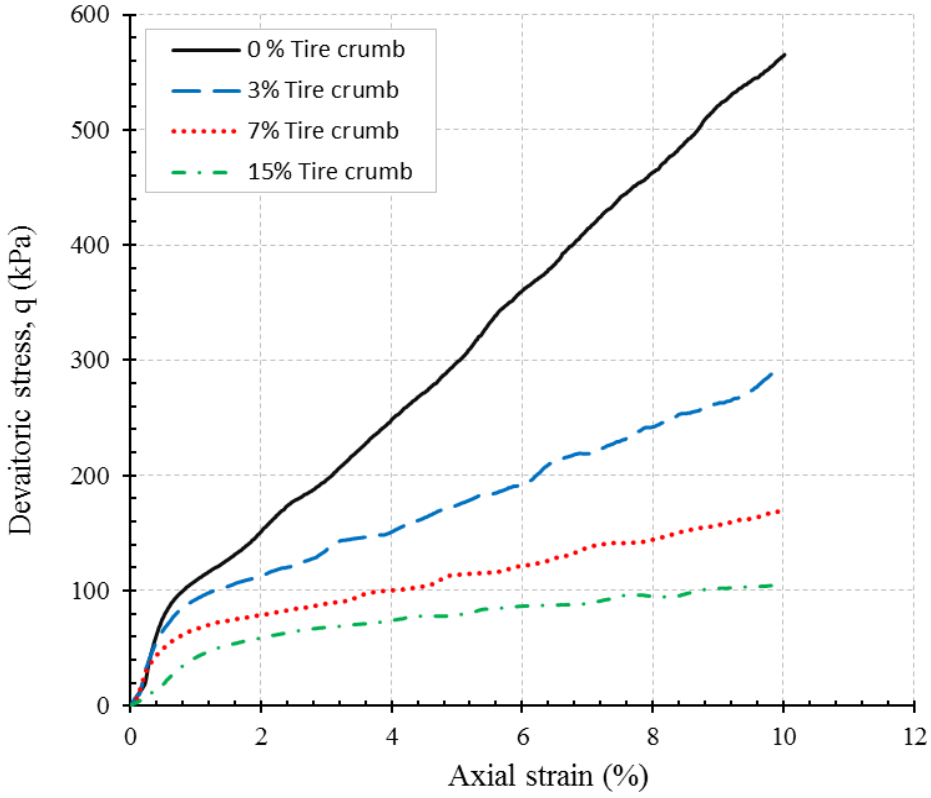

(a)

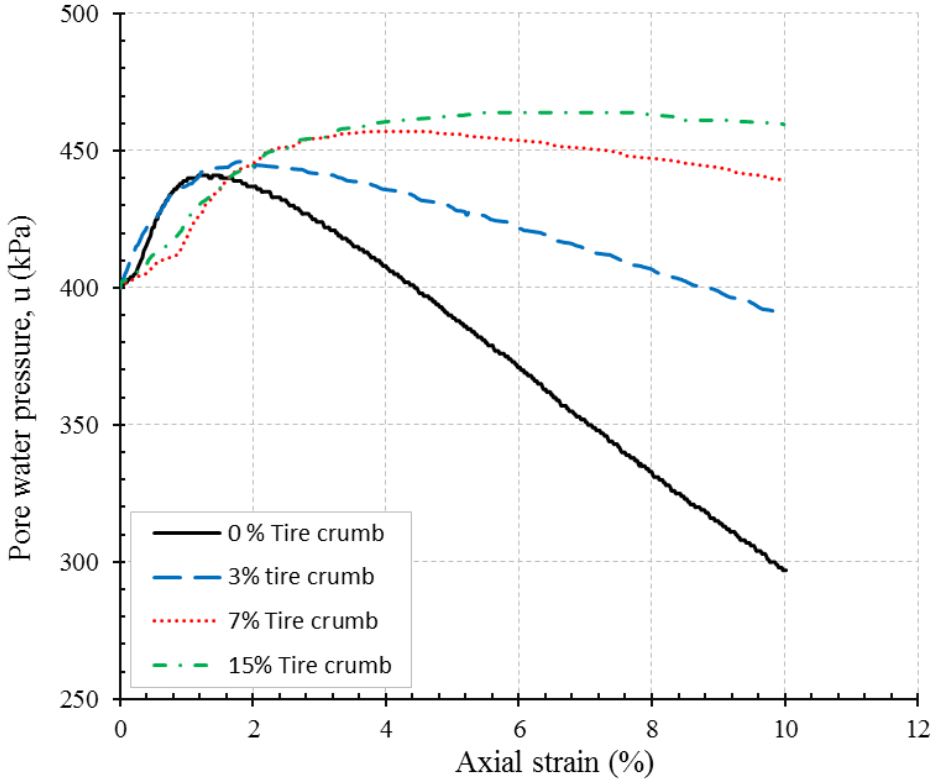

(b)

Figure 4.23 (a) stress-strain curves and, (b) pore water pressure for sand with different contents of tire crumbs.

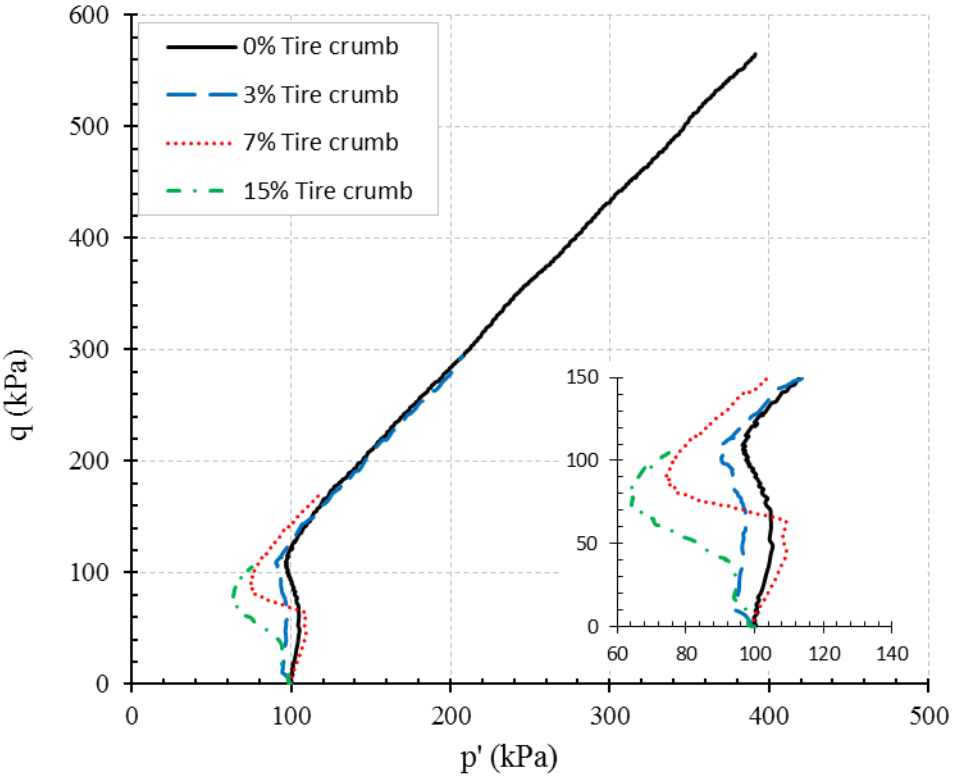

Figure 4.24 Stress path space of sand with different contents of tire crumbs.

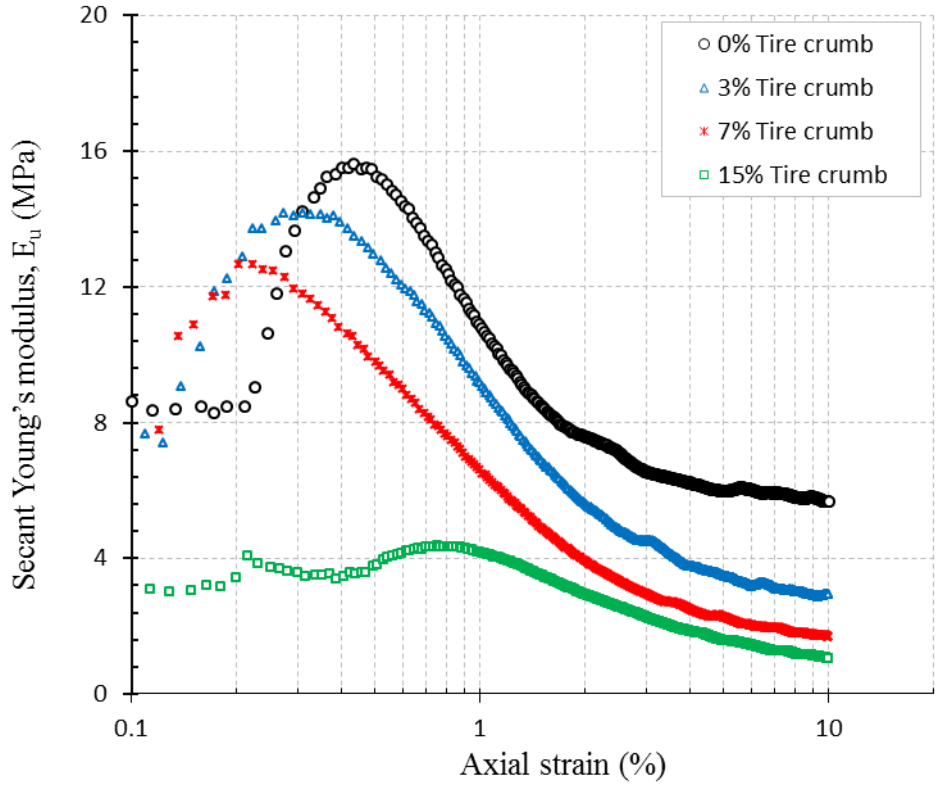

Figure 4.25 Secant Young's modulus degradation for sand with different contents of tire crumbs.

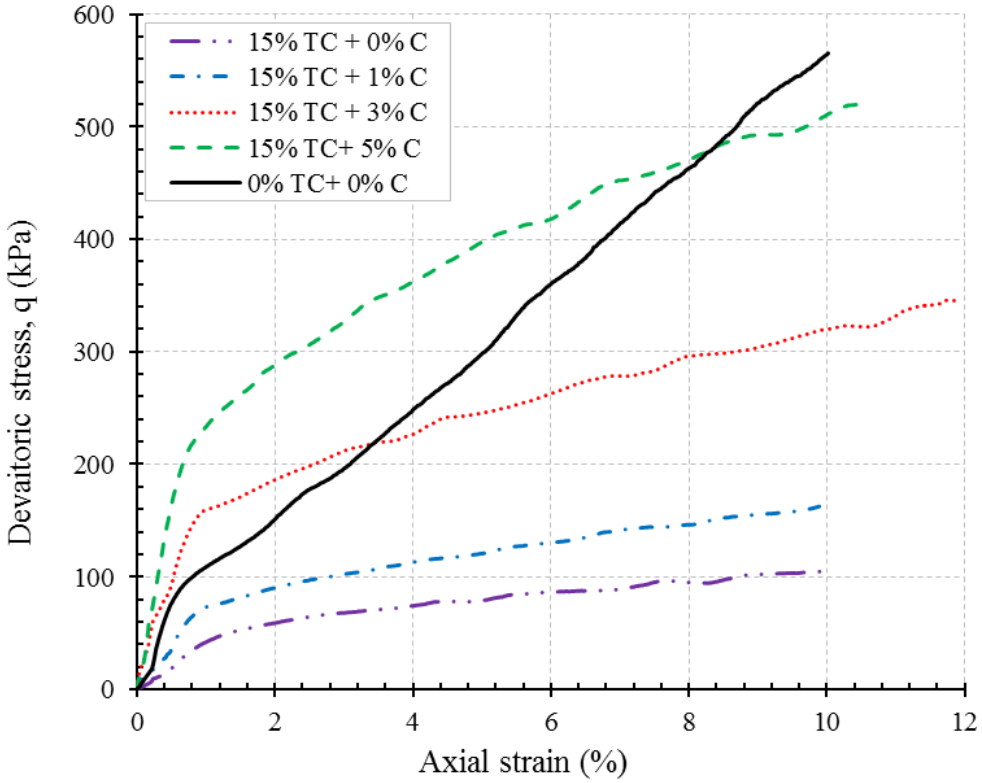

(a)

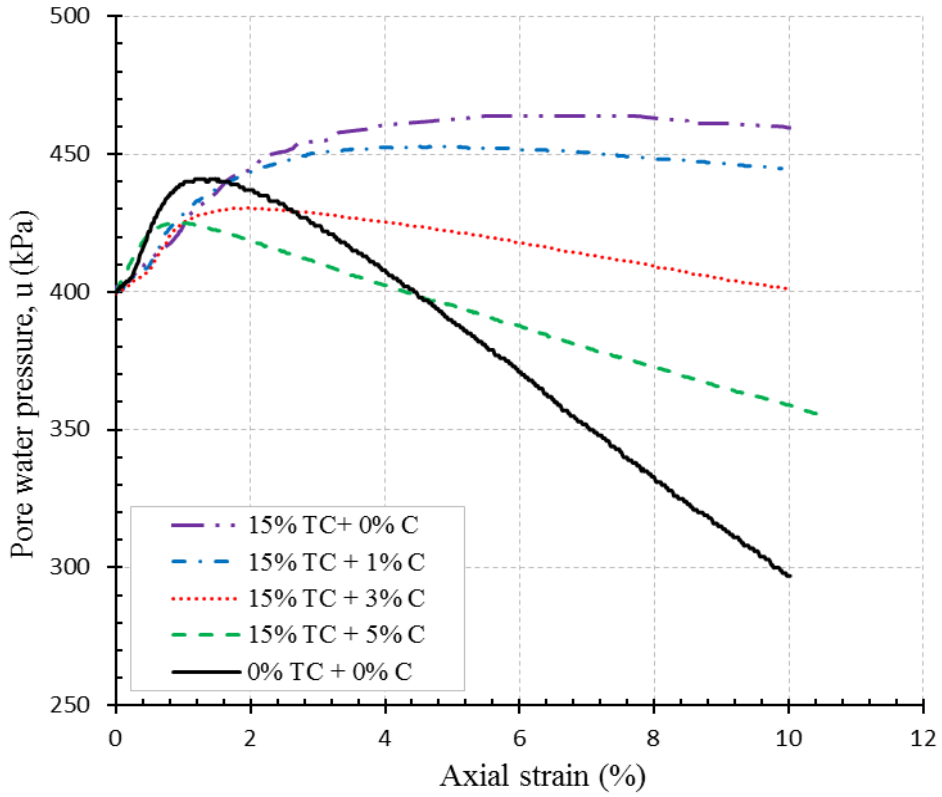

(b)

Figure 4.26 (a) stress-strain curves and, (b) pore water pressure for sand and 15% tire crumbs with different contents of the cement.

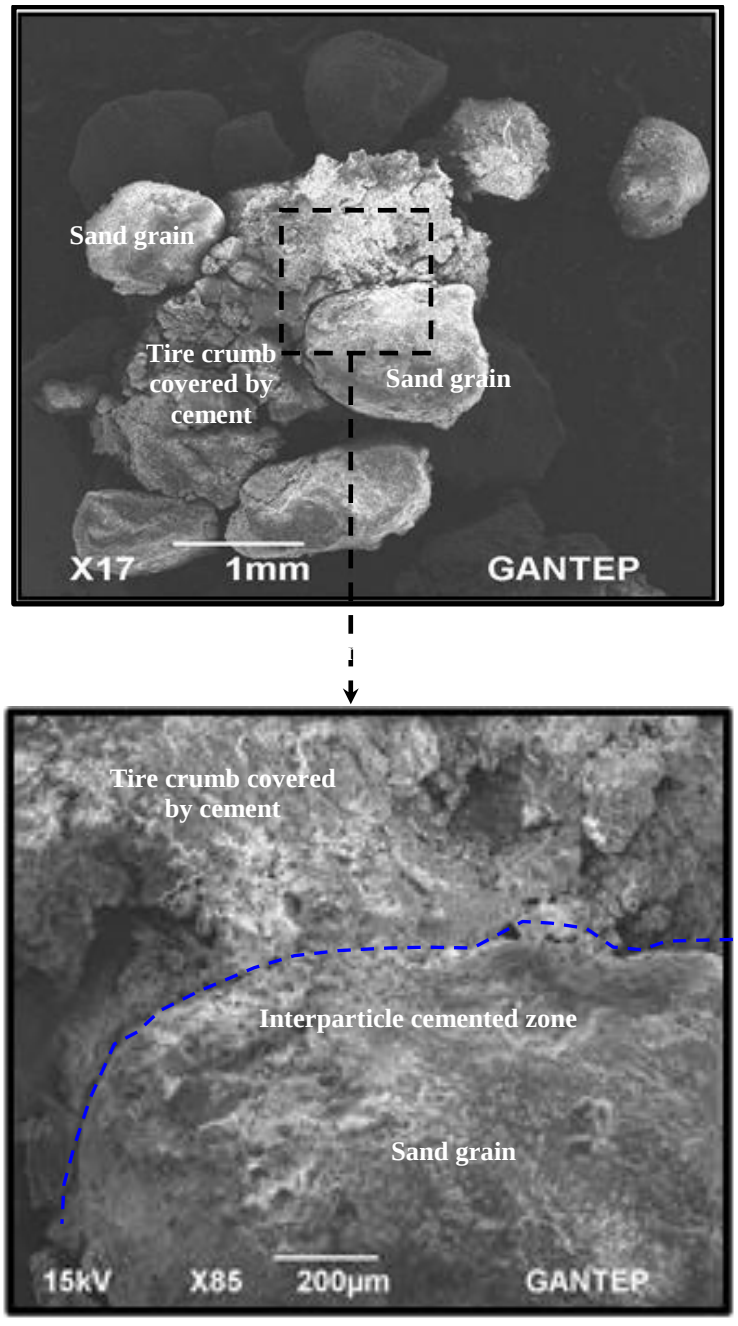

Figure 4.27 Scanning Electron Micrograph (SEM) of cemented sand and tire crumb mixture.

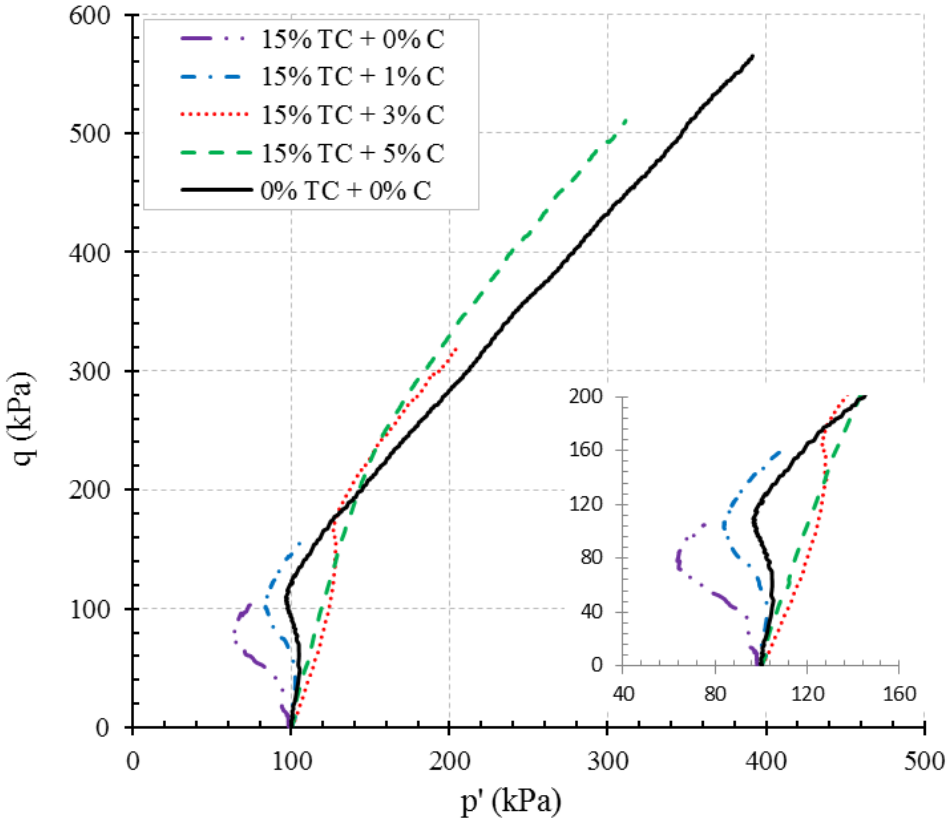

Figure 4.28 Stress paths for sand and 15% of tire crumb with different contents of cement.

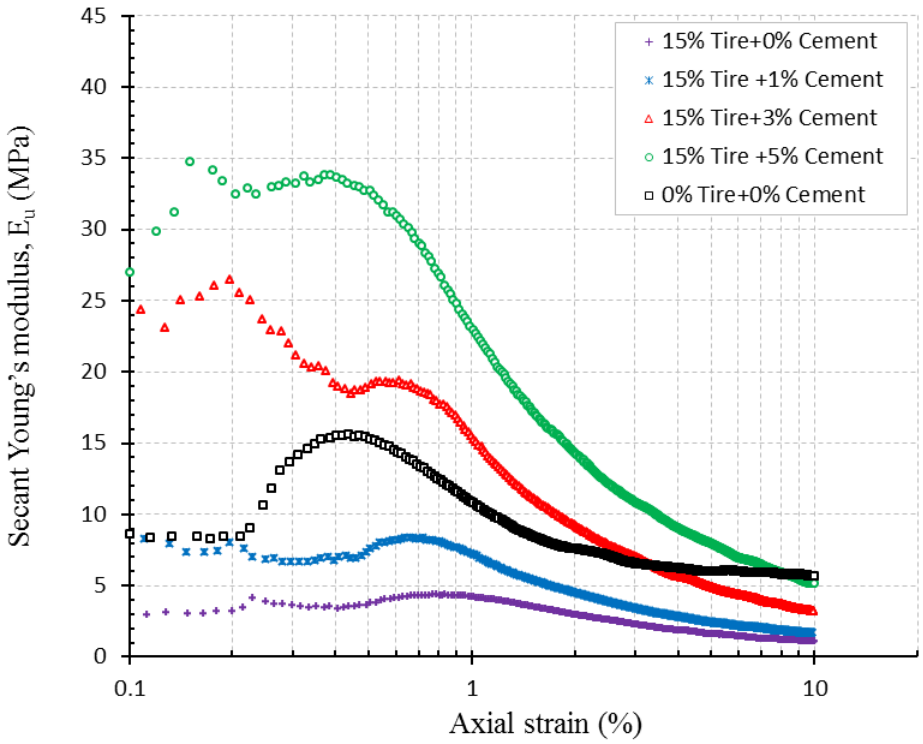

Figure 4.29 Secant Young's modulus for sand and 15% of tire crumb with different contents of cement.

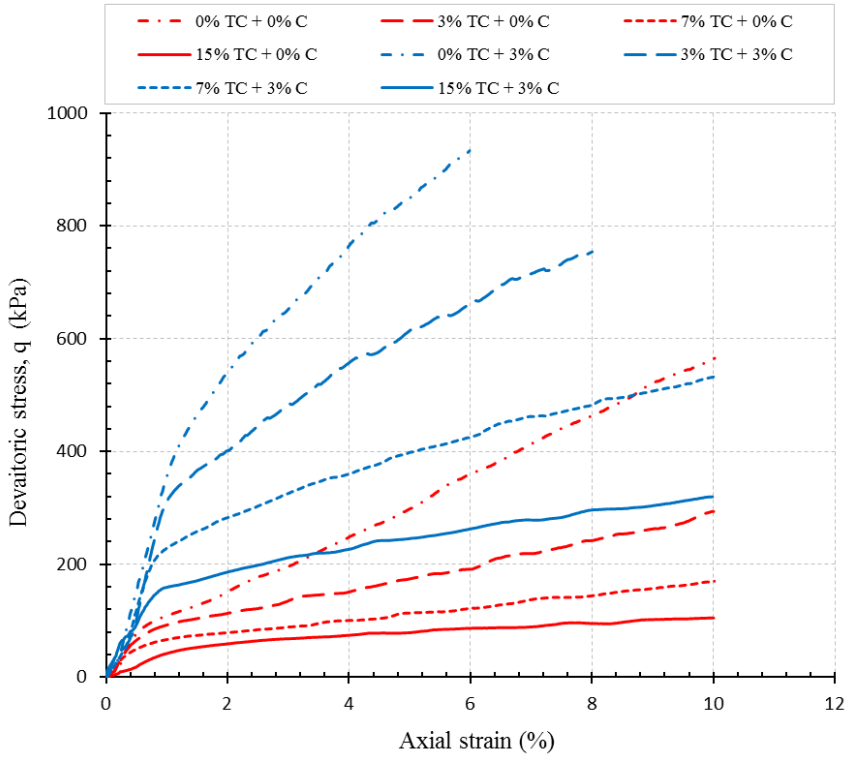

(a)

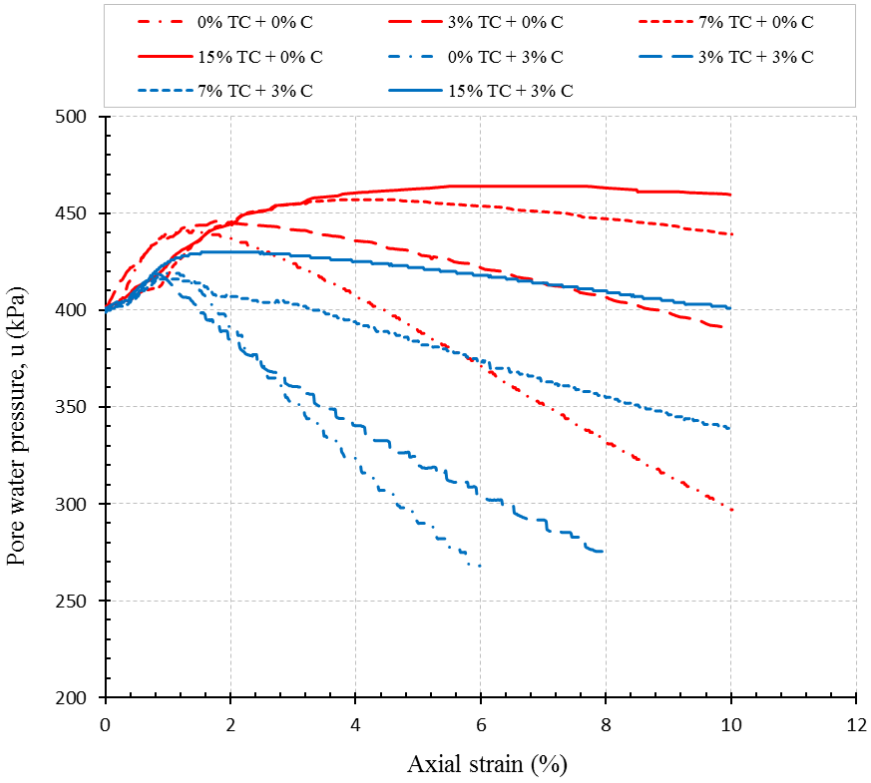

(b)

Figure 4.30 (a) stress-axial strain and, (b) Pore water pressure-axial strain, for sand and various contents of tire crumbs, with/without 3% cement.

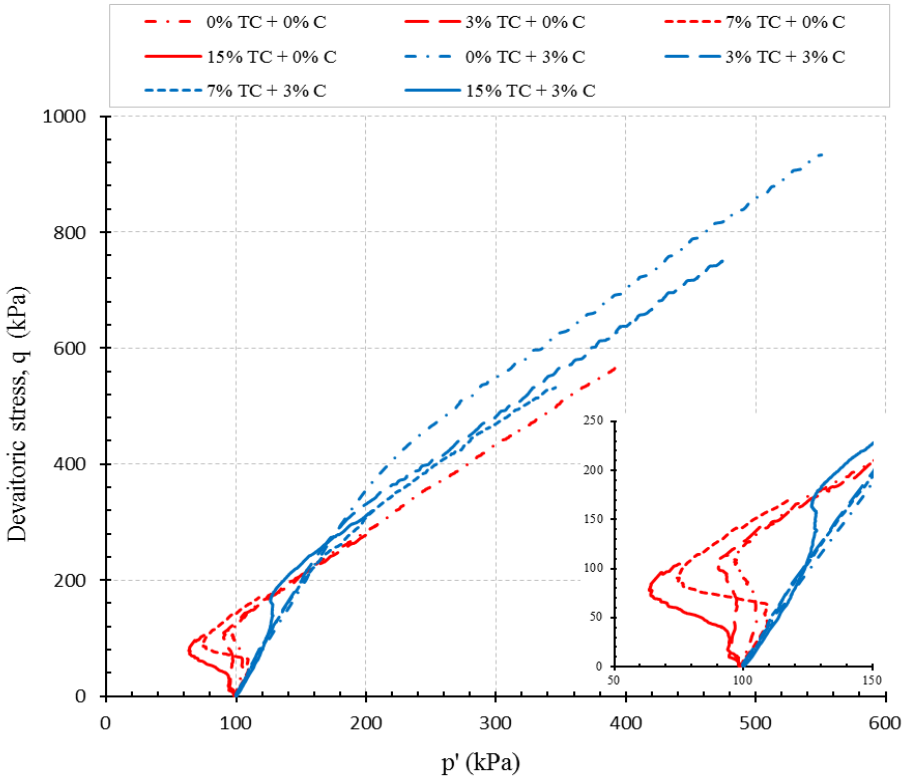

Figure 4.31 Stress path space for sand and various contents of tire crumbs, with/without 3% cement.

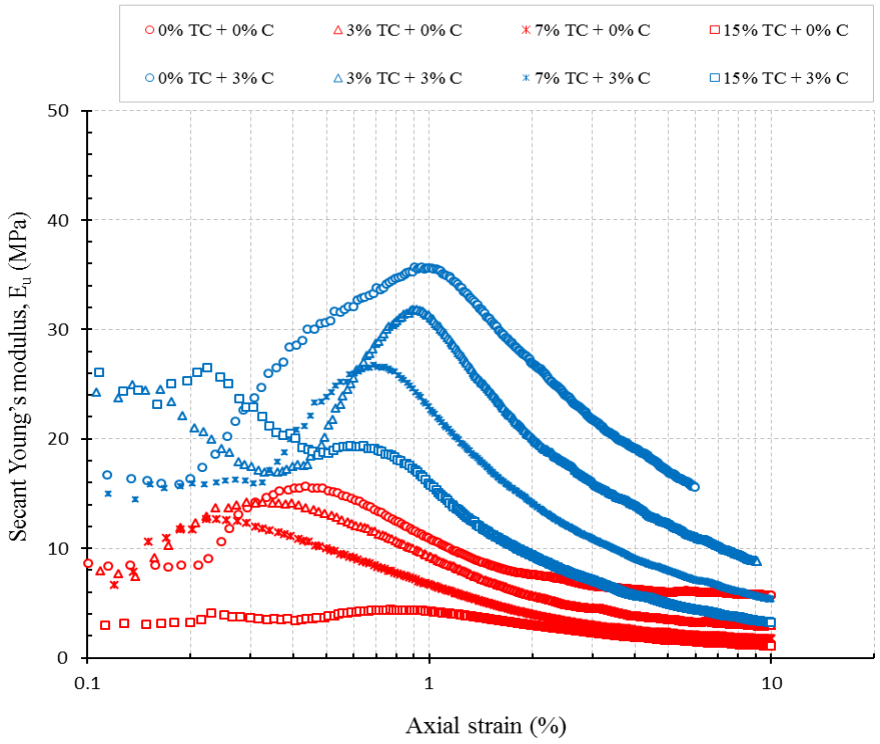

Figure 4.32 Variation of the secant Young's modulus with an axial strain for sand and various contents of tire crumbs, with/without 3% cement.

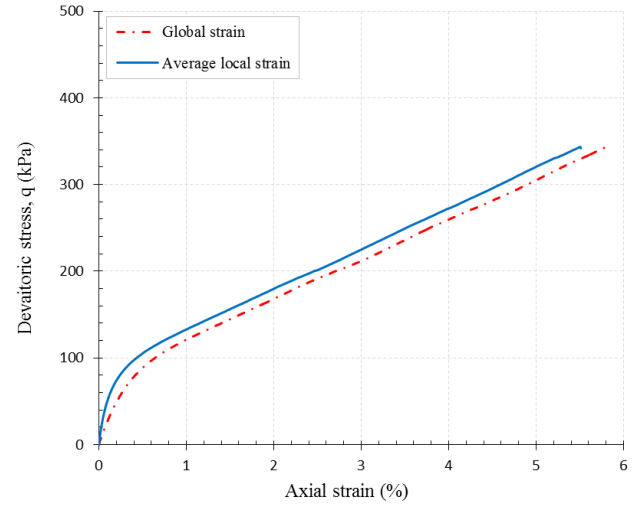

(a)

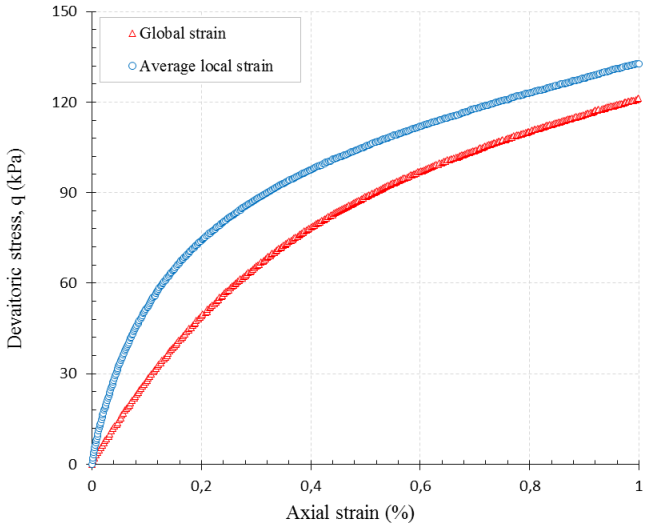

(b)

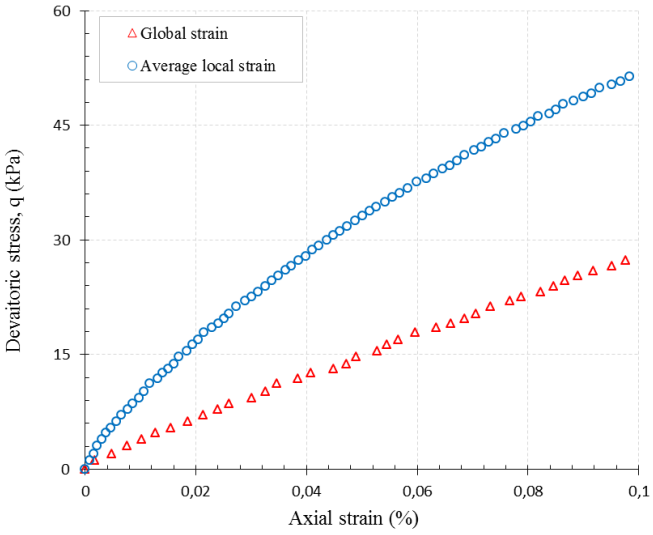

(c)

Figure 4.33 Stress-strain curves using local and global strain measurement at different scales.

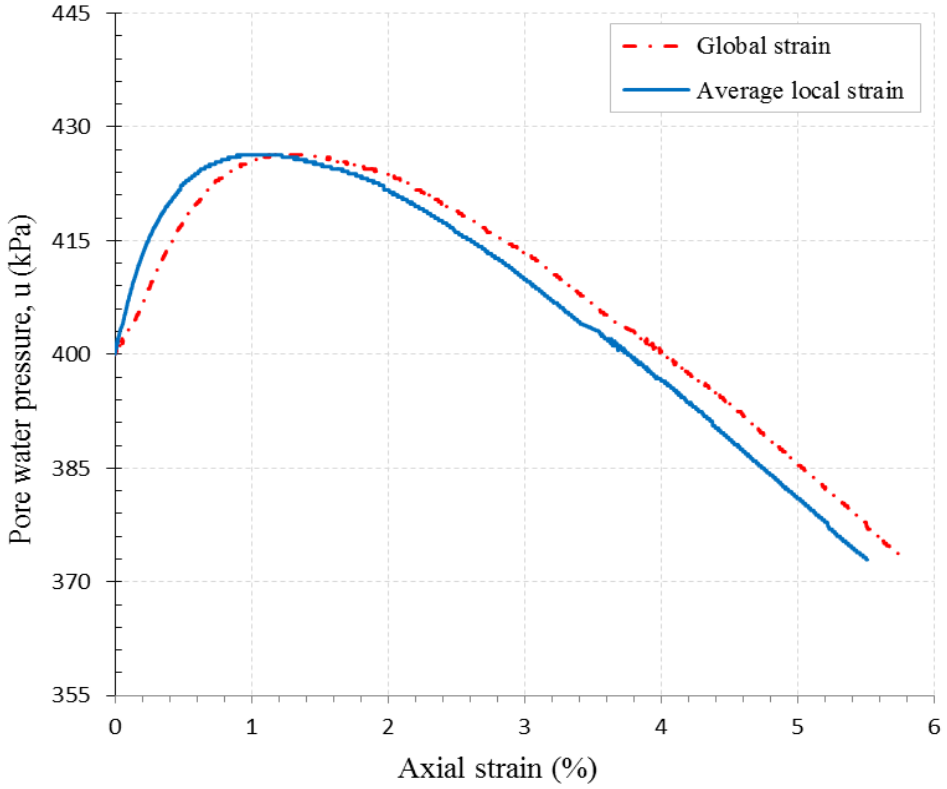

Figure 4.34 Pore water generation versus strain curves for specimens using local and global strain measurement.

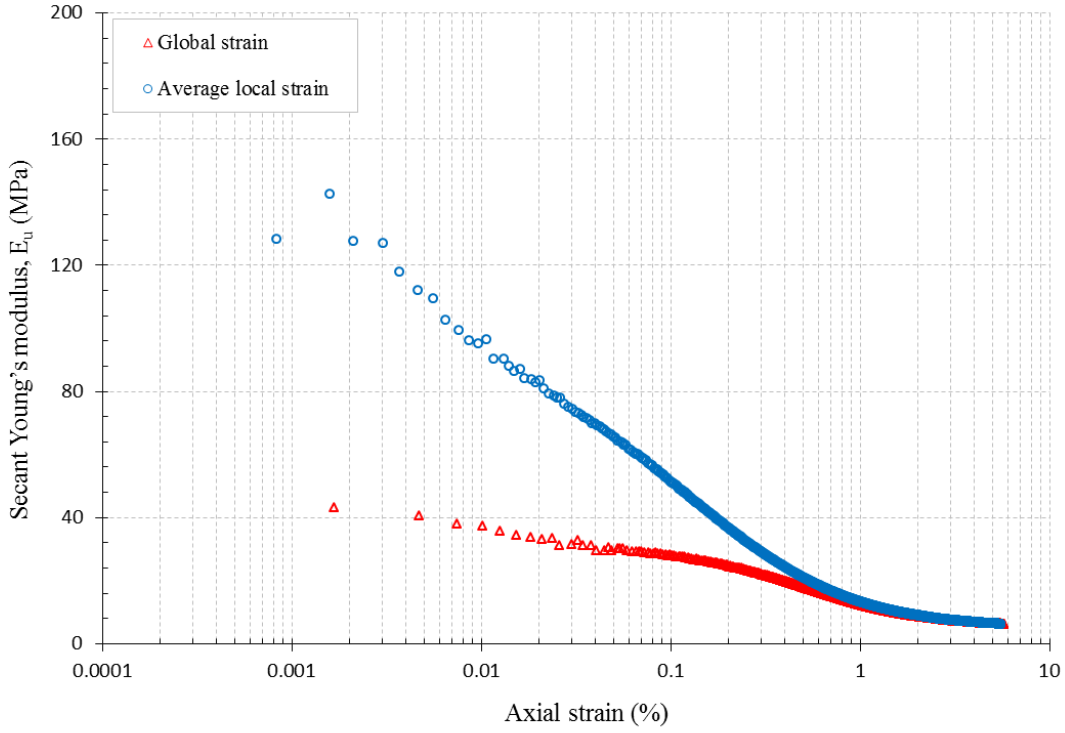

Figure 4.35 Stiffness degradation curves with the axial strain using local and global strain measurement.

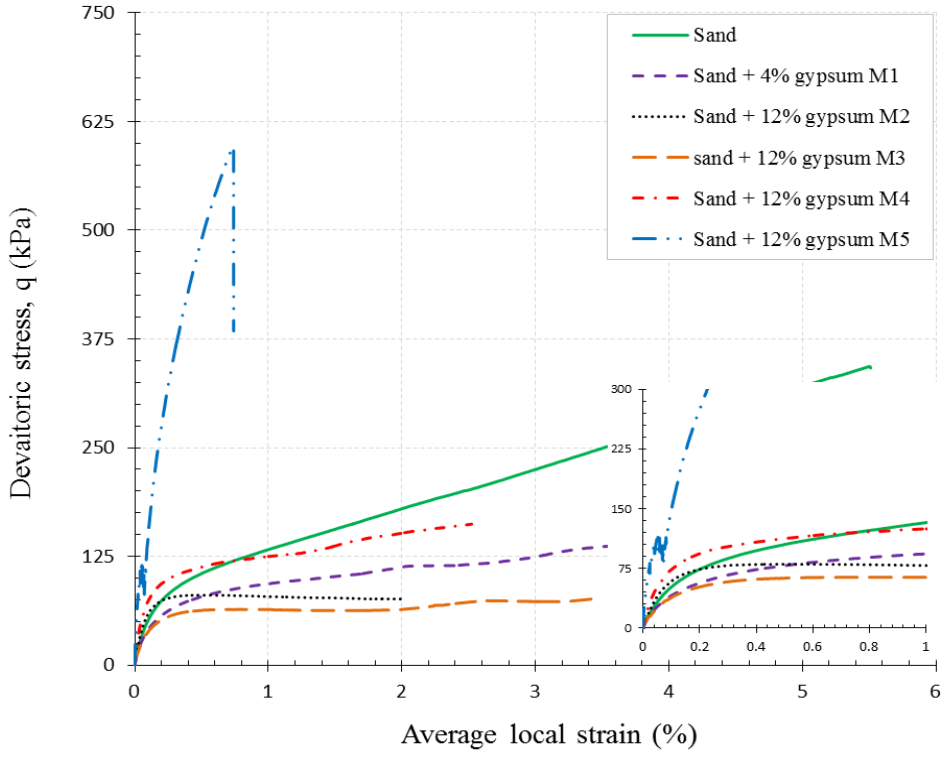

(a)

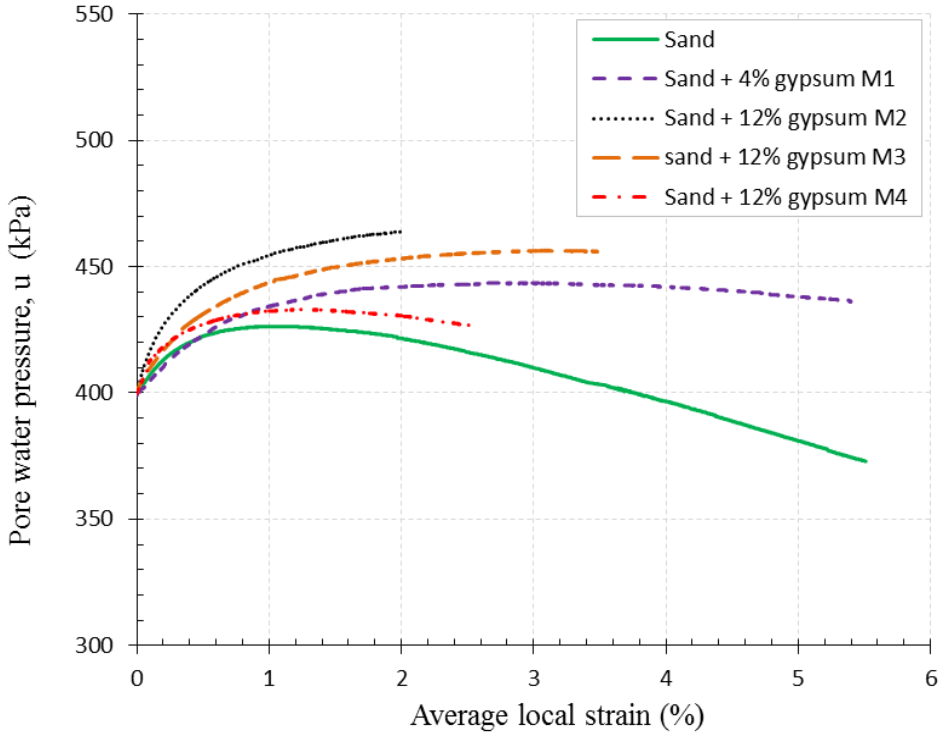

(b)

Figure 4.36 (a) stress-strain and, (b) pore water pressure versus strain curves for specimens of sand with gypsum prepared employing different techniques.

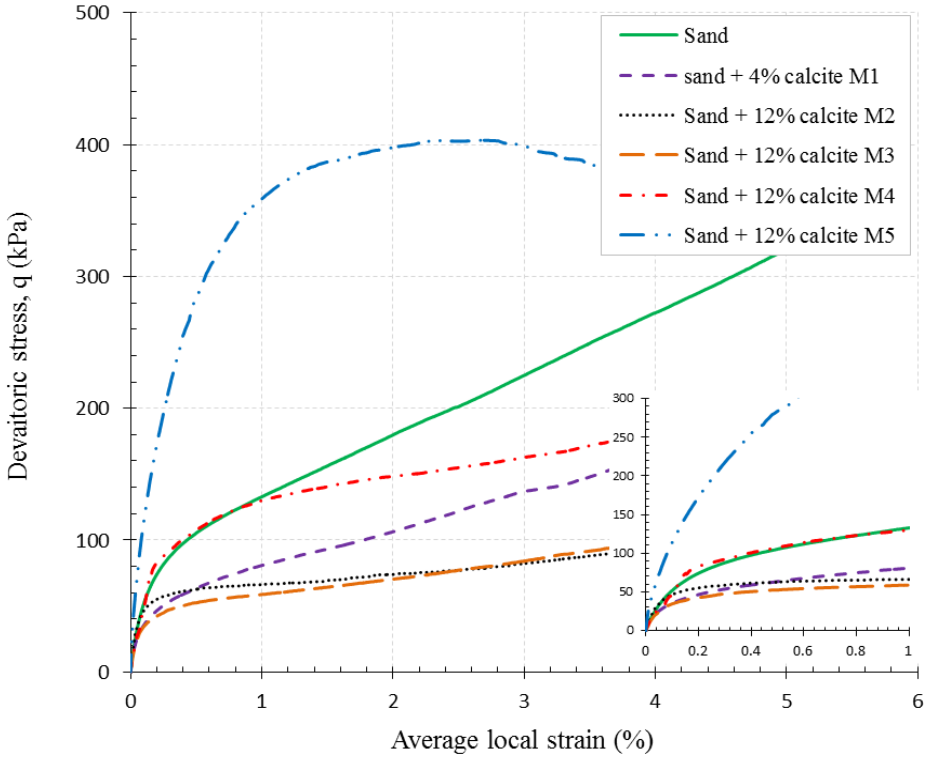

(a)

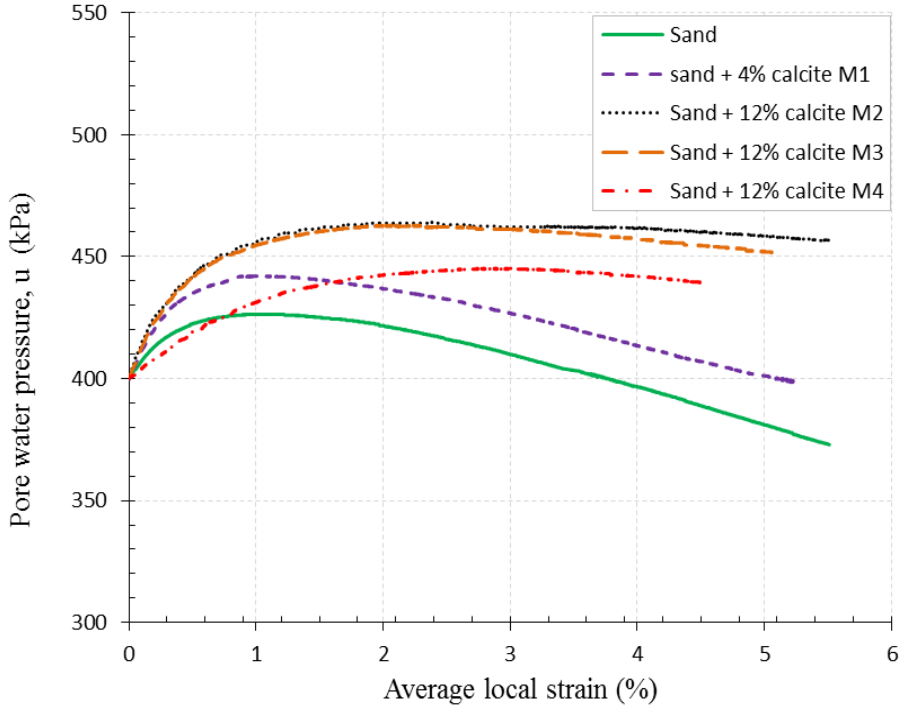

(b)

Figure 4.37 (a) stress-strain and, (b) pore water pressure versus strain curves for specimens of sand with calcite prepared employing different techniques.

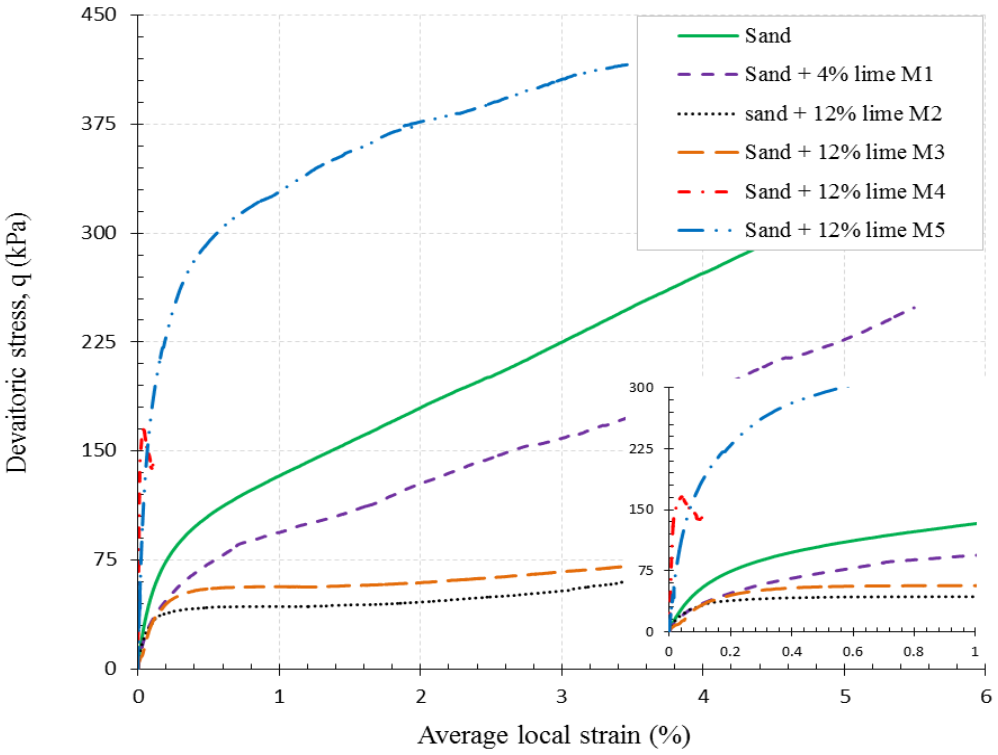

(a)

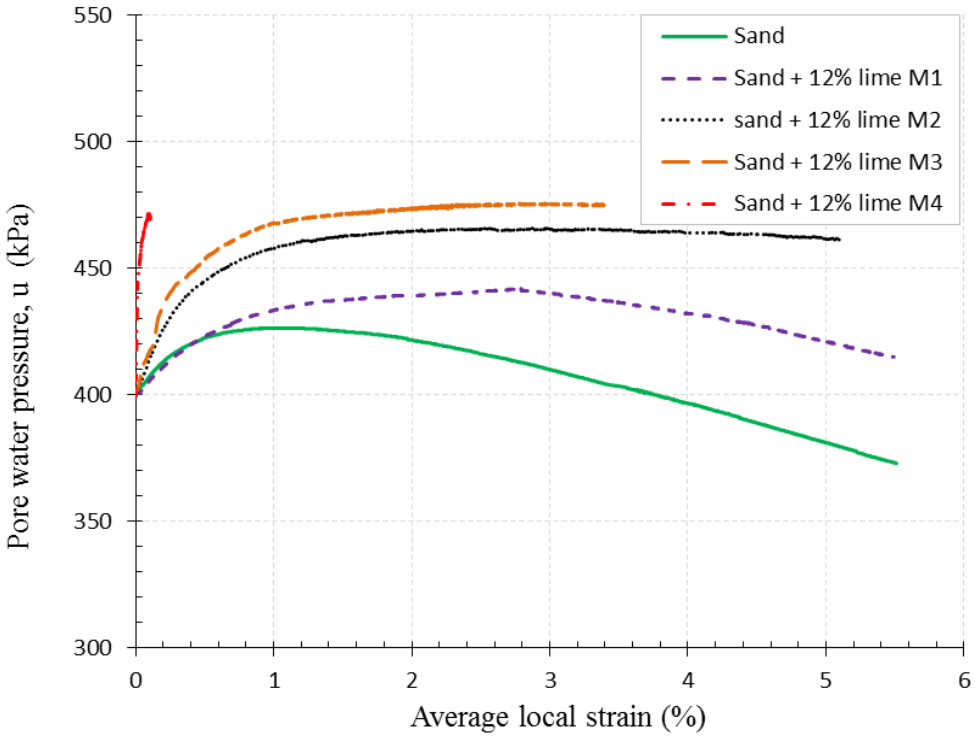

(b)

Figure 4.38 (a) stress-strain and, (b) pore water pressure versus strain curves for specimens of sand with lime prepared employing different techniques.

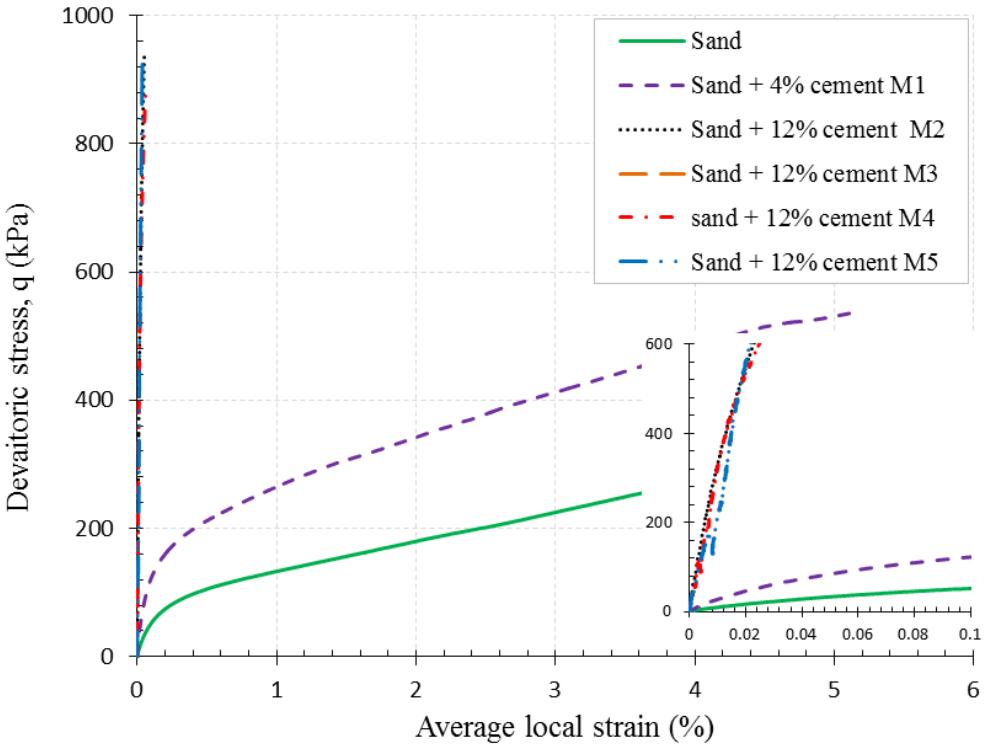

(a)

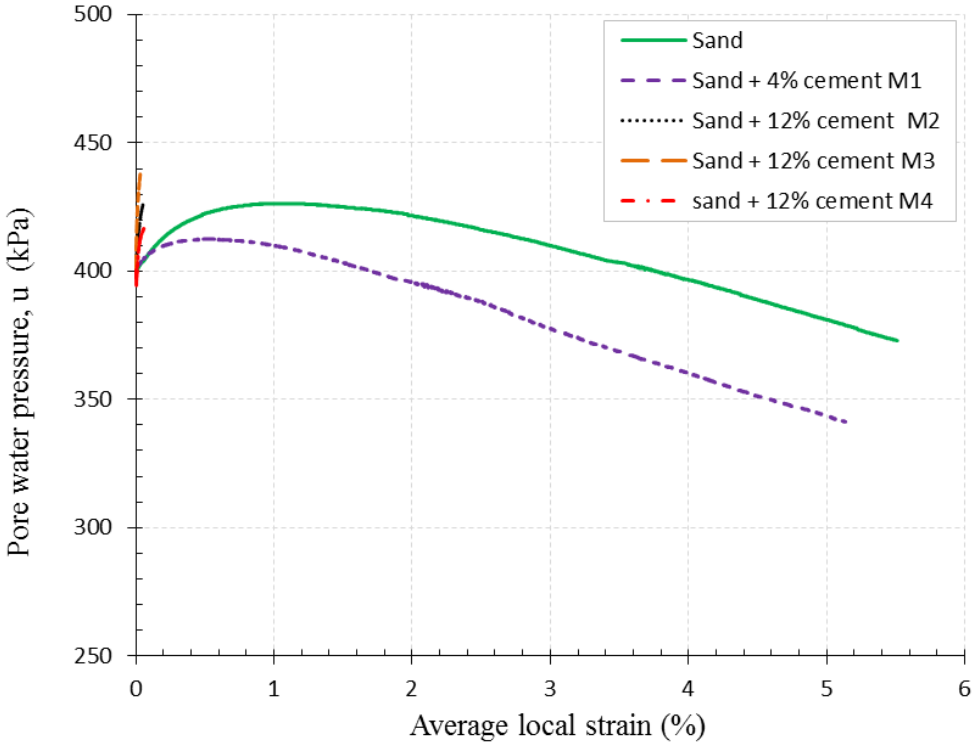

(b)

Figure 4.39 (a) stress-strain and, (b) pore water pressure versus strain curves for specimens of sand with cement prepared employing different techniques.

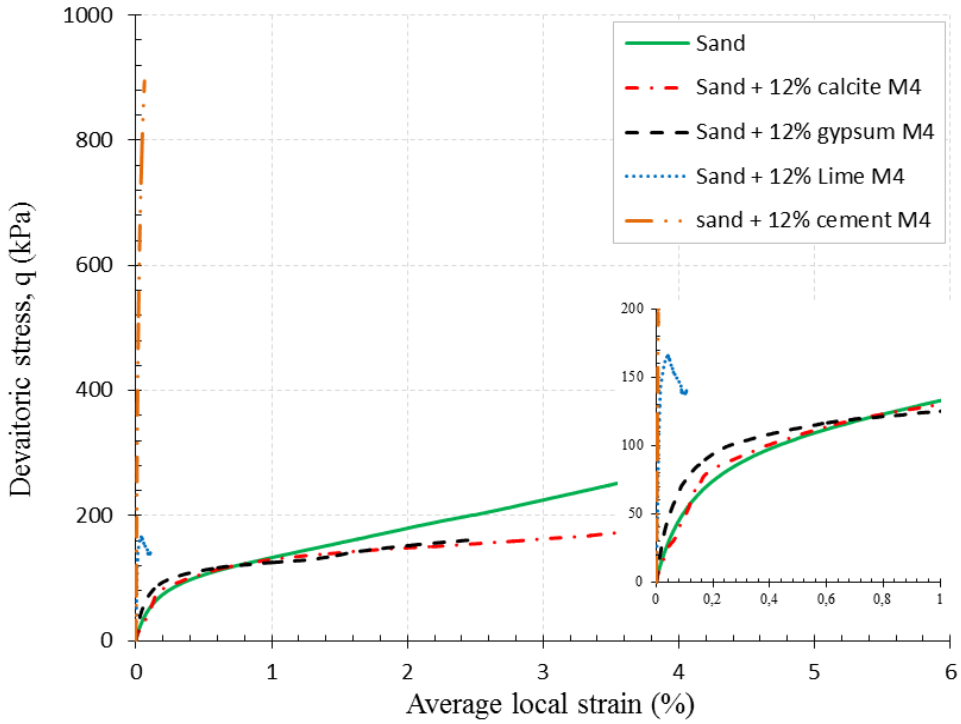

(a)

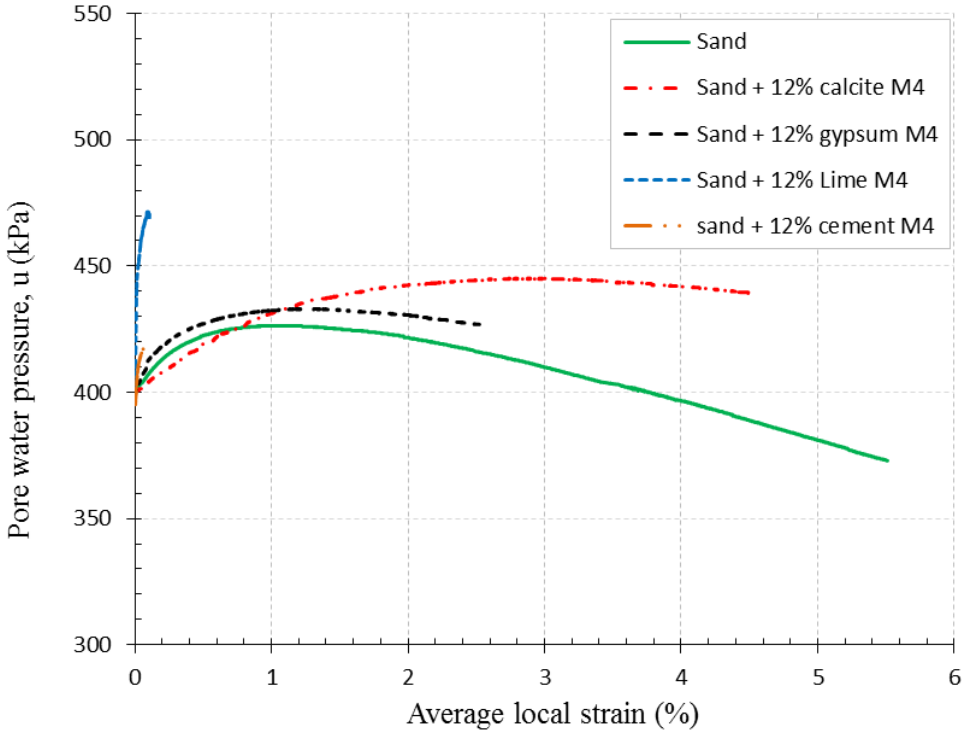

(b)

Figure 4.40 (a) stress-strain and, (b) pore water pressure versus strain curves for specimens of sand with different cementing agents prepared employing technique M4.

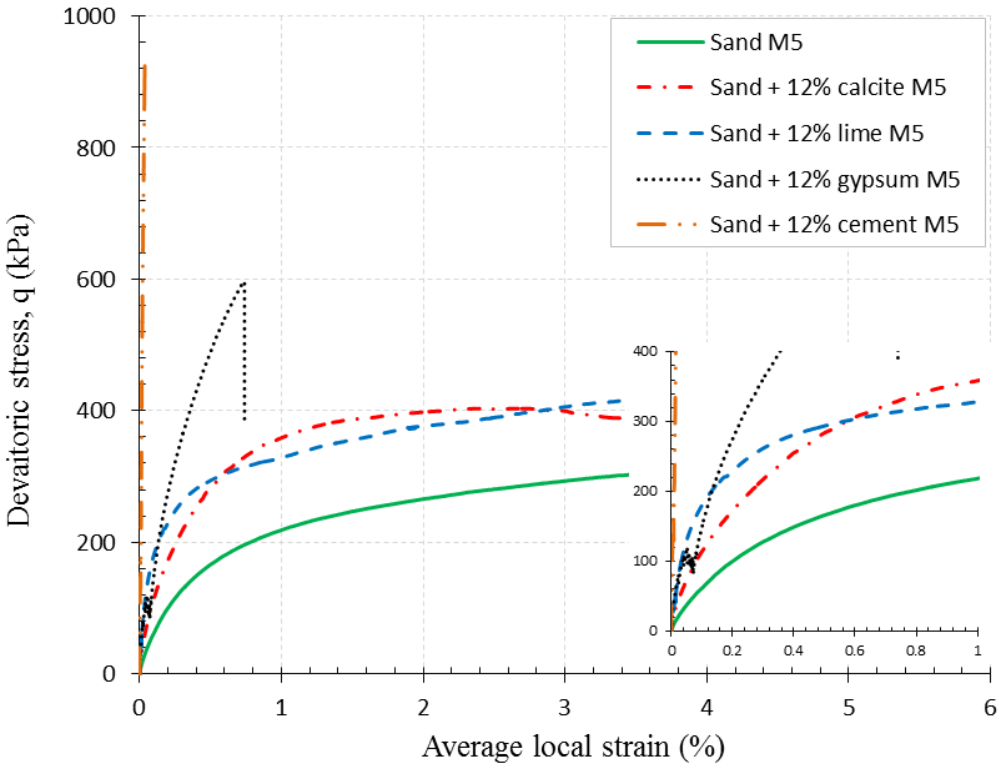

Figure 4.41 Stress-strain curves for specimens of sand with different cementing agents prepared employing technique M5.

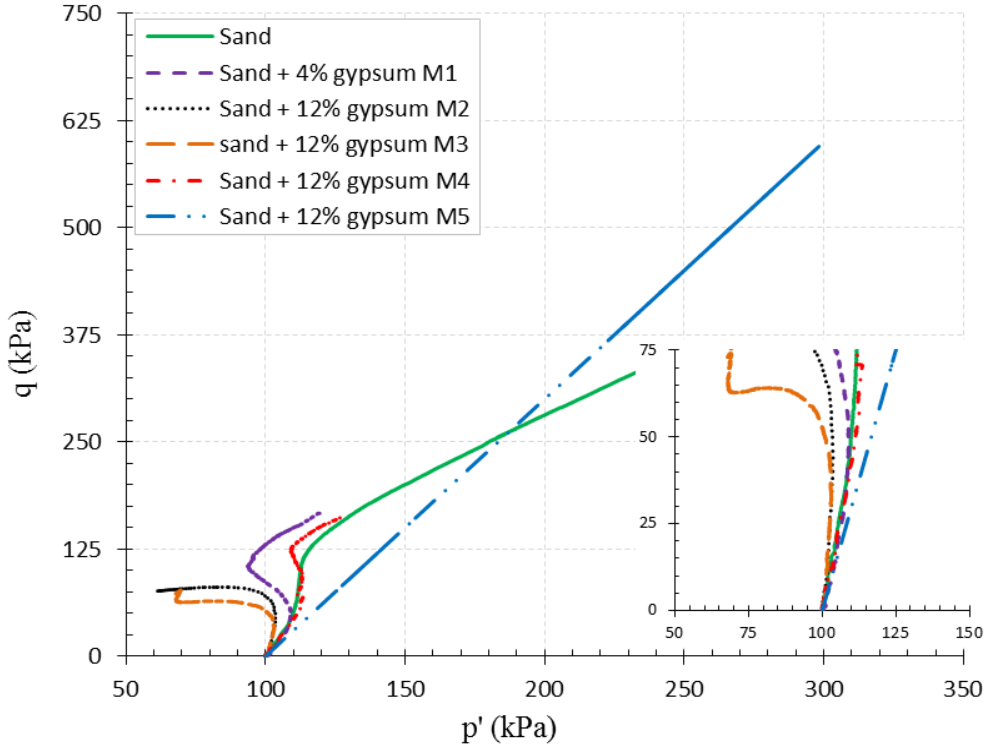

Figure 4.42 Stress space results for the specimens of sand with gypsum prepared employing different techniques.

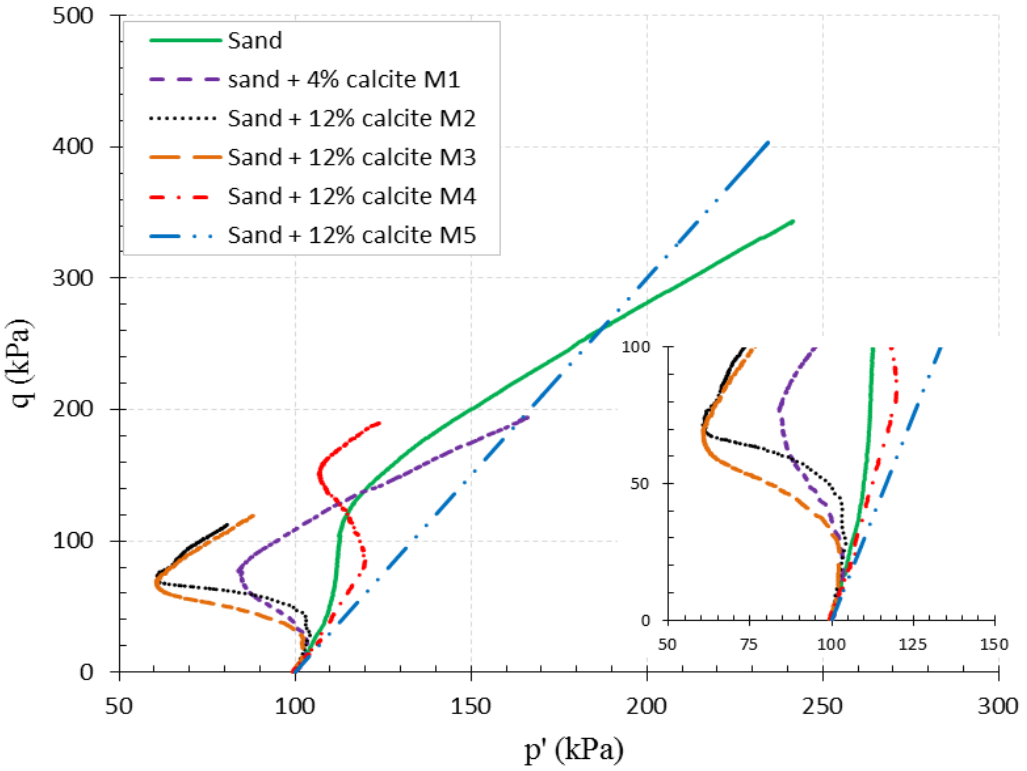

Figure 4.43 Stress space results for the specimens of sand with calcite prepared employing different techniques.

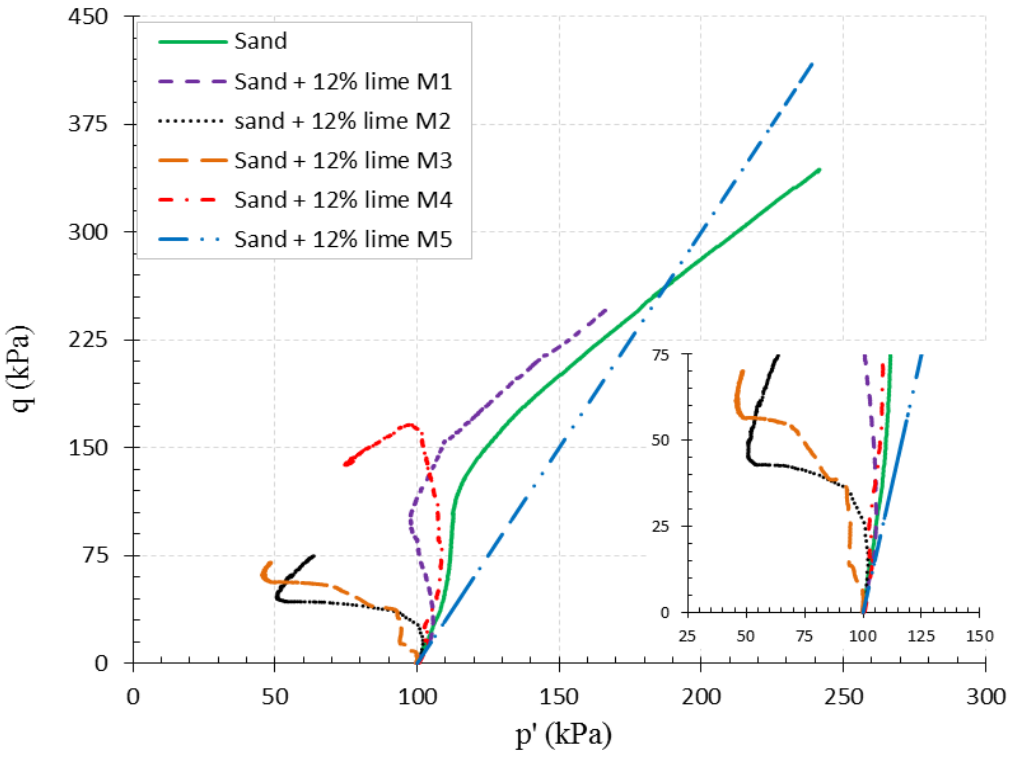

Figure 4.44 Stress space results for the specimens of sand with lime prepared employing different techniques.

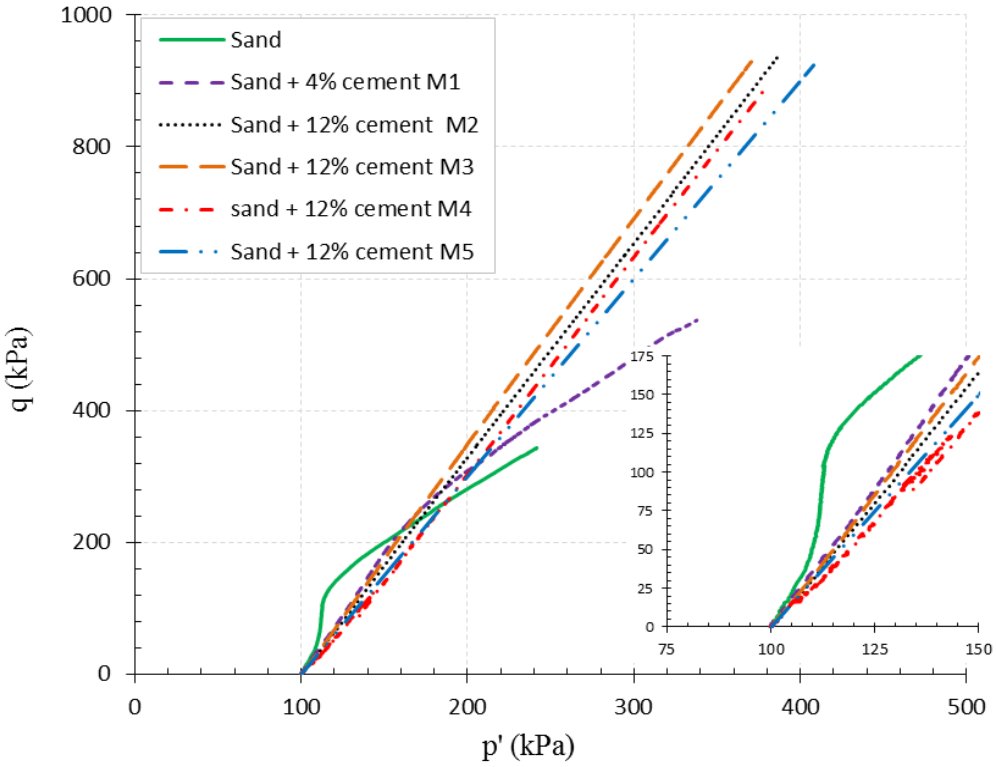

Figure 4.45 Stress space results for the specimens of sand with Portland cement prepared employing different techniques.

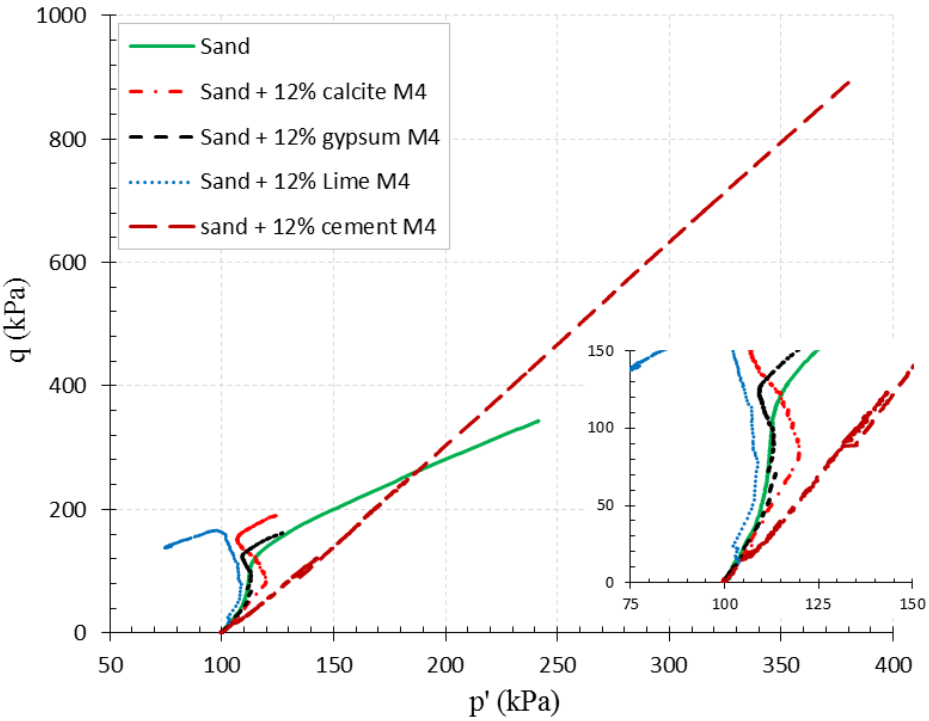

Figure 4.46 Stress space results for the specimens of sand with different cementing agents prepared employing technique M4.

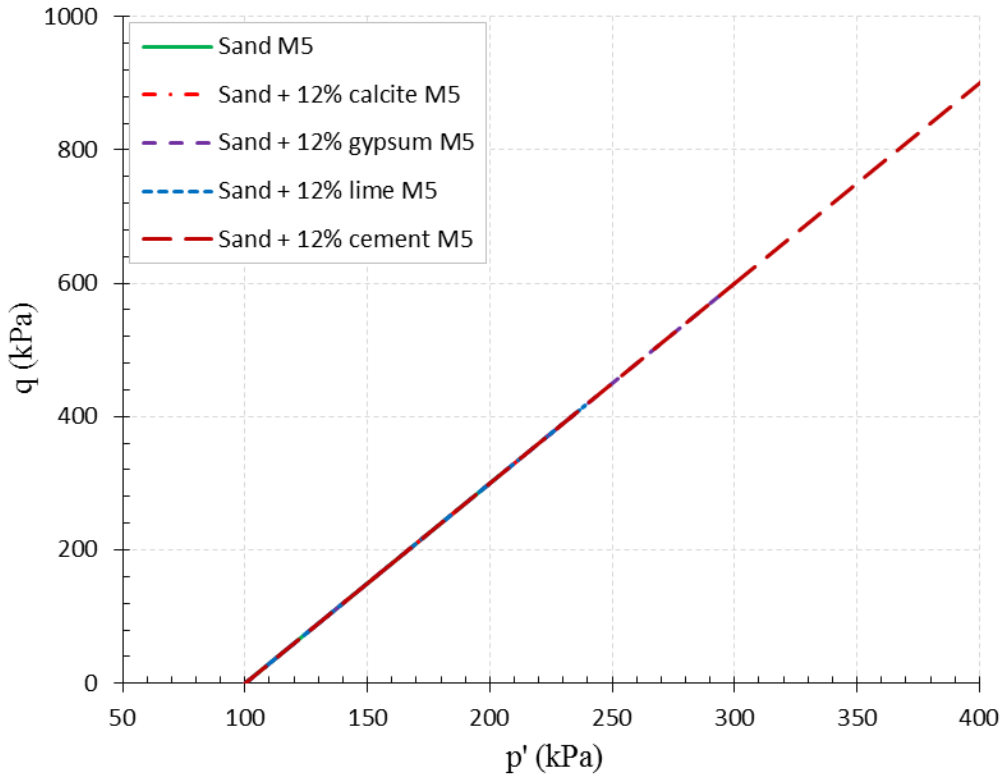

Figure 4.47 Stress space results for the specimens of sand with different cementing agents prepared employing technique M5.

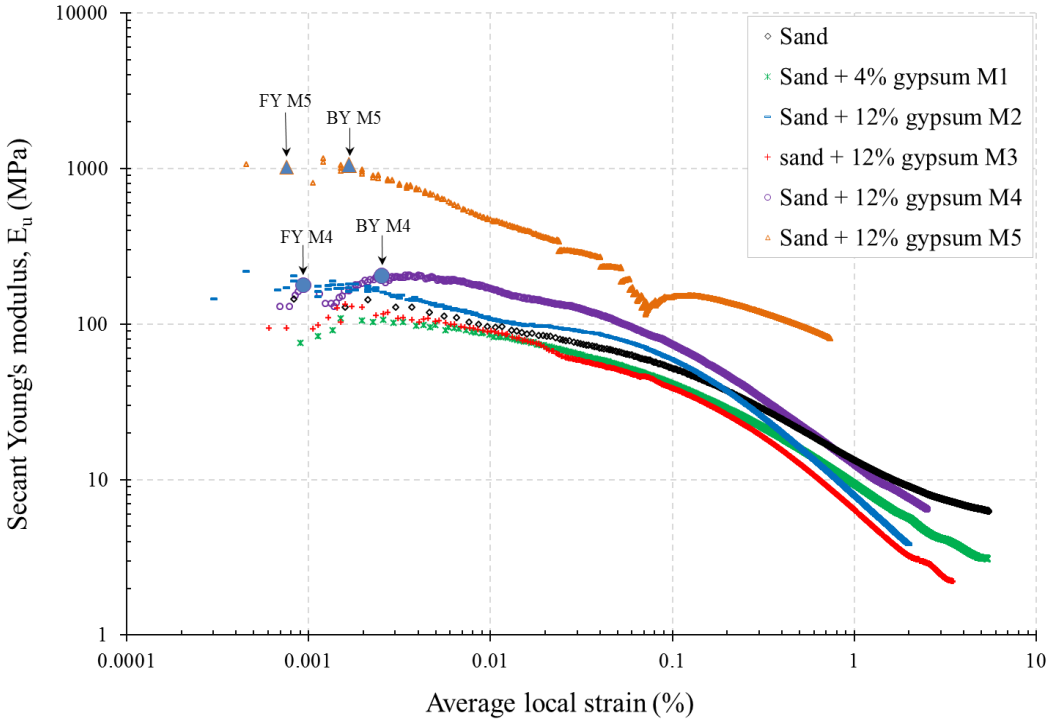

Figure 4.48 Secant Young's modulus results for the specimens of sand cemented by gypsum and prepared employing different techniques.

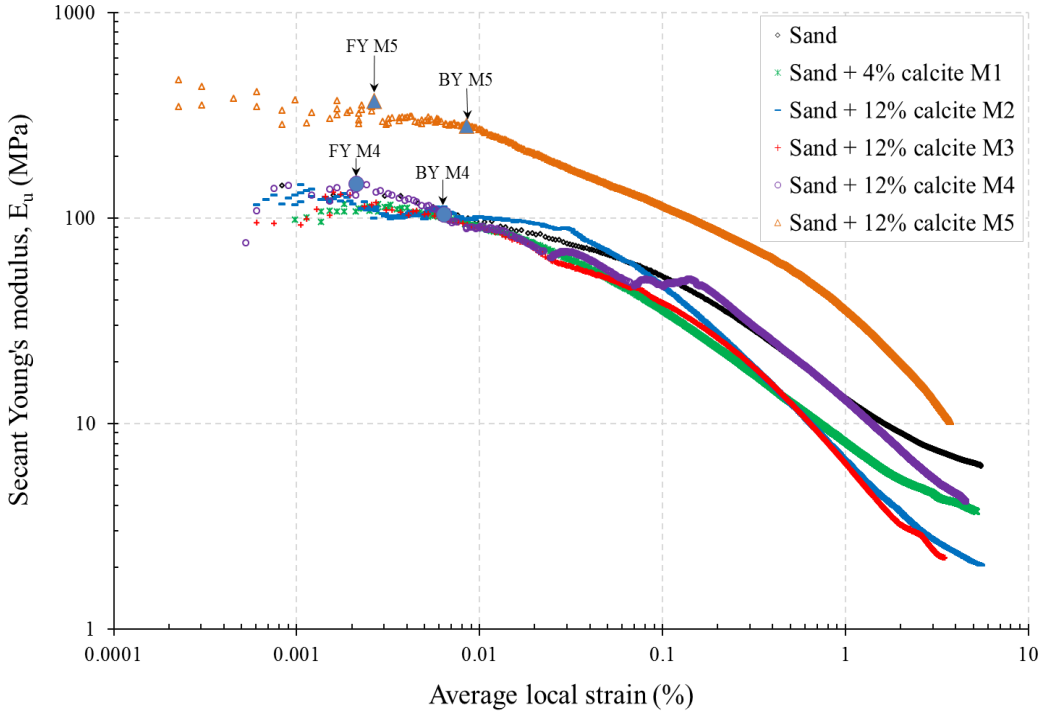

Figure 4.49 Secant Young's modulus results for the specimens of sand cemented by calcite and prepared employing different techniques.

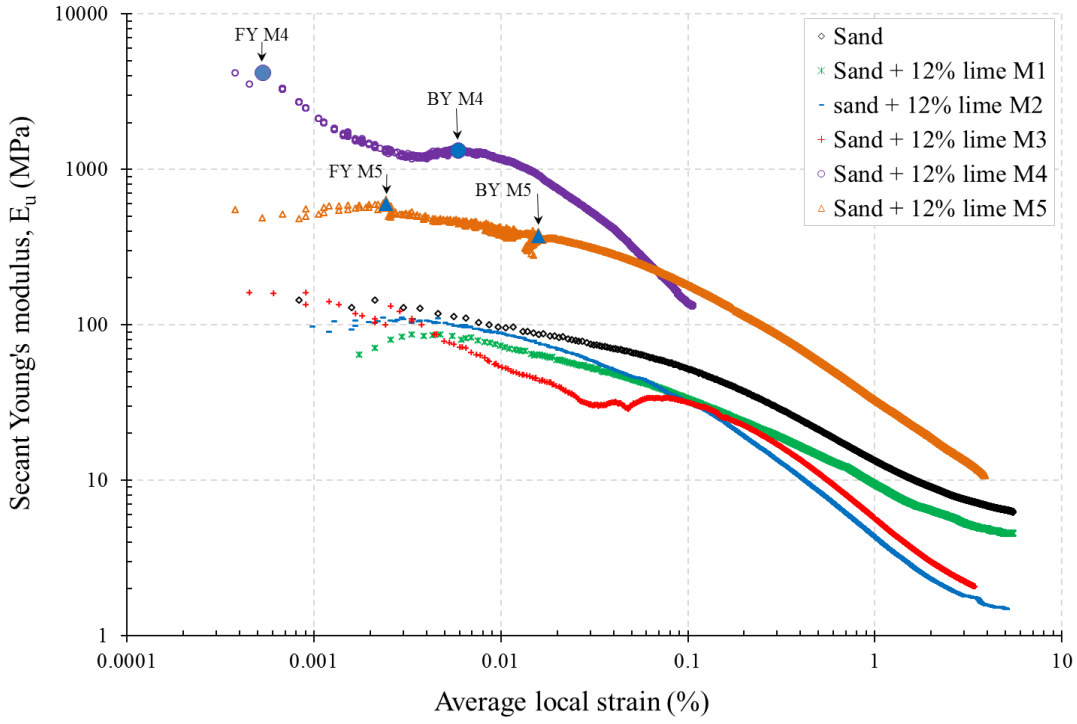

Figure 4.50 Secant Young's modulus results for the specimens of sand cemented with lime and prepared employing different techniques.

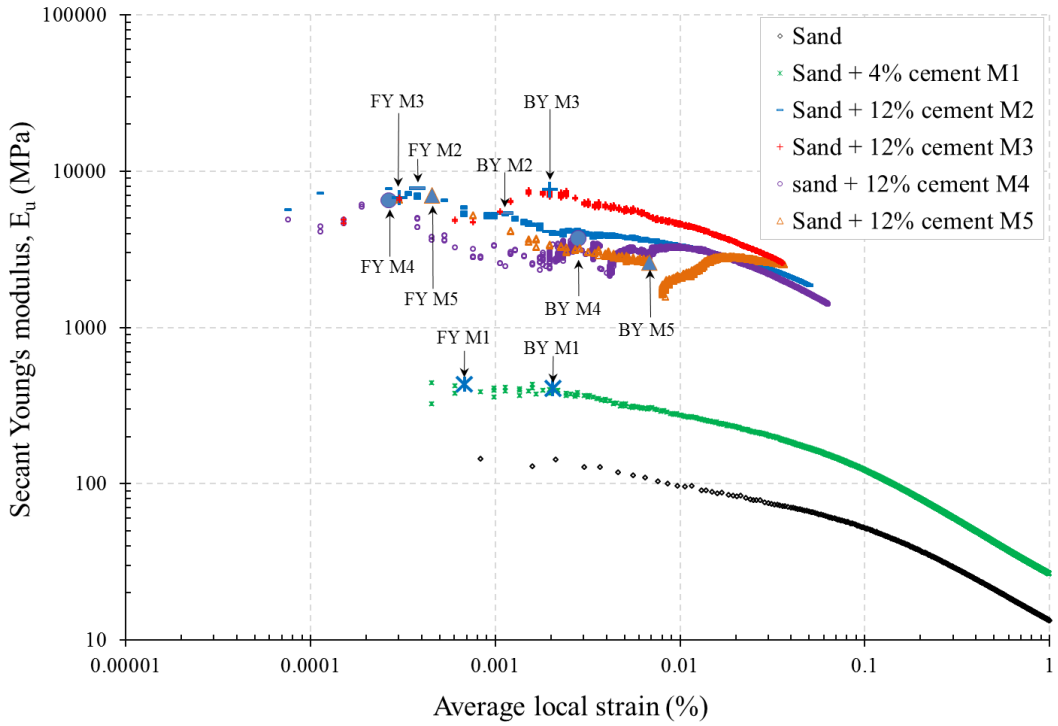

Figure 4.51 Secant Young's modulus results for the specimens of sand cemented by cement and prepared employing different techniques.

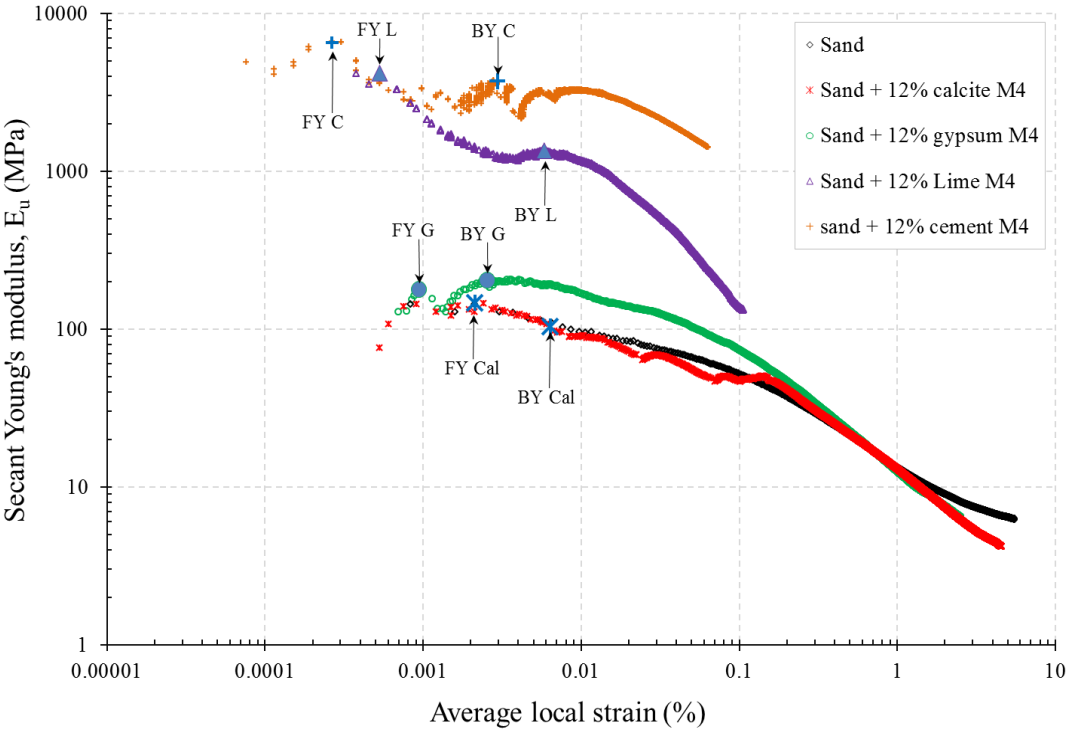

Figure 4.52 Secant Young's modulus results for the specimens of sand cemented by different cementing agents and prepated employing technique M4.

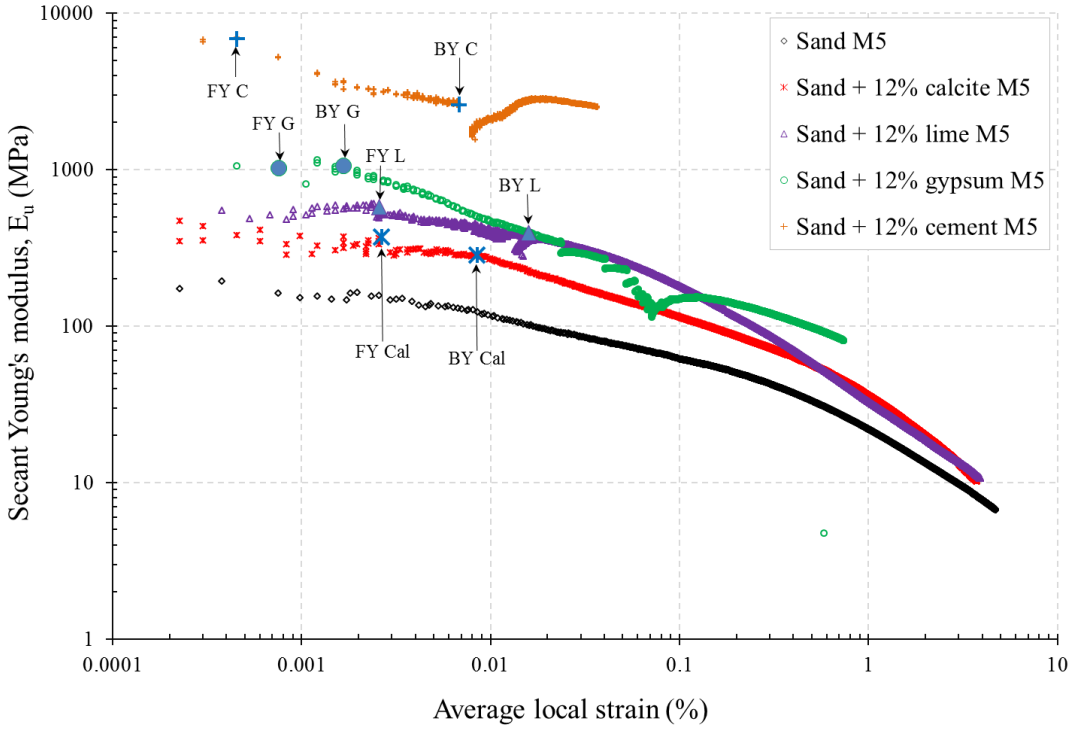

Figure 4.53 Secant Young's modulus results for the specimens of sand cemented by different cementing agents and prepared employing technique M5.

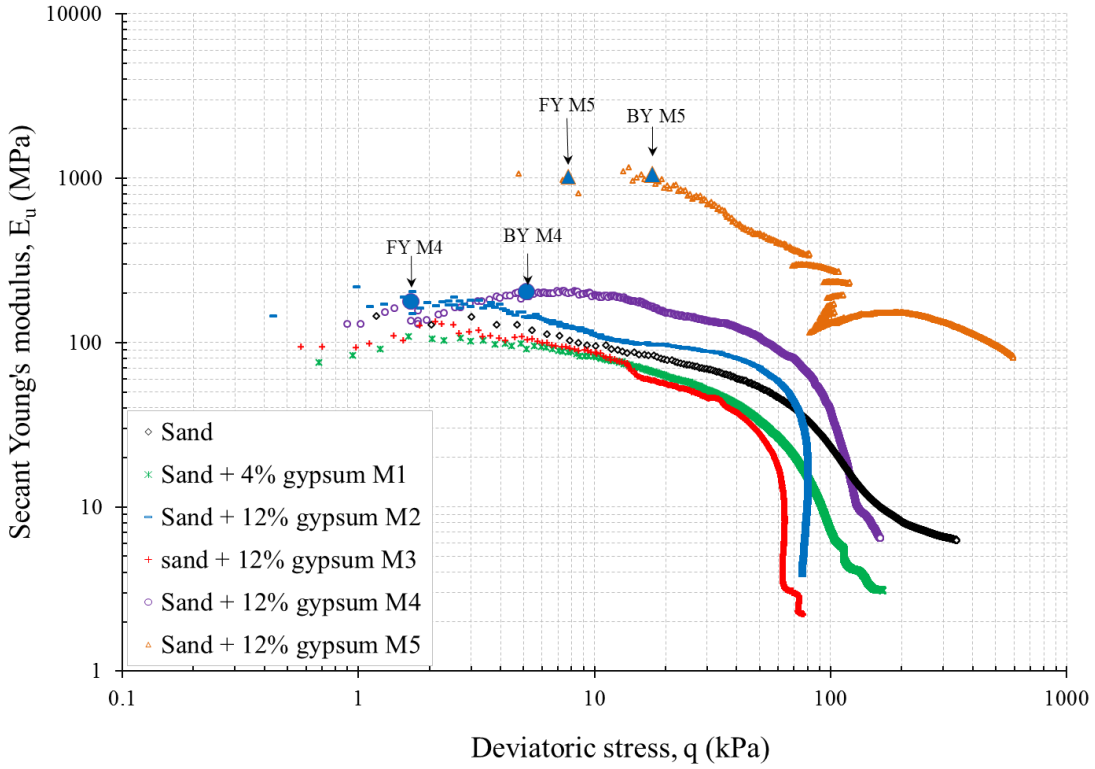

Figure 4.54 Variation of stiffness with the deviatoric stress for the specimens of sand cemented by gypsum and prepared employing different techniques.

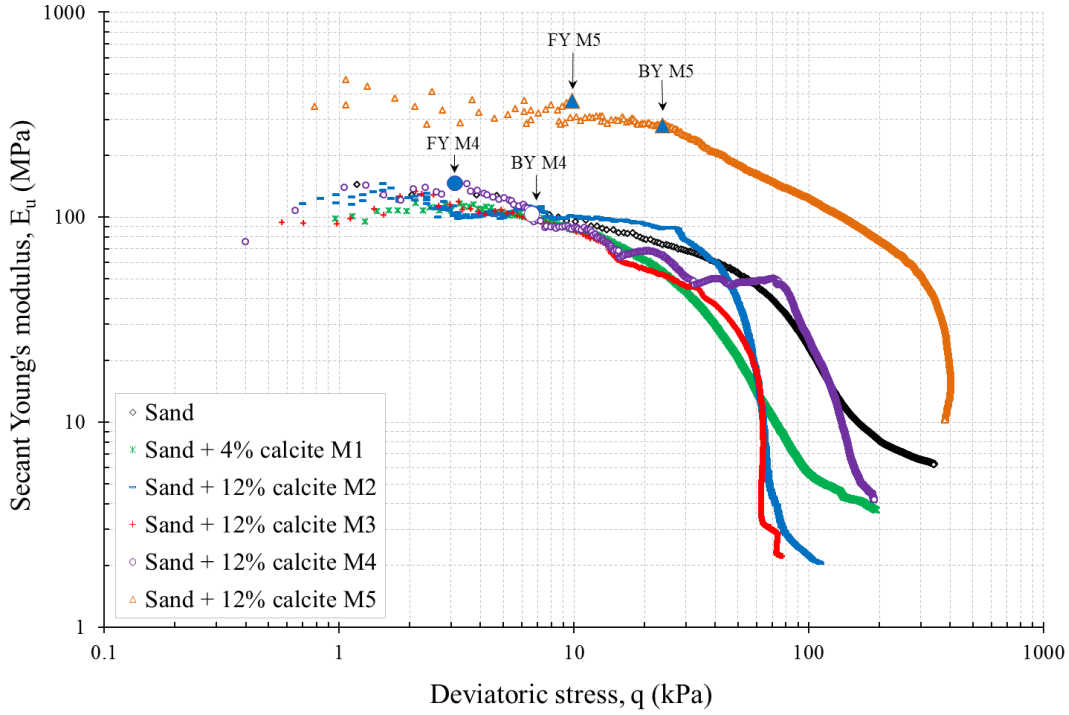

Figure 4.55 Variation of stiffness with the deviatoric stress for the specimens of sand cemented by calcite and prepared employing different techniques.

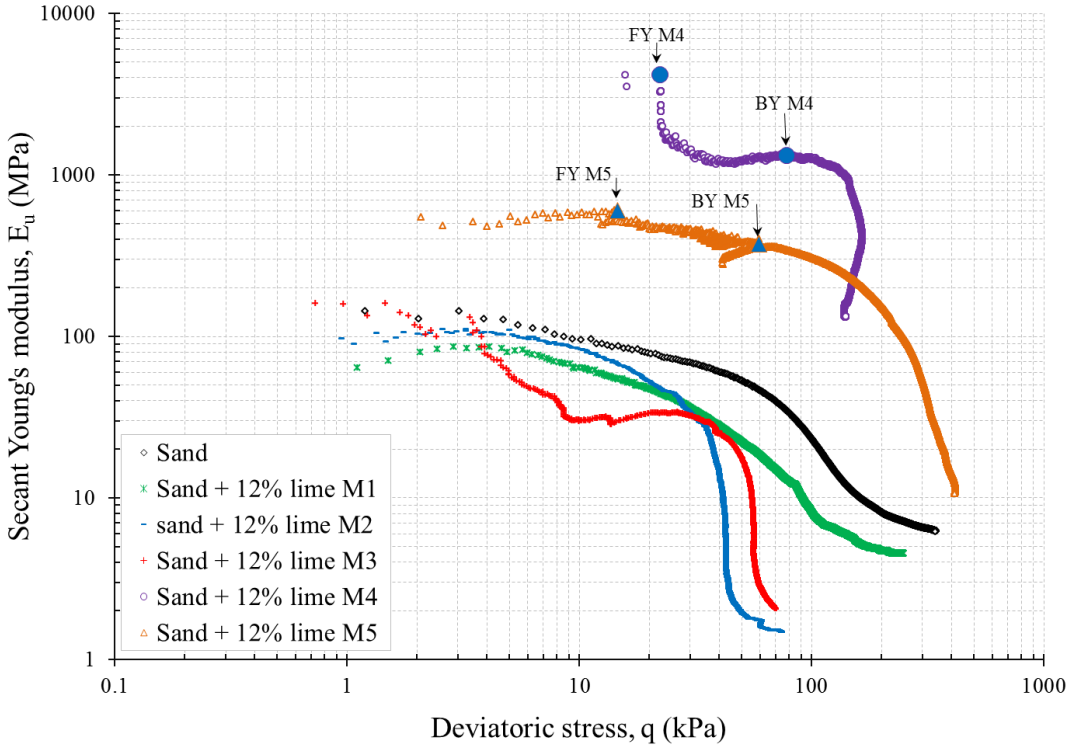

Figure 4.56 Variation of stiffness with the deviatoric stress for the specimens of sand cemented with lime and prepared employing different techniques.

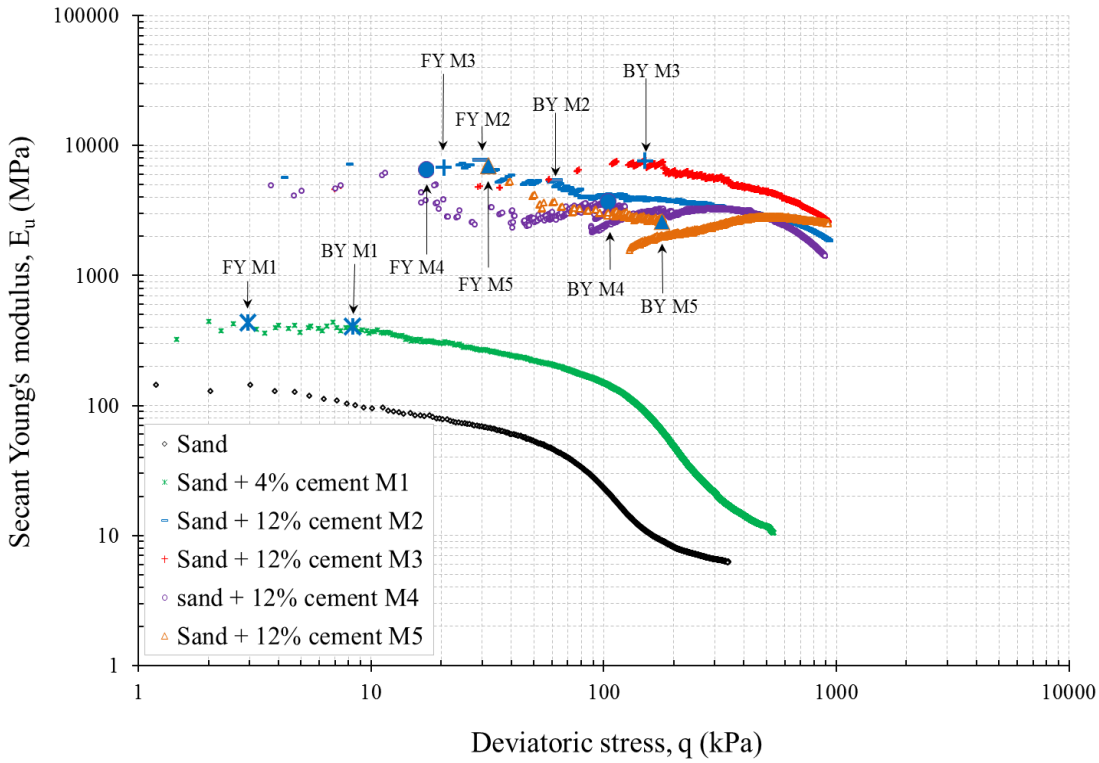

Figure 4.57 Variation of stiffness with the deviatoric stress for the specimens of sand cemented by cement and prepared employing different techniques.

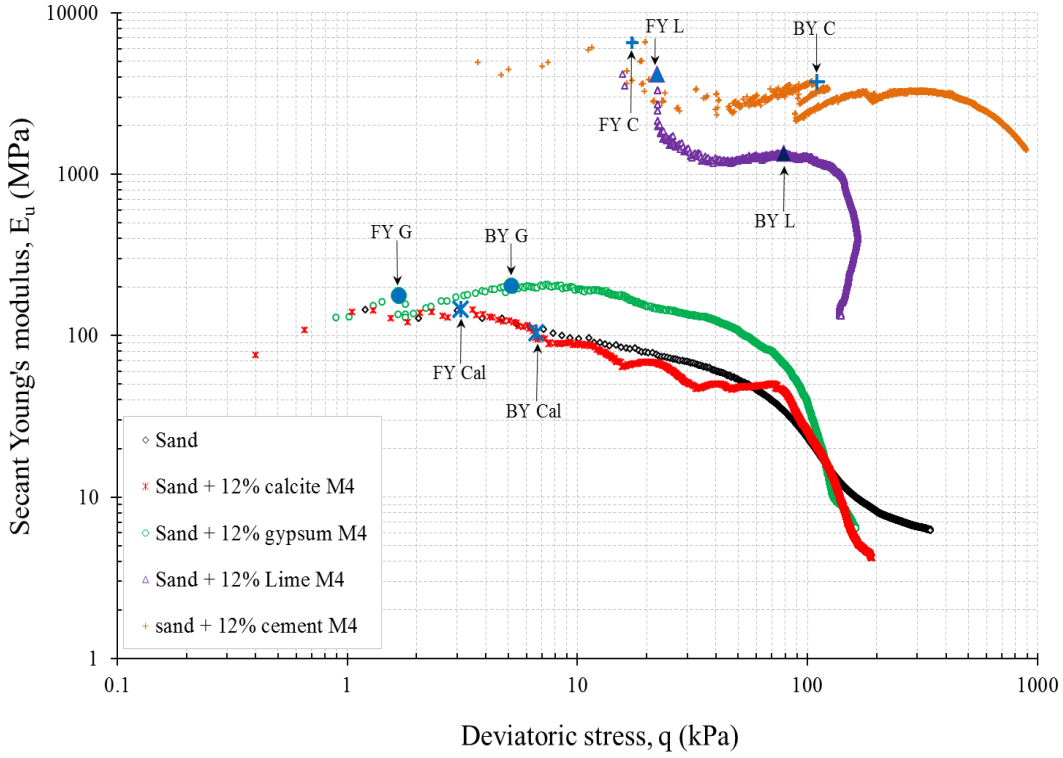

Figure 4.58 Variation of stiffness with the deviatoric stress for the specimens of sand cemented by different cementing agents and prepared using M4 techniques.

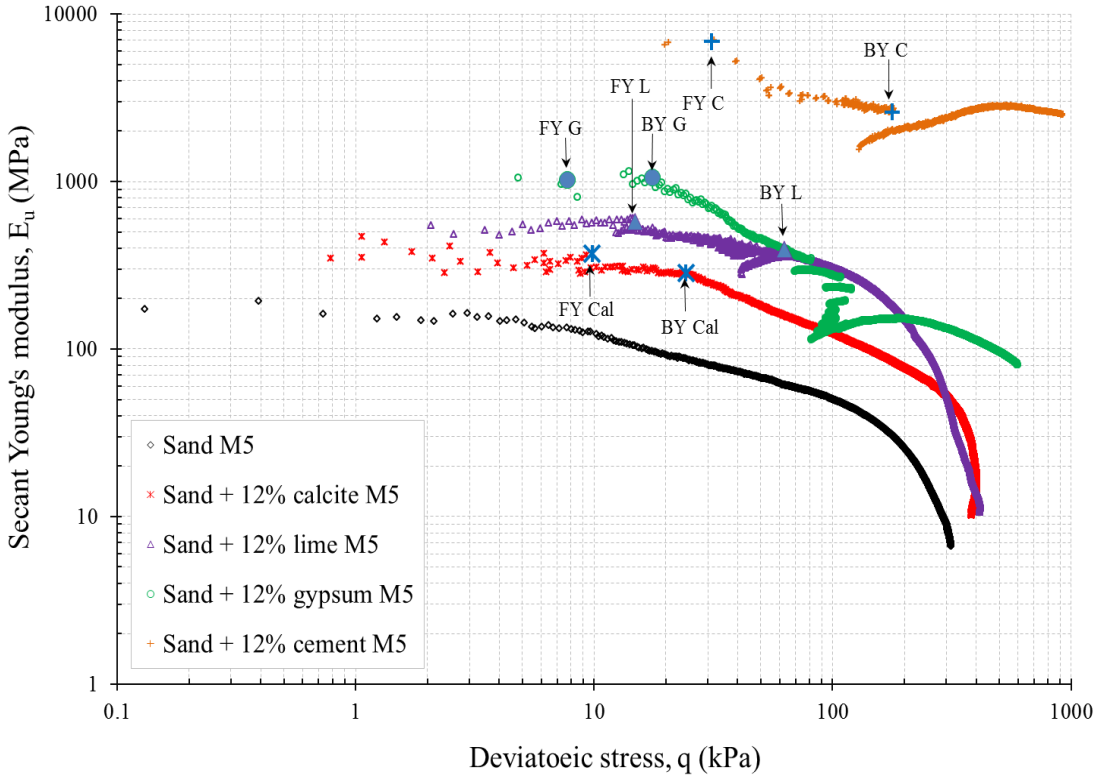

Figure 4.59 Variation of stiffness with the deviatoric stress for the specimens of sand cemented by different cementing agents and prepared using M5 techniques.

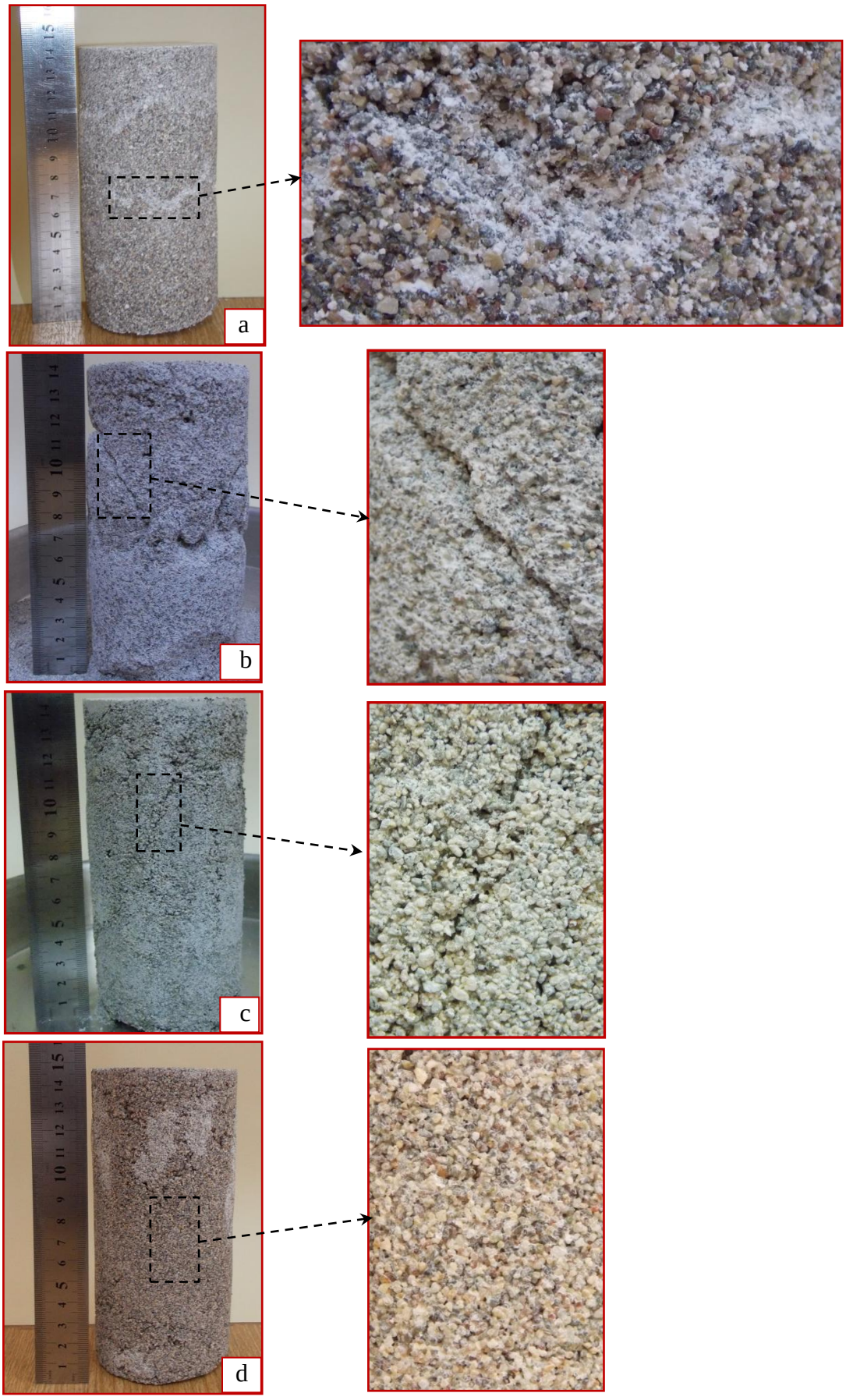

Figure 4.60 Pictures of the cemented sand specimens after testing (a) gypsum (b) calcite (c) lime (d) cement.

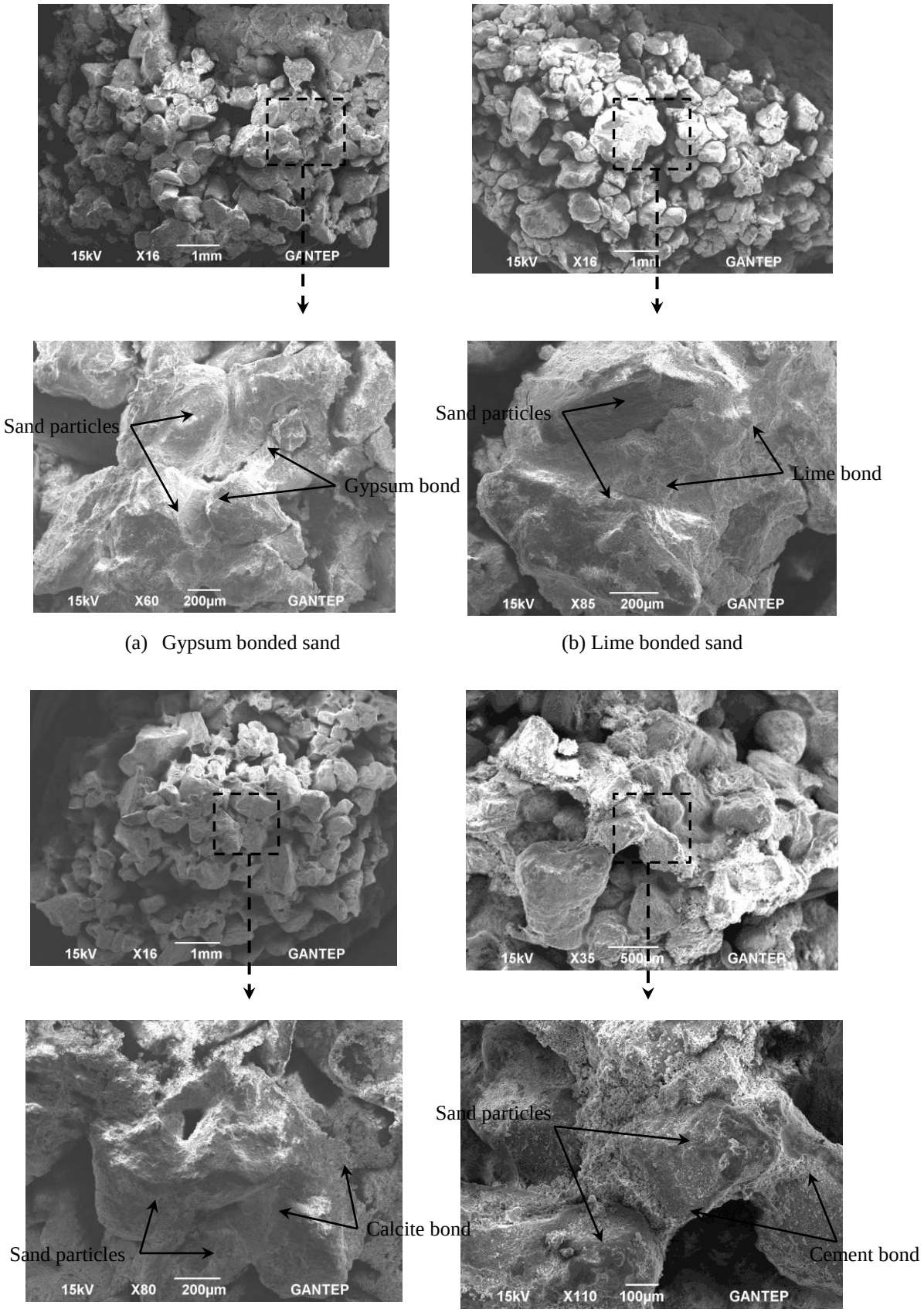

(a) Gypsum bonded sand

(b) Lime bonded sand

(c) Calcite bonded sand

(d) Cement bonded sand

Figure 4.61 SEM pictures for the sand with hydrated cementing agents.

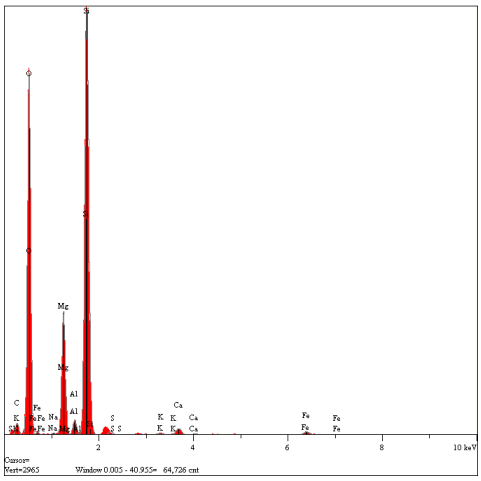

(a) Sand

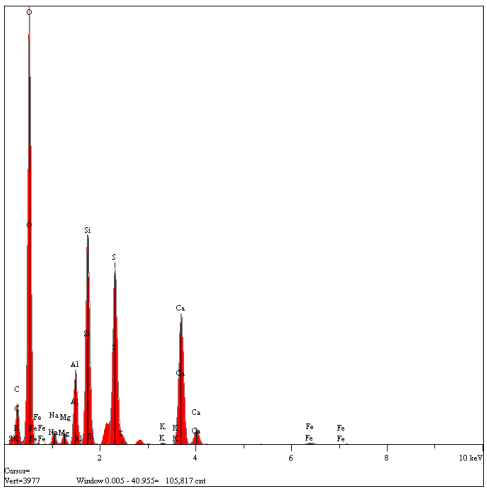

(b) Gypsum bonded sand

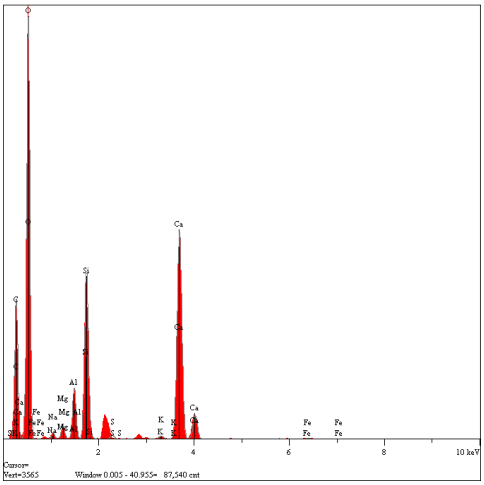

(c) Calcite bonded sand

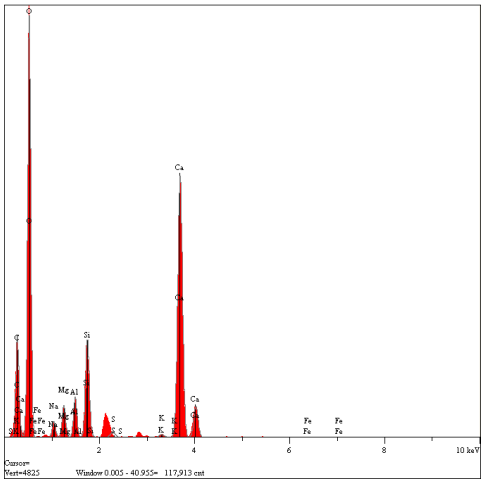

(d) Lime bonded sand

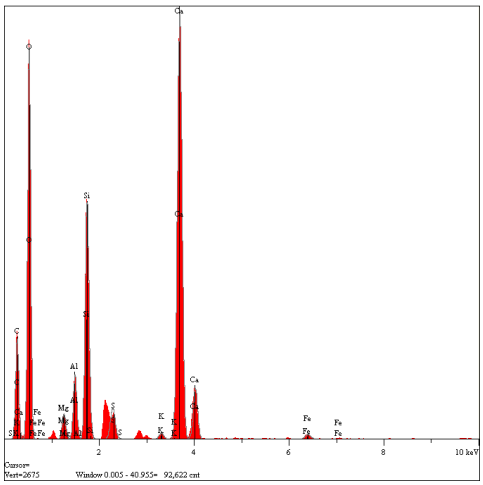

(d) Cement bonded sand

Figure 4.62 EDX results for the sand with different hydrated cementing agents.

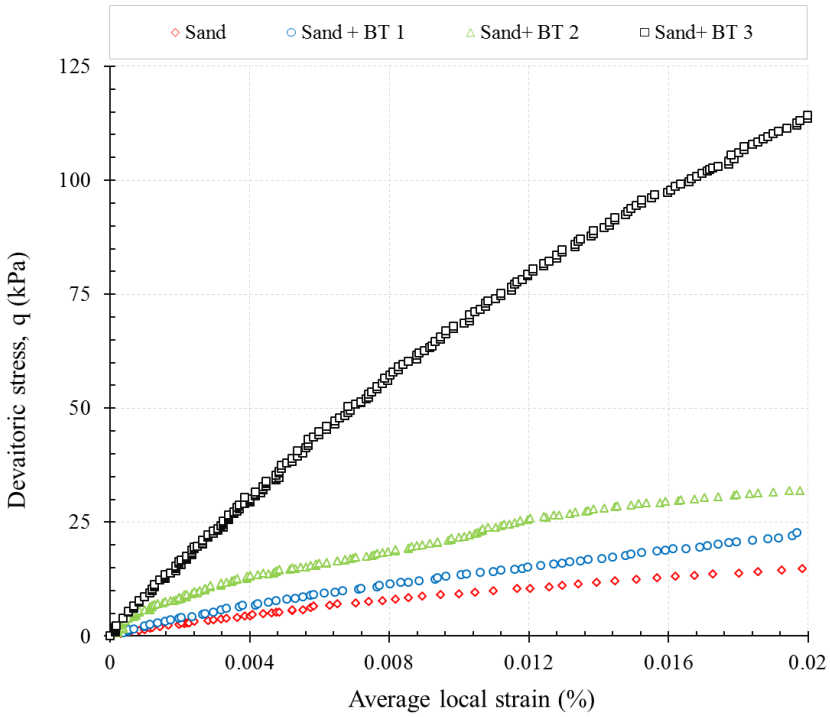

(a)

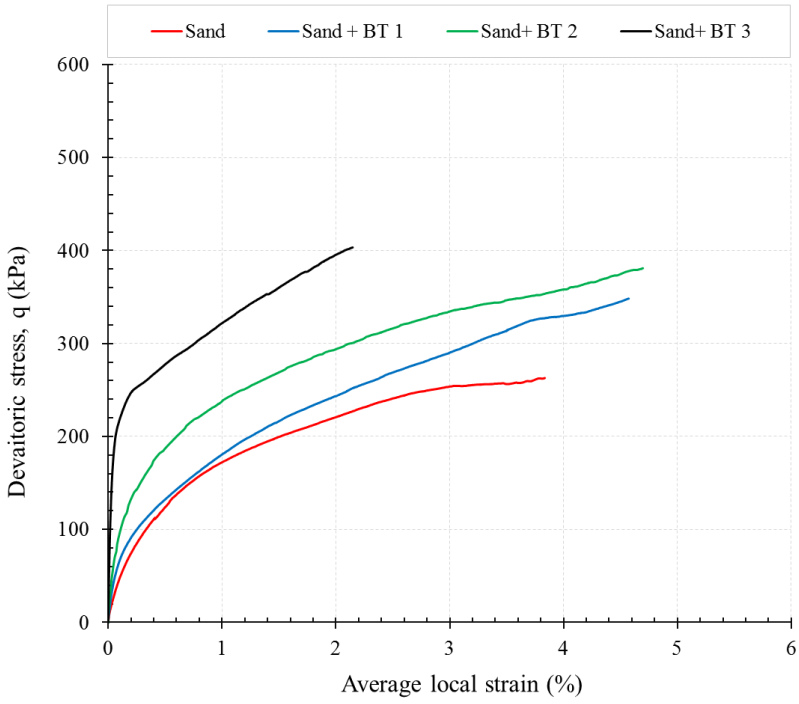

(b)

Figure 4.63 Response of the biocemented sand specimens in the triaxial tests, deviator stress verses the average local strain, for the strain levels between (a) 0.02% and 0% (b) 6% and 0%.

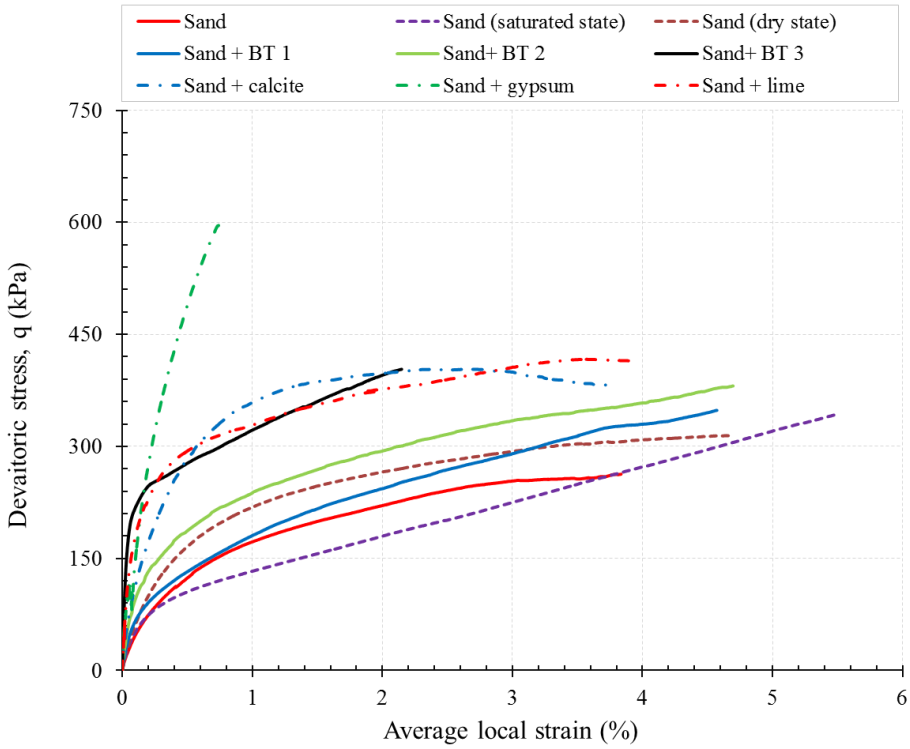

Figure 4.64 Comparison the response of the biocemented sand specimens in the triaxial tests with the cemented specimens by conventional cementing agents.

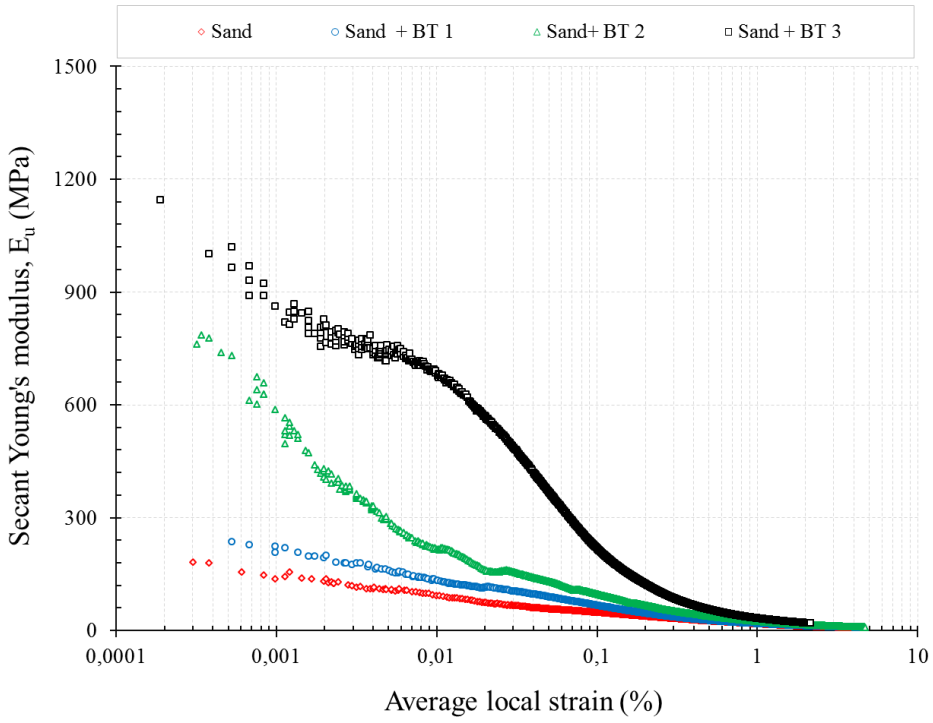

(a)

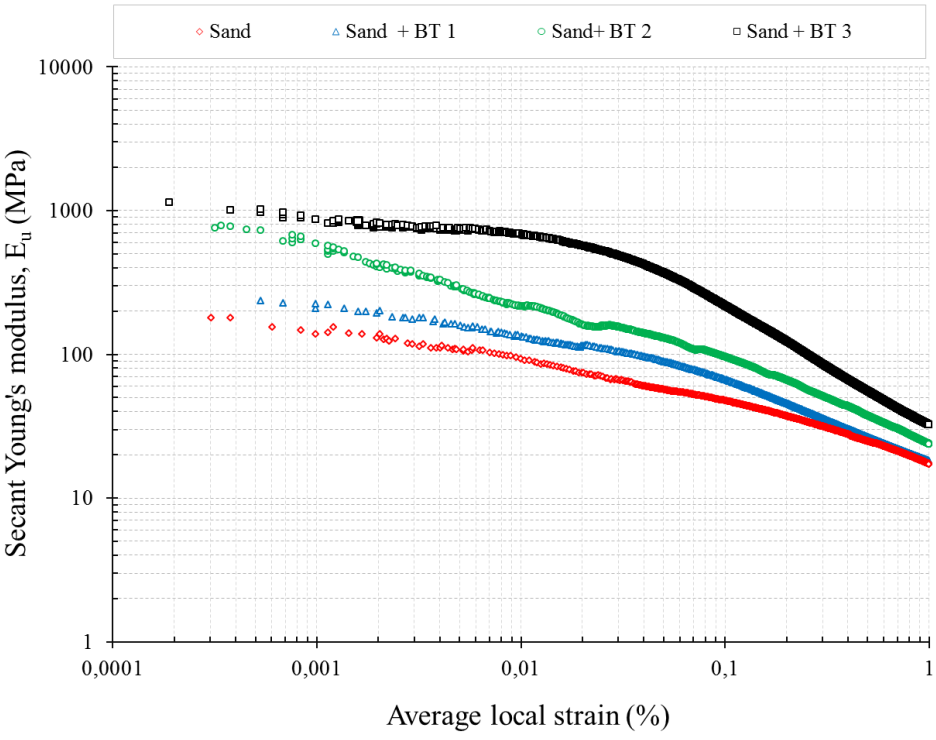

(b)

Figure 4.65 Variation of the small strain stiffness of the biocemented sand with the average local strain (a) semi-log scale (b) log-log scale.

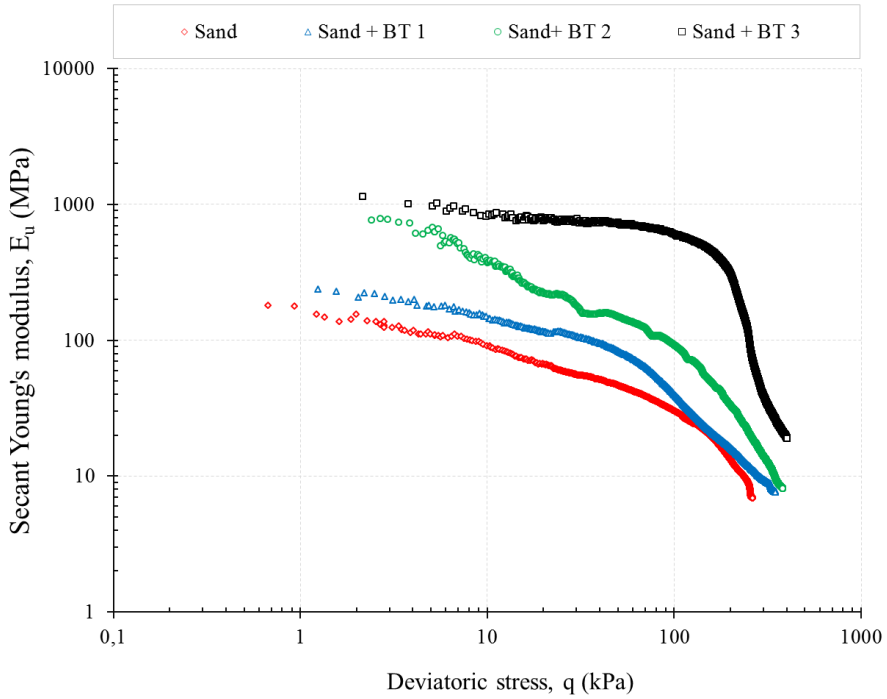

Figure 4.66 Variation of the biocemented sand stiffness with the deviatoric stress.

(a)

(b)

(c)

Figure 4.67 Biocemented specimens after extraction from the triaxial cell for (a) lightly cemented BT1 (b) moderately cemented (BT2) (c) heavily cemented (BT3).

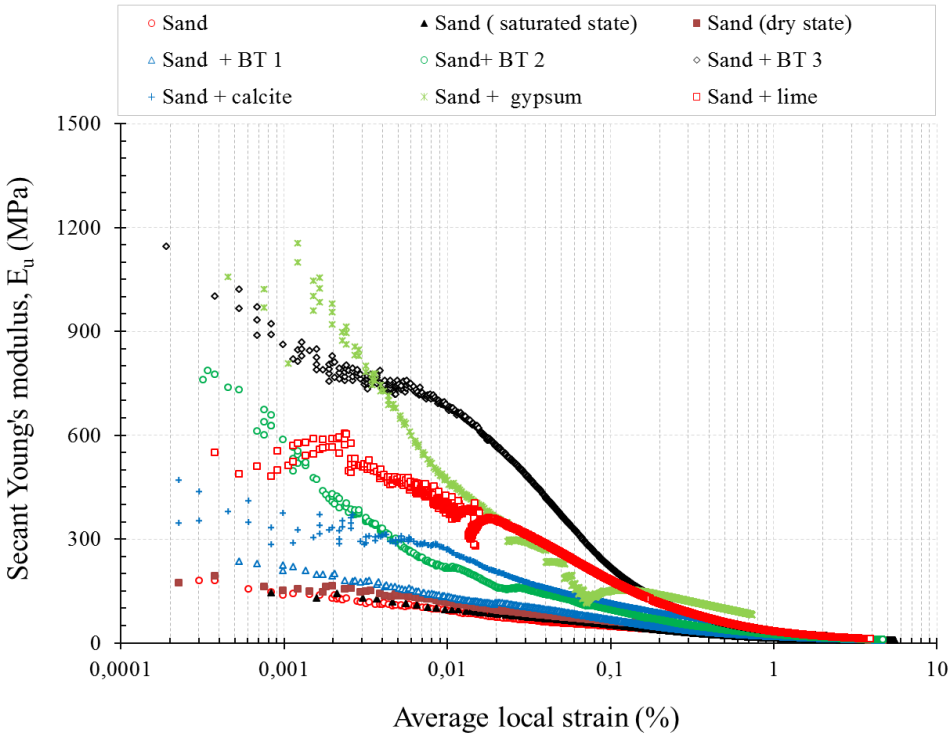

Figure 4.68 Small strain stiffness of the biocemented sands and the cemented sands by conventional cementing agents.

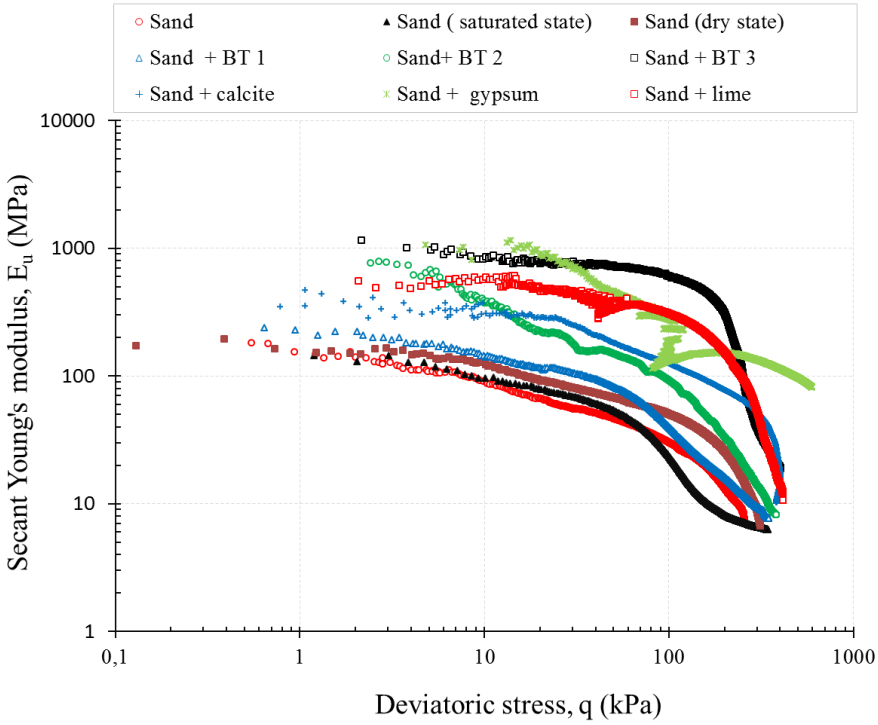

Figure 4.69 Variation of stiffness with the deviator stress of the biocemented sands and the cemented sands by conventional cementing agents.

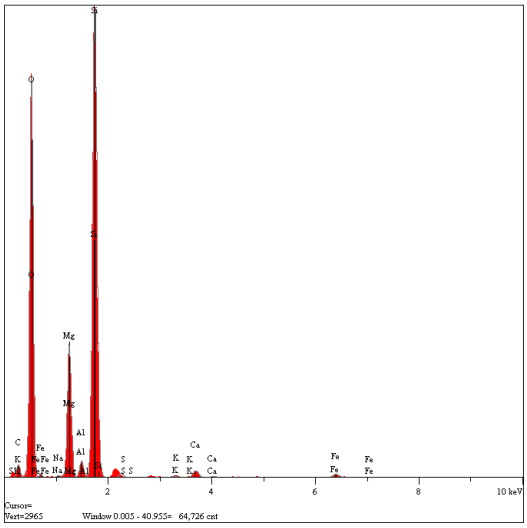

(a) Untreated sand

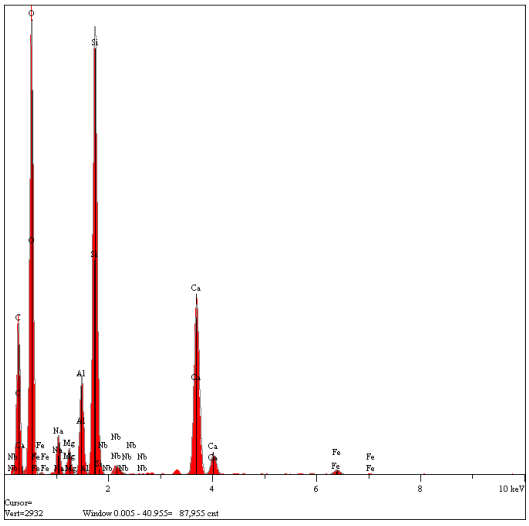

(b) Sand with BT1

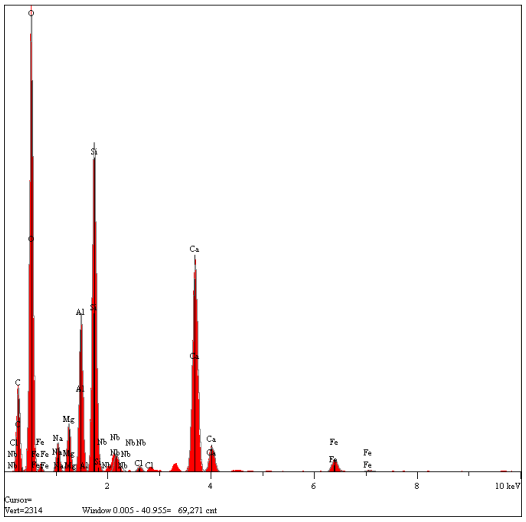

(c) Sand with BT2

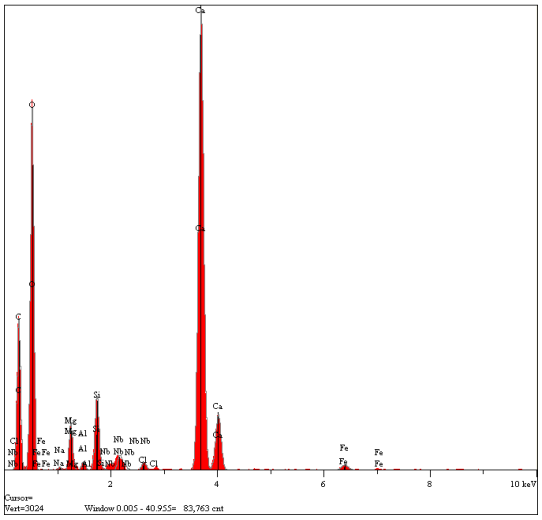

(d) Sand with BT3

Figure 4.70 Energy Dispersive X-ray (EDX) analyses results for the untreated sand and biocemented sands.

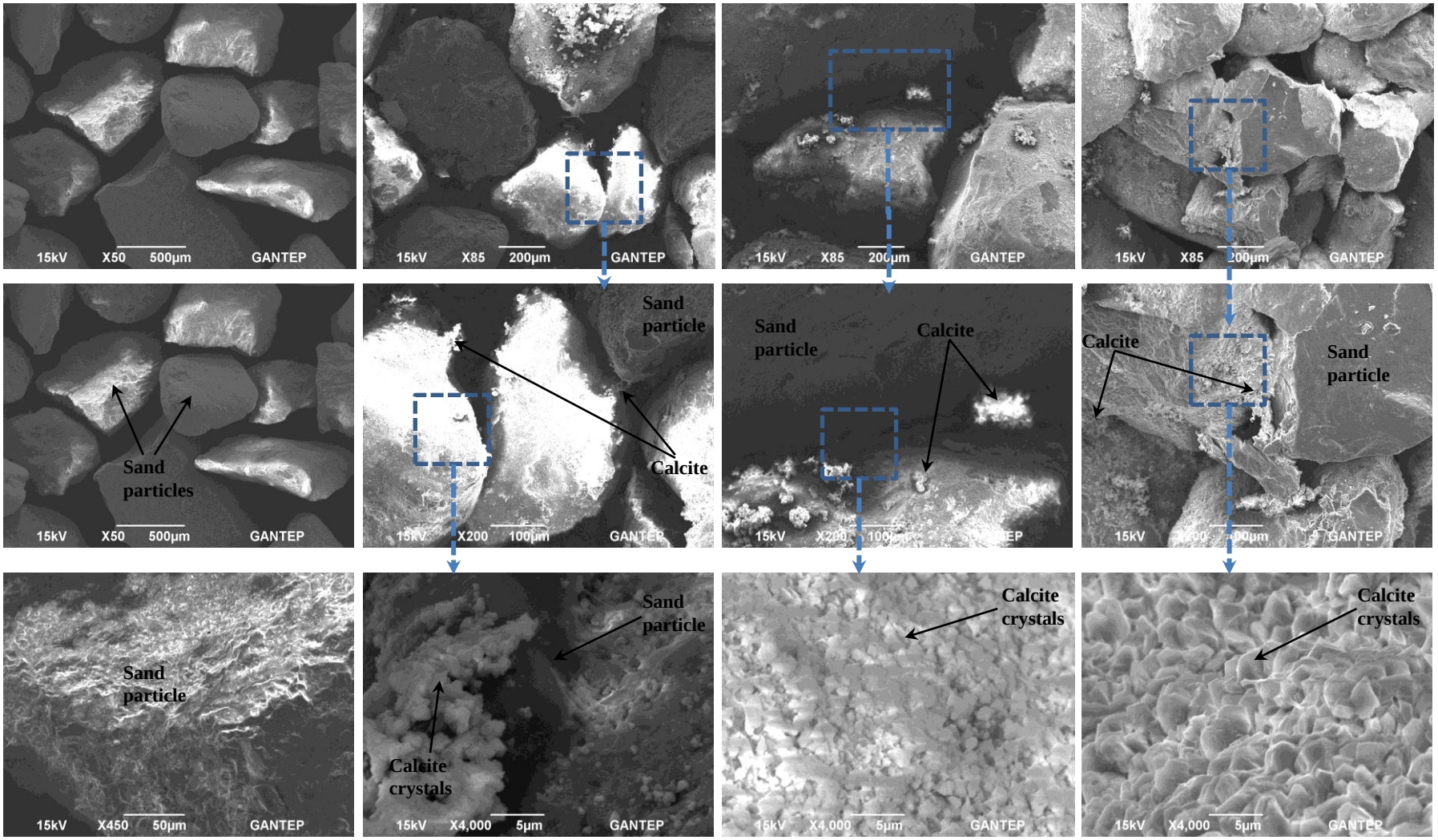

(a) Untreated sand (b) Sand with BT1 (c) Sand with BT2 (d) Sand with BT3

Figure 4.71 Scanning Electron Microscopy (SEM) pictures of the untreated sand and biocemented sands.

CHAPTER 5

CONCLUSIONS AND RECOMMENDATIONS

5.1 Conclusions

The research presented in this thesis focused on investigation of the stress-strain and small strain stiffness of the artificially cemented sand. In the initial phase of the study, a series of the preliminary triaxial tests were conducted to study the response of the natural sand. Afterwards, detailed studies were performed to investigate the behaviour of the clean and cemented sand at small strains. The triaxial system was modified for local strain measurements by using LVDTs. The effects of five different sample preparation methods, and four different cementing agents (gypsum, lime, calcite, Portland cement) on the triaxial behaviour of cemented sand were investigated. During the experimental study to investigate; emphasis was given the small strain stiffness of cemented sand. In the other part of the detailed studies, the stress-strain behaviour and small strain stiffness of the biocemented sand specimens were investigated. Also, an attempt was made to study the effect of the tire crumb inclusion on the behaviour of the clean and cemented sand. Therefore, the conclusions drawn from the current study are presented in four parts; (i) preliminary study of clean sand, (ii) behaviour of the cemented sand and tire crumbs mixture, (iii) effect of sample preparation method on the behaviour of cemented sand at small strain, and (iv) the stiffness and the stress-strain response of the biocemented sand at the small strain level.

1- Conclusions drawn from the preliminary triaxial test of clean sand:

- In general, for all types of the triaxial tests (CU and CD), the deviatoric stress and stiffness increased as the effective confining pressure and consolidation period increased. The generation of pore water pressure in the CU tests increased as the effective confining and consolidation period decreasd. The volume change and volumetric strain increase as the effective confining pressure increases.

- The sand specimens exhibit higher contractive behaviour as the consolidation period becomes shorter. Change in the effective confining pressure did not greatly influence the contractive and the dilative behaviour of the clean sand.
- Triaxial tests on the clean sand in the case of CU and CD indicated that the sand has higher deviatoric stress, stiffness, angle of internal friction in the case of CD condition than those obtained under CU condition. The clean sand specimens tested under CU condition and for all effective confining pressures, the contraction behavior was more evident than those of specimens tested under CD conditions.
- As the relative density of the clean sand increases the deviatoric stress and stiffness increase and the pore water pressure decrease. Considering the effect of the consolidation period the material behaviour becomes more contractive as the relative density decreases.

2- Conclusions on monitoring the behaviour of cemented sand and tire crumbs mixture:

Triaxial behaviours of sands-tire crumbs-cement mixtures were examined. The common aspect of the published waste tire applications is the determination of a relationship between type, aspect ratio, content of waste tires and their contribution on the behaviour of soils. The use of waste tires in civil engineering applications can reduce the tire disposal problem in an economically and environmentally beneficial way. However, use of waste tires cannot yield desired properties for some geotechnical applications always. Therefore, this part of the study has attempted to present an investigation carried out to increase the effectiveness of waste tires use in geotechnical applications by creating artificially bonding with a relatively small amount of cement. The investigation carried out to test the effect of cementation under stress on the behaviour of cemented sand and tire crumbs mixtures reports five new facets of behaviour:

- The deviatoric stress decreases as the tire crumbs content increases in the mixture within the measured strain level, and no peak shear stress values are observed in all the specimens. The deviatoric stress continues to increase with increasing axial strain. Also, the generation of the pore water pressure

decreases as the tire crumb content increases. The contraction behaviour increases as the tire crumbs content increases in the mixture.

- As the cement content in a sand with tire crumb increases, the deviatoric stress values increases. The sand-tire crumbs specimens with smaller amount of cement exhibit a higher pore water generation, in particular at larger axial strain levels.
- Hydrated cement particles cover the tire crumbs grains and sand grains, thereby, this process causes reduction in size of tire crumbs and compressibility characteristics, while it is cured under a 100 kPa effective confining stress.
- Dilative and contractive behaviour of sand with tire crumbs can be controlled by application of cement bonding. Dilatancy of the sand-tire crumbs mixtures increases as the cement content increases.
- The stiffness of the sand-tire crumb specimens decreases as the amount of tire crumbs increase in the mixture for specimens have the same percentages of cement, and increases as the percentage of the cement increase for specimens have the same amount of the tire crumbs.

3- Conclusions drawn from use of LVDTs for strain measurements and from the study of the effect of sample preparation methods on behaviour of cemented sand:

- The use of LDVTs for local strain measurements provides an accurate measurement of axial displacement over the complete range of strains.
- Determination of small strain stiffness from the stress-strain curves of the clean and cemented sand could only be obtained if axial strains were measured internally by using submersible LVDTs. This is due to the presence of significant bedding errors, tilting of the specimen and due to the effect of the apparatus compliance in the external readings. Also, using this method provides accurate observation of stiffness degradation curves that can be derived in as small as 0.002% axial strain. Furthermore, stiffness of the material that is estimated based on local strain measurements at the small strain is higher than its value when it is estimated based on the global strain measurements. Also, degradation in the stiffness value derived from the local

strain measurement is higher than its degradation in the case of external strain measurement.

- Triaxial behaviour of artificially cemented sands at small strain levels was examined. The effect of gypsum, lime, and calcite on the behaviour of the specimens differs greatly based on the preparation technique and curing conditions. However, the effect of Portland cement on the triaxial behaviour differs slightly depending on the sample preparation and the curing conditions.
- The mechanism observed in the specimens tested by employing certain techniques indicates that the cementing agents could behave like a 'fine material' in the specimen, rather than a 'bond' between the grains. The authors suggest that specimen formations and testing techniques in the way used here, mineralogical and physical properties of both sand and cementing agents could effect on the triaxial behaviour of the specimens tested.
- The specimens prepared by employing the same method and cemented with different cementing agents produce different strength, stress-strain behaviour, pore water pressure generation, stress path trend, stiffness values and degradation, yielding point position, and yielding strength.
- Generally, for all types of the cementing agents and for all sample preparation methods, there is degradation in the specimen stiffness with the axial strain. The stiffness of the cemented sand specimens at the small strain and the position of the first yield and bond yield varied depending on sample preparation methods for all types of the cementing agents. On the other hand, they depend on the characteristics of the cementing agents for the same sample preparation method.
- There is a well-defined plateau in the stiffness values at the beginning of loading which extends to relatively high values of the deviator stress. This plateau followed by a sharp decrease in the stiffness values as yielding is approached. This behaviour is same in cemented specimens that cemented with all types of the cementing agents and all sample preparation techniques.

4- Conclusions stemming from biocemented sand behaviour:

The biocementation part of this study is a pioneer investigation that presents the influence of microbial products (cementing material) on stress-strain behaviour and stiffness of sand at small strains. The objective of this part of the study was to develop an artificial cementation technique using the microorganism. The improved engineering performance of biocemented sand over its uncemented state and cemented with conventional cementing agents was assessed using local strain instrumentation with high precision and accuracy. The tests reported in this part show four new facets of behaviour:

- The biocementation process results in a significant increase in the deviatoric stress, as the period of biological treatment increases. The period of the biological treatment process caused an increase in the amount of calcite that precipitates on the sand grains.
- The stiffness of the biocemented sand specimens increase as the biocementation treatment period increase at strain levels less than 1%. However, the stiffness values for all the specimens tested were very close to each other at a strain range higher than 1% strain level. A significant amount of degradation in the stiffness appeared between 0.001% and 0.1% average axial local strain for all the specimens tested. This zone, which involves a sharp drop of the stiffness, indicates to the yielding of the cementation bonds.
- The response of the sand treated with BT3 (heavily microbial cementation) exhibit an overall trend that is similar to that of calcite and lime cemented sand specimens prepared and tested under the same conditions.
- Microscopic investigation of the sand specimens indicated that the calcite crystals precipitated on to grains' surface as well as in the contacts between grains. The cementing material made bonding bridge between the soil particles and increases the shear strength and the small strain stiffness. Amount of the calcite precipitated was seen to be higher as the period of biocementation treatment increases.

5.2 Recommendations for future works

Some recommendations can be drawn from the findings of the current research in order to observe behaviours of cemented sand in more details. Therefore, further researches are warranted in regard to the following items:

1- These studies were conducted using one type of the soil with different cementing agents and sample preparation method. These studies could be extended to use other soils with different grain shape and size to investigate effect of these properties on the response of the cemented sand.
2- The importance of the local instruments (LVDTs) that was described in this thesis for the axial displacement measurements which is very essential for stiffness determination of the soil. The techniques may be extended to use other local instruments for lateral strain measurements for more accurate observation the lateral strain.
3- It is recommended to study the influence of sample preparation techniques and other environmental conditions such as the effect of curing temperature on the behaviour of the biocemented soils.
4- Further research is required to determine the amount of calcite precipitation from the bacterial activity using the X-ray computed tomography images during the treatment process. Also, it is recommended to use bender elements to predict the amount of the biominerals that results from the treatment and to compare the stiffness values that estimated from this method with the stiffness values estimated from the triaxial test using LVDTs.
5- The biocementation technique that was described in this thesis has significantly improved the stress-strain and stiffness of the sand. Therefore, the investigation of the applicability of this method to modify the stress-strain and stiffness of the granular material used in field applications, namely sand columns is required. Also, further investigation is required to examine the performance of the biocementation technique for stabilization of the sand dunes for mitigation of dust formation.

REFERENCES

Abdulla, A., Kiousis, P. D. (1997). Behavior of cemented sands-I testing, *International Journal for Numerical and Analytical Methods in Geomechanics*, **21**, 533-547.

Acar, B. Y., El-Tahir A. E. (1986). Low strain dynamic properties of artificially cemented sands, *Journal of Geotechnical Engineering Division*, **112**, **No. 11,** 1001-1015.

Ackerley, S. K., Hellings, J. E., Jardine, R. J. (1987). Discussion on A new device for measuring local axial strains on triaxial specimens, *Géotechnique*, **37, No. 3**, 413-417.

Ahmad, I. (1993). Laboratory study on properties on rubber soils, Report No. FHWA/IN/JHRP-93/4, Joint Highway Research Project, Indiana Department of Transportation, USA.

Airey, D. W. (1993). Triaxial testing of naturally cemented carbonate soil, *Journal of Geotechnical Engineering Division*, **119, No. 9**, 1379-1398.

Airey, D. W., Fahey, M. (1991). Cyclic response of calcareous soil from the North-West Shelf of Australia, *Géotechnique*, **41**, **No. 1**, 101-121.

Akbulut, S., Arasan, S., Kalkan, E. (2007). Modification of clayey soils using scrap tire rubber and synthetic fibers, *Applied Clay Science*, **38**, 23-32.

AL-Thawadi, S. M. (2008). High strength in-situ biocementation of soil by calcite precipitation locally isolated ureolytic bacteria, PhD thesis, University of Murdoch, Western Australia.

Al-Qabany, A., Soga, K. (2013). Effect of chemical treatment used in MICP on engineering properties of cemented soils, *Géotechnique*, **63**, **No. 4**, 331-339.

Alvarado, G., Coop, M. R., Willson, S. M. (2008). On the role of unloading on the behaviour of reservoir sands and sandstones, *Géotechnique*, **62**, **No. 4**, 303-316.

Anastasiadis, A., Senetakis, K. (2011). Small-strain shear modulus and damping ratio of sand-rubber and gravel-rubber mixtures, *Geotechnical and Geological Engineering*, **30**, **No. 2**, 363-382.

Anastasiadis, A., Pitilakis, K., Senetakis, K. (2009). Dynamic shear modulus and damping ratio curves of sand/rubber mixtures, Proceedings of the earthquake geotechnical engineering satellite conference, XVIIth International Conference on Soil Mechanics and Geotechnical Engineering, Alexandria, Egypt.

ASTM. American Society for Testing and Materials. (2014). Standard test methods for maximum index density and unit weight of soils using a vibratory table. D4253-14. West Conshohocken, PA.

ASTM. American Society for Testing and Materials. (2014). Standard test methods for minimum index density and unit weight of soils and calculation of relative density. D4254-14. West Conshohocken, PA.

ASTM. American Society for Testing and Materials. (2007). Standard test method for particle-size analysis of soils. D422-63. West Conshohocken, PA.

Atkinson, J. H. (2000). Non-linear soil stiffness in routine design. The 40th Rankine Lecture, *Géotechnique*, **50**, **No. 5**, 487-508.

Atkinson, J. H., Sallfors, G. (1991). Experimental determination of stress-strain-time characteristics in laboratory and in-situ tests, Proceedings of 10th European Conference of Soil Mechnics and Foundation Engineering, Florence, No. 3, Balkema, Rotterdam, 915-956.

Atkinson, J. H., Richardson, D., Stallebrass, S. E. (1990). Effect of recent stress history on the stiffness of overconsolidated soil, *Géotechnique*, **40**, **No. 4**, 531-540.

Attom, M. F. (2006). The use of shredded waste tires to improve the geotechnical engineering properties of sands, *Environmental Geology*, **49**, 497-503.

Baig, S., Picornell, M., Nazarian, S. (1996). Low strain shear moduli of cemented sands, *Journal of Geotechnical Engineering Division*, **123**, **No. 6**, 540-545.

Baldi, G., Hight, D. W., Thomas, G. E. (1988). A re-evaluation of conventional triaxial test methods, Proceedings of ASTM Symposium on advanced triaxial testing of soil and rock, ASTM STP 977, West Conshohocken, 219-263.

Banagan, B. L., Wertheim, B. M., Roth, M. J. S., Caslake, L. F. (2010). Microbial strengthening of loose sand, *Letters in Applied Microbiology*, **51**, 138-142.

Bang, S., Min, S. H., Bang, S. S. (2011). Application of microbiologically induced soil stabilization technique for dust suppression, *International Journal of Geo-Engineering*, **3**, **No. 2**, 27-37.

Bang, S., Galinat, J. K., Ramakrishnan, V. (2001). Calcite precipitation induced by polyurethane-immobilized Bacillus pasteurii, *Enzyme and Microbial Technology*, **28**, 404-409.

Bernardi, D. J. (2012). Biologically Cemented Sandstone Bricks, MSc thesis. University of California, US.

Bhandari, A. R., Powrie, W. (2013). Strength and deformation characteristics of a locked sand at low effective stresses, *Granular Matter*, **15**, 543-556.

Bianco, A., Madonia, G. (2007). B.U.L.M. technique for increase of the bearing capacity in the pavement layers subjected to biological treatment, Proceedings of 4th International Siiv Congress, Palermo, Italy.

Blauw, M., Lambert, J. W. M., Latil, M. N. (2009). Biosealing a method for in-situ sealing of leakages, Proceedings of the International Symposium on Ground Improvement Technologies and Case Histories, Singapore, 125-130.

Bosscher, P. J., Edil, T., Kuraoka, S. (1997). Design of highway embankments using tire chips, *Journal of Geotechnical Engineering Division*, **123**, **No. 4**, 295-304.

Bressani, L. A. (1990). Experimental properties of bonded soils, PhD thesis, University of London, UK.

Bressani, L. A., Vaughan, P. R. (1989). Damage to soil structure during triaxial testing, Proceedings. XII International Conference Soil Mechanics and Foundation Engineering, Rio de Janerio 1, 17-20.

Brown, S. F., Snaith, M. S. (1974). The measurement of recoverable and irrecoverable deformations in the repeated load triaxial test, *Géotechnique*, **24**, **No. 2**, 255-259.

Burbank, M. B., Weaver, T. J., Green, T. L., Williams, B. C., Crawford, R. L. (2012). Precipitation of calcite by indigenous microorganisms to strengthen liquefiable soils, *Geomicrobiology Journal*, **28**, 301-312.

Burbank, M., Weaver, T., Lewis, R., Crawford, R. L., Williams, B. (2013). Geotechnical tests of sands following bio-Induced calcite precipitation catalyzed by indigenous bacteria, *Journal of Geotechnical and Geo-environmental Engineering*, **139**, **No. 6**, 928-936.

Burland, J. B. (1990). On the compressibility and shear strength of natural clays, *Géotechnique*, **40**, **No. 3**, 329-378.

Burland, J. B., Symes, M. (1982). A simple axial displacement gauge for use in the triaxial apparatus, *Géotechnique*, **32**, **No. 1**, 62-65.

Cabalar, A. F. (2010). Applications of the triaxial, resonant column and oedometer tests to the study of micaceous sands, *Engineering Geology*, **112**, 21-28.

Cabalar, A. F. (2010). Direct shear tests on waste tires-sand mixtures, *Geotechnical and Geological Engineering*, **29**, **No. 4**, 411-418.

Cai, Y., Shi, B., Ng, C. W. W., Tang, C. (2006). Effect of polypropylene fibre and lime admixture on engineering properties of clayey soil, *Engineering Geology*, **87**, 230-240.

Carter, J. P., Johnston, I. W., Fahey, M., Chapman, G. A., Novello, E. A., Kaggwa, W. S. (1988). Triaxial testing of North Rankin calcarenite, Proceedings of International Conference Engineering for Calcareous Sediments, Balkema, Rotterdam, 515-530.

Casagrande, A. (1932). The structure of clay and its importance in foundation engineering, *Journal of the Boston Society of Civil Engineers*, **19**, **No. 4**, 168-209.

Chen, C. W. (2006). Drained and undrained behavior of fiber-reinforced sand, Transportation Scholars Conference, November 15, Iowa State University, US.

Cheng, L., Cord-Ruwisch, R. (2012). In situ soil cementationwith ureolytic bacteria by surface percolation, *Ecological. Engineering*, **42**, 64-72.

Christopher, B. R., Atmatzidis, D. K., Krizek, R. J. (1989). Laboratory testing of chemically grouted sand, *Geotechnical Testing Journal*, **12**, **No. 2**, 109-118.

Chu, J., Ivanov, V., Naeimi, M., Stabnikov, V., Liu, H. L. (2014). Optimization of calcium-based bioclogging and biocementation of sand, *Acta Geotechnica*, **9**, 277-285.

Consoli, N. C., Rotta, G. V., Prietto, P. D. M. (2000). The influence of curing under stress on the triaxial response of cemented soils, *Géotechnique*, **50**, **No. 1**, 99-105.

Consoli, N. C., Bassani, M. A. A., Festugato, L. (2010). Effect of fiber-reinforcement on the shear strength of cemented soils, *Geotextiles and Geomembranes*, **28**, **No. 4**, 344-351.

Consoli, N. C., Casagrande, M. D. T., Prietto, P. D. M., Thome, A. (2003). Plate load test on fibre-reinforced soil, *Journal of Geotechnical and Geo-environmental Engineering*, **129**, **No. 10**, 951-955.

Consoli, N. C., Montardo, J. P., Donato, M., Prietto, P. D. M. (2004). Effect of material properties on the behaviour of sand-cement-fibre composites, *Ground Improvement*, **8, No. 2**, 77-99.

Consoli, N. C., Vendruscolo, M. A., Fonini, A., Rosa, F. D. (2009). Fiber reinforcement effects on sand considering a wide cementation range, *Geotextile and Geomembranes*, **27**, 196-203.

Consoli, N. C., DA Silva Lopes JR, L., Consoli, B. S., Festugato, L. (2014). Mohr-Coulomb failure envelopes of lime-treated soils, *Géotechnique*, **64**, **No. 2**, 165-170.

Consoli, N. C., Fonseca, A. V., Silva, S. R., Cruz, R. C., Fonini, A. (2012). Parameters controlling stiffness and strength of artificially cemented soils, *Géotechnique*, **62**, **No. 2**, 177-183.

Clayton, C. R. I. (1983). The infuence of diagenesis on some index properties of chalk in England, *Géotechnique*, **33**, **No. 3**, 225-241.

Clayton, C. R. I. (2011). Stiffness at small strain: research and practice, *Géotechnique*, **61**, **No. 1**, 5-37.

Clayton, C. R. I., Khatrush, S. A. (1987). A new device for measuring local axial strains on triaxial specimens, *Géotechnique*, **36**, **No. 4**, 593-597.

Clayton, C. R. I., Heymann, G. (2001). Stiffness of geomaterials at very small strains, *Géotechnique*, **51**, **No. 3**, 245-255.

Clayton, C. R. I., Hababa, M. B., Simons, N. E. (1984). Dynamic penetration resistance and the prediction of the compressibility of fine-grained sand-a laboratory study, *Géotechnique*, **35**, **No. 1**, 19-31.

Clayton, C. R. I., Hight, D. W., Hopper, R. J. (1992). Progressive destructuring of Bothkennar clay: implications for sampling and reconsolidation procedures, *Géotechnique*, **42**, **No. 2**, 219-240.

Clayton, C. R. I., Priest, J. A., Rees, E. V. L. (2010). The effects of hydrate cement on the stiffness of some sands, *Géotechnique*, **60**, **No. 6**, 435-445.

Clayton, C. R. I., Khatrush, S. A., Bica, A. V. D., Siddique, A. (1989). The use of hall effect semi-conductors in geotechnical instrumentation, *Geotechnical Testing Journal*, **12**, 69-76.

Clough, G. W., Kuck, W. M., Kasali, G. (1979). Silicate-stabilized sands, *Journal of the Geotechnical Engineering Division*, **105**, **No.1**, 65-82.

Clough, G. W., Sitar, N., Bachus, R. C., Shaffi Rad, N. (1981). Cemented sands under static loading, *Journal of the Geotechnical Engineering Division*, **107**, **No. 6**, 799-817.

Coop, M. R., Atkinson, J. H. (1993). The mechanics of cemented carbonate sands, *Géotechnique*, **43**, 53-67.

Coop, M. R., Willson, S. M. (2003). On the behavior of hydrocarbon reservoir sands and sandstones, *Journal of Geotechnical and Geo-environmental Engineering*, **129**, **No. 11**, 1010-1019.

Costa-Filho, L. M., Vaughan, P. R. (1980). Discussion on 'A computer model for the analysis of ground movements in London clay' by Simpson et al. (1979), *Géotechnique*, **30**, **No. 3**, 336-339.

Cuccovillo, T. (1995). Shear behaviour and stiffness of naturally cemented sands, PhD thesis, City University, London, UK.

Cuccovillo, T., Coop, M. R. (1993). The influence of bond strength on the mechanics of carbonate soft rocks, Proceedings of International Conference on Geotechnical Engineering of Hard Soils-Soft Rocks (A. Anagnostopoulos et al., eds), Athens, Greece, Balkema: Rotterdam, 447-455.

Cuccovillo, T., Coop, M. R. (1997a). The measurement of local axial strains in triaxial tests using LVDTs, *Géotechnique*, **47**, **No. 1**, 167-171.

Cuccovillo, T., Coop, M. R. (1997b). Yielding and pre-failure deformation of structured sands, *Géotechnique*, **47**, **No. 3**, 491-508.

Cuccovillo, T., Coop, M. R. (1999). On the mechanics of structured sands, *Géotechnique*, **49**, **No. 6**, 741-760.

Dalla Rosa, F., Consoli, N. C., Baudet, B. A. (2008). An experimental investigation of the behaviour of artificially cemented soil cured under stress, *Géotechnique*, **58**, **No. 8**, 675-679.

DeJong, J. T., Fritzges, M. B., Nusslein, K. (2006). Microbially induced cementation to control sand response to undrained shear, *Journal of Geotechnical and Geoenvironmental Engineering*, **132, No.11**, 1381-1392.

DeJong, J. T., Mortensen, M. B., Martinez, B. C., Nelson, D. C. (2010). Biomediated soil improvement, *Ecological. Engineering*, **36**, **No. 2**,197-210.

DeJong, J. T., Martinez, B. C., Ginn, T. R., Hunt, C., Major, D., Tanyu, B. (2014). Development of a scaled repeated five-spot treatment model for examining microbial induced calcite precipitation feasibility in field applications, *Geotechnical Testing Journal*, **37**, **No. 3**, 424-435.

DeJong, J. T., Soga, K., Kavazanjian, E., Burns, S., Van passen, L. A., AL-Qabany, A., et al. (2013). Biogeotechnical processes and geotechnical applications: progress, opportunities and challenges, *Géotechnique*, **63**, **No. 4**, 287-301.

Della, N., Arab, A., Belkhatir, M. (2011). Effect of confining pressure and depositional method on the undrained shearing response of medium dense sand, *Journal of Iberian Geology*, **37, No.1**, 37-44.

Diaz-Rodríguez, J. A., Antonio-Izarraras, V. M. (2004). Mitigation of liquefaction risk using colloidal silica stabilizer, 13th World Conference on Earthquake Engineering, Vancouver, B.C., Canada, No. 509.

Dickson, T. H., Dwyer, D. F., Humphrey, D. N. (2001). Prototypes tire-shred embankment construction, Transportation Research Record 1755, TRB, National Research Council, Washington, DC, 160-167.

Dosier, G. K. (2013). Methods for making construction material using enzyme producing bacteria, *US Provisional Patent Application*, **13**, 093-335.

Dongliang, Y., Yutian, W., Yan, D. (2011). The evaluation of soil cementation generated from the function of microorganism, *Research Journal of Chemical Sciences*, **1**, **No. 1**, 13-17.

Dupas, J. M., Pecker, A. (1979). Static and dynamic properties of sand-cement, *Journal of the Geotechnical Engineering Division*, **106**, **No. 3**, 275-297.

Edil, T., Bosscher, P. (1994). Engineering properties of tire chips and soil mixtures, *Geotechnical Testing Journal*, **14**, **No. 4**, 453-464.

Edincliler, A. (2007). Using waste tire-soil mixtures for embankment construction, International Workshop on Scrap Tire Derived Geomaterials ‘‘Opportunities and Challenges”. Kanto Branch of Japanese Geotechnical Society, 319-328.

Edincliler, A., Baykal, G., Dengili, K., (2004). Determination of static and dynamic behaviour of recycled materials for highways, *Conservation and Recycling*, **42**, **No. 3**, 223-237.

Edincliler, A., Baykal, G., Saygili, A. (2010). Influence of different processing techniques on the mechanical properties of used tires in embankment construction, *Waste Management*, **30**, 1073-1080.

Edincliler, A., Cabalar, A. F., Cagaty, A., Cevik, A. (2012). Triaxial compression behavior of sand and tire wastes using neural networks, *Neural Computing and Applications*, **21**, 441-452.

Ehrlich, HL. (1996). Geomicrobiology, 3rd edition, New York, Marcel Dekker Inc.

Etemadi, O., Petrisor, I. G., Kim, D., Wan, M. W., Yen, T. F. (2003). Stabilization of metals in subsurface by biopolymers: Laboratory drainage flow studies, *Soil Sediment Contamination: An International Journal.*, **12**, **No. 5**, 647-661.

Fearon, R. E., Coop, M. R. (2000). Reconstitution: what makes an appropriate reference material, *Géotechnique*, **50**, **No. 4**, 471-477.

Feng, Z. Y., Sutter, K. G. (2000). Dynamic properties of granulated rubber/sand mixtures, *Geotechnical Testing Journal*, **23**, **No. 3**, 338-344.

Fernandez, A. L., Santamarina, J. C. (2001). Effect of cementation on the small-strain parameters of sands, *Canadian Geotechnical Journal*, **38**, 191-199.

Ferris, F. G., Stehmeier, L. G., Kantzas, A., Mourits, F. M. (1996). Bacteriogenic mineral plugging, *Journal of Canadian Petroleum Technology*, **35**, **No. 8**, 56-61.

Foose, G. J., Benson, C. H., Bosscher, P. J. (1996). Sand reinforced with shredded waste tires, *Journal of Geotechnical and Geoenvironmental Engineering*, **122**, **No. 9**, 760-767.

Fujita, Y., Taylor, J. L., Wendt, L. M., Reed, D. W., Smith, R. W. (2010). Evaluating the potential of native ureolytic microbes toremediate a^{90}Sr contaminated environment, *Environmental Science and Technology*, **44**, **No. 19**, 7652-7658.

Gallagher, P. M., Mitchell, J. K. (2002). Influence of colloidal silica grout on liquefaction potential and cyclic undrained behavior of loose sand, *Dynamics and Earthquake Engineering*, **22**, 1017-1026.

Georgiannou, V. N. (2006). The undrained response of sands with additions of particles of various shapes and sizes, *Géotechnique*, **56**, **No. 9**, 639-649.

Ghazavi, M. (2004). Shear strength characteristics of sand-mixed granular rubber, *Geotechnical and Geological Engineering*, **22**, 401-416.

Gollapudi, U. K., Knutson, C. L., Bang, S. S., Islam, M. R. (1995). A new method for controlling leaching through permeable channels, *Chemosphere*, **30**, 695-705.

Goto, S., Tatsuoka, F., Shibuya, S., Kim, Y. S., Sato, T. (1991). A simple gauge for local small strain measurements in the laboratory, *Soils and Foundations*, **31**, **No. 1**, 169-180.

Gotteland, P., Lambert, S., Balachowski, L. (2005). Strength characteristics of tyre chips-sand mixtures, *Studia Geotechnica et Mechanica*, **27**, 1-2.

Guleria, S. P., Dutta, R. K. (2012). Effect of addition of tire chips on the unconfined compressive strength of fly ash-lime-gypsum mixture, *International Journal of Geotechnical Engineering*, **6**, 1-13.

Haeri, S. M., Seiphoori, A., Rahmati, A. (2008). The behavior of a limy cemented gravely sand under static loading-case study of Tehran alluvium, *Electronic Journal of Geotechnical Engineering*, **13**.

Haeri, S. M., Hamidi, A., Hosseini, S. M., Asghari, E., Toll, D. G. (2006). Effect of cement type on the mechanical behavior of a gravely sand, *Geotechnical and Geological Engineering Journal*, **24**, **No. 2**, 335-360.

Hamidi, A., Haeri S. M. (2008). Stiffness and deformation characteristics of a cemented gravely sand, *International Journal of Civil Engineering*, **6**, **No. 3**, 159-173.

Hamidi, A., Hooresfand, M. (2013). Effect of fiber reinforcement on triaxial shear behavior of cement treated sand, *Geotextiles and Geomembranes*, **36**, 1-9.

Hammes, F., Boon, N., de Villiers, J., Verstraete, W., Siciliano, S. D. (2003). Strain specific ureolytic microbial calcium carbonate precipitation, *Applied and Environmental Microbiology*, **69**, **No. 8**, 4901-4909.

Hardin, B. O., Drnevich, V. P. (1972). Shear modulus and damping in soil: measurement and parameter effects, *Journal of the Soil Mechanics and Foundations Division*, **98**, **No. 7**, 603-624.

He, J., Chu, J., Ivanov, V. (2013). Mitigation of liquefaction of saturated sand using biogas, *Géotechnique*, **63**, **No. 4**, 267-275.

Heymann, G. (1998). The stiffness of soils and weak rocks at very small strains, PhD thesis, University of Surrey, UK.

Heymann, G., Clayton, C. R. I., Reed, G. T. (2005). Triaxial ultra-small strain measurements using laser interferometry, *Geotechnical Testing Journal*, **28, No. 6**, 544-552.

Hight, D. W., Boese, R., Butcher, A. P., Clayton, C. R. I., Smith, P. R. (1992). Disturbance of bothkennar clay prior to laboratory testing, *Géotechnique*, **42**, **No. 2**, 199-218.

Hird, C. C., Yung, P. C. Y. (1989). The use of proximity transducers for local strain measurements in triaxial tests, *Geotechnical Testing Journal*, **12**, **No. 4**, 292-296.

Huang, J. T., Airey, D.W. (1998). Properties of artificially cemented carbonate sand, *Journal of the Geotechnical Engineering Division*, **124**, **No. 6**, 492-499.

Humphrey, D., Manion, W. (1992). Properties of tire chips for lightweight fill, *Grouting Soil Improvement and Geosynthetics*, **2**, 1344-1355.

Ivanov, V., Chu, J. (2008). Applications of microorganisms to geotechnical engineering for bioclogging and biocementation of soil in-situ, *Reviews in Environmental Science and Bio/Technology*, **7**, **No. 2**, 139-153.

Ismail, M. A., Joer, H. A., Randolph, M. F., (2000). Sample preparation technique for artificially cemented soils, *Geotechnical Testing Journal*, **23**, **No. 2**, 171-177.

Ismail, M. A., Joer, H. A., Sim, W. E., Randolph, M. F. (2002). Effect of cement type on shear behaviour of cemented calcareous soil, *Journal of Geotechnical and Geoenvironmental Engineering*, **128**, **No. 6**, 520-529.

James, G. A., Warwood, B. K., Hiebert, R., Cunningham, A. B. (2000). Microbial barriers to the spread of pollution, *Bioremediation*, 1-13.

Jardine, R. J. (1985). Investigation of pile-soil behaviour, with special reference to the foundations of offshore structures, PhD thesis, Imperial College, University of London, UK.

Jardine, R. J. (1992). Some observations on the kinematic nature of soil stiffness, *Soils and Foundations*, **32**, **No. 2**, 111-124.

Jardine, R. J. (1995). One perspective of the pre-failure deformation characteristics of some geomaterials, Proceedings of the 1st International Conference on CreFailure Deformation of Geomaterials, Shibuya, Mitachi and Miura (eds), Sapporo, Japan, 855-885.

Jardine, R. J., Symes, M. J., Burland, J. B. (1984). The measurement of soil stiffness in the triaxial apparatus, *Géotechnique*, **34**, **No. 3**, 323-340.

Jardine, R. J, Smith, P. R., Nicholson, D. P. (2002). Properties of the soft Holocene clays from Queenborough, Kent, Workshop Characterisation and Engineering Properties of NaturalS-Tan et al. (eds.), Lisse: Swets and Zeitlinger, **1**, 599-644.

Jardine, R. J., Potts, D. M., John, H. D., Hight, D. W. (1991). Some paractical applications of a non-linear ground model, Proceedings of the 10th European Conference on Soil Mechanics and Foundation Engineering, **1**, 223-228.

Jardine, R. J, Gens, A., Hight, D. W., Coop, M. R. (2004). Developments in understanding soil behaviour: Keynote paper, In Advances in Geotechnical Engineering, Proceedings of the Skempton Memorial Conference, London: Thomas Telford, **1**, 103–207.

Khachatoorian, R., Petrisor, I. B., Kwan, C. C., Yen, T. F. (2003). Biopolymer plugging effect: laboratory-pressurized pumping flow studies, *Journal of Petroleum Science and Engineering*, **38**, **1-2**, 13-21.

Kim, H. K., Santamarina, J. C. (2008). Spatial variability: drained and undrained deviatoric load response, *Géotechnique*, **58**, **No. 8**, 805-814.

Kokusho, T. (1980). Cyclic triaxial test of dynamic soil properties for wide strain range, *Soil and Foundations*, **20**, **No. 2**, 45-60.

Kucharski, E., Price, G., Li, H., Joer, H. A. (1996). Engineering properties of CIPS cemented calcareous sand, In Engineering Geology: Proceedings of the 30th International Geological Congress, Beijing, China, August 4-14, W. Sijing and P. Marinos (eds). Brill Academic Publisher, Amsterdam, Netherlands**. 23**, 92-97.

Kung, G. T. C. (2007). Equipment and testing procedures for small strain triaxial tests, *Journal of the Chinese Institute of Engineers*, **30**, **No. 4**, 579-591.

Kuwano, R. (1999). The stiffness and yielding anisotropy of sand, PhD thesis, Imperial College, University of London, UK.

Kuwano, R., Jardine, R. J. (2007). A triaxial investigation of kinematic yielding in sand, *Géotechnique*, **57**, **No. 7**, 563-579.

Lambert, J. W. M., Novakowski, K., Blauw, M., Latil, M. N., Knight, L., Bayona, L. (2010). Pamper bacteria, they will help us: application of biochemical mechanisms in geo-environmental engineering, Proceedings GeoFlorida: Advances in Analysis, Modeling and Design (eds D. O. Fratta, A. J. Puppala and B. Muhunthan), Geotechnical Special Publication 199, Reston, VA, USA, 618-627.

Lee, J. H., Salgado, R., Bernal, A., Lovell, C. W. (1999). Shredded tires and rubber-sand as light weight backfill, *Journal of Geotechnical and Geoenvironmental Engineering*, **125**, **No. 2**,132-141.

Leroueil, S., Vaughan, P. R. (1990). The general and congruent effects of structure in naturel soils and weak rocks, *Géotechnique*, **40**, 467-488.

Maccarini, M. (1987). Laboratory studies of weakly bonded artificial soil, PhD thesis, University of London, UK.

Macleod, F. A., Lappin-Scott, H. M., Costerton, J. W. (1988). Plugging of a model rock system by using starved bacteria, *Applied and Environmental Microbiology*, **54, No.6**, 1365-1372.

Maccarini, M. (1987). Laboratory studies of weakly bonded artificial soil, PhD thesis, University of London, UK.

Madigan, MT., Martinko, JM. (2003). Brock biology of microorganisms, 11th edition, Upper Saddle River, USA, Prentice Hall.

Maher, M. H., Ho, Y. C. (1993). Behavior of fiber-reinforced cement sand under static and cyclic loads, *Geotechnical Testing Journal*, **16**, **No. 3**, 330-338.

Mair, R. J. (1993). Developments in geotechnical engineering research: applications to tunnels and deep excavations, Proceedings of Institution of Civil Engineers: Civil Engineering, **93**, 27-41.

Malandraki, V. (1994). The engineering behaviour of a weakly bonded artificial soil, PhD thesis, University of Durham, UK.

Malandraki, V., Toll, D. G. (1996). The definition of yield for bonded materials, *Geotechnical and Geological Engineering*, **14**, **No.1**, 67-82.

Malandraki, V., Toll, D. G. (2000). Drained probing triaxial tests on a weakly bonded artificial soil, *Géotechnique*, **50**, **No. 2**, 141-151.

Malandraki, V., Toll, D. G. (2001). Triaxial tests on weakly bonded soil with changes in stress path, *Journal of Geotechnical and Geoenvironmental Engineering*, **127**, **No. 3**, 282-291.

Makki-Szymkiewicz, L., Hibouche, A., Taibi, S., Herrier, G., Lesueur, D., Fleureau, J. M. (2015). Evolution of the properties of lime-treated silty soil in a small experimental embankment, *Engineering Geology*, **191**, 8-22.

Martinez, B. C., DeJong, J. T. (2009). Bio-mediated soil improvement load transfer mechanisms at the micro-and macro-scales, Proceedings of Advances in Ground Improvement, US-China Workshop on Ground Improvement Technologies, March 14, Orlando, Florida, US.

Masad, E., Taha, R., Ho, C., Papagiannakis, T. (1996). Engineering properties of tire/soil mixtures as a lightweight fill material, *Geotechnical Testing Journal*, **19**, **No. 3**, 297-304.

Meyer, F. D., Bang, S., Min. S., Stetler, L. D., Bang, S. S. (2011). Microbiologically-induced soil stabilization: application of sporosarcina pasteurii for fugitive dust control, Proceedings Geo-Frontiers, March 13-16, Dallas, Texas, US.

Mitchell, A., Ferris, F. (2006). The influence of bacillus pasteurii on the nucleation and growth of calcium carbonate, *Geomicrobiology Journal*, **23**, **No. 3**, 213-226.

Mitchell, JK. (1976). Fundamentals of soil behaviour, 1st edition, Printed in the US John Wiley and Sons, Inc.

Mitchell, JK. (1993). Fundamentals of soil behaviour, 2nd edition, Printed in the US, John Wiley and Sons, Inc.

Mitchell, J. K., Santamarina, J. C. (2005). Biological considerations in geotechnical engineering, *Journal of Geotechnical and Geoenvironmental Engineering*, **131**, **No. 10**, 1222-1233.

Montoya, B. M., DeJong, J. T., Boulanger, R. W. (2013). Dynamic response of liquefiable sand improved by microbial-induced calcite precipitation, *Géotechnique*, **63**, **No. 4**, 302-312.

Moo-Young, H., Sellasie, K., Zeroka, D., Sabnis, G. (2003). Physical and chemical properties of recycled tire shreds for use in construction, *Journal of Geotechnical and Geoenvironmental Engineering*, **129**, **No. 10**, 921-929.

Murff, G. D. (1987). Pile capacity in calcareous sands, state-of-the art, *Journal of Geotechnical Engineering*, **113**, **No.5**, 490-507.

Nishimura, S. (2005). Laboratory study on anisotropy of natural London clay, PhD thesis, Imperial College, University of London, UK.

Ozdogan, A. (2010). Study on the triaxial shear behavior and microstructure of the biologically treated sand specimens, MSc thesis, University of Delaware, US.

Ozkul, Z. H., Baykal, G. (2006). Shear strength of clay with rubber fiber inclusions, *Geosynthetics International*, **133**, **No. 7**, 767-781.

Pamukcu, S., Akbulut, S. (2006). Thermoelastic enhancement of damping of sand using granular synthetic rubber, *Journal of Geotechnical and Geoenvironmental Engineering*, **132**, **No. 4**, 501-510.

Park, C. S., Tatsuoka, F. (1994). Anisotropic strength and deformation of sands in plane strain compression, Proceedings of the 13th International Conference on Soil Mechanics and Foundation Engineering, **1**, 1-6.

Park, S. (2011). Unconfined compressive strength and ductility of fiber-reinforced cemented sand, *Construction and Building Materials*, **25**, 1134-1138.

Park, S. S., Jeong, S. W. (2015). Effect of specimen size on undrained and drained shear strength of sand, *Marine Georesources and Geotechnology*, **33**, 361-366.

Pathak, S. R., Dalvi, R. S. (2011). Effect of sample preparation method on liquefaction of sandy soil, *Electronic Journal of Geotechnical Engineering*, **16**, 1411-1426.

Perkins, S. W., Gyr, p., James, G. (2000). The influence of the biofilm on the mechanical behavior of the sand, *Geotechnical Testing Journal*, **23**, **No. 3**, 300-312.

Polito, C. P. (1999). The effects of non-plastic and plastic fines on the liquefaction of sandy soils, PhD thesis, Faculty of the Virginia Polytechnic Institute and State University, US.

Porcino, D., Marcianò, V., Granata, R. (2012). Static and dynamic properties of a lightly cemented silicate-grouted sand, *Canadian Geotechnical Journal*, **49**, 1117-1133.

Porovic, E., Jardine, R. (1994). Some observations on the static and dynamic shear stiffness of Ham river sand, Proceedings of the 1st International Conference on Pre-failure Deformation Characteristics of Geomaterials, Balkema Rotterdam, **1**, 25-30.

Ramachandran, S. K., Ramakrishnan, V., Bang, S. S. (2001). Remediation of concrete using micro-organisms, *ACI Material Journal*, **98**, **No. 1**, 3-9.

Ramakrishnan, V., Bang, S. S., Deo, K. S. (1998). A novel technique for repairing cracks in high performance concrete using bacteria, Proceedings of the International Conference on High Performance High Strength Concrete, Perth, Australia, 597-618.

Rebata-Landa, V., Santamarina, J. C. (2012). Mechanical effects of biogenic nitrogen gas bubbles in soils, *Journal of Geotechnical and Geoenvironmental Engineering*, **138**, **No. 2**, 128-137.

Rippa, F., Picarelli, L. (1977). Some considerations on index properties of Southern Italian shales, Proceedings of the International Symposium on the Geotechnics of Structurally Complex Formations, Capri, **1**, 401-406.

Rios, S., Fonseca, A. V., Baudet, B. A. (2014). On the shearing behaviour of an artificially cemented soil. *Acta Geotechnica*, **9**, 215-226.

Rolo, R. (2003). The anisotropic stress-strain-strength behaviour of brittle sediments, PhD thesis, University of London, London, UK.

Rotta, G. V., Consoli, N. C., Prietto, P. D. M., Coop, M. R., Graham, J. (2003). Isotropic yielding in an artificially cemented soil cured under stress, *Géotechnique*, **53**, **No. 5**, 493-501.

Salgado, R., Bandini, P., Karim, A. (2000). Shear strength and stiffness of silty sand, *Journal of Geotechnical and Geoenvironmental Engineering*, **126, No. 5,** 451-462.

Sangrey, D. A. (1972). Naturally cemented sensitive soils, *Géotechnique*, **22**, **No. 1**, 139-152.

Santagata, M. C. (1998). Factors effecting the initial stiffness and stiffness degradation of cohesive soils, PhD thesis, Massachusetts Institute of Technology, Department of Civil and Environmental Engineering, University of Cambridge, US.

Sarda, D., Choonia, S., Sarode, D. D., Lele, S. S. (2009). Biocalcification by Bacillus pasteurii urease: a novel application, *Journal of Industrial Microbiology and Biotechnology*, **36**, **No.8**, 1111-1115.

Sari, Y. D. (2015). Soil Strength Improvement by Microbial Cementation, *Marine Georesources and Geotechnology*, **33**, 567-571.

Saxena, S. K., Lastrico, R. M. (1978). Static properties of lightly cemented sand, *Journal of the Geotechnical Engineering Division*, **104**, **No.12**, 1449-1464.

Scholey, G. K., Frost, J. D., Lo Presti, D. C. F., Jamiolkowski, M. (1995). A Review of instrumentation for measuring small strain during triaxial testing of soil specimens, *Geotechnical Testing Journal*, **18**, **No. 2**, 137-156.

Schnaid, F., Prietto, P. D., Consoli, N. (2001). Characterization of cemented sand in triaxial compression, *Journal of Geotechnical and Geoenvironmental Engineering*, **127**, **No. 10**, 857-868.

Seki, K., Miyazaki, T., Nakano, M. (1998). Effects of microorganisms on hydraulic conductivity decrease in infiltration, *European Journal of Soil Science*, **49**, **No. 2**, 231-236.

Sel, I., Ozhan, H. B., Cibik, R., Buyukcangaz, E. (2015). Bacteria-induced cementation process in loose sand medium, *Marine Georesources and Geotechnology*, **33**, 403-407.

Senetakis, K., Anastasiadis, A., Pitilakis, K., Souli, A. (2012). Dynamic behavior of sand/rubber mixtures, Part II: Effect of rubber content on G/Go-c-DT curves and volumetric threshold strain, *Journal of ASTM International*, **9**, **No. 2**.

Skempton, A. W. (1944). Notes on the compressibility of clays, *Quarterly Journal of Geological Society*, **100**, 119-135.

Smith, P. R. (1992). The behaviour of natural high compressibility clay with special reference to construction on soft ground, PhD thesis, Imperial College, University of London, UK.

Stal, L. J. (2010). Microphytobenthos as a biogeomorphological force in intertidal sediment stabilization, *Ecological Engineering*, **36**, **No. 2**, 236-245.

Stocks-Fischer, S., Galinat, J. K., Bang, S. S. (1999). Microbiological precipitation of $CaCO_3$, *Soil Biology and Biochemistry*, **31**, **No. 11**, 1563-1571.

Stoke, K. H., Santamarina, J. C. (2000). Seismic-wave based testing in geotechnical engineering, Proceeding International Conference on Geotechnical and geological Rngineering, Melbourne, Australia, **1**, 1490-1536.

Sung-Jin, P., Young-Chun, W., Kim, W. J., Ghim, S. Y. (2012). Application of alkaliphilic biofilm-forming bacteria to improve compressive strength of cement-sand mortar, *Journal of Microbiology and Biotechnology*, **22**, **No. 3**, 385-389.

Suzuki, M., Fujimoto, T., Taguchi, T. (2014). Peak and residual strength characteristics of cement-treated soil cured under different consolidation conditions, *Soils and Foundations*, **54**, **No.4**, 687-698.

Taheri, A., Tatsuoka, F. (2015). Small- and large-strain behaviour of a cement-treated soil during various loading histories and testing conditions, *Acta Geotechnica*, **10**, 131-155.

Tanchaisawat, T., Bergado, D. T., Voottipruex, P., Shehzad, K. (2010). Interaction between geogrid reinforcement and tire chip-sand lightweight backfill, *Geotextiles and Geomembranes*, **28**, 119-127.

Tang, C., Shi, B., Gao, W., Chen, W., Cai, Y. (2007). Strength and mechanical behavior of short polypropylene fiber reinforced and cement stabilized clayey soil, *Geotextiles and Geomembranes*, **25**, **No. 3**, 194-202.

Tatlisoz, N., Benson, C., Edil, T. (1997). Effect of fines on mechanical properties of soil-tire chip mixtures, Testing Soil Mixed with Waste or Recycled Materials. ASTM International, West Conshohocken, PA, 93-108.

Terzaghi, K. (1925). Erdbaumechanik auf bodenphysikalischer grundlage, Vienna, Deuticke, Leipzig.

Terzaghi, K., Peck, RB. (1962). Soil mechanics in engineering practice, 12th edition, US, John Wiley and Sons, Inc.

Thullner, M., Baveye, P. (2008). Computational pore network modeling of the influence of biofilm permeability on bioclogging in porous media, *Biotechnology and Bioengineering*, **99**, **No. 6**, 1337-1351.

Toll, D. G., Malandraki, V. (1993). Triaxial testing of a weakly bonded soil, Geotechnical Engineering of Hard Soils-Soft Rocks, A. Anagnostopoulos et al., (eds), Athens, Greece, Balkema: Rotterdam, 817-825.

Tsang, H. H. (2008). Seismic isolation by rubber-soil mixtures for developing countries, *Earthquake Engineering and Structural Dynamics*, **37**, **No. 2**, 283-303.

Tsoi, W. Y., Lee, K. M. (2011). Mechanical properties of cemented scrap rubber tyre chips, *Géotechnique*, **61**, **No. 2**, 133-141.

Tweedie, J. J., Humphrey, D. N., Sandford, T. C. (1998). Full scale field trials of tire shreds as lightweight retaining wall backfill, at-rest conditions, *Transportation Research Record*, **1619**, 64-71.

Ud-din, S., Marri, A., Wanatowski, D. (2011). Effect of high confining pressure on the behaviour of fibre reinforced sand, *Geotechnical Engineering Journal of the SEAGS and AGSSEA*, **42**, **No.4**, 69-76.

Van Paassen, L. A., Harkes, M. P., Van Zwieten, G. A., Van der Zon, W. H., Van der Star, W. R. L., Van Loosdrecht, M. C. M. (2009). Scale up of BioGrout: a biologicalground reinforcement method, Proceedings of the 17th International Conference on Soil Mechanics and Geotechnical Engineering, 2328-2333.

Van Paassen, L. A., Van Loosdrecht, M. C. M., Pieron, M., Mulder, A., Ngan-Tillard, D. J. M., Van Der Linden, T. J. M. (2010). Strength and deformation of biologically cemented sand stone, Rock Engineering in Difficult Ground Conditions-Soft Rocks and Karst-Vrkljan (ed), London, 405-410.

Vesic, A. B., Clough, G. W. (1968). Behaviour of granular materials under high stresses, *Journal of the Soil Mechanics and Foundation Division*, **94**, **No. 3**, 661-688.

Viggiani, G., Atkinson, J. H. (1995). Stiffness of fine-grained soil at very small strains, *Géotechnique*, **45**, **No. 2**, 249-265.

Waller III, J. T. (2011). Influence of bio-cementation on shearing behavior in sand using X-ray computed tomography, MSc thesis, University of California, US.

Weaver, T. J., Burbank, M., Lewis, A., Lewis, R., Crawford, R., Williams, B. (2011). Bio-induced calcite, iron, and manganese precipitation for geotechnical engineering applications, Proceedings Geo-Frontiers, Dallas, Texas, US, March 13-16, 3975-3983.

Weil, M. H., DeJong, J. T., Martinez, B. C., Mortensen, B. M. (2011). Seismic and resistivity measurements for real-time monitoring of microbially induced calcite precipitation in sand, *Geotechnical Testing Journal*, **35**, **No. 2**. 1-12.

Wen Chou, C. (2007). Biomodification of geotechnical properties of sand, MSc thesis, University of Maryland, US.

Whiffin, V. S., Van Paassen, L. A., Harkes, M. P. (2007). Microbial carbonate precipitation as a soil improvement technique, *Geomicrobiology Journal*, **24**, 417-423.

Wu, W. Y., Benda, C. C., Cauley, R. F. (1997). Triaxial determination of shear strength of tire chips, *Journal of Geotechnical and Geoenvironmental Engineering*, **123**, **No. 5**, 479-482.

Young, H. M., Sellasie, K., Zeroka, D., Sabris, G. (2003). Physical and chemical properties of recycled tire shreds for use in construction, *Journal of Environmental Engineering*, **129**, **No.10**, 921-929.

Yun, T. S., Santamarina, J. C. (2005). Decementation, softening, and collapse: changes in small-strain shear stiffness in K_o loading, *Journal of Geotechnical and Geoenvironmental Engineering*, **131**, No. 3, 350-358.

Zhu, F., Clark, J. I., Paulin, M. J. (1995). Factors affecting at-rest lateral stress in artificially cemented sands, *Canadian Geotechnical Journal*, **32**, **No. 2**, 95-103.

Zimmermann, T., Truty, A., Podles, K. (2010). Numerics in geotechnics and structures, Poland, Elmepress International.

Zornberg, J. G., Cabral, A. R., Viratjandr, C. (2004). Behavior of tire shred-sand mixtures, *Canadian Geotechnical Journal*, **41**, **No. 2**, 227-241.

CURRICULUM VITAE

PERSONAL INFORMATION

Name and Surname : Zuheir Ismaeel Mosa KARABASH

Nationality : Iraqi

Birth place and date : Tallafar-Mosul-Iraq / 26-02-1979

Marital status : Married-3 child

Phone number : 0342 317 24 50

E-mail : zuheirkra@gmail.com

EDUCATION

Degree	Graduate School	Year
MS	University of Mosul	2005
BS	University of Mosul	2001
High School	Tallafer High School	1997

WORK EXPERIENCE

Year	Place	Enrollment
2005-present	Mosul University	Assistant lecturer

PUBLICATIONS

A. International Journals

1- **Karabash, Z**., Cabalar, A. F. (2015). Effect of tire crumb and cement addition on triaxial shear behavior of sandy soils, *Geomechanics and Engineering*, **8**, **No. 1**, 1-15.

2- Cabalar, A. F., **Karabash, Z.** (2015). California bearing ratio of a sub-base material modified with tire buffings and cement addition, *Journal of Testing and Evaluation*, **43**, **No. 6**, 1-9.

3- Cabalar, A. F., **Karabash, Z**., Mustafa, W. S. (2014). Stabilising a clay using tyre buffings and lime, *Road Materials and Pavement Design*, **15**, **No. 4**, 872-891.

4- **Karabash, Z.**, Al-Atalla, M. A. A., Abdullah, F. A. M. A. (2011). Relation between ultrasonic pulse velocity and some mechanical properties of clayey soil treated with lime, *Al-Rafidain Engineering*, **19**, **No. 1**, 15-25.

5- **Karabash, Z**., Cabalar, A. F. (2015). Influence of sample preparation and cement type on the small-strain behaviour of cemented sands, *ACTA Geotechnica Slovenica*, (under review).

6- **Karabash, Z**., Cabalar, A. F., Erkmen, O. (2015). Stiffness of biocemented sand at small strains, *Candian Geotechical Journal*, (under review).

7- **Karabash, Z**., Cabalar, A. F. (2015). Undrained and drained triaxial shear behaviour of Narli sand, *Bulletin of Engineering Geology and the Environment*, (under review).

8- **Karabash, Z**., Cabalar, A. F. (2015). Influence of grain shape on triaxial shear behavior of sand-clay mixtures, *Soil Mechanics and Foundation Engineering*, (accepted).

9- Abdulnafaa, M. D., Cabalar, A. F., **Karabash, Z.** (2015). Influences of various constraction and demolition materials on the behaviour of a clay, *Journal of Material in Civil Engineering*, (under review).

B. International/National Congress, Conference and Symposium

1- **Karabash, Z.,** Cabalar, A. F., Isik, H. (2015). Stabilization of clayey soil by waste steel pieces, International Conference on Civil and Environmental Engineering, ICOCEE, May 20-23, Nevşehir/Turkey, 1538-1545.

2- Karabash, Z., Ozakca, M., Cabalar, A. F. (2014). Modeling of embankment stabilized with geogrid, 11th International Congress on Advances in Civil Engineering, ACE, 21-25 October, Istanbul/ Turkey.

3- **Karabash, Z**., Cabalar, A. F. (2014). Narli kumunun çok küçük gerinimlerdeki elastisite modülü, Zemin Mekaniği ve Temel Mühendisliği Onbeşinci Ulusal Kongresi,16-17 Ekim, Orta Doğu Teknik Üniversitesi, Ankara/Turkey, 199-204.

4- **Karabash, Z.,** Cabalar, A. F., Mustafa, W. S. (2014). A study of a clay with tire buffings and lime, Internatıional Civil Engineering and Architecture Symposium for Academicians, ICESA, May 17-20, Side/Antalya/Turkey, 222-229.

5- AL-Layla, M. T., **Karabash, Z.** (2010). Study of piping in gypseous soils and lime stabilized soils, The 2nd Regional Conference for Engineering Science, 1-2 December, Baghdad/Iraq, 689-692.

6- **Karabash, Z.,** Cabalar, A. F., Akbulut, N. (2015). The behaviour of clayey soil reinforced with waste aluminium pieces, World Multidisciplinary Earth Sciences Symposium, WMESS, Prague, Procedia Earth and Planetary Science, **15**, 353-358.

7- **Karabash, Z.,** Cabalar, A. F., Akbulut, N. (2015). A study of a clay with biopolymer by compaction and unconfined compression tests, 6. Geotechnic Symposium, Çukurova University, Adana, (accepted).